Covalently Bound Organic Monolayers on Hydrogen-Terminated Silicon Surfaces

Promotor: prof. dr. E. J. R. Sudhölter, hoogleraar in de Fysisch-Organische Chemie.

Co-promotor: dr. H. Zuilhof, universitair docent verbonden aan de leerstoelgroep Organische Chemie.

Samenstelling promotiecommissie:

Prof. dr. W. C. Sinke (ECN, Petten)

Dr. A. Goossens (Technische Universiteit Delft)

Prof. dr. M. A. Cohen Stuart (Wageningen Universiteit)

Prof. dr. L. W. Jenneskens (Universiteit Utrecht)

pH2231.293

Alexander B. Sieval

Covalently Bound Organic Monolayers on Hydrogen-Terminated Silicon Surfaces

Covalent Gebonden Organische Monolagen
op
Waterstof-Getermineerde Siliciumoppervlakken

Proefschrift
ter verkrijging van de graad van doctor
op gezag van de rector magnificus
van Wageningen Universiteit,
prof. dr. ir. L. Speelman,
in het openbaar te verdedigen
op vrijdag 20 april 2001
des namiddags te vier uur in de Aula.

161326g

Dankwoord

Silicium: atoomnummer 14, diamantrooster, halfgeleider, basismateriaal voor computerprocessoren en zonnecellen. Als fysisch-organisch chemicus was dat wel zo ongeveer mijn parate kennis over dit element. Ook organische monolagen waren weinig aan bod gekomen tijdens mijn studie scheikunde. In mijn promotieonderzoek moesten deze twee onderwerpen verenigd worden: waar was ik aan begonnen? Nu, vijf jaar later, is er een dik proefschrift over het maken en karakteriseren van diezelfde organische monolagen op siliciumoppervlakken. Een lange periode, waarin ik met veel plezier aan dit onderzoek gewerkt heb en waarin ik veel geleerd heb. Die periode zou echter niet zo plezierig, leerzaam en succesvol geweest zijn zonder de medewerking van veel mensen. Die wil ik hieronder graag bedanken.

Als eerste wil ik mijn promotor, Ernst Sudhölter, noemen. Ernst, je eerste opdracht aan mij luidde zo ongeveer "Doe dat eerst maar eens na", waarbij met 'dat' het maken van de monolagen op silicium volgens de methode van Linford werd bedoeld, die een jaar eerder was gepubliceerd. Ik denk dat we daar wel in geslaagd zijn, en dat we er een heleboel leuke dingen uit hebben gekregen. Bedankt voor jouw immer aanwezige enthousiasme voor dit onderzoek en de grote vrijheid die ik heb gehad in de afgelopen jaren.

Mijn co-promotor, Han Zuilhof, wil ik bedanken voor de dagelijkse begeleiding en de goede adviezen. Ik heb veel geleerd van de vele discussies die we hebben gevoerd over de resultaten van mijn onderzoek en de artikelen die op basis daarvan werden geschreven. Ook jouw enthousiasme voor dit onderzoek was een goede stimulans.

Op het laboratorium voor Organische Chemie was niet alle benodigde meetapparatuur aanwezig die nodig was voor dit onderzoek. Gelukkig kon er veelvuldig gebruik worden gemaakt van hulp van buiten. Willem Nissink en prof. J. van der Maas van de Universiteit Utrecht wil ik bedanken voor hun hulp bij de infraroodmetingen zoals beschreven in Hoofdstuk 3. I also want to thank dr. Levent Demirel, dr. Ricarda Opitz, and prof. Wim de Jeu, from the AMOLF institute in Amsterdam, for performing the X-ray reflectivity experiments as described in Chapters 3 and 5. Dr. Ralf Linke van de Universiteit Eindhoven wil ik bedanken voor de XPS metingen.

Oppervlaktepassivering van halfgeleiders is geen dagelijkse kost voor organisch chemici, maar vormde wel een onderdeel van dit onderzoek. Hoofdstuk 7 is dan ook het resultaat van een goede samenwerking met ECN en de Technische Universiteit Delft. Frank Schuurmans wil ik

Stellingen

1. Bij het nauwkeurig meten van watercontacthoeken van organische monolagen op vaste substraten met de Wilhelmy-plaat methode is ervaring met de betreffende techniek belangrijk om foute interpretaties te voorkomen.

2. De bewering van Effenberger et al., dat in de UV-geïnduceerde reactie van octadecanal met het waterstofgetermineerde Si(111) oppervlak aan 97% van de silicium oppervlakteatomen een organisch molecuul wordt gebonden, is onjuist.
   - Effenberger, F.; Götz, G.; Bidlingmaier, B.; Wezstein, M. *Angew. Chem., Int. Ed. Engl.* **1998**, *37*, 2462–2464.
   - Dit proefschrift.

3. De conclusie van Bateman et al., dat in de reactie van undeceen met deuteriumgetermineerde siliciumoppervlakken geen C–D bindingen gevormd worden, valt niet af te leiden uit het door de auteurs gepresenteerde IR spectrum van de resulterende monolaag.
   Bateman, J. E.; Eagling, R. D.; Horrocks, B. R.; Houlton, A. *J. Phys. Chem. B* **2000**, *104*, 5557–5565 (Figuur 9).

4. Zhu et al. vergelijken ten onrechte hun monolagen van alcoholen op chloorgetermineerde Si(100) oppervlakken niet met de monolagen van 1-alkenen op H-getermineerde Si(100) oppervlakken zoals beschreven door Sieval et al.
   - Zhu, X.-Y.; Boiadjiev, V.; Mulder, J. A.; Hsung, R. P.; Major, R. C. *Langmuir* **2000**, *16*, 6766–6772.
   - Sieval, A. B.; Demirel, A. L.; Nissink, J. W. M.; Linford, M. R.; van der Maas, J. H.; de Jeu, W. H.; Zuilhof, H.; Sudhölter, E. J. R. *Langmuir* **1998**, *14*, 1759–1768 (Hoofdstuk 3 van dit proefschrift).

5. Het kunnen meten van high resolution electron energy loss spectra (HREELS) met een resolutie beter dan 8 cm^{-1} in plaats van ongeveer 30 cm^{-1} betekent nog niet dat er gemeten wordt met ultieme resolutie.
   Tautz, F. S.; Schaefer, J. A. "Ultimate resolution electron energy loss spectroscopy at H/Si(100) surfaces." *J. Appl. Phys.* **1998**, *84*, 6636–6639.

6. Het modeleren van de driedimensionale structuur van de vaste fase van (vloeibaar-) kristallijne organische verbindingen leidt vaak tot foutieve simulaties doordat gekozen wordt voor een te kleine eenheidscel.

7. Een sollicitatieplicht in de laatste maand voor aanvang van een nieuwe baan is zinloos.

8. Een goed onderzoeker is tenminste eigenwijs.

Stellingen behorende bij het proefschrift:

Covalently Bound Organic Monolayers on Hydrogen-Terminated Silicon Surfaces

Wageningen, 20 april 2001 Alexander B. Sieval

bedanken voor de eerste (zeer succesvolle!) levensduurmetingen aan Si wafers gepassiveerd met MeA11. Dr. Axel Schönecker en prof. Wim Sinke hebben het mogelijk gemaakt dat ik gedurende een vijftal weken zelf levensduurmetingen kon doen bij ECN. Arvid van der Heide en Axel wil ik bedanken voor technische assistentie bij de MFCA experimenten. De Kelvin probe metingen zijn uitgevoerd samen met Carolien Huisman en dr. Albert Goossens van de Technische Universiteit Delft. De Kelvin probe werkte niet altijd mee, maar de uiteindelijke resultaten hebben een belangrijke bijdrage geleverd voor de verklaring van het tijdsafhankelijke gedrag van de effectieve levensduur, τ_{eff}.

Edwin Currie, Joost Maas en prof. Martien Cohen Stuart van het laboratorium voor Fysische chemie en Kolloïdkunde van Wageningen Universiteit wil ik bedanken voor hun verzoek om te proberen monolagen van styreen en polystyreen te maken. We waren eerst nogal sceptisch, maar er zijn toch hele mooie resultaten uitgekomen. Van hetzelfde laboratorium wil ik Remko Fokkink bedanken voor het oplossen van de technische problemen met de FT-IR opstelling, waarmee de ATR infraroodmetingen in Wageningen werden uitgevoerd.

Het in dit proefschrift beschreven onderzoek viel binnen het interdisciplinaire Novem-project Organische Zonnecellen. Iedereen die in de afgelopen jaren bij de vergaderingen en werkbesprekingen aanwezig is geweest, wil ik bedanken voor hun bijdrage.

Tijdens mijn onderzoek heb ik het genoegen gehad maar liefst zes studenten te mogen begeleiden: Bram en Huub kwamen van Wageningen Universiteit, Geert, Vincent, Michael en Gert van het Rijn-IJsselcollege te Arnhem. Ik wil jullie graag bedanken: mede dankzij jullie inspanningen is dit boekje zo dik geworden.

Alle medewerkers van het laboratorium voor Organische Chemie wil ik bedanken voor de gezellige jaren die ik heb gehad: "OC" was een fijne werkplek. In het bijzonder wil ik Beb van Veldhuizen bedanken voor zijn hulp bij het opnemen van de NMR spectra, Kees Teunis voor de massaspectra, en Ronald en Pleun voor het leveren en bestellen van de benodigde chemicaliën en het glaswerk. De glasblazers Jurrie en Gert wil ik bedanken voor het maken van de speciale reactiebuizen en reactiekolven die nodig waren voor dit onderzoek.

Geen promovendus zonder collega-promovendi, postdocs en analisten. Gelukkig maar, want de ontelbare (on)zinnige gesprekken tijdens de koffie-, lunch- en theepauzes, alsmede de borrels, twee AIO-reizen, drie oranje-groen roeitoernooien, diverse labreisjes, Hansje Brinker, wekelijkse zwemuurtjes, sinterklaasgedichten en vele andere activiteiten hebben de afgelopen

jaren in Wageningen tot een onvergetelijke tijd gemaakt. Het is helaas niet mogelijk om jullie specifieke bijdragen hier allemaal apart te noemen: dit dankwoord zou dan wel eens heel erg lang kunnen worden. Hendra, Theo, Yvonne, Matthew, Gert Jan, Roel, Helma, Tina en alle anderen: allemaal ontzettend bedankt!

Mijn ouders, mijn broer Paul, alsmede Marijke, Joop, Ingrid en Mark wil ik bedanken voor de belangstelling die zij al die jaren getoond hebben in de voortgang van mijn onderzoek. Jullie hadden geen goed idee van wat ik nu precies deed, daar in Wageningen, maar het was "iets met zonnecellen". Tot op zekere hoogte klopt dat ook wel, maar in dit proefschrift is toch geen zonnecel te vinden. Het hele onderzoek draaide namelijk allemaal om dat simpele figuurtje op de omslag. En daar kun je dus vier jaar mee bezig zijn!

Tot slot wil ik Sandra bedanken voor al die dingen buiten de chemie. Ook jij begreep niet precies wat ik nu deed, maar gelukkig begrijp je mij meestal wel.

Alex

Contents

Chapter		Page
1	**General Introduction**	1
2	**Organic Monolayers on Silicon Surfaces**	9
3	**Monolayers of 1-Alkenes on the Hydrogen-Terminated Si(100) Surface**	27
4	**1-Alkene Monolayers on the Hydrogen-Terminated Si(100) Surface: Solvent Effects**	57
5	**Monolayers of 1-Alkynes on the Hydrogen-Terminated Si(100) Surface**	69
6	**Molecular Modeling of Alkyl Monolayers on the H-Terminated Si(111) Surface**	101
7	**Silicon Surface Passivation by Monolayers of 1-Alkenes: Minority Charge Carrier *Lifetime Measurements and Kelvin Probe Investigations***	133
8	**Amino-Terminated Monolayers on Silicon Surfaces**	155
	Appendix	171
	Summary	175
	Samenvatting	181
	Curriculum vitae	187
	List of Publications	189

Chapter 1

General Introduction

1.1 Introduction

The present technological developments require a continuous downsizing of electronic devices, like microprocessor chips and sensors. Consequently, the surface properties of the inorganic materials that are used in these devices become more important, as the relative number of surface atoms in the device increases rapidly.[1] Therefore, control of the surface structure, preferably even down to the molecular level, becomes increasingly important.

Monolayers of organic compounds on solid substrates, also called organic monolayers, form an important candidate for such molecular control of surface properties. These monolayers have been investigated extensively for many years and they can be easily prepared on a large variety of substrates, ranging from inorganic oxides, like mica and silicon oxide, to all kinds of metals.[2,3] In general, they are formed by either the transfer of an already ordered monolayer of organic material onto a substrate (so-called Langmuir-Blodgett monolayers; see Section 1.2.1), or the spontaneous adsorption of dissolved molecules onto a substrate (so-called self-assembled monolayers, SAMs). A large variety of these SAMs exists,[2,3] but only three will be discussed in this thesis, as they are technologically the most

promising. These systems are the organosilicon derivatives on silicon oxide (see Section 1.2.2), the thiols on gold (see Section 1.2.3), and the covalently bound organic monolayers on oxide-free Si surfaces, which will be discussed extensively in Chapter 2.

1.2 Organic Monolayers on Solid Substrates

1.2.1 Langmuir-Blodgett Monolayers

The preparation of Langmuir-Blodgett layers on solid substrates consists of a two-step procedure. In the first step a monolayer of an organic compound is prepared on an aqueous subphase by spreading a small amount of a solution of this compound on a large water surface and allowing the solvent to evaporate. These layers were first investigated in detail by Langmuir, who realized that such a layer would have a maximum thickness of only one molecule.[4] In general amphiphilic molecules are used, which means that in the monolayer the polar head groups of these molecules are at the water surface, whereas the apolar parts are above this surface. This so-called Langmuir layer is slowly compressed until an ordered two-dimensional system is obtained, in which the molecules are closely packed and all have the same orientation. In the second step this ordered layer is transferred onto a solid substrate by slowly dipping this substrate in the water phase. This results in a monolayer of the organic compound that is adsorbed on the surface of the substrate. This technique was first reported by Blodgett,[5,6] therefore the resulting layers are referred to as Langmuir-Blodgett layers. By repeating the dipping step multilayers of the organic compound can be prepared.[6]

The orientation of the molecules with respect to the surface of the substrate depends on the properties of this surface and on the properties of the organic compound.[2] On polar substrates, like glass, the polar head groups of the amphiphilic molecule are at the glass surface and the apolar groups are at the monolayer–air interface, whereas on apolar substrates the reverse situation is formed. For multilayers two different situations are possible. The molecules can all be oriented head-to-tail, i.e., the orientation of the molecules in each layer is identical, or the molecules can be head-to-head, which means that they form a double-layered system. For amphiphilic molecules this latter situation is thermodynamically the most stable, as it results in a situation in which the interactions between adjacent layers are subsequently hydrophobic–hydrophobic and hydrophilic–hydrophilic.

An enormous amount of research has been done on the preparation, characterization, and properties of these Langmuir-Blodgett layers, using a large variety of organic molecules,

including polymers. A review of this work is beyond the scope of this Introduction. For more information the reader is referred to reference 2.

1.2.2 Monolayers of Organosilicon Derivatives on Silicon Oxide

Monolayers of organosilicon derivatives on silicon oxide[7] have for a long time been called monolayers on silicon, most likely to distinguish them from monolayers on silica.[8] They were first prepared by Sagiv in 1980, who reported the spontaneous formation of ordered monolayers of octadecyltrichlorosilane on glass.[9] Soon after, the reaction was extended to oxidized silicon.[10,11,12] Well-ordered monolayers were obtained with *n*-alkyltrichlorosilanes of various lengths, as well as with some ω-functionalized derivatives. The molecules in the monolayers are oriented nearly perpendicular to the surface. The reaction works equally well for trialkoxysilanes,[13,14] which have the advantage that these organic reagents are more stable toward side-reactions, like polymerization (*vide infra*). The reaction is schematically shown in Figure 1.

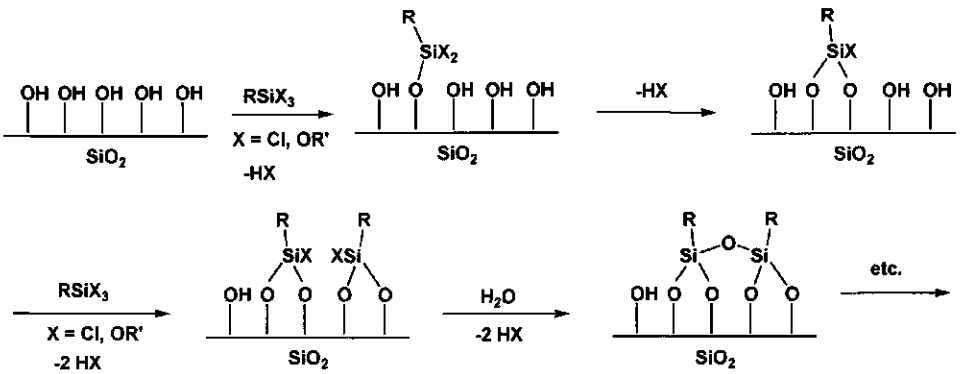

Figure 1. Reaction of organosilicon derivatives with a silicon oxide surface.

It has been shown that a large variety of functionalized organosilanes can be used. The compounds that were used in the early years can be found in references 2 and 3. Nowadays, many researchers develop special, highly functionalized molecules for specific purposes, investigating the properties of mixed monolayers, the possibilities for application in non-linear optics (NLO), the development of sensors, etc. It is beyond the scope of this Introduction to give a review of this subject.

The preparation of these self-assembled monolayers is not limited to silicon oxide. Other surfaces can be used as well, provided that hydroxyl groups are present,[2,3,15] as is

evident from Figure 1. It has been shown that on a dehydrated surface monolayer formation is not possible or leads to disordered systems.[16] However, there is still considerable debate about the precise reaction mechanism and about the exact structure of the new "SiO" layer that is formed at the interface.[15,17,18]

It should be noted that, although the reaction shown in Figure 1 is quite straightforward from a chemical point of view, there can be some practical problems in the actual preparation of the monolayers. Adsorption of the molecules will, of course, always occur, because of the chemical reaction that takes place between the surface Si–OH groups and the reactive Si–Cl or Si–OR groups of the silane derivative. However, the successful formation of high-quality monolayers is influenced both by the residual water content and by the reaction temperature. It is known that incomplete monolayer formation occurs in the absence of water, whereas an excess of water leads to extensive polymerization of the silanes in solution, and, consequently, the (co–)adsorption of polysiloxanes.[19,20] The reaction temperature not only influences the reaction kinetics, but threshold temperatures are known to exist, above which disordered monolayers are formed.[19,21] These threshold temperatures even vary within a series of derivatives that only vary in the length of the alkyl chain.[21] The occurrence of these threshold temperatures contrasts with the behavior as found for monolayers of thiols on gold[22] and, especially, that of 1-alkenes on H-terminated Si surfaces (see Section 2.3.1 and Chapter 4), where the quality of the monolayers improves if the reaction temperature is increased. Apart from these practical problems concerning the actual monolayer formation, it should also be noted that the required silane derivatives, especially the trichlorosilanes, can be difficult to purify and are very sensitive towards moisture.

1.2.3 Monolayers of Thiols on Gold

The strong affinity of sulfur compounds to transition metal surfaces is well known, and many different combinations have been investigated.[2,3] Most of the research in this field has been done on the interaction between thiols and the noble metals, in particular the Au(111) surface. The first self-assembled monolayers of sulfur-containing compounds on gold were prepared from organic disulfides.[23,24,25] Soon after, it was found that the reaction works equally well for alkanethiols[26] and it has been shown that these derivatives give monolayers that are indistinguishable from those of the corresponding disulfides.[27] A hexagonal packing structure is observed for the molecules in the monolayer, which is commensurate with the underlying Au(111) surface.[24] For *n*-alkyl thiols the alkyl chains in the monolayers are tilted approximately 27° from the surface normal.[25,26] This tilting results in

an increase in the favorable Van der Waals interactions between the alkyl chains, as the surface area that is available per molecule (~21.4 $Å^2$) is larger than that required for molecules oriented perpendicular to the surface (~19 $Å^2$).[3]

As for the alkylsilanes (see Section 1.2.2), a large variety of functionalized derivatives have successfully been used in the monolayer preparations, especially ω-functionalized thiols.[23,24,25,28] Just as for the silane derivatives, all kinds of special molecules are now used for the monolayer preparation. The results from the early years have been reviewed in references 2 and 3.

The advantage of the thiol monolayers over the alkylsilanes is the better compatibility of the thiol group with other functional groups in the organic compound. The major drawback is that they are bound to the surface by relatively weak, ionic $Au^+—S^-$ interactions. Consequently, the monolayers of thiols can be relatively easily desorbed from the Au surface, e.g., by heating in a solvent.[28,29]

1.3 Outline of this Thesis

The purpose of this investigation is the preparation of covalently bound, Si–C linked organic monolayers on hydrogen-terminated silicon surfaces by wet-chemical reactions between organic compounds and the Si surface. These monolayers are part of the class of the organic monolayers on oxide-free Si surfaces, as mentioned in the Introduction of this Chapter (see Section 1.1).

Chapter 2 gives a literature review of the various methods that have been developed in recent years for the preparation of organic monolayers on oxide-free silicon surfaces. Both wet-chemical reactions as well as vacuum processes are discussed. This Chapter also gives a short introduction into the preparation and structure of oxide-free and of hydrogen-terminated Si surfaces.

Chapter 3 describes the reaction of neat 1-alkenes with the H-terminated Si(100) surface, which results in the formation of covalently bound monolayers of these compounds on the Si surface. Both functionalized and nonfunctionalized 1-alkenes were used, in order to investigate the possibilities and limitations of the reaction.

An improved method for monolayer preparation, using solutions of 1-alkenes instead of neat 1-alkenes, is described in Chapter 4. The use of dilute solutions would constitute an

important improvement of the original method as used in Chapter 3, because the amount of 1-alkene needed is considerably reduced.

The reaction of 1-alkynes with the H-terminated Si(100) surface is the subject of Chapter 5. The properties of the resulting monolayers are compared to those of the corresponding 1-alkenes. Three-dimensional models show that 1-alkynes can bind to the Si(100) surface in several different ways. Therefore, the exact binding geometry of the 1-alkynes to the Si surface is also investigated.

In Chapter 6 a method is developed to investigate the structure of monolayers of 1-alkenes on H-terminated Si surfaces by molecular modeling simulations. The results of these calculations provide additional information on the structure of the monolayers and the geometry of the molecules in these layers.

A possible application of these monolayers, namely the passivation of Si surfaces, is investigated in Chapter 7. Surface passivation is important in the semiconductor industry and for silicon solar cells, and these monolayers can provide a valuable and relatively cheap alternative for the methods that are currently used. Lifetimes of the minority charge carriers in the modified Si substrates are determined, which gives information on the achieved surface passivation. The modified substrates are also investigated by Kelvin probe measurements.

The preparation of amino-terminated monolayers is described in Chapter 8. A new approach has been developed, which involves the reaction of mixtures of protected amine derivatives and nonfunctionalized 1-alkenes. This is the first method for the preparation of covalently attached amino-terminated monolayers on Si surfaces in which there is complete control over the composition of the monolayers and thus over the surface density of the amino groups.

References and Notes

[1] Sailor, M. J.; Lee, E. J. *Adv. Mater.* **1997**, *9*, 783–793.

[2] Ulman, A. *An Introduction to Ultrathin Organic Films*; Academic Press: Boston, MA, USA, 1991.

[3] Ulman, A. *Chem. Rev. (Washington, DC)* **1996**, *96*, 1533–1554.

[4] Langmuir, I. *J. Am. Chem. Soc.* **1917**, *39*, 1848–1906.

[5] Blodgett, K. B. *J. Am. Chem. Soc.* **1935**, *57*, 1007–1022.

[6] Blodgett, K. B.; Langmuir, I. *Phys. Rev.* **1937**, *51*, 964–982.

[7] Both the term 'silicon oxide', as well as the term 'oxidized silicon' are used in literature. The exact chemical composition of the oxidized layer on top of a silicon wafer is unknown. It is almost certainly not SiO_2, and sometimes referred to as SiO_{2-x}. The term silica is used for SiO_2 powder or plates.

[8] A second reason might be that there was no wet-chemical method for the preparation of organic monolayers directly on oxide-free silicon surfaces, which was first reported in 1993 (see Section 2.3.1). Evidently, these are the "real" organic monolayers on silicon surfaces. However, despite the fact that such layers are now known for several years, the description "monolayers on silicon" is still sometimes used in literature for monolayers on silicon oxide.

[9] Sagiv, J. *J. Am. Chem. Soc.* **1980**, *102*, 92–98.

[10] Netzer, L.; Iscovici, R.; Sagiv, J. *Thin Solid Films*, **1983**, *99*, 235–241.

[11] Netzer, L.; Iscovici, R.; Sagiv, J. *Thin Solid Films*, **1983**, *100*, 67–76.

[12] Pomerantz, M.; Segmüller, A.; Netzer, L.; Sagiv, J. *Thin Solid Films*, **1985**, *132*, 153–162.

[13] Siewierski, L. M.; Brittain, W. J.; Petrash, S.; Foster, M. D. *Langmuir* **1996**, *12*, 5838–5844.

[14] Heid, S.; Effenberger, F.; Bierbaum, K.; Grunze, M. *Langmuir* **1996**, *12*, 2188–2120.

[15] Vallant T.; Kattner, J.; Brunner, H.; Mayer, U.; Hoffmann, H. *Langmuir* **1999**, *15*, 5339–5346.

[16] See, e.g., Angst, D. L.; Simmons, G. W. *Langmuir* **1991**, *7*, 2236–2242.

[17] Bierbaum, K.; Grunze, M.; Baski, A. A.; Chi, L. F.; Schrepp, W.; Fuchs, H. *Langmuir* **1995**, *11*, 2143–2150.

[18] Stevens, M. J. *Langmuir* **1999**, *15*, 2773–2778.

[19] Silberzan, P.; Léger, L.; Ausserré, D.; Benattar, J. J. *Langmuir* **1991**, *7*, 1647–1651.

[20] Wasserman, S. R.; Tao, Y.-T.; Whitesides, G. M. *Langmuir* **1989**, *5*, 1074–1087.

[21] Rye, R. R. *Langmuir* **1997**, *13*, 2588–2590.

[22] Yamada, R.; Wano, H.; Uosaki, K. *Langmuir* **2000**, *16*, 5523–5525.

[23] Nuzzo, R. G.; Allara, D. L. *J. Am. Chem. Soc.* **1983**, *105*, 4481–4483.

[24] Nuzzo, R. G.; Zegarski, B. R.; Dubois, L. H. *J. Am. Chem. Soc.* **1987**, *109*, 733–740.

[25] Nuzzo, R. G.; Fusco, F. A.; Allara, D. L. *J. Am. Chem. Soc.* **1987**, *109*, 2358–2368.

[26] Porter, M. D.; Bright, T. B.; Allara, D. L.; Chidsey, C. E. D. *J. Am. Chem. Soc.* **1987**, *109*, 3559–3568.

[27] Biebuyck, H. A.; Bain, C. D.; Whitesides, G. M. *Langmuir* **1994**, *10*, 1825–1831.

[28] Bain, C. D.; Troughton, E. B.; Tao, Y.-T.; Evall, J.; Whitesides, G. M.; Nuzzo, R. G. *J. Am. Chem. Soc.* **1989**, *111*, 321–335.

[29] Jennings, G. K.; Laibinis, P. E. *Langmuir* **1996**, *12*, 6173–6175.

Chapter 2

Organic Monolayers on Silicon Surfaces

2.1 Silicon and Silicon Surfaces

Silicon was discovered as an element by Berzelius in 1824, when it was isolated as an amorphous, brown powder.[1,2] In 1854 Deville prepared crystalline silicon, which is grey and shows a metallic luster. Silicon is generally prepared by reduction of silica, for which various reductants are possible. The crystal structure is similar to that of diamond, with a Si–Si bond length of 2.34 Å.[3] The unit cell is depicted in Figure 1.

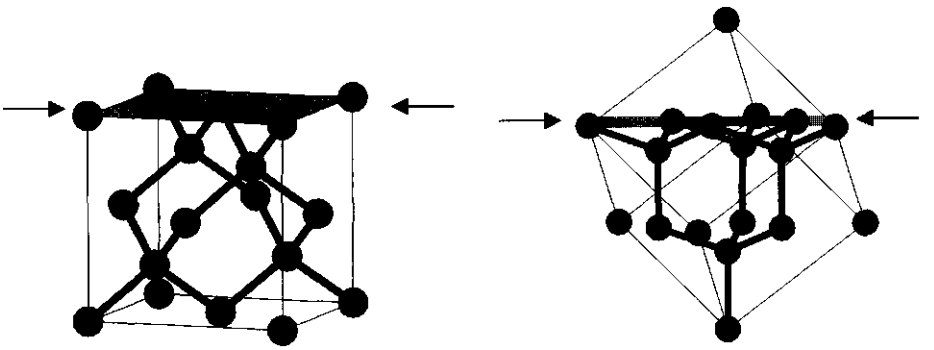

Figure 1. The unit cell of crystalline silicon. Two different orientations are shown, to show a Si(100) and a Si(111) Miller plane (in grey), which are indicated by the arrows (left and right picture, respectively; for an explanation see text).

Upon cleavage of a silicon crystal a large variety of surfaces can be formed. Thus, investigation of the chemical modification of Si surfaces is not possible without some knowledge about the structure of these surfaces. Many different surfaces have been prepared and their structures investigated under ultra-high vacuum (UHV) conditions.[4,5,6] The surfaces are characterized by their Miller indices, which refer to the plane through which the crystal was originally cleaved. This latter point is important, as in some cases the final structure of the resulting surface can differ considerably from that predicted from the Si unit cell, because of rearrangement of the surface atoms.[4,5,6]

The most common Si surface orientations are the Si(100) and the Si(111) surface, and consequently almost all investigations focus on their properties and reactivity. Both surfaces rearrange under UHV conditions. In the case of the Si(100) surface, which is the surface of any side of the unit cell as shown in Figure 1 (structure on the left),[7] the Si surface atoms would end up with two singly occupied sp^3-orbitals (so-called 'dangling bonds'). This situation is energetically unfavorable and results in dimerization of the Si surface atoms. The resulting reorganized surface is called the Si(100)-(2x1) surface. Several different dimerizations are possible, which give rise to different substructures of this (2x1)-reconstructed surface.[4,5,6]

A much more complicated reconstruction occurs for the Si(111) surface, which is formed upon cleavage of the Si unit cell through a plane perpendicular to one of the diagonals of the box, i.e., by horizontally cutting the structure on the right in Figure 1. This Si(111) surface should consist of a double-layered structure, in which each Si atom has three bonds to atoms in the other layer and one bond to an atom in a different layer. Consequently, the Si atoms at the top layer would have one dangling bond perpendicular to the Si surface. However, this Si(111) surface rearranges into the highly complicated Si(111)-(7x7) surface, which consists of a structure with 102 Si atoms in a four-layered system.[4,5,6,8,9]

2.2 Hydrogen-Terminated Si Surfaces

2.2.1 Adsorption of Hydrogen on Clean Si Surfaces

The adsorption of atomic hydrogen on silicon surfaces under ultra-high vacuum conditions has been studied extensively.[4,6] In general, complete saturation of all the dangling bonds on the Si surface occurs. On the Si(111) surface, the structure of the H-terminated surface strongly depends on the coverage, i.e., on the amount of hydrogen that has reacted

with the Si surface. At the early stages of hydrogen adsorption the Si(111)-(7x7) surface does not reconstruct, however, at higher coverage reorganization of the Si atoms occurs. This leads to a variety of complex surface structures. For more information the reader is referred to references 4 and 6.

In the case of the Si(100) surface the situation is more clear. Only three different structures are formed, again depending on the reaction conditions used.[4,6] Formation of the (2x1)-monohydride phase (Figure 2a) is the most evident process, as this does not require a reconstruction of the Si dimers that are present on the clean Si(100) surface (*vide supra*). Each Si surface atom is saturated by one hydrogen atom. However, formation of a dihydride phase (the (1x1) structure; Figure 2b) is also possible. This is the surface that would be formed if all dangling bonds on the unreconstructed Si(100) surface would be saturated with hydrogen atoms. Besides these two surfaces with only one type of Si–H groups, a 1 : 1 mixed surface of the two structures can also be formed, which is called the (3x1) structure (Figure 2c). On this surface, alternating rows are formed of the monohydride and dihydride groups.

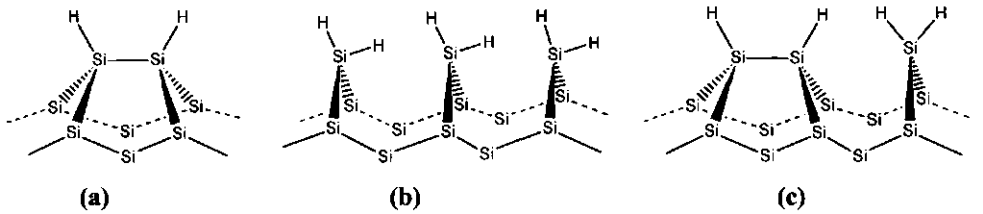

(a) **(b)** **(c)**

Figure 2. (a) The H-terminated Si(100)-(2x1) surface. (b) The H-terminated Si(100)-(1x1) surface. (c) The H-terminated Si(100)-(3x1) surface.

2.2.2 Wet-Chemical Preparations of Hydrogen-Terminated Si Surfaces

Hydrogen-terminated Si surfaces can also be prepared by dissolution of the native oxide in fluoride-containing aqueous solutions. This process is called etching of silicon and results in the formation of the H-terminated Si surface according to a series of reactions as schematically depicted in Figure 3.[10,11,12] After formation of the H-terminated Si surface, fluoride ions continue to break Si–Si bonds, which means the etching process does not stop, and new Si–F groups are formed. As a result, etching times are as important as the F^- concentration.

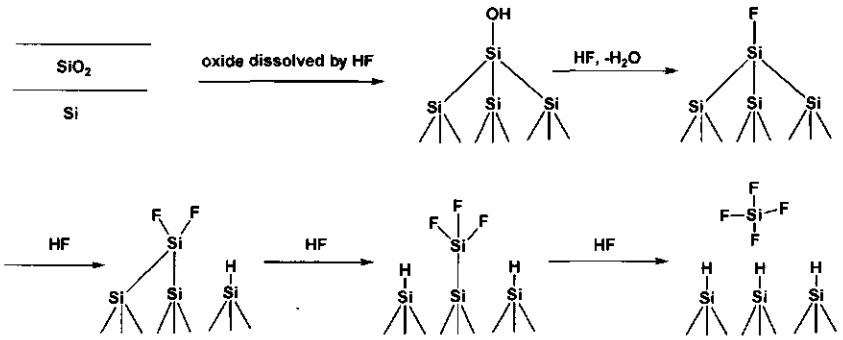

Figure 3. Reaction of fluoride solutions with a Si/SiO_2 surface, resulting in the formation of the H-terminated Si surface.

The actual structure of the H-terminated Si surface that is formed depends not only on the type of Si surface (i.e., Si(111), Si(100), or some other Si surface), but also on the pH of the solution. For the Si(111) surface the so-called "ideal" H-terminated Si(111) surface is usually formed by etching in 40% NH_4F solutions in water (pH = 7.8),[13,14] or by reaction of a HF-treated Si(111) surface with boiling water.[15,16] A flat Si surface is formed, with terraces >100 Å,[17,18] on which each Si surface atom is occupied by only one hydrogen atom. In other words, all dangling bonds of the unreconstructed Si(111) surface, as would be obtained directly after cleavage of the Si crystal (see Section 2.1), are simply saturated with hydrogen atoms. The use of buffered fluoride solutions (usually mixtures of NH_4F and HF)[18,19,20] or HF solutions[17,18,21] results in the formation of a rougher surface with smaller terraces. The "ideal" H-terminated Si(111) surface is depicted in Figure 4a.

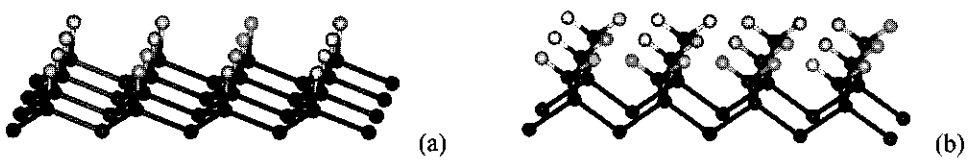

Figure 4. (a) The H-terminated Si(111) surface. (b) The H-terminated Si(100) surface.

In the case of the H-terminated Si(100) surface the corresponding "ideal" H-terminated surface would be that on which each Si surface atom is saturated with two hydrogen atoms (Figure 4b). This surface is identical to the dihydride surface that is obtained

under high-vacuum conditions (the H-terminated Si(100)-(1x1) surface, see Figure 2b). The formation of this surface under wet-chemical conditions has indeed been reported, using a 19 : 1 mixture (v/v) of concentrated HCl and HF.[22] However, the structure of the resulting surface still was not as perfect as for the Si(111) surface. In practice, Si(100) surfaces are etched in dilute HF solutions. This results in the formation of a surface that is mainly occupied with SiH_2 groups, but that also contains considerable amounts of SiH and SiH_3 groups.[20,21] Consequently, the H-terminated Si(100) surface is not atomically flat.

The use of other etching conditions has been investigated, but this does not lead to a flatter Si(100) surface, i.e., with a higher percentage of SiH_2 groups at the surface. In concentrated HF the amount of fluoride groups on the surface increases.[23] In buffered solutions formation of Si(111) facets starts to occur, a process which becomes more important in NH_4F solutions.[20,24] This is the result of two effects: the etch rates along the various directions are not equal,[18,24,25] and the H-terminated Si(111) surface is thermodynamically the most stable surface under these conditions.[20,25]

A special form of H-terminated silicon is porous silicon. This is generally prepared by galvanostatic etching or chemical corrosion of crystalline Si,[26] which results in the formation of a layer of porous, H-terminated material on the Si surface. The structure of this irregular layer is highly complex and consists of mono-, di-, and trihydride groups and Si nanocrystallites. A schematic representation of the H-terminated Si surface in this porous material is shown in Figure 5. The presence of the SiH_2 and SiH_3 groups makes the reactivity of porous silicon somewhat comparable to that of the H-terminated Si(100) surface. Porous Si has an interesting property, as, unlike crystalline Si, it is photoluminescent.[26]

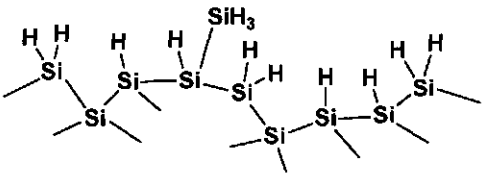

Figure 5. Schematic representation of a porous silicon surface.

2.2.3 Stability of Hydrogen-Terminated Si Surfaces

None of the H-terminated Si surfaces is stable in air at ambient temperature. Oxidation of the surface occurs in the presence of oxygen, as this reaction regenerates a silicon oxide

layer on the Si surface, which is thermodynamically the most stable situation. The oxidation is catalyzed by the presence of water.[27,28] The first steps involve the back-side oxidation of the Si–Si bonds to Si–O–Si bonds.[29] The last step is the oxidation of the resulting O_3Si–H groups to O_3Si–OH groups.[28,29,30]

The rate of the oxidation reactions is strongly influenced by all kind of factors. In the case of the crystalline H-terminated Si surfaces, formation of a monolayer of silicon oxide has been reported to take anywhere from one hour[27,28,30] to a week,[29,31] or even up to a month.[32] The silicon oxide growth strongly depends on several factors, like the type of surface (Si(111) or Si(100)),[28,30] the environmental conditions (e.g., humidity),[30] and the etching conditions.[28,29] For porous silicon the same factors influence the oxidation, however, an additional factor for this material is the adsorption of (organic) contaminants in the pores.[26]

2.3 Covalently Bound Organic Monolayers on Si Surfaces

2.3.1 Alkenes and Alkynes on Hydrogen-Terminated Si Surfaces

In 1993 Linford and Chidsey reported the first wet-chemical preparation of organic monolayers that were covalently bound to crystalline Si surfaces without an intermediate oxide layer.[33] Pyrolysis of diacyl peroxides at 100 °C in the presence of a H-terminated Si surface gave stable, well-ordered monolayers, that were linked to the surface via a covalent Si–C bond and inhibited the oxidation of the Si surface. Soon after the reaction was shown to work equally well with mixtures of 1-alkenes and diacylperoxides.[34,35] Deuterium labeling experiments showed that the latter compounds mainly serve as initiator for the monolayer formation and that most of the surface-bound alkyl chains originate from the 1-alkene. It was proposed[34] that the acyl radicals (R–C(O)O·) that are formed due to thermal cleavage of the peroxide bond generate Si radical sites on the H-terminated Si surface by hydrogen abstraction, which subsequently react with a 1-alkene to form a covalent Si–C bond between the Si radical and the terminal carbon atom of the 1-alkene. This generates a carbon-centered radical, which can abstract a hydrogen atom from a neighboring Si surface atom, which generates a new site for binding of a 1-alkene (Figure 6). Recent investigations suggested a more active role of the solvent,[36] but this hypothesis is rather doubtful (see Chapters 5 and 6).

Control experiments with neat 1-alkenes showed that the monolayers could also be formed without a radical initiator, though higher temperatures were needed (200 °C) to obtain monolayers that were of similar quality as those prepared with diacylperoxides as the

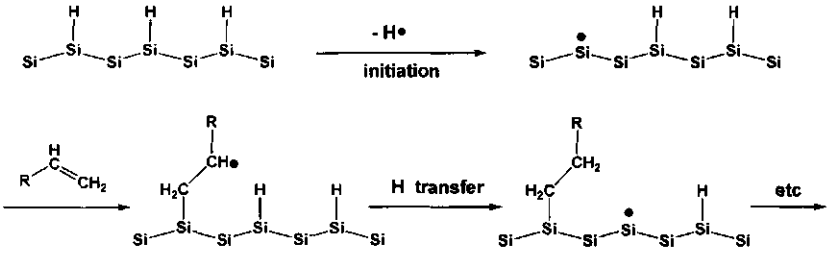

Figure 6. Proposed mechanism for the formation of monolayers in the reaction of 1-alkenes with H-terminated Si surfaces.[34]

initiator.[34,37] The advantage of the reaction with neat 1-alkenes over that with the peroxide initiator was that in the latter case the acyl radicals themselves also reacted with the Si surface, to give Si–O–C(O)–R structures. These siloxane esters are susceptible to hydrolysis, as was demonstrated by heating such monolayers in the presence of water.[34] Thus, their presence is undesirable, and yields defects in the monolayer. In addition, diacylperoxides are thermally explosive compounds.

The reaction can also be initiated by UV light, which cleaves the Si–H groups on the surface. The quality of the monolayers of 1-alkenes prepared by this method is comparable to those prepared by the thermal reaction,[38,39,40,41] and the procedure can be used for photopatterning of the organic monolayer on the Si surface, as only the illuminated areas react. The reaction also works for ω-functionalized alkenes.[42,43]

The reaction of 1-alkenes with porous silicon has also been explored.[44,45] In this case the thermal reaction as employed for the crystalline Si surfaces is not used often,[46] as it is not completely compatible with the delicate structure of the Si material. The high reaction temperatures generally cause the complete loss of the photoluminescent properties of the porous silicon.[47] Therefore alternative strategies are used, which are either based on Lewis acid-catalyzed reactions or on photochemical initiation.

In the Lewis acid-based modification of porous Si a catalytic amount of a Lewis acid, usually ethylaluminum dichloride (CH_3CH_2–$AlCl_2$), is added.[47,48,49] This well-known type of catalysis is frequently used in organic solution chemistry, i.e., in the hydrosilylation of 1-alkenes.[50,51] Although other catalysts (Rh(I)- and Pd(II)-based) can be used as well, the aluminum derivative has been found to give the best results.[49] A large variety of alkenes has been used, including ω-functionalized derivatives[47,48] and internal alkenes (i.e., 2-alkenes, tri-, and tetrasubstituted alkenes).[47,48,49] The functionalized derivatives give good results, with

packing densities that are comparable to the nonfunctionalized alkenes, provided that the functional groups are compatible with the reaction.[47] The internal alkenes give considerably lower surface coverage, due to steric hindrance between the surface-bound molecules.[47] The Al-catalyzed reaction has also been applied to crystalline Si surfaces, however, the packing density of the alkyl chains was found to be considerably lower compared to the monolayers prepared by the thermal reaction.[40] This reaction has also been shown to work with a Pt(0)-catalyst.[52]

Porous silicon also reacts with 1-alkenes by photochemical initiation.[53] Unlike for crystalline Si, where UV light is required,[39,41] this reaction can be performed using white light. The reason for this difference is not clear, but it suggests that on porous Si the reaction mechanism does not involve the direct photochemical cleavage of the surface Si–H bonds, as the energy of white light is insufficient to accomplish this reaction.[39,41] Just as for the crystalline surfaces, the 1-alkene is only bound to those areas which have been illuminated.

The surface modification has also been explored for 1-alkynes,[44,45] which react similarly to the analogous 1-alkenes in the case of the peroxide-catalyzed,[34] photochemical,[41,53] or Lewis acid-catalyzed reaction.[47,48,49] Only one Si–C bond is formed per reacting molecule, which means that a C=C double bond remains near the surface. Interestingly, the thermal reaction of 1-alkynes with porous Si seems to give two Si–C bonds per molecule, as, unlike in the case of the above mentioned situations, no C=C stretching vibrations could be detected with IR spectroscopy.[46]

2.3.2 Grignard Reagents on Hydrogen-Terminated Si Surfaces

Alkyl magnesium (Grignard) and alkyl lithium reagents can react with H-terminated Si surfaces, forming covalent Si–C bonds. Reaction of 1-decylmagnesium bromide with the Si(111) surface was found to give Si–C bonded monolayers that were as ordered as monolayers of 1-decene prepared using UV irradiation.[40] The mechanism for the reaction is not known, but is likely different from that of the comparable reaction that occurs on porous Si (vide infra).

On porous silicon the reaction has been shown to work either with[54] or without[55,56,57,58,59] an external electrical bias, via different reaction mechanisms. In the reaction with an electronic bias the Si–H groups on the surface are consumed and Si–alkyl groups are formed.[54] A methyl-terminated Si surface was obtained, using either methyl lithium or methyl magnesium derivatives. Without an electronic bias a different reaction occurs. Compounds of the general structure R–M, in which R = alkyl,[55,56,57,58] aryl,[59] or

alkynyl[59] and M = Li or MgBr, have all been shown to react with porous silicon surfaces. The Si–Si bonds at the surface are cleaved and both the organic moiety R as well as the metal ion M bind to the Si surface (Figure 7), which means that in this case no Si–H groups are consumed. The Si–M bonds, in which the Si atom is partially negatively charged, can subsequently be reacted with electrophilic reagents E–X, which results in binding of the electrophile to the surface. Several different electrophiles, like protons and acyl groups,[57,59] have been used successfully.

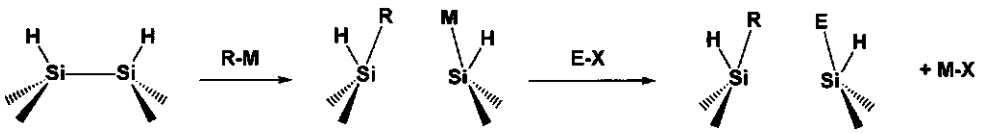

Figure 7. Reaction of Grignard reagents with porous silicon without an electronic bias.

2.3.3 Grignard Reagents on Halogen-Terminated Si Surfaces

Alkyl magnesium and alkyl lithium derivatives can also react with halogen-terminated Si surfaces. Ordered monolayers, that inhibit oxidation of the underlying Si surface, were obtained using a Cl-terminated Si(111) surface (Figure 8).[60,61,62] It was found that the quality of the monolayer depends on the length of the alkyl chain of the molecule.[61] Alkyl chains up to a length of six CH_2 groups give monolayers that are more densely packed (replacing most but not all Cl atoms on the surface) compared to monolayers of longer derivatives, as evidenced from changes in the wettability of these latter layers. 2-Lithiothiophenes have been bound to the surface via the same procedure, using a Br-terminated Si(111) surface.[63]

The reaction has also been used to confirm the formation of the covalent Si–C bond in a comparative study of monolayers of methyl lithium on Cl-terminated Si(111) and monolayers of 1-alkenes on H-terminated Si(111). Both the results from X-ray Photoelectron Spectroscopy (XPS)[38] and core-level Photoelectron Emission Spectroscopy (PES)[64] showed the formation of a Si–C bond between the Si surface and the organic reagent.

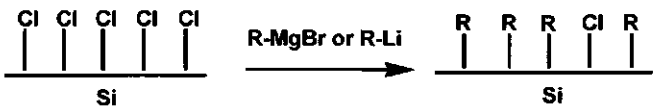

Figure 8. Schematic of the reaction of Grignard reagents with Cl-terminated Si surfaces.

2.3.4 Adsorption of Organic Compounds on Clean Si Surfaces

The physisorption and chemisorption of organic compounds on clean Si surfaces under ultra-high vacuum conditions has been studied extensively,[4,6] because these reactions are a major source for the contamination of these Si surfaces, and because they are used for the preparation of silicon carbide (SiC) layers.

n-Alkanes do not react with the Si surface, but only show physisorption at low temperatures (< 100 K).[65,66] At higher temperatures the compounds desorb from the surface. In contrast, branched alkanes do react with the Si surface.[65] A fraction of the material that is physisorbed binds dissociatively to the surface at low temperatures, which means that covalent Si–C bonds are formed between the surface and the organic compound. Upon heating of the substrate, these chemisorbed derivatives can decompose, leaving Si–$(CH_x)_y$ groups (x = 0–3, y = 1–3) on the surface.

Unsaturated hydrocarbons, i.e., alkenes, alkynes, and dienes, as well as aromatic compounds (benzene) have all been shown to react with the Si radical sites on clean Si surfaces, which leads to the formation of covalent Si–C bonds between the organic molecule and the Si surface. Much of this work has been reviewed,[4,6] however, many new developments in this field have occurred over the last years.

Relatively little work has been done on the reactivity of unsaturated organic compounds on the Si(111)-(7x7) surface, most likely because of the complex structure of this surface (see Section 2.1). Only the reactions of ethylene,[67,68] acetylene,[69,70] and benzene[71,72,73] have been studied. In general, the organic compound makes one Si–C bond to one of the so-called Si adatoms of the Si(111)-(7x7) surface, which form the top layer of this surface, and a second bond to a close-by Si surface atom in one of the lower-lying layers.

Far more information is available on the chemisorption of unsaturated compounds on the Si=Si dimers of the Si(100)-(2x1) surface. Alkenes give an addition reaction with these dimers, which can formally be considered as a [2+2] cycloaddition. This leads to the formation of two Si–C bonds per reacting molecule (Figure 9a).[65,74,75,76,77,78,79,80] It was generally believed that acetylenes reacted in the same way,[81,82,83] however, it has recently been shown that these derivatives form four Si–C bonds to the surface (Figure 9b).[84]

Unsaturated organic compounds with more than one C=C bond also react with the Si(100) surface. In the case of 1,3-dienes (cyclic and noncyclic), in which the organic compound has two C=C double bonds that are conjugated, both [2+2] and [4+2] cycloadditions have been reported.[85,86,87,88,89,90,91] The [2+2] cycloaddition is analogous to the reaction of nonconjugated alkenes, which means that one double bond reacts with the Si

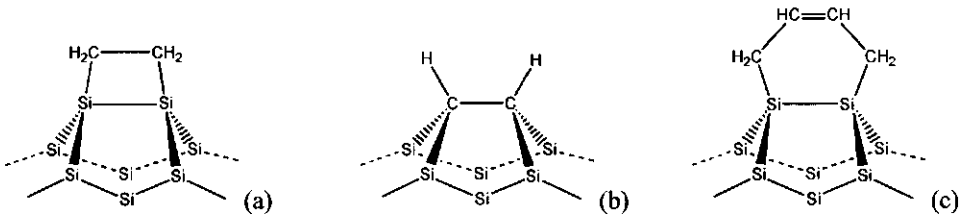

Figure 9. (a) Ethene bound to the Si(100) surface. (b) Ethyne bound to the Si(100) surface. (c) The [4+2] cycloaddition of butadiene on the Si(100) surface.

surface and the other double bond in the compound remains intact. In the [4+2] cycloaddition both double bonds react with one Si=Si dimer, i.e., a Diels-Alder type of reaction occurs, which gives structures as shown in Figure 9c. For nonconjugated dienes the reactivity depends on the three-dimensional structure of the compound. If, after the first C=C bond has reacted with a Si=Si dimer on the surface, the second C=C bond can easily react with another Si=Si dimer, this will occur.[92,93] If this second reaction step becomes complicated, e.g., because the C=C bond can not reach a Si=Si dimer due to steric problems, this C=C double bond does not react and thus remains intact.[90,93,94] A cyclic polyene (1,3,5,7-cyclooctatetraene) has also been investigated and for this molecule two out of four C=C bonds bind to the surface.[95,96]

Finally, benzene has also been shown to give chemisorption reactions with the Si(100)-(2x1) surface.[97,98] Two covalent σ-type Si–C bonds are formed, implying that the aromaticity is lost. This loss of aromaticity also occurs for the chemisorption of benzene on the Si(111)-(7x7) surface.[73]

2.3.5 Other Reactions of Organic Compounds with Oxide-Free Si Surfaces

There is a large variety of other reactions that leads to the covalent binding of organic molecules on Si surfaces. Regarding the ultra-high vacuum reactions, methyl iodide is known to adsorb dissociatively on clean Si surfaces, which results in the formation of CH_3 groups bound to the surface.[99] In contrast, methyl chloride seems to give CH_2Cl type species bound to the surface.[100] Organic amines,[101,102,103] azo compounds,[104] alcohols,[105] and acids[101,106] are also known to react, though this generally results in the formation of Si–N or Si–O linked species, instead of in the formation of Si–C bonds. A remarkable reaction occurs for C=O bonds in aldehydes and ketones, which give a [2+2]-type cycloaddition to the Si=Si dimers of the Si(100)-(2x1) surface, i.e., both a Si–O and a Si–C bond are formed simultaneously.[107]

Acetaldehyde has also been chemisorbed on the Si(111)-(7x7) surface,[108] however, the precise structure of this modified surface is unknown. This [2+2]-type of cycloaddition to the Si surface has also been found for phenyl isothiocyanate (C_6H_5–N=C=S), which gives selective addition of the C=N bond to the Si=Si dimers.[109]

Alternative wet-chemical functionalization strategies are also available. Alkylamines react with Cl-terminated porous Si surfaces to give Si–N linked species.[102] Alcohols react with H-terminated Si surfaces, which leads to Si–O–R linked monolayers.[110,111,112] Acids can react under various conditions with H-terminated Si surfaces to give siloxane esters.[113,114,115] This addition reaction also occurs on Si surfaces that are mainly terminated with Si–F groups (Si(111) etched in 50% HF).[116,117,118] Aldehydes react with H-terminated surfaces under illumination with UV-light, to give again Si–O–R linked monolayers.[39] These surface modifications usually give ordered monolayers. However, as mentioned before (see Section 2.3.1), the drawback of all these Si–O and Si–N linked monolayers is that these bonds can be easily hydrolyzed, which limits the application of such systems in semiconductor technology.

A more interesting reaction is the electrochemical attachment of benzene diazonium salts on H-terminated Si surfaces,[119] as this reaction does result in the formation of covalent Si–C bonds between the organic compound and the Si surface. Nitrogen gas is eliminated from the organic compound after uptake of an electron, and the remaining phenyl radicals bind to the surface. A monolayer of phenyl groups can thus be prepared on the surface, also if functionalized aromatics are used. A similar reaction occurs for alkyl and benzyl halides, which have been bound to porous silicon by electrochemical reduction.[120] Both functional and nonfunctional derivatives could be used. In a control experiment the reaction was also applied to a crystalline surface, which showed the same reactivity. However, no analytical data were given for this monolayer, thus the packing density (= the monolayer quality) is not known.

Finally, the formation of covalent Si–C bonds also occurs in the reaction of fullerenes with Si surfaces. This modification can be performed either under high-vacuum conditions on clean[121] or H-terminated[122] Si surfaces, or by wet-chemical treatment of H-terminated Si surfaces.[123]

References and Notes

[1] Gunning, J. W. *De Beginselen der Algemeene Scheikunde*, Deel I; S. E. van Nooten: Schoonhoven, the Netherlands, 1873, p 320–326.

[2] *Handbook of Chemistry and Physics*, 80th ed.; CRC Press, Inc.: Boca Raton, FL, USA, 1999, p 4-26–4-27.

[3] Cotton, F. A.; Wilkinson, G.; Murillo, C. A.; Bochman, M. *Advanced Inorganic Chemistry*, 6th ed.; John Wiley & Sons: New York, NY, USA, 1999, p 259.

[4] Neergaard Waltenburg, H.; Yates, J. T., Jr. *Chem. Rev. (Washington, DC)* **1995**, *95*, 1589–1673.

[5] Duke, C. B. *Chem. Rev. (Washington, DC)* **1996**, *96*, 1237–1259.

[6] Hamers, R. J.; Wang, Y. *Chem. Rev. (Washington, DC)* **1996**, *96*, 1261–1290.

[7] The sides of the unit cell of the Si crystal are all equal, which means that the surfaces of the unit cell, which are indicated by Si(100), Si(010), and Si(001), are also identical. The indication Si(100) is generally used in literature, though Si(001) sometimes occurs as well.

[8] Takayanagi, K.; Tanishiro, Y.; Takahashi, S.; Takahashi, M. *Surf. Sci.* **1985**, *164*, 367–392.

[9] Kádas, K.; Kugler, S.; Náray-Szabó, G. *J. Phys. Chem.* **1996**, *100*, 8462–8467.

[10] Trucks, G. W.; Raghavachari, K.; Higashi, G. S.; Chabal, Y. J. *Phys. Rev. Lett.* **1990**, *65*, 504–507.

[11] Hoshino, T.; Nishioka, Y. *J. Chem. Phys.* **1999**, *111*, 2109–2114.

[12] Knotter, D. M. *J. Am. Chem. Soc.* **2000**, *122*, 4345–4351.

[13] Higashi, G. S.; Chabal, Y. J.; Trucks, G. W.; Raghavachari, K. *Appl. Phys. Lett.* **1990**, *56*, 656–658.

[14] Jakob, P.; Chabal, Y. J.; Raghavachari, K.; Dumas, P.; Christman, S. B. *Surf. Sci.* **1993**, *285*, 251–258.

[15] Watanabe, S.; Nakayama, N.; Ito, T. *Appl. Phys. Lett.* **1991**, *59*, 1458–1460.

[16] Watanabe, S.; Horiuchi, K.; Ito, T. *Jpn. J. Appl. Phys.* **1993**, *32*, 3420–3425.

[17] Higashi, G. S.; Becker, R. S.; Chabal, Y. J.; Becker, A. J. *Appl. Phys. Lett.* **1991**, *58*, 1656–1658.

[18] Pietsch, G. J.; Köhler, U.; Henzler, M. *J. Appl. Phys.* **1993**, *73*, 4797–4807.

[19] Jakob, P.; Chabal, Y. J. *J. Chem. Phys.* **1991**, *95*, 2897–2909.

[20] Dumas, P.; Chabal, Y. J. *Surf. Sci.* **1992**, *269/270*, 867–878.

[21] Chabal, Y. J.; Higashi, G. S.; Raghavachari, K.; Burrows, V. A. *J. Vac. Sci. Technol. A* **1989**, *7*, 2104–2109.

[22] Morita, Y.; Tokumoto, H. *Appl. Phys. Lett.* **1995**, *67*, 2654–2656.

[23] Schlaf, R.; Hinogami, R.; Fujitani, M.; Yae, S.; Nakato, Y. *J. Vac. Sci. Technol. A* **1999**, *17*, 164–169.

[24] Neuwald, U.; Hessel, H. E.; Feltz, A.; Memmert, U.; Behm, R. J. *Surf. Sci. Lett.* **1993**, *296*, L4–L14.

[25] Kasparian, J.; Elwenspoek, M.; Allongue, P. *Surf. Sci* **1997**, *388*, 50–62.

[26] For an excellent review on porous Si, see: Cullis, A. G.; Canham, L. T.; Calcott, P. D. J. *J. Appl. Phys.* **1997**, *82*, 909–965.

[27] Morita, M.; Ohmi, T.; Hasegawa, E.; Kawakami, M.; Ohwada, M. *J. Appl. Phys.* **1980**, *68*, 1272–1281.

[28] Niwano, M.; Kageyama, J.-i.; Kurita, K.; Kinashi, K.; Takahashi, I.; Miyamoto, N. *J. Appl. Phys.* **1994**, *76*, 2157–2163.

[29] Kluth, G. J.; Maboudian, R. *J. Appl. Phys.* **1996**, *80*, 5408–5414.

[30] Miura, T.-a.; Niwano, M.; Shoji, D.; Miyamoto, N. *J. Appl. Phys.* **1996**, *79*, 4373–4380

[31] Gräf, D.; Grundner, M.; Schulze, R.; Mühlhoff, L. *J. Appl. Phys.* **1990**, *68*, 5155–5161.

[32] Olsen, J. E.; Shimura, F. *J. Vac. Sci. Technol. A* **1989**, *7*, 3275–3278.

[33] Linford, M. R.; Chidsey, C. E. D. *J. Am. Chem. Soc.* **1993**, *115*, 12631–12632.

[34] Linford, M. R.; Fenter, P.; Eisenberger, P. M.; Chidsey, C. E. D. *J. Am. Chem. Soc.* **1995**, *117*, 3145–3155.

[35] Linford, M. R.; Chidsey, C. E. D. *US Patent 5429708* (July 4, 1995).

[36] Bateman, J. E.; Eagling, R. D.; Horrocks, B. R.; Houlton, A. *J. Phys. Chem. B* **2000**, *104*, 5557–5565.

[37] Sung, M. M.; Kluth, G. J.; Yauw, O. W.; Maboudian, R. *Langmuir* **1997**, *13*, 6164–6168.

[38] Terry, J.; Linford, M. R.; Wigren, C.; Cao, R.; Pianetta, P.; Chidsey, C. E. D. *Appl. Phys. Lett.* **1997**, *71*, 1056–1058.

[39] Effenberger, F.; Götz, G.; Bidlingmaier, B.; Wezstein, M. *Angew. Chem., Int. Ed. Engl.* **1998**, *37*, 2462–2464.

[40] Boukherroub, R.; Morin, S.; Bensebaa, F.; Wayner, D. D. M. *Langmuir* **1999**, *15*, 3831–3835.

[41] Cicero, R. L.; Linford, M. R.; Chidsey, C. E. D. *Langmuir* **2000**, *16*, 5688–5695.

[42] Boukherroub, R.; Wayner, D. D. M. *J. Am. Chem. Soc.* **1999**, *121*, 11513–11515.

[43] Strother, T.; Cai, W.; Zhao, X.; Hamers, R. J.; Smith, L. M. *J. Am. Chem. Soc.* **2000**, *122*, 1205–1209.

[44] Buriak, J. M. *Chem. Commun.* **1999**, 1051–1060.

[45] Stewart, M. P.; Buriak, J. M. *Adv. Mater.* **2000**, *12*, 859–869.

[46] Bateman, J. E.; Eagling, R. D.; Worrall, D. R.; Horrocks, B. R.; Houlton, A. *Angew. Chem., Int. Ed. Engl.* **1998**, *37*, 2683–2685.

[47] Buriak, J. M.; Stewart, M. P.; Geders, T. W.; Allen, M. J.; Choi, H. C.; Smith, J.; Raftery, D.; Canham, L. T. *J. Am. Chem. Soc.* **1999**, *121*, 11491–11502.

[48] Buriak, J. M.; Allen, M. J. *J. Am. Chem. Soc.* **1998**, *120*, 1339–1340.

[49] Holland, J. M.; Stewart, M. P.; Allen, M. J.; Buriak, J. M. *J. Solid State Chem.* **1999**, *147*, 251–258.

[50] Lukevics, E. *Russ. Chem. Rev. (Engl. Transl.)* **1977**, *46*, 264–277.

[51] Speier, J. L. *Adv. Organomet. Chem.* **1979**, *17*, 407–477.

[52] Zazzera, L. A.; Evans, J. F.; Deruelle, M.; Tirrell, M.; Kessel, C. R.; McKeown, P. *J. Electrochem. Soc.* **1997**, *144*, 2184–2189.

[53] Stewart, M. P.; Buriak, J. M. *Angew. Chem., Int. Ed. Engl.* **1998**, *37*, 3257–3260.

[54] Veillard, C.; Warntjes, M.; Oxaham, F.; Chazalviel, J.-N. *Proc. Electrochem. Soc.* **1996**, *95*, 250–258.

[55] Kim, N. Y.; Laibinis, P. E. *J. Am. Chem. Soc.* **1998**, *120*, 4516–4517.

[56] Kim, N. Y.; Laibinis, P. E. *J. Am. Chem. Soc.* **1999**, *121*, 7162–7163.

[57] Song, J. H.; Sailor, M. J. *Inorg. Chem.* **1999**, *38*, 1498–1503.

[58] Vermeir, I. E.; Kim, N. Y.; Laibinis, P. E. *Appl. Phys. Lett.* **1999**, *74*, 3860–3862.

[59] Song, J. H.; Sailor, M. J. *J. Am. Chem. Soc.* **1998**, *120*, 2376–2381.

[60] Bansal, A.; Li, X.; Lauerman, I.; Lewis, N. S.; Yi, S. I.; Weinberg, W. H. *J. Am. Chem. Soc.* **1996**, *118*, 7225–7226.

[61] Bansal, A.; Lewis, N. S. *J. Phys. Chem. B* **1998**, *102*, 1067–1070.

[62] Bansal, A.; Lewis, N. S. *J. Phys. Chem. B* **1998**, *102*, 4058–4060.

[63] He, J.; Patitsas, S. N.; Preston, K. F.; Wolkow, R. A.; Wayner, D. D. M. *Chem. Phys. Lett.* **1998**, *286*, 508–514.

[64] Terry, J.; Linford, M. R.; Wigren, C.; Cao, R.; Pianetta, P.; Chidsey, C. E. D. *J. Appl. Phys.* **1999**, *85*, 213–221.

[65] Bozack, M. J.; Taylor, P. A.; Choyke, W. J.; Yates, J. T., Jr. *Surf. Sci.* **1986**, *177*, L933–L937.

[66] Simons, J. K.; Frigo, S. P.; Taylor, J. W.; Rosenberg, R. A. *Surf. Sci.* **1996**, *346*, 21–30.

[67] Yoshinobu, J.; Tsuda, H.; Onchi, M.; Nishijima, M. *Solid State Commun.* **1986**, *60*, 801–805.

[68] Rochet, F.; Jolly, F.; Bournel, F.; Dufour, G.; Sirotti, F.; Cantin, J. L. *Phys. Rev. B* **1998**, *58*, 11029–11042.

[69] Chung, Y. W.; Siekhaus, W.; Somorjai, G. A. *Surf. Sci.* **1976**, *58*, 341–348.

[70] Yoshinobu, J.; Fukushi, D.; Uda, M.; Nomura, E.; Aono, M. *Phys. Rev. B* **1992**, *46*, 9520–9524.

[71] Taguchi, Y.; Fujisawa, M.; Nishijima, M. *Chem. Phys. Lett.* **1991**, *178*, 363–368.

[72] Brown, D. E.; Moffatt, D. J.; Wolkow, R. A. *Science* **1998**, *279*, 542–544.

[73] Cao, Y.; Wei, X. M.; Chin, W. S.; Lai, Y. H.; Deng, J. F.; Bernasek, S. L.; Xu, G. Q. *J. Phys. Chem. B* **1999**, *103*, 5698–5702.

[74] Bozack, M. J.; Taylor, P. A.; Choyke, W. J.; Yates, J. T., Jr. *Surf. Sci.* **1987**, *179*, 132–142.

[75] Liu, H.; Hamers, R. J. *J. Am. Chem. Soc.* **1997**, *119*, 7593–7594.

[76] Clemen, L.; Wallace, R. M.; Taylor, P. A.; Dresser, M. J.; Choyke, W. J.; Weinberg, W. H.; Yates, J. T., Jr. *Surf. Sci.* **1992**, *268*, 205–216.

[77] Hamers, R. J.; Hovis, J. S.; Lee, S.; Liu, H.; Shan, J. *J. Phys. Chem. B* **1997**, *101*, 1489–1492.

[78] Padowitz, D. F.; Hamers, R. J. *J. Phys. Chem. B* **1998**, *102*, 8541–8545.

[79] Lopinski, G. P.; Moffatt, D. J.; Wayner, D. D. M.; Zgierski, M. Z.; Wolkow, R. A. *J. Am. Chem. Soc.* **1999**, *121*, 4532–4533.

[80] Lopinski, G. P.; Moffatt, D. J.; Wayner, D. D. M.; Wolkow, R. A. *J. Am. Chem. Soc.* **2000**, *122*, 3548–3549.

[81] Cheng, C. C.; Wallace, R. M.; Taylor, P.A.; Choyke, W. J.; Yates, J. T., Jr. *J. Appl. Phys.* **1990**, *67*, 3693–3699.

[82] Taylor, P. A.; Wallace, R. M.; Cheng, C. C.; Weinberg, W. H.; Dresser, M. J.; Choyke, W. J.; Yates, J. T., Jr. *J. Am. Chem. Soc.* **1992**, *114*, 6754–6760.

[83] Liu, Q.; Hoffmann, R. *J. Am. Chem. Soc.* **1995**, *117*, 4082–4092.

[84] Zu, S. H.; Keeffe, M.; Yang, Y.; Chen, C.; Yu, M.; Lapeyre, G. J.; Rotenberg, E.; Denlinger, J.; Yates, J. T., Jr. *Phys. Rev. Lett.* **2000**, *84*, 939–942.

[85] Konecny, R.; Doren, D. J. *J. Am. Chem. Soc.* **1997**, *119*, 11098–11099.

[86] Teplyakov, A. V.; Kong, M. J.; Bent, S. F. *J. Am. Chem. Soc.* **1997**, *119*, 11100–11101.

[87] Teplyakov, A. V.; Kong, M. J.; Bent, S. F. *J. Chem. Phys.* **1998**, *108*, 4599–4606.

[88] Hovis, J. S.; Liu, H.; Hamers, R. J. *J. Phys. Chem. B* **1998**, *102*, 6873–6879.

[89] Choi, C. H.; Gordon, M. S. *J. Am. Chem. Soc.* **1999**, *11*, 11311–11317.

[90] Cao, Y.; Yong, K. S.; Wang, Z. Q.; Chin, W. S.; Lai, Y. H.; Deng, J. F.; Xu, G. Q. *J. Am. Chem. Soc.* **2000**, *122*, 1812–1813.

[91] Kong, M. J.; Teplyakov, A. V.; Jagmohan, J.; Lyubovitsky, J. G.; Mui, C.; Bent, S. F. *J. Phys. Chem. B* **2000**, *3000–3007.*

[92] Abeln, G. C.; Lee, S. Y.; Lyding, J. W.; Thompson, D. S.; Moore, J. S. *Appl. Phys. Lett.* **1997**, *70*, 2747–2749.

[93] Wang, G. T.; Mui, C.; Musgrave, C. B.; Bent, S. F. *J. Phys. Chem. B* **1999**, *103*, 6803–6808.

[94] Hovis, J. S.; Hamers, R. J. *J. Phys. Chem. B* **1997**, *101*, 9581–9585.

[95] Hovis, J. S.; Hamers, R. J. *J. Phys. Chem. B* **1998**, *102*, 687–692.

[96] Jolly, F.; Bournel, F.; Rochet, F.; Dufour, G.; Sirotti, F.; Taleb, A. *Phys. Rev. B* **1999**, *60*, 2930–2940.

[97] Taguchi, Y.; Fujisawa, T.; Takaoka, T.; Okada, T.; Nishijima, M. *J. Chem. Phys.* **1991**, *95*, 6870–6876.

[98] Lopinski, G. P.; Moffatt, D. J.; Wolkow, R. A. *Chem. Phys. Lett.* **1998**, *282*, 305–312.

[99] Kong, M. J.; Szetsen, S. L.; Lyubovitsky, J. G.; Bent, S. F. *Chem. Phys. Lett.* **1996**, *263*, 1–7.

[100] Küster, R.; Christmann, K. *Ber. Bunsenges. Phys. Chem.* **1997**, *101*, 1799–1810.

[101] Bitzer, T.; Alkunshalie, T.; Richardson, N. V. *Surf. Sci.* **1996**, *368*, 202–207.

[102] Bergerson, W. F.; Mulder, J. A.; Hsung, R. P.; Zhu, X.-Y. *J. Am. Chem. Soc.* **1999**, *121*, 454–455.

[103] Zhu, X.-Y.; Mulder, J. A.; Bergerson, W. F. *Langmuir* **1999**, *15*, 8147–8154.

[104] Ellison, M. D.; Hovis, J. S.; Liu, H.; Hamers, R. J. *J. Phys. Chem. B* **1998**, *102*, 8510–8518.

[105] Eng, J., Jr.; Raghavachari, K.; Struck, L. M.; Chabal, Y. J.; Bent, B. E.; Flynn, G. W.; Christman, S. B.; Chaban, E. E.; Williams, G. W.; Radermacher, K.; Mantl, S. *J. Chem. Phys.* **1997**, *106*, 9889–9898.

[106] Bitzer, T.; Richardson, N. V. *Surf. Sci.* **1999**, *427–428*, 369–373.

[107] Armstrong, J. L.; White, J. M.; Langell, M. *J. Vac. Sci. Technol. A* **1997**, *15*, 1146–1154.

[108] Bu, Y.; Breslin, J.; Lin, M. C. *J. Phys. Chem. B* **1997**, *101*, 1872–1877.

[109] Ellison, M. D.; Hamers, R. J. *J. Phys. Chem. B* **1999**, *103*, 6243–6251.

[110] Cleland, G.; Horrocks, B. R.; Houlton, A. *J. Chem. Soc. Faraday Trans.* **1995**, *91*, 4001–4003.

[111] Kim, N. Y.; Laibinis, P. E. *J. Am. Chem. Soc.* **1997**, *119*, 2297–2298.

[112] Sweryda-Krawiec, B.; Cassagneau, T.; Fendler, J. H. *J. Phys. Chem. B* **1999**, *103*, 9524–9529.

[113] Lee, A. J.; Ha, J. S.; Sailor, M. J. *J. Am. Chem. Soc.* **1995**, *117*, 8295–8296.

[114] Green, W. H.; Lee, E. J.; Lauerhaas, J. M.; Bitner, T. W.; Sailor, M. J. *Appl. Phys. Lett.* **1995**, *67*, 1468–1470.

[115] Lee, E. J.; Bitner, T. W.; Ha, J. S.; Shane, M. J.; Sailor, M. J. *J. Am. Chem. Soc.* **1996**, *118*, 5375–5382.

[116] Mitsuya, M. *Langmuir* **1994**, *10*, 1635–1637.

[117] Mitsuya, M.; Sugita, N. *Langmuir* **1997**, *13*, 7075–7079.

[118] Mitsuya, M.; Sato, N. *Langmuir* **1999**, *15*, 2099–2102.

[119] Henry de Villeneuve, C.; Pinson, J.; Bernard, M. C.; Allongue, P. *J. Phys. Chem. B* **1997**, *101*, 2415–2420.

[120] Gurtner, C.; Wun, A. W.; Sailor, M. J. *Angew. Chem., Int. Ed. Engl.* **1999**, *38*, 1966–1968.

[121] Dunn, A. W.; Moriarty, P.; Upward, M. D.; Beton, P. H. *Appl. Phys. Lett.* **1996**, *69*, 506–508.

[122] Schmidt, J.; Hunt, M. C. R.; Miao, P.; Palmer, R. E. *Phys. Rev. B* **1997**, *56*, 9918–9924.

[123] Feng, W.; Miller, B. *Langmuir* **1999**, *15*, 3152–3156.

Chapter 3

Monolayers of 1-Alkenes on the Hydrogen-Terminated Si(100) Surface [1]

Abstract

Monolayers that are bonded via a covalent Si–C bond are prepared on a Si(100) surface by reaction of a 1-alkene with the hydrogen-terminated silicon surface. The monolayers have been analyzed by infrared spectroscopy, X-ray reflectivity, and water contact angle measurements, and display a remarkably high thermal stability. The reaction also works well for ω-functionalized 1-alkenes, provided that the functional group is properly protected. After formation of the monolayer, the protecting group can be easily removed without noticeable disturbance of the monolayer integrity, and the now reactive sites at the monolayer can be used for further functionalization, as has been shown in the case of ester-protected alcohol and carboxylic acids. Functional groups that are too close to the alkene moiety interfere with monolayer formation and yield disordered monolayers.

[1] This Chapter contains the full text of the article that was originally published in April 1998 (and consequently already written in the summer of 1997), a period that can now be considered as the early days of these covalently bound organic monolayers on silicon surfaces. Since then, much more information has become available about these monolayers. Footnotes have been added in those cases where these new data affect the results described in this Chapter.

Original publication: A. B. Sieval, A. L. Demirel, J. W. M. Nissink, M. R. Linford, J. H. van der Maas, W. H. de Jeu, H. Zuilhof, and E. J. R. Sudhölter *Langmuir* **1998**, *14*, 1759–1768.

3.1 Introduction

The preparation of monolayers on solid substrates is technologically important and has been studied for many years. Apart from the monolayers prepared by the Langmuir-Blodgett method, much work has been done in the field of self-assembled monolayers of thiols on gold, and on the chemisorption of trichlorosilanes on oxidized silicon. In both cases dense, well-ordered monolayers are obtained. Many different monolayers have been prepared and their structures thoroughly characterized.[1,2]

A major drawback of almost all of these monolayers is their low stability. Monolayers of thiols on gold can be quite easily removed when heated in solvents.[3] Trichlorosilane-derived layers show good stability, but the silicon–oxygen bonds that are formed are susceptible toward hydrolysis and are thermally labile.[4] Furthermore, the reproducibility of the synthesis of monolayers by this method is sometimes problematic as well.

Recently, the preparation of dense alkyl monolayers that are covalently bonded to the silicon surface has been reported.[5,6] It was shown that neat 1-alkenes react efficiently with a hydrogen-terminated Si(111) surface when heated to 200 °C. This hydrosilylation reaction (Figure 1) results in the formation of very stable silicon–carbon bonds,[7] which yields dense monolayers as evidenced from infrared spectroscopy, ellipsometry, and wetting experiments. These monolayers are at least as stable as similar monolayers on oxidized silicon, as shown in the case of several 1-alkenes and one ω-chloro-1-alkene. The thermal stability up to 615 K of the monolayers in ultrahigh vacuum has very recently been demonstrated.[8]

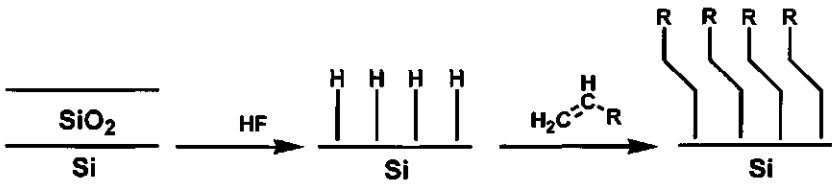

Figure 1. Schematic representation of the reaction of 1-alkenes with a hydrogen-terminated silicon surface.

In this Chapter, the preparation of highly stable monolayers on the hydrogen-terminated Si(100) surface is reported, using a variety of both functionalized and nonfunctionalized 1-alkenes. The preparation of functionalized monolayers has been

extensively explored for thiols on gold and trichlorosilanes on silicon oxide.[1,2] However, in contrast to thiols and trichlorosilanes, many functionalized alkenes are readily available or can be easily synthesized. This makes this new reaction, in combination with the stability of the resulting monolayers, potentially very interesting for many applications, e.g., in nonlinear optics[9] and adsorption experiments.[10] As nonfunctionalized 1-alkenes, 1-octadecene (**I**), 1-hexadecene (**II**), and 1-dodecene (**III**) were used, to study the dependence of the alkane chain length on the monolayer formation. To obtain information about the possibility of further functionalization of the thus formed monolayers, ω-ester functionalized 1-alkenes were chosen, since the wide-spread use of ester groups as protecting groups in organic chemistry and their expected —and observed— unreactivity towards the hydrogen-terminated silicon surface. The unprotected ω-undecenoic acid (CH_2=CH–C_8H_{16}–COOH, **IV**) and ω-undecenyl alcohol (CH_2=CH–C_8H_{16}–CH_2OH, **V**) were employed to study the effects of the presence of two potentially reactive groups in one molecule. The effects of protection of the alcohol and carboxylic acid functionality via ester formation were studied using ω-ester-functionalized 1-alkenes. ω-Undecenyl derivatives CH_2=CH–C_8H_{16}–C(O)O–CH_3 (**VI**), CH_2=CH–C_8H_{16}–C(O)O–C_3H_7 (**VII**), and CH_2=CH–C_8H_{16}–CH_2O–C(O)CH_3 (**VIII**) were used to study the effect of ester functionalities far from the reactive alkene moiety, while allyl esters CH_2=CH–CH_2–O(O)C–$C_{11}H_{23}$ (**IX**) and CH_2=CH–CH_2–O(O)C–$C_{17}H_{35}$ (**X**) were used to investigate the effect of the sterically demanding ester group close to the reactive site.

3.2 Experimental

3.2.1 General

All chemicals, unless noted otherwise, were commercially available and used as received. Solvents for substrate cleaning were distilled. 1-Octadecene, 1-hexadecene, 10-undecylenic acid, and lauroyl chloride (98%) were obtained from Acros Organics; 1-dodecene, 10-undecen-1-ol, and stearic acid (95%) were obtained from Aldrich. All alkenes for monolayer preparation were distilled at reduced pressure and stored at +4 or –20 °C until used. The silicon substrates were either pieces of double-polished silicon (Si(100), n- or p-type, 250 μm thickness), shards of single-polished silicon (Si(100), n- or p-type, 500 μm thickness) or Si(100) parallellogram plates (ATR-plates) designed for multiple internal reflection spectroscopy (Harrick Scientific, 45°, 50 x 10 x 1 mm^3, 50 reflections).

^{1}H NMR spectra were recorded in $CDCl_3$ at 200 MHz on a Bruker AC200 FT-NMR spectrometer at ambient temperature. ^{13}C NMR spectra were measured in $CDCl_3$ at 50 MHz. To obtain more reliable integrations of the ^{13}C NMR signals for the compounds **IX** and **X**, pulse sequences with a longer relaxation time, T_1 (up to 20 s), were used. Chemical shifts are in ppm relative to tetramethylsilane. Infrared spectra (IR) of the synthesized alkenes were recorded on a Biorad FTS-7 infrared spectrometer. All liquids were measured between NaCl windows; solids were dissolved in CCl_4. Melting points were determined on a Mettler FP80 HT melting point apparatus. The measurement conditions for the investigation of the monolayers are described below.

3.2.2 Syntheses

10-Undecylenic Acid Methyl Ester. A mixture of 10-undecylenic acid (15 g, 81 mmol), 35 ml of methanol, and 0.2 ml of sulfuric acid was refluxed for 3 h. The methanol was removed *in vacuo,* and the resulting material was dissolved in ether. The organic layer was washed with a sodium bicarbonate solution (2x), water (2x), and brine. Drying over magnesium sulfate and concentration yielded 15.5 g of the crude ester as a yellow oil. Vacuum distillation yielded 13.2 g (67 mmol, 82%) of pure (> 99%, GC analysis) 10-undecylenic acid methyl ester (bp 115 °C, 11 mmHg).[11]

^{1}H NMR: δ 5.90–5.70 (m, 1H), 5.04–4.89 (m, 2H), 3.67 (s, 3H), 2.30 (t, J = 7.5 Hz, 2H), 2.09–1.98 (m, 2H), 1.66–1.57 (m, 2H), 1.40–1.23 (m, 10H). **^{13}C NMR**: δ 174.10, 138.98, 114.03, 51.25, 33.97, 33.68, 29.18, 29.10, 29.03, 28.95, 28.80, 24.84. **IR** (cm^{-1}): 3075 (m); 2925 (m); 2853 (m); 1740 (s); 1638 (m).

10-Undecylenic Acid Propyl Ester. A mixture of 10-undecylenic acid (15 g, 81 mmol), 1-propanol (7 g, 0.11 mol), and 3 drops of sulfuric acid in 60 ml of toluene was heated in a Dean–Stark setup for 2 h. The toluene was removed *in vacuo,* and the resulting material dissolved in ether. Workup similar to that used for the methyl ester yielded 18.9 g of the crude ester as a brown oil. Vacuum distillation yielded 15.7 g (69 mmol, 85%) of 10-undecylenic acid propyl ester (bp 137–138 °C, 12 mmHg; lit. 139.5 °C at 7 mmHg).[12]

^{1}H NMR: δ 5.90–5.70 (m, 1H), 5.04–4.88 (m, 2H), 4.01 (t, 2H, J = 6.7 Hz), 2.29 (t, 2H, J = 7.4 Hz), 2.08–1.97 (m, 2H), 1.72–1.55 (m, 4H), 1.41–1.25 (m, 10H), 0.93 (t, 3H, J = 7.4 Hz). **^{13}C NMR**: δ 174.22, 139.42, 114.48, 66.12, 34.97, 34.14, 29.65, 29.57, 29.48, 29.41, 29.25, 25.36, 22.37, 10.73. **IR** (cm^{-1}): 3077 (m); 2967 (m); 2928 (m); 2855 (m); 1738 (s); 1640 (m).

10-Undecylenyl Acetate. A mixture of 10-undecylenyl alcohol (12 g, 70 mmol) and acetic acid anhydride (8 ml, 85 mmol) was refluxed for 1 h. The resulting liquid was poured onto 50 ml of ice water. The organic layer was separated and the water layer extracted with 50 ml of ether. The organic layers were combined and washed with a sodium bicarbonate solution (2x), water (2x), and brine. Drying over magnesium sulfate and concentration yielded 14.0 g of product as a yellow oil. Distillation yielded 11.8 g (56 mmol, 79%) of 10-undecylenyl acetate (bp 128–129 °C, 11 mmHg; lit. 125–127 °C at 7 mmHg).[13]

^{1}H NMR: δ 5.93–5.70 (m, 1H), 5.03–4.89 (m, 2H), 4.04 (t, 2H, J = 6.7 Hz), 2.03 (s, 3H), 2.05–1.98 (m, 2H), 1.65–1.56 (m, 2H), 1.40–1.22 (m, 12H). **^{13}C NMR**: δ 171.09, 139.07, 114.05, 64.55, 33.73, 29.38, 29.32, 29.16, 29.02, 28.84, 28.54, 25.84, 20.90. **IR** (cm^{-1}): 3076 (w); 2927 (m); 2855 (m); 1743 (s); 1640 (m).

Allyl Dodecanoate. Lauroyl chloride (23.1 ml, 0.10 mol) was added dropwise with stirring to 10 ml of allyl alcohol at 0 °C. The resulting mixture was stirred for one hour, allowing it to warm to room temperature. The solution was poured onto 100 ml of water. Extraction with 50 ml of petroleum ether (40–60 °C) yielded an organic layer which was subsequently washed with a sodium bicarbonate solution and brine. The combined water layers were made alkaline and extracted with a small portion of petroleum ether. The organic layers were combined and dried over magnesium sulfate. Concentration yielded 25.6 g of crude allyl dodecanoate as a yellow oil. Distillation yielded 20.4 g (85 mmol, 85%) of the pure ester (bp 149–150 °C, 10 mmHg; lit. 162–164 °C at 20 mmHg).[14]

^{1}H NMR: δ 6.02–5.83 (m, 1H), 5.37–5.20 (m, 2H), 4.58 (dt, 2H, J = 5.7 Hz, J = 1.4 Hz (2x)), 2.33 (t, 2H, J = 7.5 Hz), 1.71–1.56 (m, 2H), 1.32–1.22 (m, 16H), 0.88 (t, 3H, J = 6.8 Hz). **^{13}C NMR**: δ 173.27, 132.35, 117.84, 64.79, 34.17, 31.87, 29.56 (2 C), 29.41, 29.30, 29.22, 29.10, 24.90, 22.63, 14.02. **IR** (cm^{-1}): 3085 (w); 2925 (m); 2854 (m); 1741 (s); 1649 (m).

Allyl Octadecanoate. A mixture of stearic acid (20 g, 70 mmol), allyl alcohol (6 g, 0.10 mol), and 3 drops of sulfuric acid in 60 ml of toluene was heated in a Dean–Stark setup for 2 h. The toluene was removed *in vacuo*, and the resulting oil poured onto 150 ml of a 10% NaCl solution. The water layer was subsequently extracted with 50 ml of ether and 50 ml petroleum ether (40–60 °C). The organic layers were combined, washed with brine, and dried over magnesium sulfate. The solvent was removed, yielding 23.4 g of crude product as a yellow, wax-like material. This was dissolved in 200 ml of ethanol (96%) at 60 °C and crystallized via slow cooling to 0 °C. The product was filtered, washed with a small amount of

cold ethanol, and thoroughly dried *in vacuo* at room temperature, yielding 14.8 g (46 mmol, 65%) of allyl stearate (mp 34.5–35 °C; lit. 35 °C).[15] A further 3.4 g of product was isolated from the filtrate by removal of the ethanol and recrystallizing the resulting material from 40 ml of ethanol (96%) following the same procedure.

^{1}H NMR: δ 6.03–5.80 (m, 1H), 5.36–5.20 (m, 2H), 4.58 (dt, 2H, J = 5.7 Hz, J = 1.4 Hz (2x)), 2.33 (t, 2H, J = 7.5 Hz), 1.70–1.56 (m, 2H), 1.38–1.20 (m, 28H), 0.88 (t, 3H, J = 6.5 Hz). **^{13}C NMR**: δ 173.34, 132.36, 117.90, 64.83, 34.22, 31.92, 29.69 (large signal, 7 C), 29.59, 29.45, 29.36, 29.25, 29.14, 24.93, 22.67, 14.06. **IR** (cm^{-1}): 3087 (w); 2926 (m); 2854 (m); 1740 (s); 1647 (m).

3.2.3 Monolayer Preparation

Approximately 2 ml of the distilled alkene was placed in a small glass tube and deoxygenated with dry nitrogen for at least 30 min. A piece of silicon was etched for 1 min in 2% hydrofluoric acid, blown dry with nitrogen, and immediately placed in the deoxygenated alkene. The tube was then placed in an oil bath of 200 °C for 2 h, while slowly bubbling nitrogen through the alkene. Subsequently, the silicon piece was removed from the solution, rinsed 3 times in petroleum ether (40–60 °C) and ethanol (96%), sonicated for 5 min in dichloromethane, and dried in a stream of nitrogen. For the 10-undecenoyl ester-derived monolayers, methanol or propanol was used instead of ethanol.

For large samples such as attenuated total reflection (ATR)-crystals, a flattened glass tube with a screw cap was used, which was filled with sufficient alkene to completely immerse the silicon substrate. The alkene was deoxygenated with nitrogen for at least 1 h. These samples were cleaned in boiling dichloromethane instead of by sonication. The modified ATR-crystals were cleaned in between monolayer preparations by a UV/ozone treatment. The crystal was placed approximately 1 cm from the lamp and each side was illuminated for 10–15 min.[16,17] After this oxidation, drops of water completely spreaded on the silicon substrate, showing the complete removal of the monolayer. The crystals were subsequently etched in HF prior to renewed use.

Stability tests and modifications of the monolayers were performed in a small flask or, in the case of the ATR-crystals, in a large glass tube (50 ml) with a reflux condenser. For the acidification of solvents, a few drops of sulfuric acid were used.

3.2.4 Contact Angle Measurements

Water contact angles were measured with a KSV Sigma 701 Tensiometer, using a computer-controlled contact angle calculation program, available from the manufacturer. The silicon sample (double-polished, approximately 15x7 mm^2, thickness 250 μm) was placed vertically in a counterbalanced, homemade clamp and used as a Wilhelmy-plate. This method is often used for the determination of static contact angles but can be used for dynamic contact angles as well.[18] For both advancing and receding contact angles at least six measurements were made. For the monolayers of **I–VIII** the reproducibility for advancing contact angles is ±1° and for the receding angles ±1–2°. For the monolayers of **IX** and **X** the experimental errors are estimated to be ±3°.

3.2.5 Infrared Spectroscopy

Infrared spectra of the monolayers were recorded on a Perkin Elmer 2000 FT-IR spectrometer, equipped with a liquid-nitrogen-cooled MCT-detector, using a fixed angle multiple reflection attachment (Harrick Scientific). The infrared light was incident on one of the 45° bevels of the ATR-plate. Spectra of the monolayers were recorded with s- and p-polarized light. Measurement conditions were as follows: resolution 4 cm^{-1}, at least 256 scans, apodization medium Norton-Beer. The spectra were measured in the range of 4000–1500 cm^{-1}, following from the high absorbance of the silicon ATR-crystals below 1500 cm^{-1}. An ATR-crystal was cleaned with ethanol and chloroform and used as a background. No corrections were made for water vapour or CO_2. In some cases a linear baseline correction or a fringe correction was applied.[19] To remove physisorbed material, the samples were rinsed extensively in chloroform before mounting.

The reproducibility of the peak positions in different measurements, e.g., after repositioning of the sample or cleaning of the monolayer-modified crystal, was within 0.5 cm^{-1}. The use of a freshly etched and cleaned silicon background crystal instead of the oxidized surface gave no improvement.

From the measurement of the independent s- and p-polarized spectra the dichroic ratio $D = A_s/A_p$ can be calculated, in which A is the intensity of the absorbance measured with s- or p-polarized light.[20] The determination of D allows for an estimate of the angle α between the transition dipole moment of the vibration and the surface normal[21]

$$\alpha = \tan^{-1}\left[\frac{2DE_z^2}{E_y^2 - DE_x^2}\right]$$

in which $E_{x,y,z}$ are the electric fields of the polarized light for the x, y, and z-directions, respectively.[22] For the ATR conditions in our experiments $E_x = 1.409$, $E_y = 1.476$, and $E_z = 0.684$, using refractive indices of $n_{Si} = 3.5$ and $n_{monolayer} = 1.5$.[21] From the determination of α for both the antisymmetric (α_a) and symmetric (α_s) methylene stretching vibrations, an estimated tilt angle, Φ_{tilt}, of the molecule, with respect to the surface normal can be calculated using:[23]

$$\cos^2 \Phi_{tilt} = 1 - \cos^2 \alpha_s - \cos^2 \alpha_a$$

3.2.5 X-ray Reflectivity

X-ray reflectivity measurements were performed using a rotating anode Rigaku RU-300H generator having a maximum power of 18 kW and a triple-axis reflectometer. This setup has been described in detail previously.[24] The incident beam (Cu Kα radiation, λ = 1.5405 Å) was monochromatized and focused using a bent graphite (002) crystal. The incident and outgoing divergences, as defined by the slit widths, were 0.064° and 0.082°, respectively, corresponding to in-plane resolutions of $\Delta q_z = 7.4 \times 10^{-3}$ Å^{-1} and $\Delta q_x = 3.2 \times 10^{-3}$ Å^{-1}. Samples were mounted on a substrate holder and measured in ambient air. No sign of beam damage or contamination was observed. The 10-undecylenyl alcohol-derived monolayer (**V**) was rinsed in acetic acid and water prior to measurement, and measured in a cell that was vacuum-pumped continuously to avoid contamination through air exposure.

X-ray reflectivity data are background subtracted, and standard geometrical correction for the beam footprint has been applied. The alkyl monolayers were modeled as having a constant electron density throughout the film. For the end group-functionalized monolayers a three-layer model was used. The root mean square roughness of the air/film and film/substrate interfaces was described by a Gaussian function. Fits were calculated with an iterative matrix solution of the Fresnel equations for the reflectivity of the air/film/substrate system, using periodic slab profiles of electron densities.[24]

3.3 Results and Discussion

3.3.1 Monolayer Properties: Ordering and Packing Structures

The monolayers were analyzed by contact angle measurements, multiple internal reflection infrared spectroscopy, and X-ray reflectivity (*vide infra*). A combination of the results obtained from these measurements provides information on the ordering and packing of the monolayers. The water contact angles, as observed for the monolayers on Si(100), are listed in Table 1 (column 2). This table also contains the infrared peak positions, as observed with p-polarized light, for the antisymmetric (ν_a) and symmetric (ν_s) methylene stretching vibrations (columns 3 and 4, respectively).

Table 1. Water contact angles (in degrees) and infrared absorptions (in cm^{-1}) for the antisymmetric (ν_a) and symmetric (ν_s) methylene stretching vibrations of the monolayers.

Alkene	Θ_a/Θ_r [a]	ν_a	ν_s
CH_2=CH–$C_{16}H_{33}$ (**I**)	110/96	2920	2851
CH_2=CH–$C_{14}H_{29}$ (**II**)	109/95	2921	2852
CH_2=CH–$C_{10}H_{21}$ (**III**)	109/94	2920 [b]	2849 [b]
CH_2=CH–C_8H_{16}–COOH (**IV**)	0 [c]	2925	2854
CH_2=CH–C_8H_{16}–CH_2OH (**V**)	0 [c]	2923	2853
CH_2=CH–C_8H_{16}–COO–CH_3 (**VI**)	77/70	2923	2854
CH_2=CH–C_8H_{16}–COO–C_3H_7 (**VII**)	85/73	2920	2850
CH_2=CH–C_8H_{16}–CH_2O–C(O)CH_3 (**VIII**)	73/65	2919	2850
CH_2=CH–CH_2–OOC–$C_{11}H_{23}$ (**IX**)	101/89	2925	2856
CH_2=CH–CH_2–OOC–$C_{17}H_{35}$ (**X**)	106/91	2923	2854

Notes: [a] Advancing and receding contact angles for water. [b] Maximum shifted to lower value due to low absorption and subsequent problems with negative peaks as a result of background contamination. [c] Directly after cleaning of the substrate in acetic acid and water, a small drop of water tends to spread on the surface. However, these contact angles are not stable in time.[3,26,34]

The measurement of water contact angles is a quick and useful tool in monolayer analysis.[25] It can also be used to study the monolayer stability, if measured as a function of time, as monolayers that are disordered or not stable will show decreasing contact angles. No such changes were observed for any of the monolayers listed in Table 1.

From the high values of the water contact angles ($\Theta_{a/r}$ = 109–110°/94–96°) as measured for the unfunctionalized 1-alkenes (**I–III**), it is clear that the surface of the monolayer is completely terminated by methyl groups. The advancing contact angles are comparable to those of thiols on gold,[26,27] and to the monolayers on Si(111) prepared by Linford *et al.*[6] This shows that a sufficiently high percentage of the hydrogenated silicon atoms has reacted with a 1-alkene to give a complete coverage of the surface. The surface properties of the monolayer are therefore not affected by residual Si–H and Si–OH groups that are present on the silicon surface.[6] The receding contact angles are somewhat lower than the reported literature values as a result of surface roughness, which leads to an increase in the contact angle hysteresis $\Delta\Theta$ (defined as $\Delta\Theta = \Theta_a - \Theta_r$).[28] However, the comparatively large hysteresis may also be the result of a slightly higher number of defects in the monolayers when compared to the trichlorosilane monolayers.

Infrared spectroscopy reveals that for the samples **I–III** the anti-symmetric and symmetric methylene stretching vibrations appear near 2920 cm^{-1} and 2850 cm^{-1}, respectively (Table 1). It is well-known that shifts from 2928 to 2920 cm^{-1} and from 2856 to 2850 cm^{-1} for the methylene stretching vibrations occur on going from a liquid to a solid alkane.[29] The observed wavenumbers are therefore indicative of a densely packed monolayer of alkyl chains.[30] The IR-spectrum of the monolayer of **I** is shown in Figure 2.

The contact angles, as observed for the functionalized monolayers of **IV–VIII**, do not provide conclusive information in all cases. The acid- and alcohol-terminated monolayers (samples **IV** and **V**, respectively) show very low contact angles. This is expected for a surface terminated by hydrophilic groups, but might also be due to a disordered surface. Unfortunately, contact angle measurements cannot resolve this matter. For a methyl ester-terminated surface, different values are reported for thiols on gold (Θ_a = 67°)[26] and trichlorosilanes on silicon oxide (Θ_a = 72°–79°).[31] The advancing contact angle as observed for the monolayer of **VI** (Θ_a = 77°) is comparable to these values and indicates that the surface is terminated with methyl ester groups. The small hysteresis ($\Delta\Theta$ = 7°) suggests that the methyl groups are close together and a closely packed monolayer is formed. A similarly small

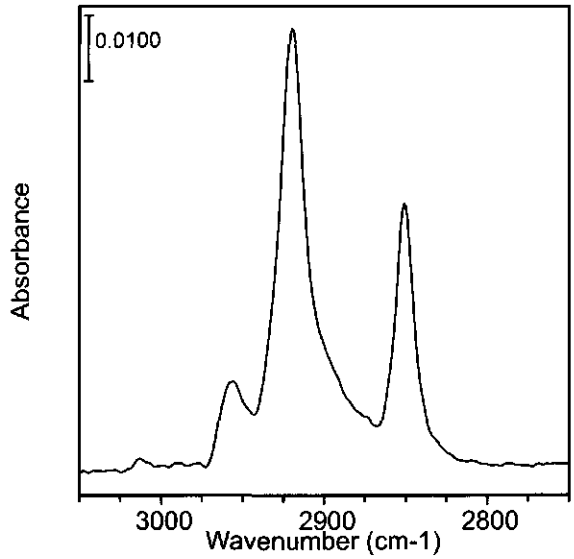

Figure 2. Infrared spectrum (C–H stretching region) of a monolayer of **I** on Si(100).

hysteresis ($\Delta\Theta$ = 8°) is observed for the acetate-terminated surface (**VIII**), which shows $\Theta_{a/r}$ = 73/65°. These values are comparable to the recently published data ($\Theta_{a/r}$ = 64/58°) for an acetate-terminated monolayer on gold.[32] The monolayers of both **VI** and **VIII** show contact angles that are slightly higher than those on gold. This is probably caused by the surface roughness of the silicon substrate, which will expose some underlying CH_2 groups. As this moiety has a low dipole moment and polarizability, this extra exposure will result in an increased hydrophobicity. The observed advancing contact angle for the propyl ester surface **VII** (Θ_a = 85°) shows that the hydrophobicity increases as the ester group gets buried in the monolayer. This value gets closer to the values observed for the long alkyl chains **I–III**, which confirms that the ester groups in the monolayers of **VI–VIII** are at the air/monolayer interface.

The infrared data of samples **VI**, **VII**, and **VIII** show that well-ordered monolayers are obtained if the functional end groups are protected as ester moieties. Monolayers of **VII** and **VIII** show absorption maxima that indicate very closely packed molecules. Apparently, the ester groups are not too big and still allow for dense packing of the monolayer. The observed maxima for the monolayer of **VI** are somewhat higher, in line with the reported observation that methylene stretching frequencies shift to higher values as the alkyl chains in alkyl

monolayers get shorter and suffer from gauche defects, but a close packing is also obtained with this protecting group.[31,33]

The unprotected undecylenic acid (**IV**) seems to give a quite disordered surface. In the infrared spectrum of the monolayer (Figure 3) the methylene stretching vibrations appear as somewhat broadened peaks with maxima at 2925 and 2854 cm^{-1}, which indicates that the monolayer is not as well-ordered as the alkyl monolayers of **I–III**. The shift of the absorption maximum to a higher frequency is the result of gauche conformations, which are possible if the molecules in the monolayer are not close together. However, a similar shift is observed when an originally ordered monolayer reorganizes, e.g., by a folding of the alkyl chains to remove the polar headgroups from the outside of the surface.[34] In the carbonyl-stretching region two peaks are observed: one at 1711 cm^{-1}, which can be attributed to the normal, hydrogen-bonded C=O vibration of carboxylic acid dimers, and one at 1740 cm^{-1}, corresponding to the carbonyl stretching vibration of a free carboxylic acid.[35] On the other hand, if the acid group is bound to the silicon surface, the C=O vibration of the resulting Si-O–C=O-ester is at ~1710 cm^{-1} as well.[5,6,36,37] The latter situation did, however, not seem to occur, as no terminal alkene vibrations were observed in the IR spectrum.

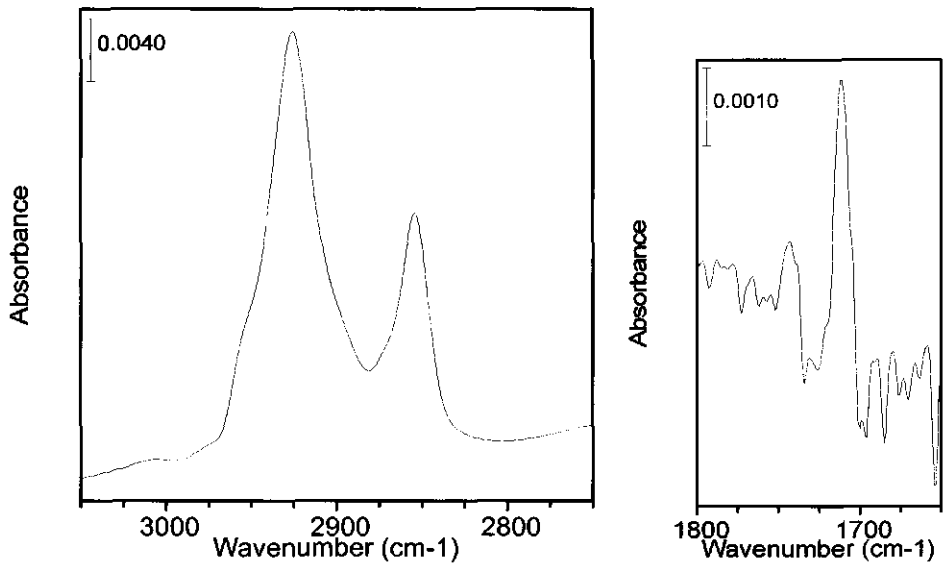

Figure 3. Infrared spectra (C–H and C=O stretching regions) of a monolayer of **IV** on Si(100).

To further investigate this surface, it was reacted with boiling acidic methanol for 20 min to hydrolyze any siloxane esters present and to introduce the methyl ester functionality. The resulting removal of any molecules from the monolayer will yield a shift of the vibrational frequencies of the methylene groups to higher wavenumbers, as observable by IR spectroscopy. After the reaction, the C=O vibration at 1710 cm^{-1} had disappeared and a broad peak at 1743 cm^{-1} showed the presence of terminal methyl ester groups. The maximum of the anti-symmetric methylene absorption had shifted to 2928 cm^{-1}, was considerably broadened, and had decreased about 40% in intensity. These observations indicate that siloxane esters are formed in the reaction of the bifunctional alkene **IV** with the hydrogen-terminated silicon surface and that the peak at 1710 cm^{-1} must arise, at least partially, from these siloxane esters that are apparently formed by a reaction of the carboxylic acid moiety with this surface. Consequently, a disordered monolayer is obtained, instead of an acid-terminated monolayer that reorganizes in time. The reaction of organic acids with a hydrogen-terminated silicon surface has been reported in literature, but only under the influence of UV light[36,37] or with an applied bias.[38] The reaction with a clean, oxide-free silicon surface has been reported as well.[39] Our results suggest that this also occurs at high temperatures, although a reaction with either defects or silanol groups at the surface cannot be fully excluded.

The unprotected alcohol **V** showed broad bands with maxima at 2923 and 2853 cm^{-1}, which is indicative of a disordered monolayer. Alcohols can react with a hydrogen-terminated silicon surface at elevated temperatures,[40,41] but as the quality of the infrared spectrum obtained was very poor, no reliable conclusion about the presence of any terminal alkene groups could be drawn. Upon treatment of this surface with acetic anhydride, a small peak around 1740 cm^{-1} was observed, and the absorption maximum of the CH_2 stretching vibration appeared at 2925 cm^{-1}. The peak at 1740 cm^{-1} is assigned to the formation of ester groups, which shows that alcohol groups were still present in the monolayer. However, if an ordered, but reorganized,[34] hydroxyl-terminated monolayer had been formed on the surface, a shift of the methylene stretching vibrations to a lower wavenumber is expected, because the resulting monolayer, after reaction with acetic anhydride, should be comparable to the acetate-terminated surface **VIII**.

To investigate the reactivity of an alcohol group towards the hydrogen-terminated surface under our experimental conditions, the surface was modified with neat dodecanol. After cleaning of the surface in petroleum ether (40–60 °C) and cold dichloromethane, it did not show hydrophobicity when a drop of water was placed on a slightly tilted sample. The infrared spectrum showed broad absorptions for the methylene stretches with maxima at 2926

and 2854 cm^{-1}. The corresponding monolayer prepared from dodecene (compound **III**) is hydrophobic and has methylene absorption maxima at 2920 and 2850 cm^{-1} (Table 1). This indicates that the alcohol does indeed react with the surface, but that a well-packed monolayer is not formed.

The allyl esters **IX** and **X** both give disordered monolayers. The water contact angles are significantly lower than for the alkyl monolayers of **I–III**, suggesting that the surface is not completely methyl-terminated. The infrared data show that the alkyl chains are not as densely packed as the corresponding monolayers from the 1-alkenes **I–III**, since the maxima of the antisymmetric methylene absorptions are observed at slightly higher wavenumbers (2923–2925 cm^{-1} compared to 2920–2921 cm^{-1}). The same difference is observed for the symmetric methylene stretches. It has been reported that an ordered monolayer was obtained for a similar compound on a gold surface, indicating that this class of compounds can give dense monolayers if enough space is available for the ester group.[42] The steric hindrance of an ester group near the silicon surface apparently hampers the alkene to approach the nearest silicon atom and prohibits formation of a closely-packed monolayer on the Si(100) surface.

3.3.2 Monolayer Properties: Electron Density, Thickness and Roughness

As the ordering and close packing of the monolayers has been established, more detailed information is desirable to further characterize this type of structures, such as the thickness of the layer and the interfacial roughness. This type of data can be obtained via X-ray reflectivity, which is sensitive to changes in the average electron density ρ along the momentum transfer vector Q, which is related to the momentum of the X-ray photons during the reflection process.[43] In specular reflectivity, where the angle Θ of the incoming X-ray beam with the surface is equal to the angle of the reflected beam, $Q(\Theta) = (4\pi/\lambda)\sin(\Theta)$ and the vector is perpendicular to the film surface. The reflectivity profile is a function of the momentum transfer $Q(\Theta)$. Below the critical value of momentum transfer Q_c, total reflection is observed; beyond Q_c, the reflectivity follows the Fresnel law for a single sharp interface. Therefore, from deviations from Fresnel reflectivity of the substrate, information about the density profile along the surface normal (i.e., the electron density variation within the monolayer), film thickness, and interface roughnesses of a monolayer can all be derived in one experiment. This makes it a powerful technique for the analysis of thin films on solid substrates. The monolayers of **I–III**, **V** and **VIII** were studied by X-ray specular reflectivity measurements, and the results reported in Figures 4–6.

Figure 4 shows the X-ray reflectivity as a function of momentum transfer Q for the alkane monolayers of **I–III** on the Si(100) surface. For all three layers Q_c is 0.028 $Å^{-1}$, which corresponds to a critical angle of 0.2°, a typical value for the underlying silicon substrate.[44] The angle of incidence was increased up to 5°, corresponding to a maximum Q value of 0.7 $Å^{-1}$. This allowed for the observation of a second minimum in the reflectivity profile for the relatively thick samples **I** and **II**, which results in an accurate determination of the film thickness. With increasing film thickness, going from top to bottom in Figure 4, the period of the reflectivity minima decreases and the position of the reflectivity minima shifts to lower Q values. The solid lines in Figure 4 are single layer best fits to the data, as described in the experimental section. The electron density of the silicon substrate was fixed at 7.89 $e^-/Å^3$ and the mass absorption coefficient at 5.49 x 10^{-6} $Å^{-1}$.

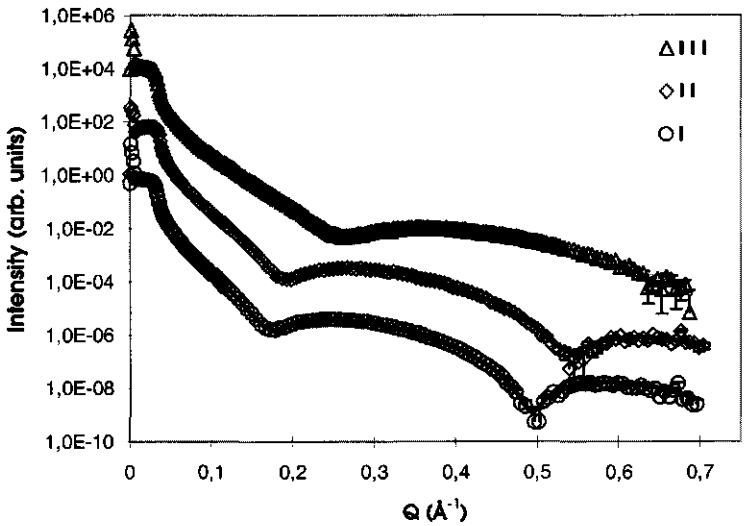

Figure 4. X-ray reflectivity profiles of monolayers of **I–III** on Si(100), also showing best-fit curves and error bars.

For some data points at large Q values, the error bars due to counting statistics are also shown. It should be noted that the total error is likely to be somewhat larger due to other contributions, such as instrumental misalignment. The measurements cover an intensity range of more than 8 orders of magnitude before the background is reached. It is clear from the relatively large error bars that the second minima observed in monolayers of **I** and **II** are close

to the background, leading to increased deviations between the data and the fitted curves in this part of the reflectivity profile. This results in a slight increase of the uncertainty in the monolayer thickness.

The calculated film thickness, electron density, and interface roughnesses of the monolayers of **I**–**III** are listed in Table 2. For the film thickness a clear linearity is observed, as expected for a series of long alkyl chains. Each methylene group adds approximately 1 Å to the monolayer thickness. The values are consistent with a constant tilt angle of 27° for all three layers, as will be discussed below.

Table 2. Various films properties as obtained from single-layer fits to the X-ray reflectivity measurements.[a]

Monolayer [b]	Thickness (Å)	e density ($e^-/Å^3$)	σ_2 (Å) [c]	σ_3 (Å) [d]	Tilt angle [e] (deg)
I	19.5	0.32	2.6	2.9	29
I (on Si(111))	19.7	0.30	2.6	4.1	28
II	17.8	0.31	2.5	3.5	26
III	13.2	0.30	1.7	2.7	26
V	17.1 (14.4)	0.52	1.6 (3.8)	1.6 (2.0)	n.d. [f]
VIII	16.1 (16.4)	0.34	2.5 (2.0)	2.4 (2.9)	17

Notes: [a] When improved fits are possible using more layers, the results are placed between parentheses. Approximate errors, based on the scatter of values determined from measurements of different samples of monolayers **I**, **II**, and **III**, are as follows: thickness ±1%, e density ±3%, σ_2 ±2%, σ_3 ±10%. [b] Monolayer on Si(100), unless otherwise specified. [c] Roughness of air/monolayer interface. [d] Roughness of monolayer/silicon interface. [e] Tilt angle as determined from X-ray reflectivity results. [f] Not determined (see below for explanation).

The average electron density for all three layers is nearly constant at a value of 0.31 ± 0.02 $e^-/Å^3$. For comparison, the density of crystalline $C_{33}H_{68}$ is 0.35 $e^-/Å^3$,[45] which again indicates that the alkyl chains in the monolayers of **I**–**III** are closely packed. The interface roughnesses are 1–4 Å, comparable to the roughness of 2–4 Å usually found for silicon, while the roughness at the air/monolayer interface is smaller than at the monolayer/substrate

interface. Apparently the outside of the monolayer can somewhat reorganize and form a smooth outer layer, while at the monolayer/silicon interface, the roughness is determined by the original hydrogen-terminated Si(100) surface. A similar smoothing of the outside of the monolayer has been observed for mono- and multilayers of behenic acid on silicon oxide.[46]

To compare the results on the Si(100) surface with monolayers on Si(111), a monolayer of **I** on this latter surface was prepared following a literature procedure.[6] The similarity of the X-ray specular reflectivity data for the two monolayers can be seen in Figure 5. The solid lines are the best fits to the data and error bars are due to counting statistics. As shown in Table 2, the thicknesses determined from the fits are almost identical, differing by only 1%. The electron densities differ by 7%, which is within the scatter of values obtained from different fits, e.g., when using an optimized or the literature value for the electron density of the silicon substrate.

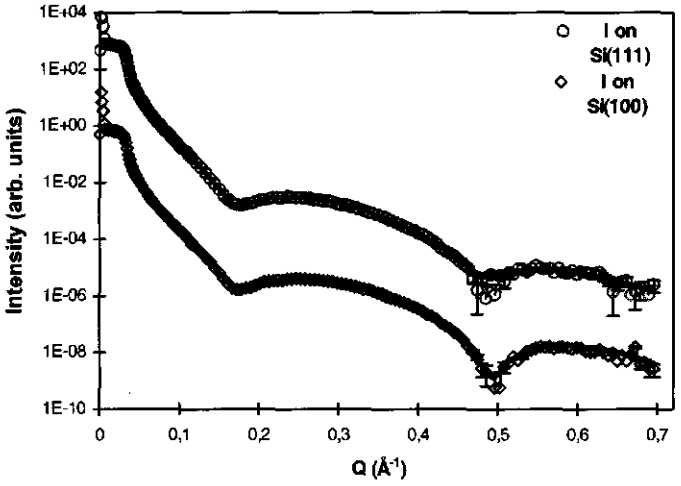

Figure 5. X-ray reflectivity profiles of a monolayer of **I** on Si(111) and Si(100).

The similarity of the monolayer of **I** on the Si(111) and (100) surface is not unexpected. The two hydrogen-terminated surfaces are very different, but from a simple ball-and-stick model it is clear that on both surfaces only 50% of the hydrogenated silicon atoms can react with an alkene due to steric hindrance, as was already suggested by Linford *et al.* for their monolayers on the Si(111) surface.[6] Consequently, the resulting monolayers on both surfaces are as closely packed as possible. The ball-and-stick model shows that the unit cells

of the modified silicon surfaces have approximately the same size. Therefore, the electron density and thickness of the monolayer of **I** on the two surfaces will be similar as well. [II]

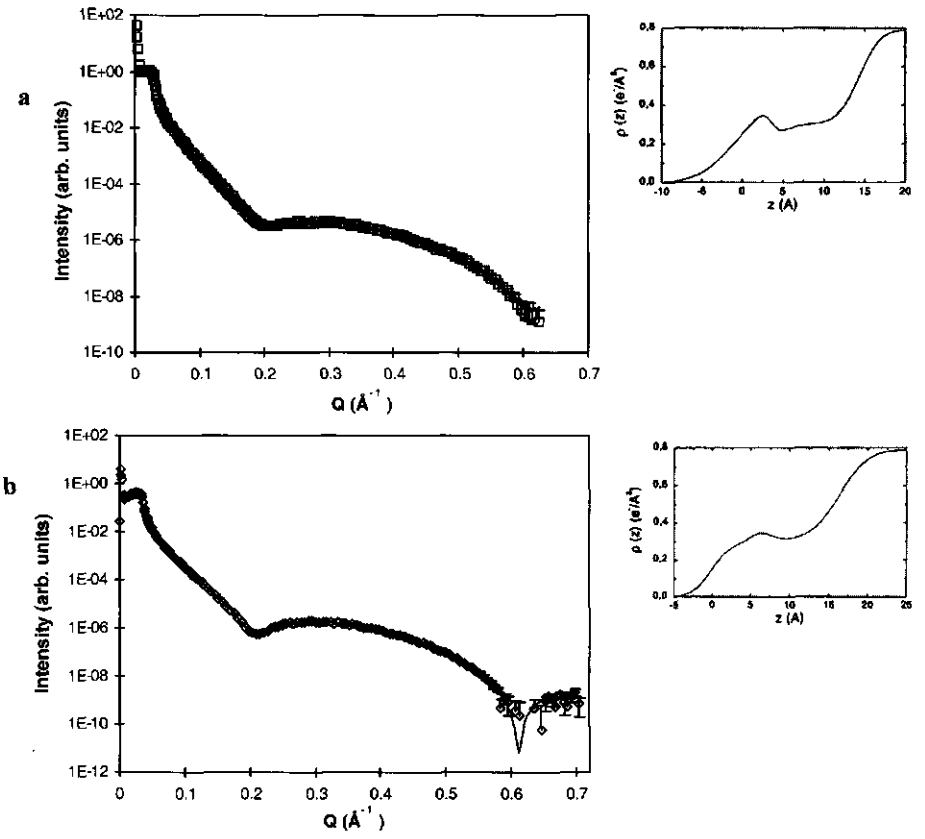

Figure 6. (a) X-ray reflectivity profile of a monolayer of **V** on Si(100). The inset shows the electron density profile as calculated from a three-layer model (see text). (b) X-ray reflectivity profile of a monolayer of **VIII** on Si(100). The inset shows the electron density profile as calculated from a three-layer model (see text).

[II] Although ball-and-stick models of the surfaces indeed suggest that the unit cells have approximately the same size, there is in fact a difference of almost 2 Å^2 between the two. The unit cell of the Si(111) surface is 12.77 Å^2, whereas that of the Si(100) surface is 14.75 Å^2. Consequently, on the Si(100) surface the number of Si surface atoms bound to an alkyl chain will actually be larger than on the Si(111) surface. Assuming an area of 24 Å^2 per alkyl chain (see Section 3.3.4), approximately 61% of the Si(100) surface atoms is bound to an alkyl chain, compared to approximately 53% of the Si(111) surface atoms.

Figure 6 shows the reflectivity data for the unprotected alcohol **V** (top) and the protected monolayer of **VIII** (bottom). The single layer best fits resulted in significant deviation from the data at large Q values and unreasonably high electron densities as seen in Table 2. From the IR-analysis of the alcohol-terminated monolayer (**V**) *–vide supra–* it was already clear that this alkene does not give a closely-packed monolayer. For the monolayer of **VIII**, a single layer model might be insufficient, because the acetate group in the monolayer is relatively electron-rich compared to the underlying alkyl chain. This can be accounted for by using a three-layer model, as schematically depicted in Figure 7.

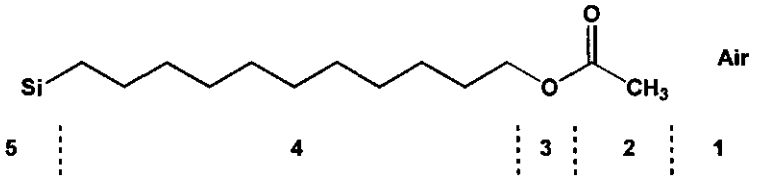

Figure 7. Schematic representation of the three-layer model for a monolayer on silicon, as used for the analysis of the X-ray data of a monolayer of **VIII** on Si(100). The numbers represent the number of each layer (air = layer 1) in the model. The same model was used for the monolayer of **V**, in which the end group is OH instead of an acetate group.

The solid lines in Figure 6 are the best fits to a three-layer model, consisting of a chain of CH_2 groups on the substrate, a narrow electron-rich intermediate layer that corresponds to the oxygen atoms in the monolayer, and a cap layer (see Figure 7). The electron density of the first layer was fixed at 0.31 $e^-/Å^3$, as determined previously from the alkyl monolayers of **I–III**. The insets show the resulting electron densities corresponding to the best fits. The resulting fitting parameters for each layer are listed in Table 3.

The total film thickness of 16.40 Å for the protected monolayer of **VIII** is consistent with the chain length. The peak electron density, 6.33 Å below the free surface, is smeared out to 0.35 $e^-/Å^3$, because the interface roughness on both sides of this electron-rich intermediate layer is comparable to the thickness of the layer. The electron density of the cap layer is 0.29 $e^-/Å^3$, as expected for methyl termination.

For the monolayer of **V**, a total film thickness of 14.44 Å is still too high for a monolayer with this chain length. The peak electron density is 2.68 Å below the surface and

has a value of 0.34 $e^-/Å^3$. Monolayer **V** is probably still contaminated, which yields an estimate of the film thickness that is too high. This result confirms the observation that the unprotected alcohol gives a disordered layer.

Table 3. Monolayer properties derived for **V** and **VIII** from best fits using a three-layer model (see Figure 7).

Parameter [a]	**V**	**VIII**
σ_{21} (Å)	3.8	2.0
t_2 (Å)	2.2	5.4
ρ_2 ($e^-/Å^3$)	0.51	0.29
σ_{32} (Å)	2.1	1.2
t_3 (Å)	1.5	1.1
ρ_3 ($e^-/Å^3$)	0.46	0.43
σ_{43} (Å)	0.75	1.5
t_4 (Å)	10.7	9.9
ρ_4 ($e^-/Å^3$)	0.31	0.31
σ_{54} (Å)	2.0	2.9

Note: [a] σ_{xy} = interface roughness of the interface between layers x and y; t_x is the thickness of the layer x, ρ_x is the corresponding electron density.

3.3.3 Functionalization of Ester-Terminated Surfaces.

The hydrolysis of ester-terminated monolayers would provide a convenient route to prepare alcohol- and acid-terminated surfaces, which cannot be prepared directly as shown above for compounds **IV** and **V**. Since these latter functional groups can be easily transformed into a variety of other functionalities, hydrolysis of the ester groups under relatively mild conditions would constitute an attractive route to highly functionalized monolayers. Because alkaline hydrolysis seriously damages the silicon itself, the surfaces were hydrolyzed in boiling acidified water for 20–30 min. The alkyl monolayers of **I–III** were perfectly stable under these conditions, as would be expected for hydrophobic surfaces, but were also not affected when a mixture of 9 : 1 (v/v) of isopropanol/concentrated

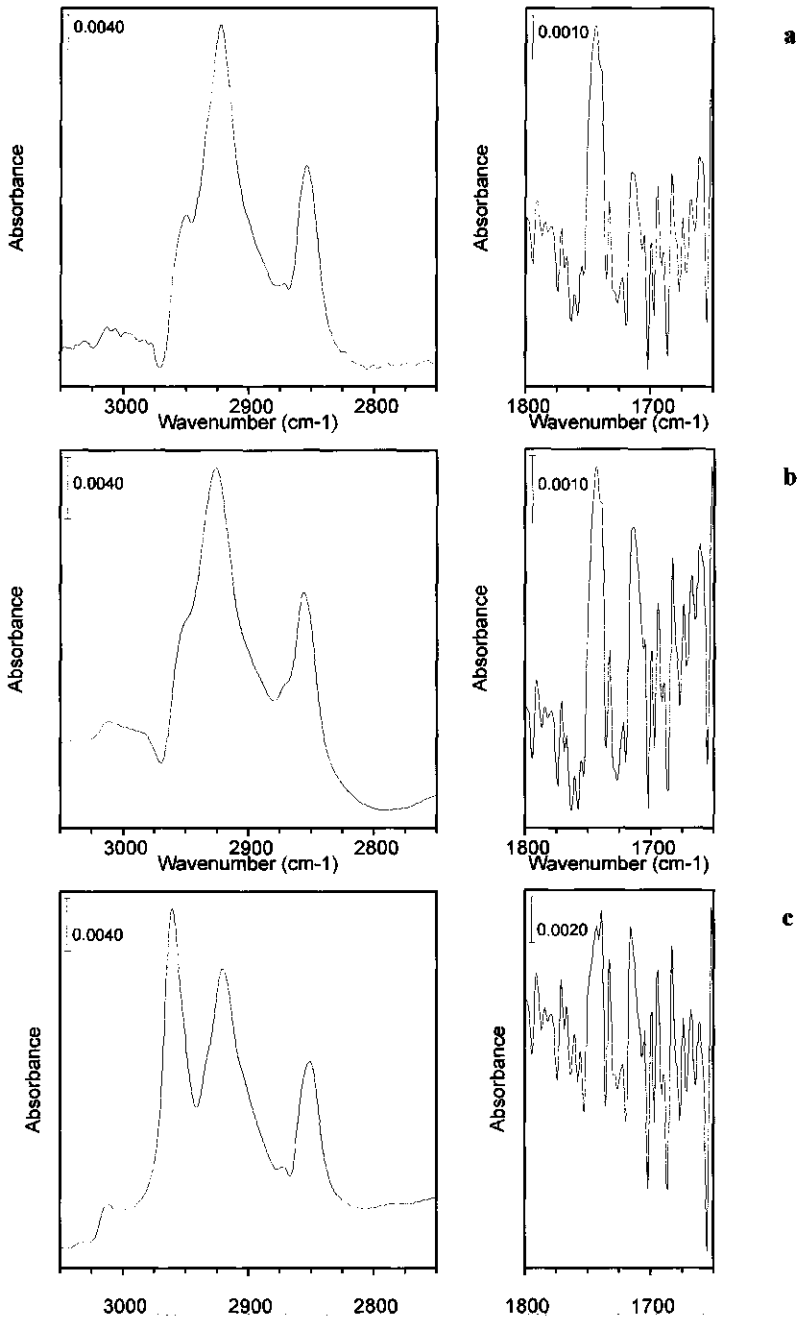

Figure 8. (a) Infrared spectra (C–H and C=O stretching regions) of a monolayer of **VI** on Si(100). (b) Infrared spectra (C–H and C=O stretching regions) of a hydrolyzed monolayer of **VI** on Si(100). (c) Infrared spectra (C–H and C=O stretching regions) of the monolayer of part b after subsequent reaction with acidic *n*-propanol.

hydrochloric acid was used. Consequently, hydrolysis in acidic water should have no effect on the ester-terminated monolayers, apart from the desired hydrolysis of the ester groups. The infrared spectra (p-polarized) of the various stages of the hydrolysis of the methyl ester surface (**VI**) are depicted in Figure 8.

The first spectrum (Figure 8a) shows the original monolayer of **VI**. The carbonyl stretching vibration is clearly visible at 1743 cm^{-1}. Upon hydrolysis, the spectrum changes considerably (Figure 8b). The anti-symmetric methylene stretching vibration has shifted to 2926 cm^{-1}, and the carbonyl stretching region shows two peaks of about the same intensity, which can be assigned to the various vibrations of carboxylic acid groups. Because the surface was rinsed in water before wiping with chloroform, some carboxylate groups may be present as well. Unfortunately, a detailed analysis of the carbonyl region is complicated, because of the low signal to noise ratio (see also Experimental Section) and the appearance of peaks from residual water vapor. [III] The signal at 1743 cm^{-1} is still present, but is decreased in intensity relatively to the 1711 cm^{-1} band (*vide infra*). This may indicate that not all the ester groups were hydrolyzed, which has been observed before.[47,48] However, the peak could also be assigned to non-hydrogen-bonded carboxylic acid groups,[35] which will be present if the acid-terminated surface reorganizes.[34] That hydrolysis did take place is evident from the water contact angles ($\Theta_{a/r}$ = 69/35°), which are lower than for the methyl-terminated surface and show a very large hysteresis. Directly after cleaning of the modified surface in water, small drops of water tend to spread on the surface, as would be expected for the hydrophilic, acid-terminated surface. Longer reaction times had no effect on the positions or intensities of the various peaks in the IR-spectrum. [IV]

The hydrolyzed monolayer was subsequently placed in acidified *n*-propanol and heated to reflux for 30 min. The subsequently measured infrared spectra (maxima at 2920 and 2851 cm^{-1}; Figure 8c) and water contact angles ($\Theta_{a/r}$ = 83/75°) were very similar to the results of a monolayer prepared directly from the propyl ester (**VII**). The carbonyl stretching region does not differ much from the hydrolyzed surface, still showing a peak at 1710 cm^{-1}. This

[III] (a) In the case of carboxylic acid-terminated thiol monolayers on gold, it has been shown that the intensity of the C=O stretch vibration is also orientation-dependent. See: Kim, T.; Ye, Q.; Sun, L.; Chan, K. C.; Crooks, R. M. *Langmuir* **1996**, *12*, 6065–6073.

[IV] Complete ester hydrolysis has been reported for a monolayer of ω-undecylenic acid ethyl ester on the hydrogen-terminated Si(111) surface, using 2.4 M HCl at 70 °C and a reaction time of 2 h. No peak at 1740 cm^{-1} was observed in the IR spectrum of that hydrolyzed monolayer, indicating that the hydrolysis of the methyl ester terminated monolayer may indeed have been incomplete. However, this observation can also be due to differences in the surface morphology of the Si–surfaces, as H-Si(111) is atomically flat over relatively large terraces, whereas H-Si(100) is more rough. See: Boukherroub, R.; Wayner, D. D. M. *J. Am. Chem. Soc.* **1999**, *121*, 11513–11515.

small peak at ~1710 cm^{-1} was observed in all IR spectra, also of the monolayers of **I–III**. The origin of this signal is, at present, unknown.[V] Refunctionalization of the original ester surface is thus easily achieved. This observation also confirms that the ester groups do not react with the hydrogen-terminated surface and shows that the methyl ester **VI** gives an ordered monolayer.[49]

Hydrolysis of the acetate surface (**VIII**) was expected to yield the hydroxy-terminated surface. Surprisingly, no changes were observed in either infrared spectra or contact angles after a reaction in boiling acidic water for 20 min. Replacing the water for ethanol lowered the contact angles by a few degrees to $\Theta_{a/r}$ = 71/62° after 20 min, but longer reaction times had no further effect. Apparently the ester groups are not accessible and hydrolysis is not possible.

In contrast, reduction of the acetate surface (**VIII**) with $LiAlH_4$ (boiling ether, 15 min) does give the hydroxyl-terminated surface. A very hydrophilic surface is obtained directly after cleaning the modified surface with water, ethanol, and dichloromethane, with contact angles of about 20°, as estimated from small drops of water that were placed on the slightly tilted silicon sample. Measurement by the Wilhelmy plate-method (see Experimental Section) showed a large hysteresis: $\Theta_{a/r}$ = 59/40°, confirming that the surface is more hydrophilic and that the acetate groups were removed. Infrared spectroscopy showed methylene stretching vibrations at 2923 and 2854 cm^{-1}, and the complete disappearance of the C=O vibration, in line with the complete reduction of the ester moiety.

3.3.4 Determination of Tilt Angles

More information about the precise structure of the monolayers can be obtained from the combination of the results from X-ray reflectivity and infrared dichroism. An average tilt angle, with respect to the surface normal, of the molecules in the monolayer can be calculated from the monolayer thickness as obtained from X-ray reflectivity, combined with the chain length of the molecule in the monolayer. The same tilt angle can be obtained from the results of infrared dichroism, if the infrared spectra are measured with s- and p-polarized light. The difference between the absolute absorptions of a certain vibration allows for the determination of this angle, using the formulas in the experimental section. Usually, the methylene stretching vibrations are used. Unfortunately, the error in the absolute absorbances can be as large as ±10%, which makes this method often quite inaccurate.[6] This error is also strongly

[V] The origin of this peak arises from Si–O vibrations within the Si crystals, the amount of which can vary slightly from crystal to crystal. This problem has later been solved by the manufacturer and new ATR crystals are now free of these Si–O vibrations. Private communication from Harrick Scientific, Co.

affected by the variation in the absolute absorbances as a result of differences in the amount of absorbed contaminants on the background or the sample.[50] This can become an important factor for thin monolayers (e.g., monolayer of **III**), and for surfaces with polar groups, like **VI** and **VIII**, which get contaminated upon prolonged exposure to air. A second problem is the large dependency of α on the variation of D in the regions where $D \approx 1$ and $D \approx 0$, corresponding to molecules that are oriented perpendicular and parallel to the surface, respectively.

Table 4. Tilt angles for alkyl monolayers of **I–III** on Si(100).[a]

Monolayer	A_a^{s-pol} / A_a^{p-pol}	α_a **(deg)**	A_s^{s-pol} / A_s^{p-pol}	α_s **(deg)**	Φ_{IR} **(deg)**	$\Phi_{X\text{-}ray}$ **(deg)**
I	0.071	72	0.047	90	18	29
	0.068		0.042			
II	0.074	64	0.042	63	39	26
	0.075		0.043			
III	0.0089 [b]	58	0.0067 [b]	90	32	26
	0.0096 [b]		0.0058 [b]			

Note: [a] $A_a^{s-pol,p-pol}$, absorbance of antisymmetric methylene stretching vibration using polarized light. $A_s^{s-pol,p-pol}$, absorbance of symmetric methylene stretching vibration using polarized light. α, angle between the surface normal and the symmetric or antisymmetric CH_2 dipole moment (see also Experimental Section). An α of 90° is assigned to dichroic ratios $D >$ 1.1. Φ_{IR}, calculated tilt angle from IR-dichroism. $\Phi_{X\text{-}ray}$, calculated tilt angle from X-ray reflectivity. [b] Large uncertainty in the absorbances (see Table 1).

Assuming that all the C–C bonds of the alkyl chain are in the *trans*-geometry, the film thicknesses of monolayers of **I–III** in Table 2 correspond to a constant tilt angle $\Phi_{X\text{-}ray}$ of 27 ± 1.5°, calculated using the following expression:[6]

$$\Phi_{X\text{-}ray} = \cos^{-1}[(d - 0.77)/(2.52\,(n - 1)/2)]$$

where d is the measured film thickness, and 2.52 Å is the distance between next-nearest carbons in an alkyl chain with n carbon atoms, and 0.77 Å is the covalent bond radius for C in a Si–C bond on the substrate.[51] In the above formula for $\Phi_{X\text{-ray}}$ it is assumed that the Si–C bond is perpendicular to the silicon surface. From a ball-and-stick model of the Si(100) surface it is evident that this is not correct. However, variation of the Si–C bond angle with respect to the surface normal changes the resulting tilt angle of the alkyl chain by only 1–2 degrees. This makes the above expression useful for the calculation of the approximate tilt angle, taking into account the uncertainty of ±0.2 Å in the monolayer thickness.

An estimated tilt angle for the alkyl chains of monolayers of **I**–**III** can also be obtained from the IR dichroism data. The resulting angles, Φ_{IR}, are listed in Table 4. For some monolayers, the dichroic ratio of the symmetric methylene stretching vibrations was found larger than 1.1, which gives unfeasible results in the calculation of α. A value for α of 90° was taken in these cases, because the value for α changes very rapidly for $D > 1$ and there is a large variation in D with changes of only a few percent in the measured absorbance. The tilt angles determined from the IR-dichroism vary between 18° and 39°. Though this is consistent with the results from X-ray reflectivity, such scattered values prevent to draw any conclusion from a combination of the two techniques.

X-ray reflectivity studies of arachidic acid on water indicate that the aliphatic tails are predominantly in the all-*trans* configuration and uniformly tilted.[52] The tilt angle decreases continuously with decreasing area per molecule from 33° at 24 Å^2/molecule to 0° at 20 Å^2/molecule. Assuming that the tilt of the chains is completely determined by Van der Waals interactions, a constant tilt angle of 27° suggests that the area/molecule is close to 24 Å^2/molecule and that not all surface Si-atoms are bonded to an alkyl chain. Another indication for this comes from the similar film thickness and electron density of **I** on the Si(100) and Si(111) surface. On the Si(111) surface only 50% of the silicon atoms is bonded to an alkyl chain.[6] Although the Si(100) surface has a different structure and subsequently a different surface density of silicon atoms, it is still not possible to occupy all silicon atoms, as can be easily seen with a ball-and-stick model of the surface.

Reflectivity data for **VIII** also show a smooth film on Si(100). The film thickness of 16.40 Å, as calculated by the three-layer model, is comparable to the total chain length of the molecule. After subtraction of 0.77 Å for the covalent radius of the surface carbon atom, a tilt angle of 17° is found. The big ester functionality at the outside of the monolayer could force the alkyl chains to a more perpendicular orientation with respect to the surface.

3.4 Conclusions

The results presented above show that closely packed, well-ordered monolayers can be obtained by heating of a hydrogen-terminated Si(100) surface to 200 °C in the presence of a 1-alkene. The monolayers prepared from long-chain alkenes (compounds **I**–**III**) are similar to those prepared on the Si(111) surface,[6] as evidenced by infrared spectra and X-ray reflectivity measurements. The advancing contact angles for water are similar as well, but the receding angles are somewhat lower, which is the result of surface roughness. It is well known that, unlike the hydrogen-terminated Si(111) surface, the Si(100) surface is not atomically flat and consists of SiH, SiH_2 and SiH_3 groups.[53] Despite this surface roughness, dense monolayers can still be prepared. Stable monolayers can be formed over a wide range of alkyl chain lengths, as, e.g., the relatively short dodecene molecules (**III**) form an ordered monolayer. This shows that in this respect the monolayers are comparable to those of *n*-alkyl thiols on gold, which are ordered for $n > 9$,[26] and the monolayers on silicon oxide, which give ordered structures for alkyl chains that contain at least 12 methylene groups.[54]

The possibility to use ω-functionalized alkenes opens the way to many interesting applications of this new method for monolayer preparation. However, dense monolayers can not be obtained in all cases. Functional groups that can react with the hydrogen-terminated surface, like carboxylic acids (**IV**) and alcohols (**V**), give rise to disordered or even very poorly ordered monolayers. In contrast, well-ordered monolayers are obtained with the ester-protected analogues of these compounds (compounds **VI**, **VII**, and **VIII**). Enough space for the ester groups is available at the outside of the monolayer to allow for a dense packing. The observed contact angles show that the ester groups are indeed at the outside of the monolayer.

Because of the exceptional stability of the monolayers, when compared to the monolayers on gold and on silicon oxide, the protecting groups can be removed or modified, even when high temperatures are necessary. The conversion of the methyl ester-terminated surface of **VI** into that of the corresponding propyl ester (**VII**) proceeds smoothly and without any noticeable damage to the monolayer. The resulting surface was identical to that prepared directly from **VII**, which confirms that esters do not react with the hydrogen-terminated surface and that the functional groups are indeed at the outside of the monolayer. This provides a completely new pathway to the preparation of many functionalized surfaces that are currently not accessible.

The monolayers prepared from the allyl esters **IX** and **X** indicate that, unlike at the outside of the monolayer, not enough space is available for the ester groups near the silicon surface. Consequently, disordered monolayers are obtained.

References and Notes

[1] Ulman, A. *Chem. Rev. (Washington, D.C.)* **1996**, *96*, 1533–1554.

[2] Ulman, A. *An Introduction to Ultrathin Organic Films*; Academic Press: Boston, MA, USA, 1991.

[3] Tillman, N.; Ulman, A.; Penner, T. L. *Langmuir* **1989**, *5*, 101–111.

[4] Calistri-Yeh, M.; Kramer, E. J.; Sharma, R.; Zhao, W.; Rafailovich, M. H.; Sokolov, J.; Brock, J. D. *Langmuir* **1996**, *12*, 2747–2755.

[5] Linford, M. R.; Chidsey, C. E. D. *J. Am. Chem. Soc.* **1993**, *115*, 12631–12632.

[6] Linford, M. R.; Fenter, P.; Eisenberger, P. M.; Chidsey, C. E. D. *J. Am. Chem. Soc.* **1995**, *117*, 3145–3155.

[7] Terry, J.; Linford, M. R.; Wigren, C.; Cao, R.; Pianetta, P.; Chidsey, C. E. D. *Appl. Phys. Lett.* **1997**, *71*, 1056–1058.

[8] Sung, M. M.; Kluth, G. J.; Yauw, O. W.; Maboudian, R. *Langmuir* **1997**, *13*, 6164–6168.

[9] For some recent examples see: (a) Roscoe, S. B.; Kakkar, A. K.; Marks, T. J.; Malik, A.; Durbin, M. K.; Lin, W.; Wong, G. K.; Dutta, P. *Langmuir* **1996**, *12*, 4218–4223. (b) Collins, T. J.; Tae Bae, I.; Scherson, D. A.; Sukenik, C. N. *Langmuir* **1996**, *12*, 5509–5511. (c) Roscoe, S. B.; Yitzchaik, S.; Kakkar, A. K.; Marks, T. J.; Xu, Z.; Zhang, T.; Lin, W.; Wong, G. K. *Langmuir* **1996**, *12*, 5338–5349. (d) Lin, W.; Lee, T.-L.; Lyman, P. F.; Lee, J.; Bedzyk, M. J.; Marks, T. J. *J. Am. Chem. Soc.* **1997**, *119*, 2205–2211.

[10] For some recent examples see: (a) Fragneto, G.; Lu, J. R.; McDermott, D. C.; Thomas, R. K.; Rennie, A. R.; Gallagher, P. D.; Satija, S. K. *Langmuir* **1996**, *12*, 477–486. (b) Madoz, J.; Kuznetzov, B. A.; Medrano, F. J.; Garcia, J. L.; Fernandez, V. M. *J. Am. Chem. Soc.* **1997**, *119*, 1043–1051. (c) Heise, A.; Menzel, H.; Yim, H.; Foster, M. D.; Wieringa, R. H.; Schouten, A. J.; Erb, V.; Stamm, M. *Langmuir* **1997**, *13*, 723–728. (d) Silin, V.; Weetall, H.; Vanderah, D. J. *J. Colloid Interface Sci.* **1997**, *185*, 94–103. (e) Petrash, S.; Sheller, N. B.; Dando, W.; Foster, M. D. *Langmuir* **1997**, *13*, 1881–1883.

[11] (a) The literature value for 10-undecylenic acid methyl ester is 124 °C at 10 mmHg,[11b] a suspicious value when compared to the ethyl ester, which has 131.5 °C at 16 mmHg.[11b] The methyl ester has been prepared several times and displayed a bp between 113 °C (10 mmHg) and 116 °C (12 mmHg) in all cases, which was not affected by repeated distillation. Because no impurities could be found upon

GC-analysis, it is assumed that the literature value is incorrect. (b) *Handbook of Chemistry and Physics*, 52nd ed.; The Chemical Rubber Co.: Cleveland, OH, USA, 1971.

[12] *Beilstein Handbook of Organic Chemistry*, 4th ed. (abbreviated as Beilstein); Springer Verlag: Berlin, Germany, vol. **2**, supplementary series III, p 1364. This ester shows the same large difference in boiling points as the methyl ester, but again NMR and GC-analysis showed no impurities.

[13] Beilstein, vol. **2**, supplementary series II, p 152.

[14] Beilstein, vol. **2**, supplementary series III, p 887.

[15] Beilstein, vol. **2**, supplementary series III, p 1019.

[16] Frantz P.; Granick, S. *Langmuir* **1992**, *8*, 1176–1182.

[17] Brunner, H.; Vallant, T.; Mayer, U.; Hoffmann, H. *Langmuir* **1996**, *12*, 4614–4617.

[18] Ramé, E. *J. Colloid Interface Sci.* **1997**, *185*, 245–251 (erratum see *189*, 383).

[19] The fringes that appear in the infrared spectra are due to minor variations between the position and the size of the ATR-samples and the background. It is possible to remove these fringes by applying a mathematical correction on the obtained interferogram. The band positions are not affected, but the intensities of the bands are lowered. The correction was only applied to the carbonyl stretching region. Nissink, J. W. M. Ph.D. Thesis, Utrecht University, January 1999.

[20] Tillman, N.; Ulman, A.; Schildkraut, J. S.; Penner, T. L. *J. Am. Chem. Soc.* **1988**, *110*, 6136–6144.

[21] Linford, M. R. Ph.D. Thesis, Stanford University, 1996.

[22] Haller, G. L.; Rice, R. W. *J. Phys. Chem.* **1970**, *74*, 4386–4393.

[23] Higashiyama, T.; Takenaka, T. *J. Phys. Chem.* **1974**, *78*, 941–947.

[24] Mol, E. A. L.; Schindler, J. D.; Shalaginov, A. N.; de Jeu, W. H. *Phys. Rev. E* **1996**, *54*, 536.

[25] Ulman, A., reference 2, p 253.

[26] Bain, C. D.; Troughton, E. B.; Tao, Y.-T.; Evall, J.; Whitesides, G. M.; Nuzzo, R. G. *J. Am. Chem. Soc.* **1989**, *111*, 321–335.

[27] Bain, C. D.; Evall, J.; Whitesides, G. M. *J. Am. Chem. Soc.* **1989**, *111*, 7155–7164.

[28] Ulman, A., reference 2, p 53, and references cited therein.

[29] Snyder, R. G.; Strauss, H. L.; Elliger, C. A. *J. Phys. Chem.* **1982**, *86*, 5145–5150.

[30] Porter, M. D.; Bright, T. B.; Allara, D. L.; Chidsey, C. E. D. *J. Am. Chem. Soc.* **1987**, *109*, 3559–3568.

[31] Pomerantz, M.; Segmüller, A.; Netzer, L.; Sagiv, J. *Thin Solid Films* **1985**, *132*, 153–162.

[32] Engquist, I.; Lestelius, M.; Liedberg, B. *Langmuir* **1997**, *13*, 4003–4012

[33] Hostetler, M. J.; Stokes, J. J.; Murray, R. W. *Langmuir* **1996**, *12*, 3604–3612.

[34] Evans, S. D.; Evall, J.; Whitesides, G. M. *J. Am. Chem. Soc.* **1989**, *111*, 7155–7164

[35] Cheng, S. S.; Scherson, D. A.; Sukenik, C. N. *Langmuir* **1995**, *11*, 1190–1195.

[36] Lee, E. J.; Ha, J. S.; Sailor, M. J. *J. Am. Chem. Soc.* **1995**, *117*, 8295–8296.

[37] Lee, E. J.; Bitner, T. W.; Ha, J. S.; Shane, M. J.; Sailor, M. J. *J. Am. Chem. Soc.* **1996**, *118*, 5375–5382.

[38] Green, W. H.; Lee, E. J.; Lauerhaas, J. M.; Bittner, T. W.; Sailor, M. J. *Appl. Phys. Lett.* **1995**, *67*, 1468–1470.

[39] Bitzer, T.; Alkunshalie, T.; Richardson, N. V. *Surf. Sci.* **1996**, *368*, 202–207.

[40] Cleland, G.; Horrocks, B. R.; Houlton, A. *J. Chem. Soc. Faraday Trans.* **1995**, *91*, 4001–4003.

[41] Kim, N. Y.; Laibinis, P. E. *J. Am. Chem. Soc.* **1997**, *119*, 2297–2298.

[42] Clegg, R. S.; Hutchison, J. E. *Langmuir* **1996**, *12*, 5239–5243.

[43] For an explanation of X-ray specular reflection analysis of thin layers see, e.g.: (a) Wasserman, S. R.; Whitesides, G. M.; Tidswell, I. M.; Ocko, B. M.; Pershan, P. S.; Axe, J. D. *J. Am. Chem. Soc.* **1989**, *111*, 5852–5861. (b) Tidswell, I. M.; Ocko, B. M.; Pershan, P. S.; Wasserman, S. R.; Whitesides, G. M.; Axe, J. D. *Phys. Rev. B* **1990**, *41*, 1111–1128.

[44] Russell, T. *Mat. Sci. Reports* **1990**, *5*, 171–271.

[45] Ewen, B.; Strobl, G. R.; Richter, D. *Faraday Discuss. Chem. Soc.* **1980**, *69*, 19–31.

[46] Asmussen, A.; Riegler, H. *J. Chem. Phys.* **1996**, *104*, 8151–8158.

[47] Fryxell, G. E.; Rieke, P. C.; Wood, L. L.; Engelhard, M. H.; Williford, R. E.; Graff, G. L.; Campbell, A. A.; Wiacek, R. J.; Lee, L.; Halverson, A. *Langmuir* **1996**, *12*, 5064–5075.

[48] Wasserman, S. R.; Tao, Y.-T.; Whitesides, G. M. *Langmuir* **1989**, *5*, 1074–1087.

[49] This monolayer has also been analyzed by X-ray reflectivity, using a commercially available 2 kW instrument (STOE&CIE GmbH, Darmstadt, Germany). A thickness of 13 Å was found, in agreement with the chain length of this molecule and therefore indicative of a well-ordered monolayer. However, the X-ray reflectivity profile could not be measured accurately, because of a considerable contribution of the background to the signal intensity from approximately $Q = 0.35$, resulting in incorrect interface roughnesses ($\sigma_2 = 4$, $\sigma_3 = 0$) and an unreasonably high electron density of 0.42 $e^-/Å^3$.

[50] Care should be taken that the observed band heights are not altered as a result of contamination of the background crystal, a process that is quite fast. Small differences from background to background —and thus in the reported absolute absorbances of monolayers **I–III**— cannot be excluded, and the results from the dichroic ratio measurements should always be interpreted with caution.

[51] This value is slightly different from that previously used in reference 6, in which 1.86 Å, corresponding to the Si–C bond length, was subtracted. Although a significant effect on the calculated tilt angle results (an increase of ca. 4°), the present approach is probably more reasonable, since the electron density will gradually change in the Si–C bond and not abruptly at the silicon surface. The film thickness as measured by X-ray reflectivity corresponds to the region between the air/monolayer interface and the monolayer/substrate interface. Since the latter interface is in the Si–C bond, the covalent radius of the Si-atom is not included in the measured film thickness. See also references 43a and 43b.

[52] Kjaer, K.; Als-Nielsen, J.; Helm, C. A.; Tippman-Krayer, P.; Möhwald, H. *J. Phys. Chem.* **1989**, *93*, 3200–3206.

[53] Dumas, P.; Chabal, Y. J.; Jakob, P. *Surf. Sci.* **1992**, *269/270*, 867–878.

[54] Hoffmann, H.; Mayer, U.; Krischanitz, A. *Langmuir* **1995**, *11*, 1304–1312.

Chapter 4

1-Alkene Monolayers on the Hydrogen-Terminated Si(100) Surface: Solvent Effects [I]

Abstract

The possibility to use dilute alkene solutions for the formation of alkene monolayers with 1-hexadecene on a hydrogen-terminated Si(100) surface has been investigated for a variety of solvents. The resulting monolayers were analyzed by water contact angles. Anisole, n-butylbenzene, and n-decane were found to be unsuitable solvents for monolayer preparation at all 1-hexadecene concentrations used. At high 1-hexadecene concentrations (25% and 10% (v/v)) well-ordered monolayers were formed in toluene, xylene (mixture of isomers), cumene, t-butylbenzene, and mesitylene. Only with mesitylene high-quality monolayers are feasible even at significantly lower alkene concentrations (down to 2.5%), making this the solvent of choice. The newly described procedure reduces the amount of alkene needed to form well-ordered monolayers by a factor of 20–40 in comparison with the original procedure that requires neat alkenes.

[I] A slightly modified version of this Chapter has been published:
A. B. Sieval, V. Vleeming, H. Zuilhof, and E. J. R. Sudhölter *Langmuir* **1999**, *15*, 8288–8291.

4.1 Introduction

In Chapter 3 the preparation of organic monolayers on a hydrogen-terminated Si(100) surface has been described using a thermal reaction between a 1-alkene and a H-terminated Si(100) surface. Although this reaction has been shown to work very well, a drawback of the current procedure is the required use of neat 1-alkene for the monolayer preparation. Consequently, large amounts of the 1-alkene are needed for the modification of the silicon substrates, whereas only a very small fraction of the alkene is actually consumed in the reaction. Thus, a major improvement would be the possibility to use a solution of the 1-alkene in a suitable organic solvent. This will considerably broaden the scope of the reaction, especially in the area of functionalized monolayers, as smaller amounts of the –often expensive or difficult to synthesize– functional 1-alkene are required. Although in one case solutions of 1-alkenes and 1-alkynes in toluene have been used,[1] no systematic investigation has been performed of the effect of the solvent on the quality of the resulting monolayer.

In the case of neat 1-alkenes, *well-ordered* monolayers on hydrogen-terminated crystalline silicon surfaces can only be prepared at temperatures around or above 150 °C,[2,3] which indicates solvents with a high boiling point are required. In this Chapter, the preparation of hexadecyl monolayers on the hydrogen-terminated Si(100) surface is reported from refluxing solutions of 1-hexadecene in various, mostly aromatic solvents. Toluene, xylene (mixture of isomers, as well as the separate *o*-, *m*-, and *p*-isomers), cumene, anisole, mesitylene (1,3,5-trimethylbenzene), *t*-butylbenzene and *n*-butylbenzene were used as the aromatic solvents. As non-aromatic solvent *n*-decane was used. 1-Hexadecene was chosen as the 1-alkene in this study, as the resulting monolayer has a sensitive quality probe: even a slight disorder in the resulting monolayers can already be easily detected via significantly smaller water contact angles of the monolayers.[2,3,4,5] Although water contact angle measurements alone can not be used to determine whether or not a monolayer is well-ordered, water contact angles are an easy, rapid tool to compare otherwise identical monolayers that are prepared under different conditions.[4,5,6] In addition, the results can be compared to the known contact angles of the well-ordered hexadecyl monolayer on Si(100) as previously prepared using neat 1-hexadecene,[4] thus giving an indication about the quality of the monolayer. This monolayer showed an advancing water contact angle of $\Theta_a = 109°$ and a receding angle of $\Theta_r = 95°$.

4.2 Experimental Details

Generally, the quality of the monolayer decreases fast with lower purity of the solvent, and purification, e.g., by distillation, of the commercially available chemicals is nearly always required. Toluene (Acros, 99%), xylene (Merck, mixture of isomers), *o*-xylene (Acros, 99%), *m*-xylene (Acros, 99+%), *p*-xylene (Acros, p.a.), cumene (Acros, 99%), and anisole (Aldrich, 99%) were distilled at atmospheric pressure. *t*-Butylbenzene (Merck, 99%), mesitylene (1,3,5-trimethylbenzene, Acros, 99%), *n*-butylbenzene (Aldrich, 99%), and *n*-decane (Acros, 99+%) were distilled at reduced pressure. All distilled solvents were stored on NaOH pellets. 1-Hexadecene (Acros, 94%) was distilled in vacuo to partially remove lower-boiling isomers and polymeric material and stored at 4 °C. The resulting distillate has a purity of ~97% (GC). The silicon substrates were pieces of double polished silicon (Si(100), n- or p-type, 250 μm thickness).

To prepare the monolayers, 10 ml of the alkene solution was placed in a small, three-necked flask fitted with a nitrogen inlet, a condenser with a $CaCl_2$ tube, and a thermometer. The solution was deoxygenated with dry nitrogen for at least 1 h. Subsequently, a piece of silicon was etched in 2.5% hydrofluoric acid for 2 min and immediately placed in the solution, temporarily removing the thermometer under vigorous N_2 flow. The solution was then refluxed by placing the flask in an oil bath of 210 °C for 2 h (220 °C for *n*–decane and *n*-butylbenzene), while nitrogen was slowly bubbled through the solution to prevent bumping. (In this set-up the nitrogen inlet should preferably be just below the surface of the liquid to minimize the possibility of damaging the forming monolayer by the relatively large nitrogen bubbles). It was observed that non-refluxing solutions sometimes gave monolayers of lower quality. After cooling to room temperature, the modified substrate was removed from the solution and cleaned by subsequent rinsing in petroleum ether (40–60 °C), ethanol, and dichloromethane.[4] All experiments were performed in triplicate. The water contact angles were measured as described previously.[4] The reproducibility of the contact angles is ±1° for the well-ordered monolayers ($\Theta_a > 104°$, $\Theta_r > 93°$) and ±2–3° for monolayers of lower quality, as these tend to yield more significant differences in the quality of the monolayer from one experiment to the other.

Computed BDE were obtained from restricted (closed-shell species) and unrestricted (radicals) B3LYP/6-311+G(d,p) computations with the Gaussian 94 suite of programs, using the functional and basis set as implemented in there.[7]

4.3 Results and Discussion

The quality of the 1-hexadecene monolayers as obtained from 10% (v/v) solutions of the alkene in various solvents is shown in Table 1. It is evident that not all solvents used are suitable for monolayer preparation, although their boiling points (110–183 °C) are such that in refluxing solutions the thermal energy necessary for the preparation of well-ordered monolayers is available.[2,3] Also, no clear trend exists with respect to the boiling point of the solvent, as can for example be concluded from the observation that xylene gives better monolayers than *n*-butylbenzene.

Table 1. Water contact angles (in °) of 1-hexadecene monolayers obtained from 10% (v/v) solutions in various solvents.[a]

Solvent	**Boiling Point (°C)**	Θ_a	Θ_r
n-Decane	174	105	93
n-Butylbenzene	183	102	88
Anisole	154	104	92
Toluene	110	107	94
Xylene (mixture of isomers)	140	107	96
Cumene	154	107	96
t-Butylbenzene	167	108	97
Mesitylene	166	109	98
Neat 1-hexadecene (reference)	–	109	95

[a] Note: The uncertainty in the water contact angles is ±1° for the well-ordered monolayers (Θ_a > 104°, Θ_r > 93°) and ±2–3° for monolayers of lower quality.

n-Decane initially gave contact angles of Θ_a = 108° and Θ_r = 97°, which are indicative of well-ordered monolayers. However, upon heating the modified substrates in ethanol for ca. 1 h, the contact angles decreased by several degrees to Θ_a = 105° and Θ_r = 93° and also decrease gradually by a few degrees during the measurements. This decrease, which is

generally found for disordered hydrophobic monolayers, indicates that physically adsorbed molecules have been removed from the monolayer and pinholes are created. As monolayers prepared using neat 1-alkene are stable under these conditions,[2,4] unbound decane molecules, which resemble 1-hexadecene in terms of molecular composition and structure, have apparently been initially trapped in the monolayer due to favorable Van der Waals interactions. This will hamper the proper arrangement of the alkene molecules in the monolayer, and consequently many pinholes are formed after evaporation or extraction of decane. Prolonged heating of the substrate in an appropriate solvent is therefore a requirement for the assessment of the long-term quality of the monolayer. The incorporation of aliphatic solvent molecules has also been observed for octadecyl monolayers prepared on H-terminated Si(111) surfaces using UV-irradiation, where disordered monolayers were obtained in the case of a 1-octadecene/hexadecane mixture (9 : 1).[8] A similar situation occurs with the use of *n*-butylbenzene, which gives as water contact angles Θ_a = 102° and Θ_r = 88° (Table 1). Comparison with the data obtained for the reference monolayer produced with the neat 1-hexadecene shows that also this solvent yields disordered monolayers. Since *t*-butylbenzene (*vide infra*) does yield high-quality monolayers, the relatively long aliphatic alkyl chain is suspected to hamper the monolayer formation. Therefore, aromatic solvents without long flexible groups in combination with sufficiently high boiling points were investigated.

Toluene, xylene (mixture of isomers), cumene, anisole, *t*-butylbenzene, and mesitylene all gave ordered monolayers as 10% (v/v) alkene solutions (i.e., both Θ-values within 5° of the reference layer; see Table 1). As this opened up the possibility of a significantly smaller use of alkene, a detailed investigation of the effects of these solvents on variation of the 1-hexadecene concentration was performed. The advancing and receding water contact angles as observed for these monolayers are shown in Figure 1. In all cases the monolayers were prepared using three or four different 1-hexadecene concentrations: 25%, 10%, 5%, and 2.5% (v/v).

It is clear that despite its boiling point anisole is not a suitable solvent. Even at the high 1-hexadecene concentration of 25% (v/v) the observed contact angles (Θ_a = 104°, Θ_r = 93°) are lower than those of the reference layer. Apparently, anisole interferes with the monolayer formation reaction, which is assumed to be a radical-based process that starts at a defect (e.g., a dangling bond) at the H-terminated surface.[2] A possible explanation for this interference is that the Si radical sites that are necessary for the initiation and propagation of the reaction are destroyed by a reaction with anisole. The O–CH_3 bond in anisole has a

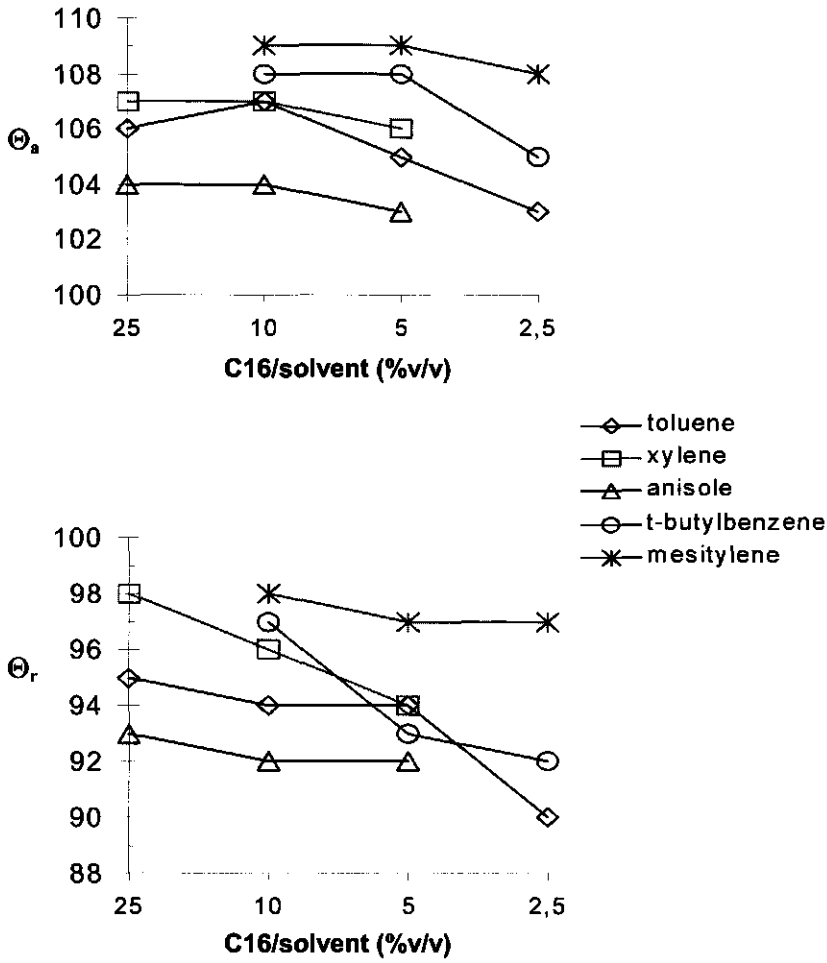

Figure 1. Advancing (top) and receding (bottom) water contact angles of the hexadecene monolayers prepared at various concentrations in the selected aromatic solvents. Note: The uncertainty in the water contact angles is ±1° for the well-ordered monolayers (Θ_a > 104°, Θ_r > 93°) and ±2–3° for monolayers of lower quality.

relatively low bond dissociation energy (BDE) of only 64 kcal mol^{-1},[9] which was confirmed by B3LYP/6-311+G(d,p) computations (computed BDE = 62.1 kcal mol^{-1}). This bond can thus be cleaved thermally, which results in the formation of a methyl and a phenoxy radical. Also, anisole can react with organic radicals, like the alkyl radicals formed during the

propagation step of the monolayer formation, which results in the formation of various reactive organic radicals.[9a] All these radicals can react with radical sites at the silicon surface (yielding, e.g., methyl or phenoxy groups at the surface), and, thus, cause defects at the silicon surface that hamper the formation of an ordered hexadecyl monolayer. Alternatively, the formed radicals can also abstract hydrogen atoms from the silicon surface, thereby creating new reactive sites. In the case of phenoxy radical the hydrogen atom abstraction from a Si–H bond at the surface is exothermic, as the BDE of the OH group in phenol (measured values: 84 – 88 kcal mol^{-1};[10] computed with B3LYP/6-311+G(d,p), 89.7 kcal mol^{-1}) is larger than the BDE of a Si–H bond on the silicon surface (approximately 80 kcal mol^{-1}).[8] This will generate a new reactive site and allows formation of the monolayer to continue. In the case of the alkyl-substituted benzenes, such hydrogen atom abstraction reactions cannot occur, as the weakest bond in these solvent molecules is the C–H bond in the alkyl group (BDE = 88 kcal mol^{-1};[11] computed with B3LYP/6-311+G(d,p), 93.7 kcal mol^{-1}), which is already stronger than the Si–H bond. Consequently, the monolayer formation is in the case of alkylated benzenes as solvents not influenced by these side-reactions between solvent molecules and the silicon surface.[12] In line with this, all these alkyl-substituted benzene derivatives, with the exception of *n*-butylbenzene (*vide supra*), give ordered monolayers (see Table 1).

If toluene or xylene is used as solvent ordered monolayers are obtained at high 1-hexadecene concentrations (25% and 10% (v/v)). However, at lower 1-hexadecene concentrations, monolayers of lower quality are obtained, as is evident from the decreasing advancing and receding contact angles (Figure 1). This indicates that at lower alkene concentrations the solvent molecules increasingly interfere with the monolayer formation process. Given the reduced possibility of hydrogen-atom abstraction from these methyl-substituted aromatic solvents in comparison to anisole (*vide supra*) and the success of using other methyl-group containing aromatic solvents (*vide infra*), the shape of the solvent molecules apparently interferes with monolayer formation. These relatively small solvent molecules fit quite well within the final small areas that have to be filled to make a well-ordered monolayer. Once these solvent molecules block surface sites for the 1-hexadecene molecules, pinholes are formed in the monolayer. At high 1-hexadecene concentrations (25% and 10 % (v/v)), this does not occur often, as there are still relatively many alkene molecules available, and, consequently, a well-ordered monolayer with only a few pinholes will be formed. Upon increase of the relative amount of solvent molecules, by using 5% and 2.5% solutions (v/v) of 1-hexadecene, more pinholes are formed in the monolayer, as can be concluded from the decrease of both the advancing and receding water contact angles of these

monolayers (Figure 1). This effect is not related to the low boiling point of these two solvents, as is evident from comparison of these results to monolayers prepared in *n*-butylbenzene (bp = 183 °C), which also gave disordered monolayers at these concentrations (Table 1). This again indicates that, for temperatures > 130 °C, the boiling point of the solvent is not a dominant factor for the successful preparation of the monolayers.

Both mesitylene (1,3,5-trimethylbenzene) and *t*-butylbenzene, two molecules that are slightly larger than xylene,[13] gave well-ordered monolayers at a 1-hexadecene concentration of 10%. At lower 1-hexadecene concentrations, the contact angles of the monolayers prepared in *t*-butylbenzene decrease considerably, to $\Theta_r = 93°$ at a 1-hexadecene concentration of 5%, a value that is comparable to that of the layer prepared in xylene at the same conditions. This was somewhat surprising, since this indicates that, apparently, the *t*-butyl group does not sufficiently increase the size of the solvent molecule[14] and thus seems to give rise to defects in the monolayer by the same mechanism as xylene.

In contrast, monolayers prepared in mesitylene show almost no change in the water contact angles upon decrease of the 1-hexadecene concentration. Even at a 1-hexadecene concentration of 2.5% the observed contact angles of $\Theta_a = 108°$ and $\Theta_r = 97°$ are still similar to those of the monolayer prepared in neat 1-hexadecene, which showed $\Theta_a = 109°$ and $\Theta_r = 95°$.[4] This indicates that the mesitylene molecules are too large to fit efficiently in the pinholes and thus cannot interfere with the monolayer formation process. Consequently, a well-ordered monolayer is formed.

A critical aspect of this procedure using solvents for the monolayer preparation is the minimization of the oxygen concentration in the reaction set-up. This was achieved by refluxing of the solution, and the construction of special glassware in order to minimize the time that the solution is non-refluxing upon introduction of the wafer. As this occurred under fair nitrogen flows from the other end of the set-up, the wafer itself could simply be transferred from the ambient atmosphere into the reaction flask. In this way elaborate glove box procedures were circumvented, without lowering the monolayer quality.

In order to further investigate the effect of the shape of the solvent molecule on the monolayer preparation, the separate use of each of the three xylene isomers was investigated, using 2.5% solutions of the 1-alkene. *Ortho*-, *meta*- and *para*-xylene have the same molecular volume[13] but a somewhat different diameter (5.0, 5.1, and 4.3 Å, respectively). If this minor variation in the molecular shape would cause *p*-xylene to fit better in the forming monolayer, this would lead to more defects, and —at low 1-alkene concentrations— to lower contact

angles compared to those prepared in *o*- and *m*-xylene. In fact, all three xylenes yielded relatively well-ordered monolayers at this concentration, with values of Θ_a = 107° and Θ_r = 97°, without statistically significant differences between the three solvents. In contrast to the values measured for mesitylene, these contact angles do, however, decrease gradually over time. Therefore, the number of defects in the monolayer is somewhat larger when this is prepared using xylenes than by using mesitylene. Again, only prolonged measurements can in this case reveal the quality of the monolayers. This shows that mesitylene (diameter 5.4 Å) is the most suitable solvent for the successful preparation of *well-ordered* monolayers and that the diameter of the solvent molecule is likely to be relevant for the quality of the monolayer formed.

4.4 Conclusions

Well-ordered monolayers of 1-alkenes on hydrogen-terminated silicon surfaces can be prepared from dilute solutions of the 1-alkene in various aromatic solvents. At high alkene concentrations xylene, cumene, *t*-butylbenzene, and mesitylene are all suitable for monolayer preparation. Mesitylene appears as the solvent of choice, as only in this solvent low alkene concentrations can be used (2.5–5 % (v/v)) to form *well-ordered* monolayers on the hydrogen-terminated Si surface.[II] If the boiling point of the alkene is below that of mesitylene, *o*- and *m*-xylene are suitable alternatives. The possibility to use dilute solutions of 1-alkenes in mesitylene for the silicon surface modification process is an important improvement over the currently used procedure to prepare these monolayers, which makes use of neat 1-alkenes. The amount of 1-alkene needed for monolayer preparation is considerably reduced (by a factor 20–40), which broadens the applicability of the reaction, especially in the area of functionalized monolayers.

[II] The procedure described in this Chapter has since successfully been used by other researchers for the modification of hydrogen-terminated germanium surfaces. Interestingly, other reactions than the thermal procedure failed for this surface. See: Choi, C. H.; Buriak, J. M. *Chem. Commun.* **2000**, 1669–1670.

References and Notes

[1] Bateman, J. E.; Eagling, R. D.; Worrall, D. R.; Horrocks, B. R.; Houlton, A. *Angew. Chem., Int. Ed. Engl.* **1998**, *37*, 2683–2685.

[2] Linford, M. R.; Fenter, P.; Eisenberger, P. M.; Chidsey, C. E. D. *J. Am. Chem. Soc.* **1995**, *117*, 3145–3155.

[3] Sung, M. M.; Kluth, G. J.; Yauw, O. W.; Maboudian, R. *Langmuir* **1997**, *13*, 6164–6168.

[4] Sieval, A. B.; Demirel, A. L.; Nissink, J. W. M.; Linford, M. R.; van der Maas, J. H.; de Jeu, W. H.; Zuilhof, H.; Sudhölter, E. J. R. *Langmuir* **1998**, *14*, 1759–1768. (Chapter 3)

[5] Folkers, J. P.; Gorman, C. B.; Laibinis, P. E.; Buchholz, S.; Whitesides, G. M.; Nuzzo, R. G. *Langmuir* **1995**, *11*, 813–824.

[6] Ulman, A. *An Introduction to Ultrathin Organic Films*; Academic Press: Boston, MA, USA, 1991; p 253.

[7] Frisch, M. J.; Trucks, G. W.; Schlegel, H. B.; Gill, P. M. W.; Johnson, B. G.; Robb, M. A.; Cheeseman, J. R.; Keith, T.; Petersson, G. A.; Montgomery, J. A.; Raghavachari, K.; Al-Laham, M. A.; Zakrzewski, V. G.; Ortiz, J. V.; Foresman, J. B.; Cioslowski, J.; Stefanov, B. B.; Nanayakkara, A.; Challacombe, M.; Peng, C. Y.; Ayala, P. Y.; Chen, W.; Wong, M. W.; Andres, J. L.; Replogle, E. S.; Gomperts, R.; Martin, R. L.; Fox, D. J.; Binkley, J. S.; Defrees, D. J.; Baker, J.; Stewart, J. P.; Head-Gordon, M.; Gonzalez, C.; Pople J. A. *Gaussian 94, Revision E.2*; Gaussian, Inc.; Pittsburgh, PA, USA, 1995.

[8] Effenberger, F.; Götz, G.; Bidlingmaier, B.; Wezstein, M. *Angew. Chem., Int. Ed. Engl.* **1998**, *37*, 2462–2464.

[9] (a) Arends, I. W. C. E.; Louw, R.; Mulder, P. *J. Phys. Chem.* **1993**, *97*, 7914–7925. (b) Jonsson, M.; Lind, J.; Reitberger, T.; Eriksen, T. E.; Merényi, G. *J. Phys. Chem.* **1993**, *97*, 8229–8233.

[10] (a) Bordwell, F. G.; Cheng, J.-P. *J. Am. Chem. Soc.* **1991**, *113*, 1736–1743. (b) Bordwell, F. G.; Zhang, X.-M. *Acc. Chem. Res.* **1993**, *26*, 510–517.

[11] McMillen, D. F.; Golden, D. M. *Annu. Rev. Phys. Chem.* **1982**, *33*, 493–532.

[12] It has been suggested, by one of the reviewers of the publication that was written on the basis of the results presented in this Chapter, that the odd behavior of anisole —the only oxygenated solvent in the series investigated— could also be the result of a higher residual water content. As traces of residual water are indeed an important factor in the modification of hydrogen-terminated silicon surfaces, this explanation can currently not be excluded, although distilled anisole was dried over NaOH prior to use.

[13] The free volumes of these solvents as calculated from the MSI-program Cerius^2, version 3.5, using the optimized structures are: xylene 115–116 Å^3 (small differences between the isomers), mesitylene 134 Å^3, and *t*-butylbenzene 152 Å^3.

[14] Although the free volume of *t*-butylbenzene is larger than that of mesitylene,[13] the diameter of the molecule with respect to that of the phenyl ring is only slightly increased by the *t*-butyl group. This group has a diameter of approximately 4.4 Å, which is similar to the diameter of approximately 4.3 Å of a phenyl ring. As mesitylene has a diameter of 5.4 Å, this difference in the width of the two molecules, combined with the presence of a relatively large alkyl group in *t*-butylbenzene, may explain the observed differences between the two solvents at lower 1-hexadecene concentrations.

Chapter 5

Monolayers of 1-Alkynes on the Hydrogen-Terminated Si(100) Surface [1]

Abstract

Monolayers of a series of 1-alkynes, from 1-dodecyne to 1-octadecyne, have been prepared on the hydrogen-terminated Si(100) surface via a thermal reaction of the organic compound with this Si surface. An efficient procedure is presented for the synthesis of 1-alkynes from the corresponding 1-alkenes. The resulting monolayers were characterized by water contact angle measurements, ATR infrared spectroscopy, and X-ray reflectivity. The results show that these 1-alkynes give well-ordered, covalently bonded monolayers, which are at least as ordered as those of the corresponding 1-alkenes.

The exact binding geometry of the 1-alkyne to the Si surface was investigated. The results from IR spectroscopy and X-ray reflectivity measurements indicate that the 1-alkynes form two Si–C bonds to the surface per reacting molecule. Quantum mechanical calculations confirm that this formation of two Si–C bonds is not only chemically possible but also energetically much more favorable than formation of only one Si–C bond per reacting molecule.

[1] A slightly modified version of this Chapter has been published:
A. B. Sieval, R. Opitz, H. P. A. Maas, M. G. Schoeman, G. Meijer, F. J. Vergeldt, H. Zuilhof, and E. J. R. Sudhölter *Langmuir* **2000**, *16*, 10359–10368.

5.1 Introduction

Covalently attached, organic monolayers on silicon surfaces, without the interfacial silicon oxide layer, are an interesting new class of monolayers on solid substrates.[1,2] These monolayers can be prepared by different routes.[2] Probably the easiest and technologically most promising method is the hydrosilylation reaction of 1-alkenes with hydrogen-terminated (H-terminated) Si surfaces (Figure 1). This reaction has been successfully performed on both H-terminated Si(111) [3,4,5] and Si(100) [6,7,8] surfaces, and on porous silicon.[9,10,11,12,13] It results in the formation of a covalently bonded,[14] stable, and well-ordered monolayer on the Si surface. Advantages of this procedure compared to other available routes are that special equipment, like a high-vacuum chamber, is not required, and that 1-alkenes are relatively harmless compounds compared to other reagents, like PCl_5 and Grignard reagents, that are to be used in other wet-chemical procedures.[15] Recently, it was shown that the monolayers can also be prepared with dilute solutions of the 1-alkene in organic (aromatic) solvents. This eliminates the previously required use of neat 1-alkenes and yields a 20–40-fold reduction of the required amount of the organic reagent.[16]

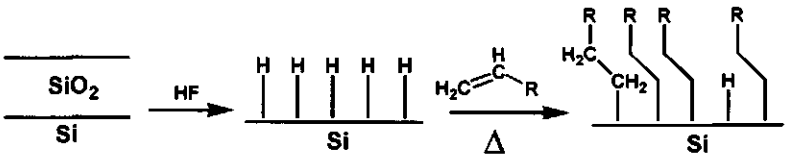

Figure 1. Schematic representation of the reaction of 1-alkenes with a H-terminated silicon surface.

Although most of the research on the hydrosilylation of Si surfaces has been done on 1-alkenes, the reaction works equally well for 1-alkynes.[3,5,9,10,11,12,13] However, so far no systematic investigations have been done on surface modifications with this latter class of compounds. Besides, the monolayers that are reported were also almost all prepared under different conditions. This has resulted in a remarkable observation: the alkyne C≡C bond has been found to react either once[3,5,9,10,11,12] or twice[13] with a surface Si–H group, depending on the reaction conditions used. On the H-terminated Si(111) surface, on which each Si surface atom bears only one hydrogen atom, the peroxide-catalyzed thermal reaction of 1-hexadecyne[3] and the photochemical reaction of 1-octyne and phenylacetylene[5] resulted in

alkenyl groups bound to the surface. A weak C=C stretch vibration was observed with infrared spectroscopy, which was interpreted to indicate the formation of only one Si–C bond per alkyne molecule. The same reactivity of 1-alkynes was reported for porous silicon, if the reaction was induced with an Al catalyst,[9,10,11] with a transition metal catalyst,[10] or with white light.[12] For all these reactions of 1-alkynes on porous silicon a C=C vibration was clearly visible in the IR spectrum of the modified silicon material.

In contrast, the thermal reaction of 1-octyne with porous silicon, this time without any catalyst, has been reported to give two Si–C bonds per molecule, as no alkene vibration was visible with IR spectroscopy.[13] The formation of a certain amount of such doubly bonded structures has also been suggested to occur in the case of the Rh^{I}-catalyzed reaction of 1-alkynes with porous silicon.[10] This 'double reaction' of the C≡C bond is not unlikely, as porous silicon has many SiH_2 and SiH_3 groups, which could easily react twice with the alkyne, especially because of the proposed radical mechanism of the thermal reaction (see Figure 2).[3]

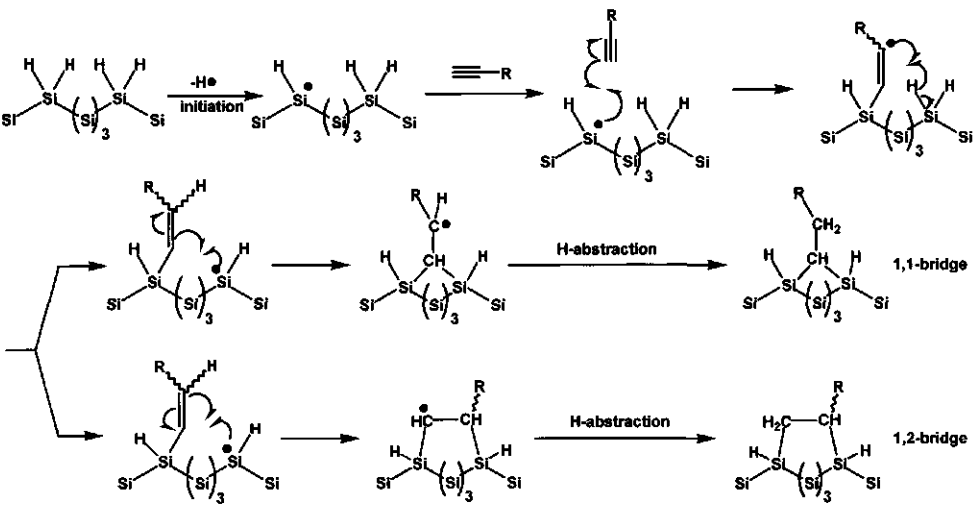

Figure 2. Mechanism of the reaction of a 1-alkyne with a SiH_2-terminated silicon surface, depicting the possible formation of 2 Si–C bonds per reacting organic molecule.

The reason for this difference in reactivity of 1-alkynes is not clear. In the case of the H-terminated Si(111) surface, the second Si–C bond has to be formed to the next-nearest Si surface atom, which would give rise to a five-membered ring structure, in which considerable

deformation of the Si–C bonds is required. This can prohibit the formation of two Si–C bonds per molecule on this surface. However, the reaction of porous silicon with a 1-alkyne can evidently give rise to the formation of two Si–C bonds per reacting 1-alkyne molecule. Thus, such structures can be formed if the reaction proceeds by a mechanism similar to that depicted in Figure 2. The reason such reactivity is observed in the thermal reaction, but is not observed with the light-induced and Lewis acid-catalyzed reactions, is unknown.[2]

There are no reports on the reaction of 1-alkynes with the H-terminated Si(100) surface. This is somewhat surprising, as this surface consists mainly of SiH_2 groups, with small amounts of SiH and SiH_3 groups present,[17] which makes the reactivity of this H-terminated Si(100) surface comparable to that of porous silicon. Thus, it could well serve as a model surface to study the reaction of 1-alkynes under more controlled conditions. In addition, the structure of the H-terminated Si(100) surface is relatively well-known compared to that of porous silicon,[2] which facilitates the interpretation of experimental results.

If 1-alkynes can indeed form two Si–C bonds per molecule, this would also be relevant for an interesting application of monolayers of these compounds. It has been shown that monolayers of 1-alkenes on Si surfaces can be used for surface passivation.[18] Formation of two stable Si–C bonds per molecule, instead of only one as in the case of alkenes, will reduce the number of surface sites for further reactions and is therefore expected to improve the passivation properties.

In this Chapter the first investigation of the thermal reaction of 1-alkynes with the H-terminated Si(100) surface is presented. Four nonfunctionalized 1-alkynes of various lengths were used: 1-octadecyne (**I**), 1-hexadecyne (**II**), 1-tetradecyne (**III**), and 1-dodecyne (**IV**). The properties of the resulting monolayers are compared to those of monolayers of the corresponding 1-alkenes, which are also prepared and investigated. All reactions were performed in refluxing mesitylene, which has been shown to be the solvent of choice for the thermal modification of H-terminated Si surfaces with 1-alkenes.[16] The monolayers were characterized by water contact angle measurements, attenuated total reflection (ATR) infrared spectroscopy, and X-ray reflectivity. To get more insight into the way in which the 1-alkynes are bound to the Si(100) surface, several possible binding structures were also investigated with molecular mechanics and quantum mechanical calculations.

5.2 Experimental

5.2.1 General Information

The 1-alkynes **I–IV** were synthesized according to the procedure described below. All 1-alkynes and 1-alkenes used for monolayer preparations were distilled under reduced pressure and stored at -20 °C, except for 1-octadecyne (**I**), which was recrystallized from methanol and stored at room temperature under vacuum.[19] Mesitylene (Acros, 99%, or Fluka, 99%) was distilled at atmospheric pressure and stored on $CaCl_2$.[20] All glassware for the distillations and the monolayer preparations was cleaned with distilled solvents only. All other chemicals are commercially available and were used as received, unless noted otherwise. The silicon substrates were either pieces of double-polished silicon (Si(100), n-type, 250 μm thickness), shards (~1 x 3 cm) of single-polished silicon (Si(100), n-type, 500 μm thickness), or Si(100) parallelogram plates (ATR-plates) designed for multiple internal reflection spectroscopy (Harrick Scientific, 45°, 50 x 10 x 1 mm^3, 50 reflections).

^1H NMR spectra were recorded in $CDCl_3$ at 200 MHz on a Bruker AC200 FT-NMR spectrometer at ambient temperature; ^{13}C NMR spectra were measured in $CDCl_3$ at 50 MHz. Chemical shifts are in ppm relative to tetramethylsilane. To obtain more reliable integrations of the ^{13}C NMR signals, pulse sequences with a longer relaxation time (T_1 = 12 s) were used. Infrared spectra of the synthesized compounds were recorded on a Biorad FTS-7 infrared spectrophotometer. IR measurements of fluids were performed between NaCl windows, while all solids were measured as solutions in CCl_4. Melting points were determined on a Mettler FP80 HT melting point apparatus. Mass spectra were recorded on a Mat95 GC/MS mass spectrometer. The measurement conditions for the investigation of the monolayers are described below.

5.2.2 Synthesis of the 1-Alkynes

All 1-alkynes were synthesized by the route depicted in Figure 3.[21] The synthesis of 1-hexadecyne (**II**) is described in full detail as an example; the analogous syntheses of the other 1-alkynes are described only briefly, except for the last step in the reaction sequence, for which the procedure differs slightly for each derivative.

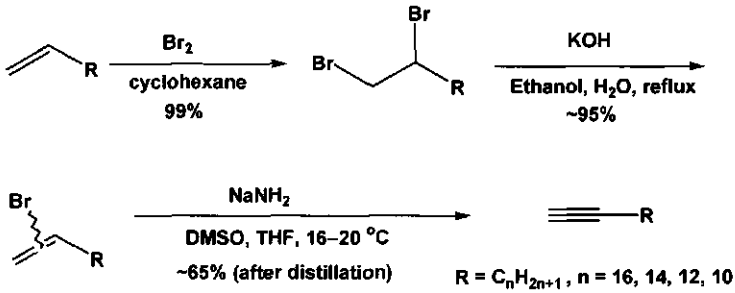

Figure 3. General route for the synthesis of the 1-alkynes.

5.2.2.1 Synthesis of 1-Hexadecyne (II)

1,2-Dibromohexadecane. A solution of 44.8 g (0.20 mol) of 1-hexadecene in 200 ml of dry cyclohexane was cooled to 0 °C. Subsequently, 11.2 ml (35.2 g, 0.22 mol) of bromine was added dropwise at this temperature over 30 min. The resulting dark red mixture was allowed to warm to room temperature and stirred overnight. The solution was washed with 200 ml of a 2% $NaHSO_3$ solution, to remove excess bromine, and with brine, and dried over $MgSO_4$. Evaporation of the solvent yielded the desired 1,2-dibromohexadecane as a yellow oil in 100% isolated yield.

^{1}H NMR: δ 4.25–4.12 (m, 1H), 3.87 (dd, 1H, J = 4.4 Hz, J = 10.2 Hz), 3.64 (dd, appears as t, 1H, J = 10.0 Hz (2x)), 2.20–2.07 (m, 1H), 1.86–1.70 (m, 1H), 1.70–1.25 (br. m, 24H), 0.90 (t, 3H, J = 6.4 Hz). **^{13}C NMR**: δ 53.10, 36.31, 35.99, 31.92, 29.65 (5C), 29.61, 29.53, 29.37, 28.81, 26.74, 22.69, 14.13. **IR** (cm^{-1}): 2923 (m); 2852 (m); 1465 (m); 1436 (m). **MS**: m/z (relative intensity) 41 (44.0), 43 (67.7), 55 (50.6), 57 (100), 69 (39.9), 71 (68.7), 83 (39.8), 85 (47.3), 97 (15.2), 111 (17.7), 226 (12.6), 303 (11.0), 305 (11.1). Exact mass: 303.1687 for $C_{16}H_{32}Br^{+\bullet}$; found 303.1687. No peak corresponding to the $M^{+\bullet}$ of $C_{16}H_{32}Br_2$ was observed.

1/2-Bromo-1-Hexadecene (Mixture of Isomers). A mixture of 77.5 g (0.20 mol) of 1,2-dibromohexadecane, 200 ml of ethanol, 16.8 g (0.30 mol) of KOH, and 20 ml of water was refluxed for 3 h. The reaction mixture was cooled down to ~40 °C and the ethanol was removed by evaporation in vacuo. Subsequently, 50 ml of water and 10 ml of brine were added to the residue. The aqueous layer was extracted with subsequently 200 ml of ether, a mixture of 100 ml of ether and 50 ml of petroleum ether (40–60 °C), and 100 ml of petroleum ether (40–60 °C). The combined organic layers were washed with 50 ml of water and with 50

ml of brine and dried over $MgSO_4$. Evaporation of the organic solvents gave 56.2 g (0.186 mol, 93%) of 1/2-bromo-1-hexadecene (mixture of the three isomers) as a yellow oil.

^{1}H NMR: δ [6.19–5.98 (m) + 5.56–5.55 (m) + 5.39–5.38 (m); total of 2H, relative integral height = ~1.5 : 1 : 1], [2.45–2.39 (m) + 2.26–2.16 (m) + 2.09–2.00 (m); total of 2H, relative integral height = ~1.5 : 1 : 1], 1.60–1.22 (br. m, 24H), 0.90 (t, 3H, J = 6.5 Hz). **IR** (cm^{-1}): 3078 (w); 2925 (m); 2851 (m); 1630 (m); 1464 (m).

1-Hexadecyne (II). In a large, three-necked flask fitted with a mechanical stirrer was placed 23.4 g of sodium amide (0.60 mol). This was dissolved in 120 ml of dry DMSO by stirring the suspension at 60 °C under a nitrogen atmosphere for 1 h. The resulting bluish solution was cooled to room temperature and the flask was placed in a large water bath of ~15 °C. Subsequently, a solution of 56.2 g (0.186 mol) of 1/2-bromo-1-hexadecene (mixture of isomers) in 30 ml of dry THF was added dropwise over 45 min, maintaining the temperature of the water bath between 16 and 20 °C. After the addition was complete, the resulting viscous brown suspension was stirred at 20 °C for another 2 h.

The reaction mixture was mixed with 400 ml of ice water and the aqueous layer was extracted four times with 100 ml of ether. The combined organic layers were washed twice with brine and dried over $MgSO_4$. Evaporation of the solvent gave the crude 1-alkyne as a dark oil. Subsequent distillation gave 29.8 g (0.134 mol, 72%) of 1-hexadecyne (bp 144–145 °C at 12 mmHg; lit. 144 °C at 10 mmHg)[22] as a colorless liquid.

^{1}H NMR: δ 2.18 (dt, 2H, J = 2.6 Hz, J = 6.9 Hz (2x)), 1.93 (t, 1H, J = 2.6 Hz), 1.63–1.20 (br. m, 24H), 0.89 (t, 3H, J = 6.4 Hz). **^{13}C NMR**: δ 84.67, 68.00, 31.94, 29.68 (3C), 29.64, 29.53, 29.39, 29.14, 28.93, 28.78, 28.51, 22.71, 18.39, 14.11. **IR** (cm^{-1}): 3315 (s); 2924 (m); 2853 (m); 2120 (w); 1464 (m). **MS**: m/z (relative intensity) 41 (52.6); 43 (49.9); 55 (48.7); 57 (27.7); 67 (63.8); 69 (26.9); 81 (100); 82 (73.8); 95 (52.3); 96 (57.4). No $M^{+\cdot}$ was observed.

5.2.2.2 Synthesis of 1-Dodecyne (IV)

1,2-Dibromododecane. This reaction was performed as described for 1,2-dibromohexadecane, but on a 0.10 mol scale. The yield of 1,2-dibromododecane was 32.2 g (0.098 mol, 98%).

^{1}H NMR: δ 4.23–4.11 (m, 1H), 3.84 (dd, 1H, J = 4.4 Hz, J = 10.2 Hz), 3.62 (dd, appears as t, 1H, J = 10.0 Hz (2x)), 2.19–2.04 (m, 1H), 1.86–1.67 (m, 1H), 1.60–1.25 (br. m, 16H), 0.89 (t, 3H, J = 6.5 Hz). **^{13}C NMR**: δ 53.07, 36.29, 35.97, 31.88, 29.56, 29.53, 29.38,

29.31, 28.80, 26.73, 22.67, 14.12. **IR** (cm^{-1}): 2953 (m); 2924 (m); 2853 (m); 1464 (m); 1460 (m). **MS**: m/z (relative intensity) 41 (59.3); 55 (69.1); 57 (82.8); 69 (74.1); 71 (72.0); 85 (77.9); 97 (77.2); 111 (68.3); 247 (100); 249 (97.0). Exact mass: 247.1062 for $C_{12}H_{24}Br^{+\bullet}$; found 247.0944. No $M^{+\bullet}$ was observed.

1/2-Bromo-1-Dodecene (Mixture of Isomers). The reaction was performed as described for 1/2-bromo-1-hexadecene, but on a different scale, using 32.2 g (0.098 mol) of 1,2-dibromododecane. The yield was 23.7 g (0.096 mol, 98%) of 1/2-bromo-1-dodecene (mixture of isomers).

^{1}H NMR: δ [6.25–5.97 (m) + 5.56–5.54 (m) + 5.39–5.38 (m); total of 2H, relative integral height = ~1.5 : 1 : 1], [2.45–2.38 (m) + 2.24–2.15 (m) + 2.10–2.00 (m); total of 2H, relative integral height = ~1.5 : 1 : 1], 1.65–1.24 (br. m, 16H), 0.89 (t, 3H, J = 6.8 Hz). **IR** (cm^{-1}): 3075 (w); 2925 (m); 2855 (m); 1628 (m); 1460 (m).

1-Dodecyne (IV). Sodium amide (11.47 g, 0.29 mol) was dissolved in 60 ml of DMSO by heating the suspension under nitrogen at 60 °C for 1 h while stirring. The resulting solution was cooled to room temperature and the reaction flask was placed in a large water bath of 20 °C. Subsequently, 23.7 g (0.096 mol) of 1/2-bromo-1-dodecene (mixture of isomers), dissolved in 10 ml of THF, was added dropwise over 45 min. The resulting solution was stirred at room temperature for 1 h and poured onto 150 ml of ice water. The aqueous layer was extracted three times with 50 ml of ether. The combined organic layers were washed with brine (2x) and dried over $MgSO_4$. Evaporation of the solvent yielded 16.0 g of crude 1-dodecyne as a dark oil. Distillation gave 10.7 g (0.065 mol, 68%) of 1-dodecyne (bp 97–98 °C at 15 mmHg; lit. 95–98 °C at 12 mmHg)[23] as a colorless liquid.

^{1}H NMR: δ 2.16 (dt, 2H, J = 2.6 Hz, J = 6.9 Hz (2x)), 1.93 (t, 1H, J = 2.6 Hz), 1.60–1.24 (br. m, 16H), 0.88 (t, 3H, J = 6.5 Hz). **^{13}C NMR**: δ 84.78, 66.01, 31.90, 29.58, 29.52, 29.33, 29.12, 28.77, 28.50, 22.69, 18.39, 14.11. **IR** (cm^{-1}): 3309 (s); 2919 (m); 2856 (m); 2114 (w); 1414 (m). **MS**: m/z (relative intensity) 41 (50.8); 43 (46.3); 54 (23.3); 55 (44.0); 67 (67.9); 68 (23.4); 81 (100); 82 (47.7); 95 (46.1); 96 (23.4). No $M^{+\bullet}$ was observed.

5.2.2.3 Synthesis of 1-Tetradecyne (III)

1,2-Dibromotetradecane. This reaction was performed on the same scale and with the same procedure as described for 1,2-dibromohexadecane. The yield was quantitative.

^{1}H NMR: δ 4.25–4.11 (m, 1H), 3.86 (dd, 1H, J = 4.4 Hz, J = 10.2 Hz), 3.64 (dd, appears as t, 1H, J = 10.0 Hz (2x)), 2.21–2.07 (m, 1H), 1.88–1.69 (m, 1H), 1.68–1.25 (br. m,

20H), 0.90 (t, 3H, J = 6.4 Hz). **^{13}C NMR**: δ 53.13, 36.34, 36.01, 31.92, 29.62, 29.60, 29.57, 29.49, 29.36, 29.32, 28.82, 26.75, 22.70, 14.14. **IR** (cm^{-1}): 2924 (m); 2852 (m); 1465 (m); 1436 (m). **MS**: m/z (relative intensity) 41 (38.9); 43 (67.9); 55 (38.1); 57 (100); 69 (32.9); 71 (66.2); 83 (22.9); 85 (44.5); 97 (17.1); 99 (14.6); 275 (12.2); 277 (12.1). Exact mass: calculated 275.1374 for $C_{14}H_{28}Br^{+}$; found 275.1371. No $M^{+\bullet}$ was observed.

1/2-Bromo-1-Tetradecene (Mixture of Isomers). This reaction was performed on the same scale and with the same procedure as described for 1/2-bromo-1-hexadecene. The yield was 53.8 g (0.195 mol, 98%).

^{1}H NMR: δ [6.21–5.97 (m) + 5.57–5.55 (m) + 5.39–5.38 (m); total of 2H, relative integral height = ~1.5 : 1 : 1], [2.45–2.38 (m) + 2.25–2.15 (m) + 2.06–1.99 (m), total of 2H, relative integral height = ~1.5 : 1 : 1], 1.65–1.24 (br. m, 20H), 0.89 (t, 3H, J = 6.5 Hz). **IR** (cm^{-1}): 3062 (w); 2923 (m); 2857 (m); 1621 (m); 1455 (m).

1-Tetradecyne (III). Sodium amide (21.1 g, 0.54 mol) was dissolved in 120 ml of DMSO by heating the suspension under nitrogen at 60 °C for 1 h while stirring. The resulting solution was cooled to room temperature and the reaction flask was placed in a large water bath of 16 °C. A solution of 53.8 g of 1/2-bromo-1-tetradecene (0.195 mol, mixture of isomers) in 30 ml of THF was added dropwise over 1 h and the solution was stirred for another 2 h. The use of a mechanical stirrer during the reaction is strongly advised.

The reaction mixture was subsequently mixed with 500 ml of ice water and the organic layer was obtained. The aqueous layer was extracted twice with 200 ml of ether. The organic layers were combined, washed with brine (2x), and dried over $MgSO_4$. Evaporation of the solvent yielded 38.3 g of crude 1-tetradecyne. Distillation gave 24.0 g (0.124 mol, 64%) of 1-tetradecyne (bp 120–122 °C at 10 mmHg; lit. 128 °C at 15 mmHg,[24] or 70–78 °C at 0.7 mmHg)[25] as a colorless liquid.

^{1}H NMR: δ 2.19 (dt, 2H, J = 2.6 Hz, J = 6.9 Hz (2x)), 1.94 (t, 1H, J = 2.6 Hz), 1.64–1.24 (br. m, 20H), 0.89 (t, 3H, J = 6.5 Hz). **^{13}C NMR**: δ 84.68, 67.99, 31.93, 29.65 (3C), 29.53, 29.37, 29.13, 28.77, 28.50, 22.69, 18.38, 14.09. **IR** (cm^{-1}): 3315 (s), 2927 (m), 2853 (m), 2120 (w), 1464 (m). **MS**: m/z (relative intensity) 41 (56.4); 43 (50.5); 55 (49.4); 57 (27.0); 67 (65.9); 69 (24.2); 81 (100); 82 (60.5); 95 (48.2); 96 (40.8). No $M^{+\bullet}$ was observed.

5.2.2.4 Synthesis of 1-Octadecyne (I)

1,2-Dibromooctadecane. This reaction was performed on the same scale and with the same procedure as described for 1,2-dibromohexadecane. The yield was quantitative. The

product is a viscous liquid, which can solidify into a sticky, wax-like solid after standing for several days.

^{1}H NMR: δ 4.25–4.12 (m, 1H), 3.83 (dd, 1H, J = 4.5 Hz, J = 10.2 Hz), 3.64 (dd, appears as t, 1H, J = 9.9 Hz (2x)), 2.22–2.06 (m, 1H), 1.89–1.72 (m, 1H), 1.70–1.23 (br. m, 28H), 0.89 (t, 3H, J = 6.5 Hz). **^{13}C NMR**: δ 53.06, 36.27, 35.99, 31.93, 29.70 (8C), 29.54, 29.39, 28.82, 26.75, 22.70, 14.13. **IR** (cm^{-1}): 2924 (m); 2853 (m); 1465 (m); 1437 (w). **MS**: m/z (relative intensity) 41 (35.1); 43 (59.6); 55 (46.4); 57 (100); 71 (75.7); 83 (45.8); 85 (55.6); 97 (24.6); 331 (23.0); 333 (26.8). Exact mass: calculated 331.2000 for $C_{18}H_{36}Br^{+\bullet}$; found 331.1998. No $M^{+\bullet}$ was observed.

1/2-Bromo-1-Octadecene (Mixture of Isomers). This reaction was performed on the same scale and with the same procedure as described for 1/2-bromo-1-hexadecene. The yield was 64.5 g (0.194 mol, 97%).

^{1}H NMR: δ [6.21–5.97 (m) + 5.57–5.55 (m) + 5.39–5.38 (m); total of 2H, relative integral height = ~1.5 : 1 : 1], [2.46–2.39 (m) + 2.24–2.15 (m) + 2.06–1.99 (m); total of 2H, relative integral height = ~1.5 : 1 : 1], 1.65–1.22 (br. m, 28H), 0.89 (t, 3H, J = 6.5 Hz). **IR** (cm^{-1}): 3079 (w); 2928 (m); 2853 (m); 1630 (m); 1468 (m).

1-Octadecyne (I). Sodium amide (20.1 g, 0.51 mol) was dissolved in 120 ml of DMSO by heating the suspension under nitrogen at 65 °C for 1 h while stirring. The resulting solution was cooled to room temperature and the reaction flask was placed in a large water bath of 16 °C. A solution of 64.5 g of 1/2-bromo-1-octadecene (0.194 mol, mixture of isomers) in 30 ml of THF was added dropwise over 1 h and the solution was stirred for another 2 h. The use of a mechanical stirrer during the whole reaction is required.

The reaction mixture was mixed with 500 ml of ice water and the organic layer was filtered off on a glass filter. The aqueous layer was extracted twice with 200 ml of ether. The solid product was dissolved in the combined ether layers. Subsequently, the organic layer was washed with brine (2x) and dried over $MgSO_4$. Evaporation of the solvent yielded 45.8 g of crude 1-octadecyne. Distillation gave 40.5 g (0.162 mol, 82%) of 1-octadecyne (bp 117–122 °C at 0.015 mmHg; lit. 175–177 °C at 13 mmHg)[26] as a colorless liquid, which rapidly solidifies upon standing. Recrystallization from methanol gave 35.5 g (0.142 mol, 73%) of pure 1-octadecyne as white flakes (mp 29–30 °C; lit. 28 °C).[26]

^{1}H NMR: δ 2.20 (dt, 2H, J = 2.6 Hz, J = 6.9 Hz (2x)), 1.95 (t, 1H, J = 2.6 Hz), 1.61–1.28 (br. m, 28H), 0.89 (t, 3H, J = 6.4 Hz). **^{13}C NMR**: δ 84.81, 68.00, 31.91, 29.67 (7C), 29.50, 29.35, 29.10, 28.75, 28.47, 22.68, 18.38, 14.12. **IR** (cm^{-1}): 3315 (s); 2923 (m); 2853

(m); 2120 (w). **MS**: m/z (relative intensity) 41 (35.4); 43 (49.9); 55 (45.2); 57 (37.6); 67 (52.9); 81 (100); 82 (87.5); 83 (30.1); 95 (49.3); 96 (75.8). No $M^{+\bullet}$ was observed.

5.2.3 Monolayer Preparation

For the water contact angle measurements, the monolayers were prepared as described previously.[16] In short, 10 ml of a 0.2 M solution of 1-alkyne or 1-alkene in mesitylene was placed in a small, three-necked flask fitted with a nitrogen inlet, a thermometer, and a reflux condenser with a $CaCl_2$ tube. The solution was deoxygenated with dry nitrogen for at least 1 h. Subsequently, a piece of double polished silicon was etched in 2.5% HF for 2 min and immediately placed in the solution. The flask was immersed in an oil bath of 210 °C and refluxed for 2 h, while maintaining a slow N_2 flow. Subsequently, the sample was removed from the solution and cleaned.[6,16]

Modification of the ATR crystals with a similar set-up as used for the samples for water contact angle measurements gave some practical problems. Due to the length of the crystals (5 cm) a large three-necked flask with a volume of at least 100 ml is required, which has to be filled with over 50 ml of the 1-alkyne or 1-alkene solution to completely immerse the crystal. This large amount of solvent takes too long to start refluxing, even if preheating is applied (*vide infra*). Modifications with this set-up were attempted, but disordered monolayers were always the result. To reduce the amount of material, the use of a flattened tube, as used previously with the neat 1-alkenes (see Chapter 3), was investigated. However, in this case superheating of the solution at the bottom of the tube caused large bubbles, as a result of which the crystal started to bounce up and down. This gives a considerable risk of damaging or even breaking of the crystal. In addition, disordered monolayers were again obtained.

The ATR crystals were successfully modified in a specially designed flask as depicted in Sketch 1. It has a flattened bottom, which reduces the amount of 1-alkyne or 1-alkene solution that is needed to immerse the crystal to 25 ml. By partially immersing this flask in an oil bath of 220 °C (instead of 210 °C), the solution was preheated to 163–164 °C, which is just below the boiling point of mesitylene (165 °C). After deoxygenation (*vide supra*), the ATR-crystal was inserted via the screw-cap opening and the flask was further lowered into the oil bath of 220 °C, immersing it as deeply as possible. By applying this procedure, the solution starts to reflux well within 60 s, which is a similar time period as with the small flask used for the small substrates. The same set-up was used for the preparation of the samples for the X-ray reflectivity experiments.

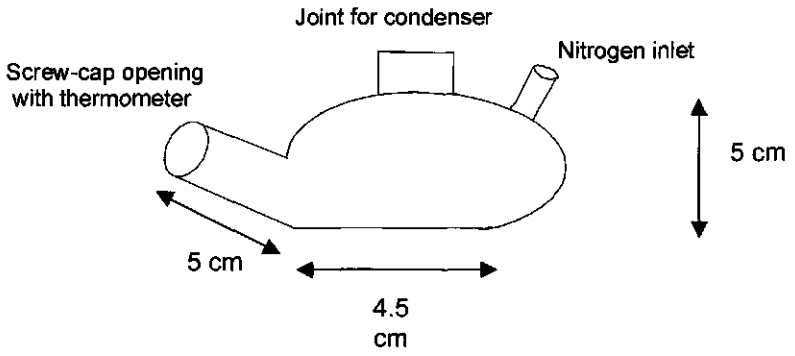

Sketch 1. The reaction flask for the modification of ATR crystals (side view with approximate dimensions). The flask was prepared from a 100 ml round bottom flask. The diameter of the screw cap opening is 2 cm.

The ATR-crystals were recycled by oxidative removal of the monolayer in "piranha solution" (30% H_2O_2 : H_2SO_4 = 1 : 2 (v/v)) at 85 °C for 60 min.[27,28] *Caution: The acidic solutions of hydrogen peroxide described in this procedure are dangerous, strong oxidants, and should be handled with great care.* The crystal was removed from the solution and rinsed extensively with water. After this cleaning, drops of water spread completely on the surface, and IR spectroscopy showed the complete absence of any C–H vibrations. This indicates that the monolayer was completely removed.

5.2.4 Contact Angle Measurements

Water contact angles were determined by the Wilhelmy-plate method as described previously.[6,16] All samples were prepared in triplicate, and for each sample at least 7 measurements were made for both advancing and receding contact angles. The reported values are the averages of the three samples. The reproducibility of the advancing contact angles is ±1°, and that of the receding angles is ±1–2°.

5.2.5 Infrared Spectroscopy

Infrared spectra of the monolayers were recorded on a Perkin Elmer 1725X FT-IR spectrophotometer, equipped with a liquid nitrogen-cooled MCT-detector, using a fixed angle multiple reflection attachment (Harrick Scientific). The infrared light was incident on one of the 45° bevels of the ATR crystal. Spectra of the monolayers were recorded with s- and p-polarized light. Measurement conditions were: resolution 0.25 cm^{-1}, with 512 scans. A

clean, untreated Si ATR crystal was used as a background. All crystals were cleaned with chloroform before mounting. The reproducibility of the peak positions in different measurements of the same samples, e.g., after repositioning of the sample or cleaning of the monolayer-modified crystal, was ±0.25 cm^{-1}. From the measurements of the independent s- and p-polarized spectra an average tilt angle with respect to the surface normal can be calculated. This procedure is described in the Appendix of this thesis.

5.2.6 X-ray Reflectivity

X-ray reflectivity measurements were performed using a rotating anode Rigaku RU-300H generator having a maximum power of 18 kW and a two-circle diffractometer. The incident beam was monochromatized (Cu K_α, λ = 1.54 Å) and converted into a parallel beam by a W/B_4C graded multilayer monochromator, which had an inherent divergence of 5.23 x 10^{-4}. Additionally, the incoming and outgoing divergences were given by the slit widths, which resulted in an in-plane resolution of $\Delta q_z = 4.3 \times 10^{-3}$ $Å^{-1}$ and $\Delta q_x = 5.3 \times 10^{-3} \times q_z$.

Before starting a measurement the samples were rinsed in chloroform. During the measurement they were kept in a cell which was continuously evacuated in order to avoid contamination through air exposure. The X-ray reflectivity data were corrected for the sample size effects at small incidence angles as well as for the background scattering, and were normalized to unit incident intensity. They were analyzed according to an iterative matrix formalism derived from the Fresnel equations by taking into account the deviation from the ideal decay of the reflectivity for a perfectly smooth surface due to the presence of roughness.[29,30] The calculated reflectivity profiles were convoluted with the experimental resolution, which is assumed to be of Gaussian statistics.

5.2.7 Molecular Mechanics Calculations

All calculations were performed with the MSI program Cerius^2 (version 3.5).[31] The structures were optimized using the "Smart Minimizer" minimization routine with "high-convergence" criteria.[32] Two different force fields were used: the Universal Force Field (UFF)[33] and the Polymer Consistent Force Field (PCFF),[34] both as implemented in Cerius^2. A cluster of 32 Si atoms was prepared from an enlarged Si crystal unit cell, which is available in the database of Cerius^2. This cluster was terminated with hydrogen atoms, which gave a cluster with four surface SiH_2 groups, which represents the H-terminated Si(100) surface. The 1-butyne or 1-butene molecule was bound to this surface in such a way that the aliphatic tail of the organic molecule was above the Si crystal surface, to include the interactions between

the alkyl chain and the Si surface in an optimal fashion. In all calculations, only the top two layers of Si atoms were allowed to move, whereas the remaining atoms were fixed at their positions. In this way the underlying Si crystal structure is properly represented, as the Si cluster was directly prepared from the Si crystal unit cell.

5.2.8 Ab-Initio Calculations

The optimized structures obtained from the molecular mechanics calculations (see Section 5.2.7) were investigated with B3LYP/6-31G(d) computations. The Gaussian 98 suite of programs was used, with the functional and basis set as implemented in there.[35] All structures were fully optimized. Natural population analysis (NPA) charges were obtained using the NBO program as implemented in Gaussian;[36] since the computations using the 6-31G(d) basis set involve the use of 752 basis functions, which is larger than the maximum of allowed basis functions in the NBO module in Gaussian 98, the LANL2DZ basis set was used for silicon in the NPA computations. Test calculations on smaller systems in which both the LANL2DZ and 6-31G(d) basis sets could be used showed only negligible differences between the resulting NPA charges.

5.3 Results and Discussion

5.3.1 Structure of the Monolayers

Information about the packing density of the molecules in the monolayers can be obtained from a combination of water contact angle and infrared spectroscopy measurements. In Table 1 the water contact angles as determined for the 1-alkyne and 1-alkene monolayers are listed (column 2 and column 3, respectively). From these results it is evident that all four 1-alkynes **I–IV** give ordered monolayers on the Si(100) surface (column 2). The advancing contact angles (Θ_a = 108–110°) are indicative of ordered monolayers that are terminated with methyl groups, as they are well comparable to the values reported for thiols on gold.[37,38] The same holds for the receding angles (Θ_r = 98–101°).

The values for the 1-alkene monolayers prepared with the recently developed solution procedure[16] (column 3) are all comparable to the values reported earlier for the well-ordered monolayers prepared on the Si(100) surface using neat 1-alkenes.[6] Comparing the results from the monolayers of the 1-alkynes to those of the 1-alkenes shows that the average values for both the advancing and the receding contact angles as observed for the monolayers of

1-alkynes are slightly higher than those of the corresponding 1-alkenes (Θ_a = 108–110° vs. 108–109°; Θ_r = 98–101° vs. 96–98°). They are also the highest values reported so far for any methyl-terminated alkyl monolayer on the Si(100) surface. This indicates that the monolayers of 1-alkynes are at least as well-ordered as these 1-alkene monolayers. The difference between the receding contact angles of the monolayers of the 1-alkynes and the 1-alkenes might be caused by differences in the orientation of the methyl groups.[39,40]

Table 1. Water contact angles (in degrees) for the 1-alkyne and 1-alkene monolayers (columns 2 and 3, respectively).

Compound **R =**	**HC≡C–R** Θ_a/Θ_r [a]	**H_2C=CH–R** Θ_a/Θ_r [a]
$C_{16}H_{33}$	110/98	109/96
$C_{14}H_{29}$	110/101	109/97
$C_{12}H_{25}$	110/100	108/98
$C_{10}H_{21}$	108/98	108/97

Note: [a] Advancing and receding contact angles for water.

The results from the infrared spectroscopy measurements on the monolayers of the 1-alkynes **I–IV** are shown in Table 2. The antisymmetric methylene stretching vibrations appear near 2921 cm^{-1} and the symmetric vibrations are near 2852 cm^{-1}. The antisymmetric CH_3 vibration is visible at 2960 cm^{-1}. As an example, the spectrum of a monolayer of **II** is shown in Figure 4. It is known that shifts occur for these vibrations on going from the liquid to the solid state. In long, linear *n*-alkanes the antisymmetric vibration shifts from approximately 2928 cm^{-1} to 2920 cm^{-1} and the symmetric vibration from 2856 cm^{-1} to 2850 cm^{-1}.[41] Consequently, the packing of the 1-alkyne molecules in the monolayers resembles that of the solid state of *n*-alkanes. This indicates that the molecules are closely packed and form a well-ordered monolayer.

The values for the monolayers of 1-octadecyne (**I**) and 1-hexadecyne (**II**) are also similar to those previously reported for the corresponding 1-octadecene and 1-hexadecene monolayers on the Si(100) surface, which gave values of 2920–2921 cm^{-1} and 2851–2852 cm^{-1}, respectively.[6] As values for a monolayer of 1-tetradecene were not available and the

Table 2. Infrared absorptions (in cm^{-1}) for the antisymmetric (ν_a) and symmetric (ν_s) methylene stretching vibrations of the monolayers of **I**–**IV**, using p-polarized light.

Monolayer	ν_a	ν_s
$HC{\equiv}C{-}C_{16}H_{33}$ **(I)**	2921.1	2851.9
$HC{\equiv}C{-}C_{14}H_{29}$ **(II)**	2921.4	2852.2
$HC{\equiv}C{-}C_{12}H_{25}$ **(III)**	2921.9	2852.4
$HC{\equiv}C{-}C_{10}H_{21}$ **(IV)**	2921.5	2852.2

values previously reported for 1-dodecene are less reliable,[6] these monolayers were prepared by the same procedure as that for the 1-alkyne monolayers. The methylene stretch vibrations of these monolayers of 1-tetradecene and 1-dodecene showed absorptions at ν_a/ν_s = 2922.2/2852.6 cm^{-1} and ν_a/ν_s = 2922.1/2852.5 cm^{-1}, respectively, again indicative of ordered monolayers in which the alkyl chains will adopt an all-*trans* conformation. In general, the absorptions of these methylene stretch vibrations shift to slightly higher values for shorter molecules.[42] The absorption values for the monolayers of 1-tetradecyne **(III)** and 1-dodecyne **(IV)** as listed in Table 2 are well comparable to these values, which confirms that also the shorter 1-alkynes give well-ordered monolayers. Thus, on the basis of the results from the water contact angle measurements and IR spectroscopy it is concluded that all four 1-alkynes **I**–**IV** give well-ordered monolayers on the Si(100) surface, and that the ordering of the alkyl chains in these monolayers is similar to, if not better than, that of the monolayers of the corresponding 1-alkenes.

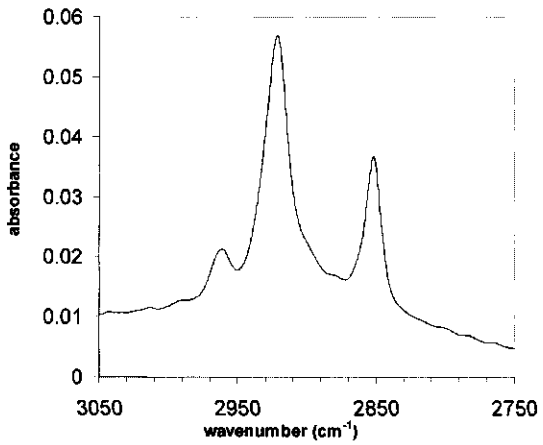

Figure 4. Infrared spectrum (C–H stretching region) of a monolayer of **II** on Si(100).

The separate measurement of s- and p-polarized IR spectra of the 1-alkyne monolayers allows for an estimate of the tilt angle of the alkyl chains with respect to the surface normal. The differences between the absolute absorbances of the antisymmetric and symmetric methylene vibrations can be used for this purpose.[6] The results are listed in Table 3. The calculated average tilt angle of the four 1-alkynes is 35±5°, which agrees with the value of 30±9° that was previously found for the 1-alkene monolayers by the same method.[6] This again confirms a high similarity between the structure of monolayers of 1-alkynes and 1-alkenes on the Si(100) surface.

Table 3. Tilt angles for the monolayers of 1-alkynes **I–IV**.[a]

Monolayer	$\mathbf{A_a^{s-pol}}$ / $\mathbf{A_a^{p-pol}}$	α_a **(deg)**	$\mathbf{A_s^{s-pol}}$ / $\mathbf{A_s^{p-pol}}$	α_s **(deg)**	Θ_{IR} **(deg)**
I	0.064	70	0.035	66	33
	0.062		0.035		
II	0.047	71	0.027	71	27
	0.045		0.026		
III	0.035	60	0.018	66	40
	0.037		0.018		
IV	0.059	64	0.035	62	40
	0.060		0.036		

Note: [a] $A_a^{s-pol,p-pol}$, absorbance of the antisymmetric methylene stretch vibration using polarized light. $A_s^{s-pol,p-pol}$, absorbance of the symmetric methylene stretch vibration using polarized light. α, angle between surface normal and the (anti)symmetric CH_2 dipole moment. Θ_{IR}, calculated tilt angle from IR-dichroism (see also Experimental Section).

5.3.2 X-ray Reflectivity

Further information about the packing of the molecules in the monolayers is obtained by X-ray reflectivity.[43] This technique is based on the condition that the resulting wave vector transfer Q is parallel to the surface normal of the sample. Thus X-ray reflectivity probes changes in the electron density perpendicular to the monolayer surface, which are used to

determine the following sample parameters: the layer thickness, the electron density of the layer, and the interfacial roughness of the monolayer.[43]

Three of the monolayers, i.e., of compounds **I–III**, were studied with X-ray reflectivity. The results are depicted in Figure 5, which shows the reflectivity profiles of the monolayers as a function of momentum transfer Q_z. The shape of the reflectivity curve is determined by two characteristic regions.[29] An intensity plateau is typical for incident angles smaller than the critical angle for external total reflection ($Q < Q_{crit}$, with $Q = 4\pi/\lambda \sin \alpha_i$, with α_i the incident angle). From the position of the critical angle of total reflection the electron density of the layers is deduced. For angles beyond this critical angle the curve is characterized by a rapid decrease of the intensity ($\sim Q^{-4}$). Superimposed to this decay a low-frequency oscillation is obtained due to interference of the reflected X-ray waves at the air–monolayer and monolayer–Si interfaces. From its period ΔQ the layer thickness may be estimated using the Bragg equation $d = 2\pi/\Delta Q$. Due to the small thickness of the monolayers the curves show in fact only one maximum and two minima, which is, however, sufficient to obtain a precise fit of the monolayer thickness. Only for the monolayer of **III**, where the smallest thickness is expected, the second minimum could not be seen, because the background at high Q_z limits the analyzable range of the measurement. This gives less accurate results for the monolayer thickness, and therefore the monolayer of **IV**, which will be even thinner, was not investigated with this technique.

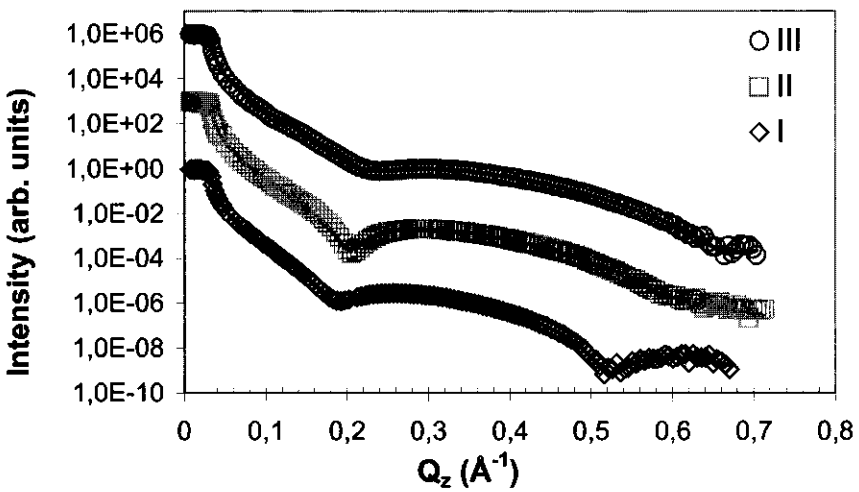

Figure 5. X-ray reflectivity profiles and fit curves for the monolayers of **I–III**.

The solid lines in Figure 5 are the best fit curves, using a two-layer model for the organic monolayer (*vide infra*). In all three cases there is a good agreement between the experimental data and the fit curve, which is not the case for fits using a single-layer model. The calculated electron density, the layer thickness, and the interfacial roughness of the various layers as obtained from these fit curves are listed in Table 4.

Table 4. Film properties as obtained from two-layer fits to the X-ray reflectivity measurements.

Layer (Air = 1)	Property [a]	I	II	III
	t_2	18.3±0.1	16.2±0.2	15.8±0.6
Monolayer	ρ_2	0.31±0.01	0.32±0.01	0.27±0.01
	σ_{12}	3.0±0.1	2.7±0.1	3.1±0.1
	t_3	1.3±0.7	0.2±0.1	1.1±0.4
Intermediate layer	ρ_3	1.21±0.02	1.21±0.02	1.21±0.02
	σ_{23}	4.2±0.1	2.4±0.2	3.5±0.3
Silicon substrate [b]	σ_{34}	5.0±0.3	1.9±0.2	3.1±0.2

Note: [a] t_x = thickness (in Å) of layer x, ρ_x = electron density (in $e^-/Å^3$) of layer x, σ_{yx} = roughness (in Å) between layer y (= x–1) and x. [b] In all fits, a value of $\rho = 0.71$ $e^-/Å^3$ was used for the electron density of Si, as well as an absorption of 1.727×10^{-7}.

The results in Table 4 show that there is an approximately linear correlation between the calculated layer thickness and the length of the organic molecule, as can be expected for ordered alkyl layers on solid substrates. The monolayer of **III** is somewhat too thick compared to the length of the 1-tetradecyne molecule, but still agrees with this linearity within experimental error, as this error is much larger in this case than that for the monolayers of **I** and **II**, because the second minimum in the reflectivity profile could not be observed. The layers of compounds **I** and **II** have an electron density of 0.31 and 0.32 $e^-/Å^3$, respectively, which is well comparable to the previously found value of 0.30–0.32 $e^-/Å^3$ for the monolayers of the corresponding 1-alkenes on the Si(100) surface. When compared to the electron density of crystalline alkanes of 0.35 $e^-/Å^3$,[44] the electron density of the alkyl chains in the monolayers shows that they are closely packed, as was already found with IR spectroscopy.

The electron density of 0.27 $e^-/Å^3$ for the monolayer of **III** is somewhat lower compared to these values. This may indicate that this monolayer is slightly less densely packed, although the larger experimental error in this measurement compared to those of monolayers of **I** and **II** precludes definitive conclusions.

For all three monolayers the roughness of ~4 Å of the Si surface is comparable to the roughness of ~3 Å of the air/monolayer interface. This shows that a smooth, densely packed film has been formed on the Si surface. These values are also similar to those measured for the corresponding 1-alkene monolayers on the Si(100) surface,[6] which confirms the high similarity between the monolayers of 1-alkenes and of 1-alkynes on this Si surface as already observed with contact angle measurements and IR spectroscopy.

As mentioned above, the fitting of the reflectivity profiles as measured for the monolayers of the 1-alkynes **I–III** required the introduction of a second layer, i.e., an intermediate layer between the organic layer and the Si surface. Such a layer was not necessary for the corresponding 1-alkene monolayers, which indicates that there is an important difference between the structure of the two layers. The calculated electron density of 1.21 $e^-/Å^3$ of this intermediate layer is the same for all three samples. Interestingly, this value is much higher than that of the alkyl layer, and also above that of Si, which has a value of 0.71 $e^-/Å^3$.[29] This indicates that there must be a very high density of probably strongly electronegative atoms in this interfacial region between the Si surface and the alkyl chains.

It is known that the Si–H groups that remain unreacted are oxidized to Si–OH groups, but further oxidation of the Si surface to SiO_2 does not occur.[3] The electron density of SiO_2 is comparable to that of Si itself,[45] and thus significantly lower than the calculated value for the intermediate layer. Besides, Si surface oxidation would generate a SiO_2 layer with a thickness of at least several Å. Thus, it is likely that this interfacial layer is not due to the presence of SiO_2.

A possible explanation for the presence of the intermediate layer is that the 1-alkynes are bound to the Si surface in a different way than the 1-alkenes (see Figure 2). The various possible structures, which will be discussed in more detail in the next section, are shown in Figure 6. If each 1-alkyne forms two bonds to the Si surface, there will be an increase in the electron density near this surface when compared to that of the rest of the alkyl chain. If both bonds are formed to the terminal carbon atom of the 1-alkyne (structure **6C**), this carbon atom comes close to the Si surface and will also have a considerable negative charge (*vide infra*), which implies an increase in the electron density on this atom. A ball-and-stick model shows that the second carbon atom of the former acetylene moiety is in such bonding situation in a

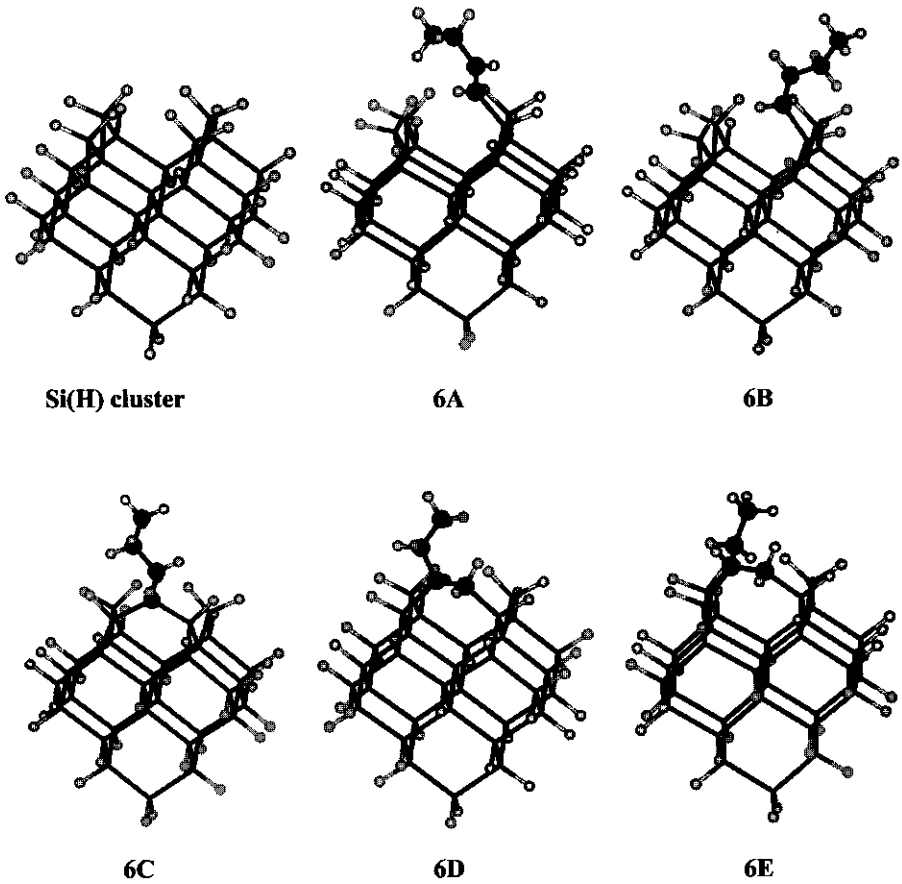

Figure 6. The Si cluster with 32 Si atoms, the top of which represents the H-terminated Si(100) surface, and the five lowest-energy optimized structures **6A–6E** of this Si cluster bound to a 1-butyne molecule in various ways. Carbon and hydrogen atoms of these clusters in their fully optimized geometries are shown as balls for reasons of clarity. For more details see text.

plane not much above this first carbon atom and that it has limited flexibility, whereas the remaining methylene groups are highly flexible. Thus, the alkyl chains can be in an all-*trans* conformation, as found with IR spectroscopy, except for the first two carbon atoms. Consequently, a thin layer is formed between the Si surface and the alkyl tails, which has a higher electron density compared to that of these alkyl tails. A similar situation occurs when the two Si–C bonds are formed to the two different carbon atoms of the 1-alkyne. In this case

these two atoms are both in the same plane and at the same height above the Si surface (structures **6D** and **6E**). If the 1-alkyne makes only one Si–C bond to the Si surface, such an electron-rich layer is not formed, as the two carbon atoms in the remaining C=C double bond are not in the same plane above the Si surface (structures **6A** and **6B**) and also have on average the same electron density as an alkyl chain (see Section 5.3.3). Thus, this gives a plausible explanation for the presence of an electron-rich intermediate layer between the Si surface and the alkyl chains.

The presence of such an intermediate layer of increased electron density makes it difficult to obtain an accurate value for the tilt angle of the alkyl chains in the monolayers of **I–III**. It can be reasoned that the interfacial region reduces the alkyl chain length by two methylene groups, as the first two carbon atoms of the former 1-alkyne are in this intermediate layer. Consequently, using the same formula as was used for the 1-alkenes[6] ($\Phi_{Xray} = \cos^{-1}[(d–0.77)/(2.52\ (n–1)/2)]$, with d = layer thickness, and n = number of C atoms in the alkyl chain), the tilt angle of the alkyl chains in the monolayer of **I** would be 22°, and the monolayer of **II** would give a tilt angle of 20°. However, both values deviate significantly from the value of 35±5° as determined with IR spectroscopy. It is known that IR dichroism can give large experimental errors in the calculated tilt angles,[3,6] which suggests that there is probably a significant uncertainty in this latter value. The tilt angles calculated from the X-ray measurements also differ significantly from those obtained for the monolayers of the corresponding 1-alkenes (29° and 26° for monolayers of 1-octadecene and 1-hexadecene, respectively).[6] This also indicates that it is not realistic to calculate a tilt angle for the monolayer of **III**, because of the large uncertainty in the thickness of that monolayer.

5.3.3 The Si–C interface: One or Two Si–C Bonds per Molecule?

The results shown above indicate that 1-alkynes form densely-packed, well-ordered monolayers on the H-terminated Si(100) surface. However, although the results from the X-ray reflectivity suggest a significant difference between the monolayers of 1-alkynes and 1-alkenes, so far no experimental evidence has been obtained about the nature of the binding between the 1-alkyne and this Si surface, i.e., whether the 1-alkynes form one or two Si–C bonds per reacting molecule (see Figure 2).

The binding structure of the 1-alkyne at the Si interface was investigated with infrared spectroscopy, as these measurements can reveal the presence of C=C and/or C=C–H vibrations in the monolayer. If the 1-alkyne reacts only once with a Si–H group, forming only one Si–C bond per molecule, such vibrations will be present; if the 1-alkyne reacts with two

Si–H groups on the surface and a doubly bonded structure is formed, these vibrations will be absent.[46]

No vibrations from alkene moieties were observed in any of the IR spectra of the 1-alkynes investigated here. As an example, the spectrum of a monolayer of 1-hexadecyne (**II**) is shown in Figure 7. This observation strongly suggests that alkene moieties are absent in the monolayers of 1-alkynes on the H-terminated Si(100) surface, as the C=C vibration has been detected with IR spectroscopy in the monolayer of a 1-alkyne on the H-terminated Si(111) surface.[3,5] Thus, the 1-alkynes seem to form two Si–C bonds per molecule to the Si(100) surface. However, it is known that the intensity of infrared absorptions in monolayers on solid substrates can be orientation-dependent, as has for example been observed for carboxyl groups in the case of thiol monolayers on gold.[47] It is not known to which degree this may also occur for the C=C vibrations in these monolayers, and, therefore, the results from IR spectroscopy on their own are not fully conclusive.

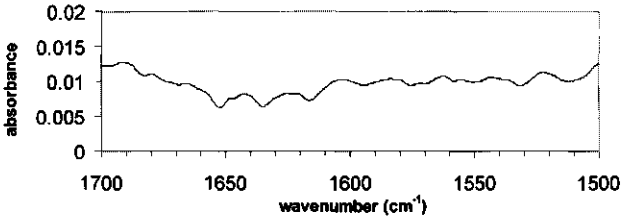

Figure 7. Infrared spectrum (C=C stretching region) of a monolayer of **II** on Si(100).

Theoretical calculations were therefore performed to obtain further insight in the way the 1-alkynes are bound to the Si(100) surface. The structure of monolayers of 1-alkenes on Si surfaces has been successfully investigated by molecular mechanics calculations, using two-dimensionally repeating boxes to describe the modified Si surface.[48] Unfortunately, this molecular mechanics approach is not suitable here, as the predominant factor that determines the overall monolayer structure is formed by the long alkyl chains, while the precise binding geometry at the Si surface has only a small influence on the layer thickness.

Therefore quantum chemical computations were performed on small Si–alkyl clusters, for which the starting structures were obtained using molecular mechanics computations. As model system was chosen a Si_{32} cluster with a single alkyne molecule (1-butyne) bound in all chemically realistic geometries that could be designed on a three-dimensional ball-and-stick

model of the surface. This Si cluster had four Si surface atoms that are terminated with two H atoms to describe the structure of the Si(100) surface (Figure 6, Si(H) cluster). The alkyl chain was always oriented above this Si surface.

Several different structures are possible for a 1-alkyne that is bound to the H-terminated Si(100) surface. The results from the molecular mechanics calculations showed that the relative order of stability of the structures depends on the force field that is used (see Table 5). Therefore, these molecular mechanics results are only suitable to select the structures that are chemically most realistic. In Figure 6 these structures are presented. If the C≡C bond reacts only once with a Si–H group, this leads to the formation of a 1-alkenyl type structure. This leaves two possibilities:[10,11] structure **6A** with the remaining C=C bond trans, and structure **6B** with the C=C bond cis. If the 1-alkyne forms two Si–C bonds to the surface, only one structure (**6C**) is possible if both bonds are formed to the terminal carbon of the 1-alkyne (1,1-bridge structure in Figure 2). Several different structures are possible if the two Si–C bonds are formed to the two different carbon atoms of the former 1-alkyne (1,2-bridge structure in Figure 2), as the second carbon atom of the 1-alkyne can reach any of the surrounding Si surface atoms and form a covalent Si–C bond to it. Only the two most suitable ones of these structures were considered, as these 1,2-bridged structures already have an energy significantly higher than that of **6A**–**6C**. They differ in the orientation of the remaining ethyl group: upward (axial) in structure **6D** and sideward (equatorial) in structure **6E**. The energy of all the other 1,2-bridged structures was considerably higher compared to that of **6D** and **6E** (> 20 kcal mol^{-1} difference). Therefore, they were eliminated from the present investigations.

More accurate calculations were performed by quantum mechanical B3LYP/6-31G(d) investigations of the structures **6A**–**6E**. The PCFF-optimized structures described above were used as starting structures for this purpose.[49] Quantum mechanical calculations have frequently been used to investigate the binding structure of small molecules adsorbed on Si surfaces under ultrahigh vacuum conditions.[50] Usually, a small Si cluster of only ~7–15 Si atoms is used to represent the Si surface, to reduce the time required for the computations. In the present calculations, however, a large cluster of 32 Si atoms was used. This has two advantages: (a) the underlying Si crystal structure is much better described by such a large Si cluster, and (b) the use of such a large cluster allows for an estimate of the positions of the valence and conduction bands of the semiconductor. This can be used to investigate possible shifts of these levels as a result of the binding of the organic molecule to the Si surface.

So far, these monolayers of 1-alkenes or 1-alkynes on H-terminated Si surfaces have not been investigated by quantum mechanical calculations, which means that there are no reference values available (e.g., for the binding energy). Therefore, three additional structures, i.e., the H-terminated Si cluster shown in Figure 6, a 1-butene molecule, and a Si surface with a butyl group bound to the surface (i.e., the structure that is formed when 1-butene reacts with the H-terminated Si(100) surface) were also investigated. The results[51] showed that it is energetically favorable to bind an organic molecule to the Si surface. The binding of a 1-butene molecule to the Si cluster, resulting in the formation of the covalent Si–C bond and rehybridization of the terminal 1-alkene from sp^2 to sp^3, yields 23.4 kcal mol^{-1}.

The results of the calculations on the various 1-alkyne structures are listed in Table 5, which shows the relative energies of the structures **6A–6E**. It is found that the 1,1-bridged structure **C** has the lowest energy. It was calculated that the energy of **6C** is 59.9 kcal mol^{-1} lower than that of the separate 1-butyne molecule plus the H-terminated Si cluster.[52] The 1,2-bridged structures **6D** and **6E** are the intermediate situations, with energies that are only 4.7 and 7.3 kcal mol^{-1} higher than that of **6C**. The two 1-alkenyl structures **6A** and **6B** have the highest energies, being approximately 20 kcal mol^{-1} less favorable than the 1,1-bridged situation, since the C=C bond is weaker than a Si–C σ-bond. The formation of two Si–C bonds, this time combined with the rehybridization of the carbon atoms of the triple bond from sp to sp^3, is not only structurally feasible, as was already found with the molecular mechanics calculations, but is apparently energetically highly favorable, despite the introduction of some ring tension in the resulting structure.

Table 5. Energies (in kcal mol^{-1}) of the structures **6A–6E** as obtained from the molecular mechanics and B3LYP/6-31G(d) calculations.

Structure [a]	E_{PCFF} [b]	E_{UFF} [c]	E_{B3LYP} [d]
6A	-49.32	-19.80	+19.57
6B	-45.64	-13.37	+21.82
6C	-51.95	-13.69	0
6D	-43.77	-9.99	+4.74
6E	-40.32	-1.11	+7.33

Note: [a] The structures are depicted in Figure 6. [b] Energy as calculated with the PCFF force field. [c] Energy as calculated with the UFF force field. [d] Relative energy as calculated with the B3LYP method (values are relative to the lowest-energy structure, i.e., to structure **6C**).

showed that there is a significant difference between the binding of 1-alkynes and 1-alkenes to the Si(100) surface. It was inferred that this intermediate layer is the result of the formation of two Si–C bonds per 1-alkyne molecule.

The binding geometry of the 1-alkynes was further investigated by quantum mechanical calculations. These results showed that the formation of two Si–C bonds per 1-alkyne is energetically much more favorable, by ~15–20 kcal mol^{-1}, than the formation of only one Si–C bond, which would leave C=C groups near the Si surface. The situation in which both bonds are to the former terminal carbon atom of the 1-alkyne (the 1,1-bridged situation **6C**) is more favorable, by ~5–7 kcal mol^{-1}, compared to the 1,2-bridged geometry (structures **6D** and **6E**). Combined with the results from IR spectroscopy and from X-ray reflectivity measurements on the monolayers it is concluded that 1-alkynes form two Si–C bonds per reacting molecule on the hydrogen-terminated Si(100) surface.

References and Notes

[1] Bishop, A. R.; Nuzzo, R. G. *Curr. Opin. Colloid Interface Sci.* **1996**, *1*, 127–136.

[2] Buriak, J. M. *Chem. Commun.* **1999**, 1051–1060.

[3] Linford, M. R.; Fenter, P.; Eisenberger, P. M.; Chidsey, C. E. D. *J. Am. Chem. Soc.* **1995**, *117*, 3145–3155.

[4] (a) Boukherroub, R.; Wayner, D. D. M. *J. Am. Chem. Soc.* **1999**, *121*, 11513–11515. (b) Strother, T.; Cai, W.; Zhao, X.; Hamers, R. J.; Smith, L. M. *J. Am. Chem. Soc.* **2000**, *122*, 1205–1209. (c) Effenberger, F.; Götz, G.; Bidlingmaier, B.; Wezstein, M. *Angew. Chem., Int. Ed. Engl.* **1998**, *37*, 2462–2464. (d) Boukherroub, B.; Morin, S.; Bensebaa, F.; Wayner, D. D. M. *Langmuir* **1999**, *15*, 3831–3835.

[5] Cicero, R. L.; Linford, M. R.; Chidsey, C. E. D. *Langmuir* **2000**, *16*, 5688–5695.

[6] Sieval, A. B.; Demirel, A. L.; Nissink, J. W. M.; Linford, M. R.; van der Maas, J. H.; de Jeu, W. H.; Zuilhof, H.; Sudhölter, E. J. R. *Langmuir* **1998**, *14*, 1759–1768 (Chapter 3).

[7] Sung, M. M.; Kluth, G. J.; Yauw, O. W.; Maboudian, R. *Langmuir* **1997**, *13*, 6164–6168.

[8] Zazzera, L. A.; Evans, J. F.; Deruelle, M.; Tirrell, M.; Kessel, C. R.; Mckeown, P. *J. Electrochem. Soc.* **1997**, *144*, 2184–2189.

[9] Buriak, J. M.; Allen, M. J. *J. Am. Chem. Soc.* **1998**, *120*, 1339–1340.

[10] Holland, J. M.; Stewart, M. P.; Allen, M. J.; Buriak, J. M. *J. Solid State Chem.* **1999**, *147*, 251–258.

[11] Buriak, J. M.; Stewart, M. P.; Geders, T. W.; Allen, M. J.; Choi, H. C.; Smith, J.; Raftery, D.; Canham, L. T. *J. Am. Chem. Soc.* **1999**, *121*, 11491–11502.

[12] Stewart, M. P.; Buriak, J. M. *Angew. Chem., Int. Ed. Engl.* **1998**, *37*, 3257–3260.

[13] Bateman, J. E.; Eagling, R. D.; Worrall, D. R.; Horrocks, B. R.; Houlton, A. *Angew. Chem., Int. Ed. Engl.* **1998**, *37*, 2683–2685.

[14] (a) Terry, J.; Linford, M. R.; Wigren, C.; Cao, R.; Pianetta, P.; Chidsey, C. E. D. *Appl. Phys. Lett.* **1997**, *71*, 1056–1058. Terry, J.; Linford, M. R.; Wigren, C.; Cao, R.; Pianetta, P.; Chidsey, C. E. D. *J. Appl. Phys.* **1999**, *85*, 213–221.

[15] See ref 2 and references cited therein.

[16] Sieval, A. B.; Vleeming, V.; Zuilhof, H.; Sudhölter, E. J. R. *Langmuir* **1999**, *15*, 8288–8291 (Chapter 4).

[17] Dumas, P.; Chabal, Y. J.; Jakob, P. *Surf. Sci.* **1992**, *269/270*, 867–878.

[18] Sieval, A. B.; Zuilhof, H.; Sudhölter, E. J. R.; Schuurmans, F. M.; Sinke, W. C. *Proceedings of the 2nd World Conference on Photovoltaic Solar Energy Conversion*, Vienna, 1998; Joint Research Center of the European Commission: Ispra, Italy, 1998, pp 322–325 (see also Chapter 7).

[19] The purity of the 1-alkynes obtained from the synthesis was found to be insufficient for the preparation of monolayers, as this reaction is very sensitive to small amounts of impurities in the reagents. Therefore, a second distillation step was always performed. No change in boiling points was observed.

[20] In some cases, mesitylene that was stored on NaOH became turbid after several weeks. Storage on $CaCl_2$ did not give this problem.

[21] (a) The original procedure[21b] lead –in contrast with claims by the authors– to the formation of large amounts of 2-alkynes (even over 50%) rather than 1-alkynes. The mistake in the interpretation of their data was most likely caused by insufficient resolution in the high-field NMR spectroscopy (60 MHz). The modified procedure used here (see Experimental Section) yields only 2–3% of the 2-alkyne (GC analysis) and 97–98% of the desired 1-alkyne. (b) Klein, J.; Gurfinkel, E. *Tetrahedron* **1970**, *26*, 2127–2131.

[22] Elsner, B. B.; Paul, P. F. M. *J. Chem. Soc.* **1952**, 893–897.

[23] Vaughn, T. H. *J. Am. Chem. Soc.* **1933**, *45*, 3453–3458.

[24] Krafft, F.; Reuter, L. *Berichte der Deutschen Chemischen Gesellschaft (Chem. Ber.)* **1892**, *25*, 2243–2251. Found in: *Beilstein Handbook of Organic Chemistry*, 4th ed.; Springer-Verlag: Berlin, Germany, Vol. 1, p 262.

[25] Jenny, E. F.; Druey, J. *Helv. Chim. Acta* **1959**, *42*, 401–406.

[26] Elsner, B. B.; Paul, P. F. M. *J. Chem. Soc.* **1951**, 893–897.

[27] (a) The following procedure was used: In a high, small cylinder (volume of 25 ml) was placed 7 ml of H_2O_2 (30% solution in H_2O). This was cooled to 0 °C and 14 ml of H_2SO_4 was added. *Caution: This addition is strongly exothermic.* The crystal was placed in the now hot (~85 °C) solution and the cylinder was immersed in an oil bath of 105–110 °C, thus maintaining the temperature of the oxidizing

solution around 85 °C. The solution was occasionally stirred with a glass rod. After 1 h the oil bath was removed and the crystal was taken from the solution using teflon tweezers. (b) Based on: Pintchovski, F.; Price, J. B.; Tobin, P. J. Peavey, J.; Kobold, K. *J. Electrochem. Soc.* **1979**, *26*, 1428–1430.

[28] In Chapter 3 a UV/ozone oxidation was used for recycling of the ATR crystals. Though this is an easier procedure compared to the piranha oxidation method, it was observed that in some cases the surface of the ATR crystals gets a brownish, matte appearance after the UV oxidation. Such crystals were found to be no longer suitable for monolayer preparations, as only monolayers of poor quality could be prepared on these surfaces. This could happen at any time, i.e., some crystals showed this effect after their first UV/ozone oxidation, whereas others could be recycled many times. The current oxidation procedure, though more elaborate, does not give any such problems and the crystals can be recycled many times without any effect on the quality of the new monolayer that is prepared.

[29] See, e.g., (a) Tolan, M. *X-ray Scattering from Soft-Matter Thin Films*, Springer Tracts in Modern Physics, Vol. 148; Springer Verlag: Berlin, Germany, 1999. (b) Holý, V.; Pietsch, U.; Baumbach, T. *High-Resolution X-Ray Scattering from Films and Multilayers*, Springer Tracts in Modern Physics, Vol. 149; Springer Verlag: Berlin, Germany, 1999.

[30] Fitting program REFGR by I. Samoilenko.

[31] (a) Cerius^2, version 3.5, Molecular Simulations Inc., September 1997. (b) Terms that are specific to the Cerius^2 program have in the text been put between quotes.

[32] Criteria for the "high-convergence" minimizations: Atom root mean square force 1 x 10^{-3} kcal mol^{-1} Å^{-1}; atom maximum force 5 x 10^{-3} kcal mol^{-1} Å^{-1}; energy difference 1 x 10^{-4} kcal mol^{-1}; root mean square displacement 1 x 10^{-5} Å; maximum displacement 5 x 10^{-5} Å.

[33] (a) Rappé, A. K.; Casewit, C. J.; Colwell, K. S.; Goddard, W. A., III; Skiff, W. M. *J. Am. Chem. Soc.* **1992**, *114*, 10024–10035. (b) Castongauy, L. A.; Rappé, A. K. *J. Am. Chem. Soc.* **1992**, *114*, 5832–5842. (c) Rappé, A. K.; Colwell, K. S.; Casewit, C. J. *Inorg. Chem.* **1993**, *32*, 3438–3450.

[34] (a) Sun, H.; Mumby, S. J.; Maple, J. R.; Hagler, A. T. *J. Phys. Chem.* **1995**, *99*, 5873–5882, and references therein. (b) Hill, J.-R.; Sauer, J. *J. Phys. Chem.* **1994**, *98*, 1238–1244. (c) Maple, J. A.; Hwang, M. J.; Stockfisch, T. P.; Dinur, U.; Waldman, M.; Ewig, C. S.; Hagler, A. T. *J. Comp. Chem.* **1994**, *15*, 162–182.

[35] Frisch, M. J.; Trucks, G. W.; Schlegel, H. B.; Scuseria, G. E.; Robb, M. A.; Cheeseman, J. R.; Zakrzewski, V. G.; Montgomery, J. A., Jr.; Stratmann, R. E.; Burant, J. C.; Dapprich, S.; Millam, J. M.; Daniels, A. D.; Kudin, K. N.; Strain, M. C.; Farkas, O.; Tomasi, J.; Barone, V.; Cossi, M.; Cammi, R.; Mennucci, B.; Pomelli, C.; Adamo, C.; Clifford, S.; Ochterski, J.; Petersson, G. A.; Ayala, P. Y.; Cui, Q.; Morokuma, K.; Malick, D. K.; Rabuck, A. D.; Raghavachari, K.; Foresman, J. B.; Cioslowski, J.; Ortiz, J. V.; Stefanov, B. B.; Liu, G.; Liashenko, A.; Piskorz, P.; Komaromi, I.; Gomperts, R.; Martin, R. L.; Fox, D. J.; Keith, T.; Al-Laham, M. A.; Peng, C. Y.; Nanayakkara, A.;

Gonzalez, C.; Challacombe, M.; Gill, P. M. W.; Johnson, B.; Chen, W.; Wong, M. W.; Andres, J. L.; Gonzalez, C.; Head-Gordon, M.; Replogle, E. S.; Pople, J. A. *Gaussian 98, Revision A.6*; Gaussian, Inc.: Pittsburgh, PA, USA. 1998.

[36] Glendening, E. D.; Reed, A. E.; Carpenter, J. E.; Weinhold, F. *NBO, version 3.1.*

[37] Bain, C. D.; Troughton, E. B.; Tao, Y.-T.; Evall, J.; Whitesides, G. M. *J. Am. Chem. Soc.* **1989**, *111*, 321–335.

[38] Bain, C. D.; Evall, J.; Whitesides, G. M. *J. Am. Chem. Soc.* **1989**, *111*, 7155–7164.

[39] Graupe, M.; Takenaga, M.; Koini, T.; Colorado, R., Jr.; Lee, T. R. *J. Am. Chem. Soc.* **1999**, *121*, 3222–3223.

[40] Colorado, R., Jr.; Villazana, R. J.; Lee, T. R. *Langmuir* **1998**, *14*, 6337–6340.

[41] Snyder, R. G.; Strauss, H. L.; Elliger, C. A. *J. Phys. Chem.* **1982**, *86*, 5145–5150.

[42] Porter, M. D.; Bright, T. B.; Allara, D. L.; Chidsey, C. E. D. *J. Am. Chem. Soc.* **1987**, *109*, 3559–3568.

[43] For an explanation of the analysis of thin organic films on solid substrates by specular X-ray reflectivity see: (a) Wasserman, S. R.; Whitesides, G. M.; Tidswell, I. M.; Ocko, B. M.; Pershan, P. S.; Axe, J. D. *J. Am. Chem. Soc.* **1989**, *111*, 5852–5861. (b) Tidswell, I. M.; Ocko, B. M.; Pershan, P. S.; Wasserman, S. R.; Whitesides, G. M.; Axe, J. D. *Phys. Rev. B* **1990**, *41*, 1111–1128.

[44] Ewen, B.; Strobl, G. R.; Richter, D. *Faraday Discuss. Chem. Soc.* **1980**, *69*, 19–31.

[45] The electron density is proportional to the mass density of a material. For Si and SiO_2 these mass densities are 2.33 g/cm^3 and 2.23 g/cm^3, respectively. This results in $\rho_{el}(Si) = 0.71$ e$^-$/Å^3 and in $\rho_{el}(SiO_2) = 0.68$ e$^-$/Å^3. In ref 43 a ratio of $\rho_{el}(SiO_2)/\rho_{el}(Si) = 0.96\pm0.01$ has been found experimentally. More information can be found in ref 29.

[46] In principle, the presence or absence of vibrations from the resulting tertiary C–H groups (methyne groups) in the doubly bonded structures could also be investigated with IR spectroscopy. However, these vibrations will most likely be too difficult to detect, as they are usually weak. Besides, the antisymmetric methyne vibration coincides with the much stronger symmetric methyl vibration and will therefore not be visible.

[47] Kim, T.; Ye, Q.; Sun, L.; Chan, K. C.; Crooks, R. M. *Langmuir* **1996**, *12*, 6065–6073.

[48] Sieval, A. B.; Van den Hout, B.; Zuilhof, H.; Sudhölter, E. J. R. *Langmuir* **2000**, *16*, 2987–2990 (see also Chapter 6).

[49] The choice to use the PCFF results is somewhat arbitrarily, as both force fields give rise to the same structures for the various clusters **A**–**E**.

[50] Recent examples are: (a) Hovis, J. S.; Hamers, R. J. *J. Phys. Chem. B* **1997**, *101*, 9581–9585. (b) Konecny, R.; Doren, D. J. *J. Am. Chem. Soc.* **1997**, *119*, 11098–11099. (c) Hovis, J. S.; Hamers, R. J. *J. Phys. Chem. B* **1998**, *102*, 687–692. (d) Lopinski, G. P.; Moffatt, D. J.; Wayner, D. D. M.; Zgierski, M. Z.; Wolkow, R. A. *J. Am. Chem. Soc.* **1999**, *121*, 4532–4533. (e) Ellison, M. D.; Hamers, R. J. *J.*

Phys. Chem. B **1999**, *103*, 6243–6251. (f) Wang, G. T.; Mui, C.; Musgrave, C. B.; Bent, S. F. *J. Phys. Chem. B* **1999**, *103*, 6803–6808. (g) Choi, C. H.; Gordon, M. S. *J. Am. Chem. Soc.* **1999**, *121*, 11311–11317.

[51] The 6-31G(d) calculations gave the following energies: Si(H) cluster = -9285.8879141 Hartree; 1-butene = -157.2210669 Hartree; butyl chain bound to Si(H) cluster = -9443.1461975 Hartree.

[52] The 6-31G(d) calculations gave the following energies: 1-butyne = -155.9668684 Hartree; structure **6C** = -9441.9503288 Hartree

[53] A table of Pauling's electronegativities for atoms can be found in most organic chemistry textbooks. In this case they were taken from: Carey, F. A.; Sundberg, R. J. *Advanced Organic Chemistry Part A: Structure and Mechanisms*, 3rd ed.; Plenum Press: New York, NY, USA, 1980, p 15.

Chapter 6

Molecular Modeling of Alkyl Monolayers on the H-Terminated Si(111) Surface [1]

Abstract

The structure of octadecyl monolayers on the H-terminated Si(111) surface is investigated by molecular modeling simulations, using substitution percentages from 33% to 100% of the Si–H moieties by Si–alkyl groups. The major part of the calculations is done on 50%-substituted surfaces. In all calculations two-dimensionally repeating boxes are used to mimic the modified Si surface. Calculations without this repeating box approach were shown to be unsuccessful.

The results on the repeating boxes show that only with a substitution percentage of ~50% there is a good correlation between the structure of the monolayers as obtained from molecular modeling and the available experimental data. The resulting steric hindrance due to interpenetration of the Van der Waals radii is compensated for by larger attractive Van der Waals forces between parts of the alkyl chains at increased distances from the Si surface. A variety of substitution patterns with this substitution percentage of 50% is investigated, which shows that a zigzag-type pattern is most suitable to describe the structure of the layers.

From the results of the investigations an important conclusion for future experimental work is drawn: the experimentally determined substitution percentage of 50–55% of the Si–H for Si–alkyl groups is close to the maximum value that can be reached on the H-terminated Si(111) surface.

[1] The results described in this Chapter have been published:
(a) A. B. Sieval, B. van den Hout, H. Zuilhof, and E. J. R. Sudhölter *Langmuir* **2000**, *16*, 2987–2990.
(b) A. B. Sieval, B. van den Hout, H. Zuilhof, and E. J. R. Sudhölter *Langmuir*, in press.

6.1 Introduction

In the previous Chapters the preparation of covalently bound, well-ordered monolayers of 1-alkenes and 1-alkynes on H-terminated Si surfaces has been described. A large variety of functionalized and underivatized compounds has successfully been used. The monolayers have been characterized in detail using several different techniques that provide information on the bulk of the monolayer or the average properties of the constituting molecules. For example, the results from IR spectroscopy, contact angle measurements, and X-ray reflectivity measurements show that densely packed, well-ordered monolayers are formed on the Si surface and also provide information about the structure of the monolayer, like the average tilt angle of the molecules. However, only the overall, i.e., bulk properties of the monolayer are obtained, as these methods measure over a relatively large area of the surface. Thus, it is at present not possible to get detailed experimental information about the geometry of individual molecules in the monolayers.

In the case of monolayers of linear 1-alkenes on the H-terminated Si(111) surface, a possible structure of the molecules in the monolayer has been proposed on the basis of the available experimental data.[1] It was deduced that approximately 50–55% of the Si–H groups on the surface had reacted with the 1-alkene, whereas the other Si–H groups remain intact.[1,2,3] The alkyl chains are tilted approximately 30° with respect to the surface normal and are in an all-*trans* conformation,[1,2] except for the first C–C bond at the surface, which is considerably twisted (torsion angle Si–C–C–C ≈ 37°).[1] From a ball-and-stick model of such a modified surface a comparable structure is found. However, in the case of ω-functionalized molecules the situation becomes more complicated, as has already been observed for, e.g., the acetate-terminated monolayer described in Chapter 3. In this monolayer the molecules are considerably less tilted compared to simple 1-alkenes of similar length without additional groups (tilt angle 17° vs. 28°). This change in the tilt angle is most likely due to both steric and electronic effects of the ester group, which force the molecules in a different orientation. However, the results of such effects on the final structure of the monolayer can not be predicted in advance by ball-and-stick models. Thus, it is evidently necessary to get more information about the structure of the layers on a molecular level.

Molecular modeling provides a unique way to atomistic information on these monolayers on Si surfaces. Monolayers of amines on Cl-terminated Si(100) surfaces, prepared by chemical vapor deposition, have been investigated by molecular modeling, using a small, finite Si surface with only 12 organic molecules bound to it.[4] Disordered structures

were found for the monolayers, which corresponded well with the available experimental data. A different approach has been used for monolayers of thiols on gold, where the modified surface was described by two-dimensionally repeating boxes with periodic boundary conditions.[5] This latter method is often used in molecular dynamics investigations of (physisorbed) organic monolayers on solid surfaces.[6]

As mentioned above, the properties of molecules in a monolayer are in general derived from measurements that investigate a relatively large surface area. Thus, the ideal way to describe the modified surfaces at a molecular level by theoretical means would be the investigation of a very large surface occupied with at least several hundreds of alkyl chains. Such calculations are possible in molecular mechanics, but they are at present limited by computational aspects. Therefore, it is desirable to reduce the size of the structure under investigation, as has been done in both methods mentioned above.

The use of small surfaces instead of large ones is one possibility for such reduction.[4] However, although the results from these calculations are consistent with the experimental data, it is doubtful that by this approach the structure of monolayers can be properly described, as will be discussed (see Section 6.3.1.1). In general, the results from such calculations suffer badly from edge effects, as molecules along the edges are not representative for molecules in the bulk of the monolayer. In calculations on small surfaces a large fraction of the molecules is located along the edges of the surface, unlike in a real monolayer, in which the total number of molecules in an ordered domain is significantly larger than the number of molecules at the domain edges. Consequently, the final structure that is obtained will likely deviate from that of an ordered monolayer, which indicates that any good correlation with experimental data is probably coincidental.

An alternative approach to reduce the required computational means is the use of repeating boxes to describe a modified surface.[5] In this method, that makes use of two-dimensionally repeating boxes, there are no edges, because of the periodic boundary conditions that are used. Thus, the molecules in the box represent the bulk of the monolayer, which means that in this case a better correlation with experimental data is to be expected for monolayers with large ordered domains. However, so far no systematic investigations on this approach have been done, and it also has not been shown that these calculations give the same (or better) results as very large non-repeating surfaces.

In this Chapter the results of molecular modeling investigations on octadecyl monolayers on the H-terminated Si(111) surface are described. The H-terminated Si(111) surface was chosen, as it displays a well-defined two-dimensional structure, in contrast to the

H-terminated Si(100) surface (see Section 2.2.2). Only one H atom is bound to each Si surface atom, which simplifies the construction of the starting structures and thus the modeling of this surface. The octadecyl monolayer was chosen, as the structure of this monolayer on the Si(111) surface is relatively well known,[1,2,3] which allows for a more direct comparison with experiment.

The methodological aspects are investigated by comparing the results of calculations on large finite surfaces to those investigated with periodic boundary conditions. Also, the effects of different substitution patterns on the monolayer structure are investigated, as many different patterns can be formed on the Si(111) surface if 50% of the Si–H groups are replaced by alkyl chains, as concluded from experimental data.[1,2,3] On the basis of the proposed radical-chain reaction mechanism for the formation of these covalently attached monolayers,[1,7] it is likely that several different substitution patterns will be present on the Si surface. However, there are currently no experimental data available about the structure of these substitution patterns. Therefore, several different patterns with 50% substitution of the Si–H groups for Si–alkyl groups will be investigated, as well as several different starting structures that actually describe the same pattern, but differ in the overall symmetry of the box.

Besides this variation in the substitution patterns, different substitution percentages of the Si–H for Si–alkyl groups are investigated. Both significantly lower (33%) and higher (67% and 100%) substitution percentages are used. Higher values than 50% have already been reported for well-ordered monolayers on the Si(111) surface. In the case of a pentyl monolayer on the Si(111) surface, it was estimated that 60% of the Si surface atoms was bound to an alkyl chain.[8] For monolayers of octadecanal on Si(111) even the unlikely high substitution percentage of 97% was claimed.[3] By investigating such surfaces with a significantly higher substitution percentage than 50% it is possible to get an idea about the maximum substitution percentage that can be reached with these alkyl monolayers on the Si(111) surface.

6.2 Experimental Details

6.2.1 General

All calculations were performed with the MSI program Cerius[2], version 3.5 or 3.8.[9] The structures were optimized with "high-convergence" criteria[10] using the "Smart Minimizer" minimization routine. Two force fields were used for the calculations: the Universal Force Field (UFF)[11] and the Polymer Consistent Force Field (PCFF),[12] both as implemented in Cerius[2]. The PCFF force field does not contain inversion parameters for Si atoms with a dangling bond, therefore the "ignore undefined terms" option was necessary in these calculations. Such atoms are present at the bottom of the Si crystal structure (*vide infra*), and as such this reduction of the system does not influence the outcome of the calculations.

In most cases the two force fields give similar results, however, in some situations the UFF force field gave unlikely differences between structures that should give (nearly) identical results. These discrepancies are most likely due to artifacts, however, their appearance is unpredictable. No such artifacts were found for PCFF calculations, and therefore only the results from these calculations are presented and discussed in this Chapter (with one exception, see Section 6.3.3.1).

6.2.2 Construction of Starting Structures

All starting structures were obtained from a small unit cell that contains one octadecyl chain and four Si atoms that represent the atoms in the first four layers of the Si surface. This structure was obtained by cleaving the Si crystal structure from the Cerius[2] database along the (111) plane. Subsequently, a pre-optimized, vertically aligned all-*trans* octadecyl molecule was attached to the dangling bond of the top Si atom. This new structure was placed in a box, with the following dimensions: $a = b = 3.840$ Å (from the Si bulk unit cell), and $c = 35$ Å, and angles $\alpha = \beta = 90°$, and $\gamma = 120°$ (see Figure 1).

Subsequently, this box was copied in the a and b direction by as many times as necessary to obtain a new structure with the dimensions of the required larger repeating box. Finally, alkyl groups were replaced by hydrogen atoms at the appropriate positions, to obtain the boxes with the various substitution percentages used to describe the modified surfaces. The various unit cells used in this investigation are depicted in the Results and Discussion section. The numbers of these unit cells (**33**, **50**, and **67**) refer to the substitution percentages of the Si–H for Si–alkyl groups (33%, 50%, and 67%, respectively). The various substitution patterns are identified by capitals (**33-A**, **33-B**, etc). To mimic the Si crystal structure, the

much smaller contribution of the attractive Van der Waals forces, confirming that these forces between the alkyl chains are not properly accounted for in these finite surface calculations.

The results in Figure 3 may suggest that by using very large surfaces, i.e., with $n >$ 162, the structure of the modified surfaces could be described properly, because of the convergence of the tilt angle and the energy with increasing n. Although larger surfaces will better resemble the terraces of the H-terminated Si(111) surface,[16] the problems associated with the edge effects will not be eliminated, as further increase of the surface size still does not produce a surface without edges. Also, increasing the surface size rapidly becomes problematic from a practical point of view, because of the rapid increase of the time needed for the computations.[17] Therefore, calculations on these large surfaces are not suitable for the modeling of these monolayers.

6.3.1.2 Simulations on Infinite Surfaces

The problem of the edge effects can be eliminated by the approach of periodic boundary conditions, i.e., the use of repeating boxes. In such calculations, the surface is described by two-dimensionally repeating units, which are themselves relatively small surfaces, but their periodic repetition in two dimensions provides a means to represent an infinitely large surface. This implies that all alkyl chains on the surface, including those along the edges of the surface, are now fully surrounded by other alkyl chains, because the molecules at one side of the box "feel" the presence of the molecules at the opposite side. Consequently, the system does no longer have edges and the problems associated with these edges will therefore disappear. Thus, this approach of periodic boundary conditions is well suitable to be used for the molecular mechanics calculations on ordered monolayers on extended solid surfaces.

For the successful modeling of the monolayer structure by this approach of two-dimensionally repeating boxes, the result of the calculations has to satisfy the criterion that a change in the box size should not influence the final structure of the monolayer if all other factors remain unchanged. This means that an increase or decrease of the number of alkyl chains n in a repeating box, without changing the substitution percentage or the substitution pattern on the surface, must not affect the outcome of the calculation. This also implies that independent of n the system has to have a constant average energy per alkyl chain. The results presented in this Chapter show that this is only the case for boxes that contain at least ~30 alkyl chains. As this section concerns the comparison of the two methods, the origin of this effect is already discussed here.

Calculations on smaller boxes with less than ~30 alkyl chains usually give results that depend strongly on the box size used. Not all alkyl chains in a monolayer will be identical, but they will have slightly different geometries, in order to achieve the optimal packing. In too small a box, some of the alkyl chains may be forced into a certain position, due to the fact that the method of repeating boxes forces alkyl chains in adjacent boxes to be similar. The observed variation in the average energy per alkyl chain E_{ave} of the various structures is mainly caused by differences in the Van der Waals energy per alkyl chain. This indicates that in a small box with only a few alkyl chains the intermolecular forces between these alkyl chains are not properly accounted for, unlike in the large boxes. Thus, the modeling of the monolayer structure is only successful with these larger boxes with many alkyl chains, and only the results of these larger boxes will be discussed in this Chapter.

6.3.2 50% Substitution of Si–H for Si–Alkyl Groups

6.3.2.1 Practical Issues in the Simulations

A projected surface area of ~24 Å^2 per alkyl chain in the monolayer and a tilt angle of ~28–30° for such chains have been derived from a combination of infrared dichroism measurements and X-ray reflectivity experiments.[1,2] The surface area of a Si–H group on the Si(111) surface is 12.77 Å^2, as can be calculated from the dimensions of the basis unit cell depicted in Figure 1. This gives a theoretical substitution percentage of ~53% of the Si–H for Si–alkyl groups on this surface, in line with the reported experimental values of 50–55%.[1,2,3] For the molecular modeling of these alkyl monolayers on the Si(111) surface a substitution percentage of 50% of the surface Si–H groups for Si–alkyl groups is an appropriate approximation, as this value is close to the aforementioned value of 53% and within the experimentally determined range of 50–55%. It is also a highly convenient value, because the Si–H : Si–alkyl ratio of 1 : 1 allows for easy construction of substitution patterns on the Si surface.[18]

6.3.2.2 Ordered, Linear Substitution Patterns

As was already discussed in Section 6.1, a variety of substitution patterns can be formed on the surface, because of the proposed radical-chain mechanism of monolayer formation.[1,7] One possible pattern on the Si(111) surface is a linear substitution pattern, with all molecules on the surface in long straight lines. With a substitution percentage of 50% there

are three different unit cells (**50-A**, **50-B**, and **50-C**; Figure 4) that can be used to describe such a surface, which differ in the overall symmetry of the box. Unit cells **50-A** and **50-B** have one plane of symmetry (along the long diagonal of the box), whereas cell **50-C** has no symmetry. As a result of the procedure followed to obtain the surfaces, each of the three repeating boxes is optimized to a local minimum. These local minima are the same if the positions of *all* atoms in the box (up to several thousands of atoms for the larger boxes) would be identical. In practice this appears to be never the case, and several very slightly different structures are obtained as end result.

The results obtained from the calculations on boxes with these patterns are shown in Figure 5, which shows the average energy per alkyl chain (E_{ave}) of the PCFF calculations. The results show that in the case of small boxes (n = 2, 8, and 18) the energy per alkyl chain E_{ave} varies with n, the number of alkyl chains in the box. For the larger boxes (n > 30) E_{ave} becomes almost independent of the box size (see Section 6.3.1.2), and also E_{ave} of the various patterns **50-A** to **50-C** becomes approximately equal at large values of n. As all three structures **50-A**, **50-B**, and **50-C** describe the same substitution pattern on the Si surface, the differences between the various boxes should disappear at large n, because in large boxes the interactions that can take place between the alkyl chains within the box become similar. However, the structures obtained from the simulations with pattern **50-C** differed from those of the other two patterns **50-A** and **50-B**. The boxes **50-A** and **50-B** give monolayers in which the alkyl chains are well-ordered, i.e., mainly all-*trans*, and show tilt angles of ~25°–30°, in agreement with experimental values.[1,2] Figure 6 gives an example of such a structure. The molecules in structures of type **50-C** were less tilted (tilt angles of ~20° instead of ~25°) and the overall structure of the monolayer was more disordered, with twist angles in almost all the C–C bonds of the alkyl chains. Both the computed tilt angle and the disordered alkyl chains are two factors that do not correspond to the ordered structure that is observed experimentally. Thus, it seems that boxes of type **50-C** do not give a good description of the monolayer structure and are therefore less suitable for the molecular modeling of these alkyl layers on Si(111) surfaces. The reason for this behavior is not clear, but it may be related to the difference in the symmetry of pattern **50-C** compared to that of the two patterns **50-A** and **50-B** (*vide supra*).

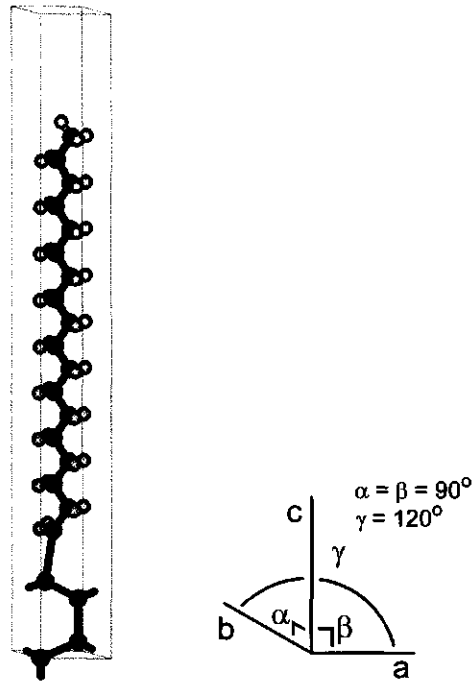

Figure 1. Structure of the basis unit cell as used for the construction of the repeating boxes.

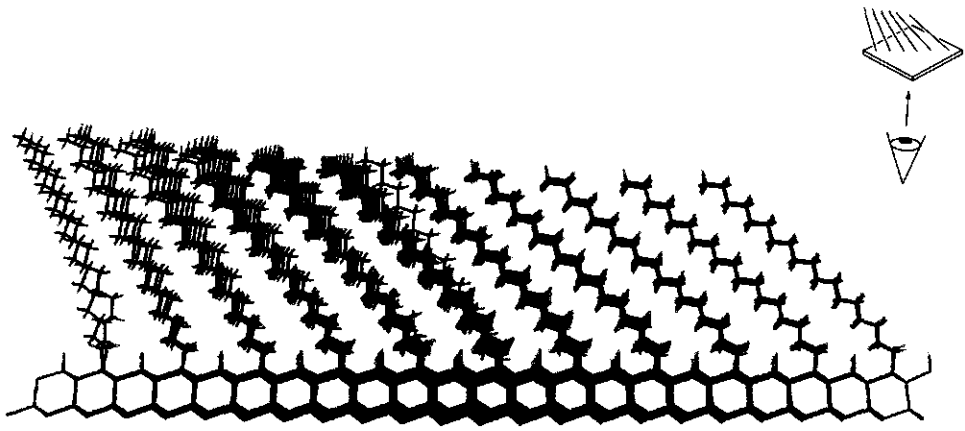

Figure 2. The influence of edge effects on the monolayer structure: calculation on a Si surface with 72 alkyl chains without periodic boundary conditions (side view). Inset: view direction in Figure 2.

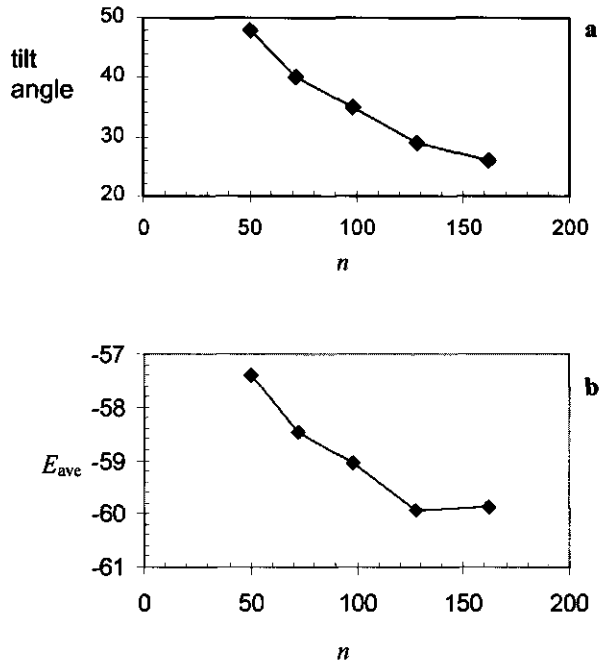

Figure 3. (a) Dependence of the tilt angle (degrees) of the central molecules on the number of alkyl chains n on the Si surface in calculations without periodic boundary conditions. (b) The average energy (kcal mol^{-1}) per alkyl chain from the PCFF calculations for these Si surfaces without periodic boundary conditions.

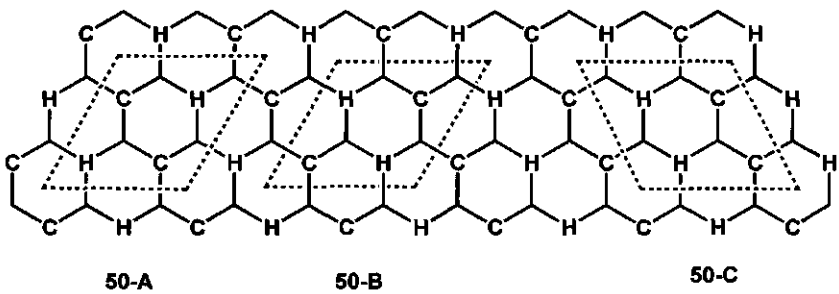

Figure 4. Unit cells **50-A**, **50-B**, and **50-C** for the linear patterns with a substitution percentage of 50%. The **C** and **H** indicate the alkylated and H-terminated Si surface atoms, respectively.

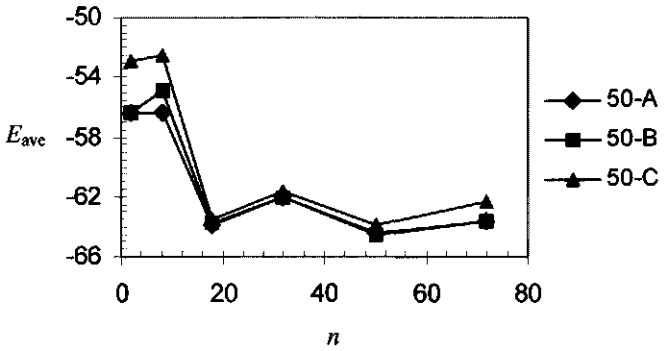

Figure 5. Results (E_{ave} (kcal mol^{-1}) per alkyl chain vs. n) of the PCFF calculations on cells **50-A**, **50-B**, and **50-C**.

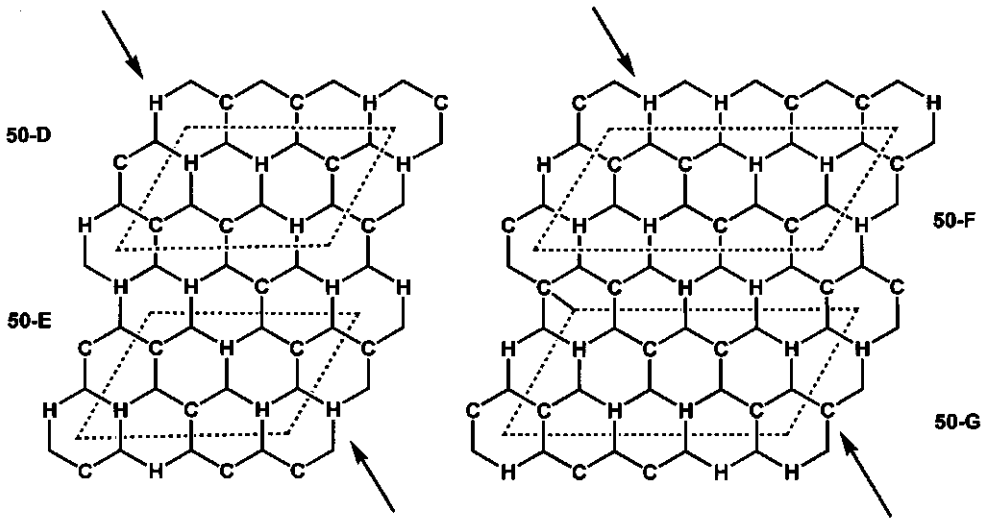

Figure 7. Unit cells **50-D**, **50-E**, **50-F**, and **50-G** for the two types of zigzag patterns with a substitution percentage of 50%. For an explanation of the arrows see the text.

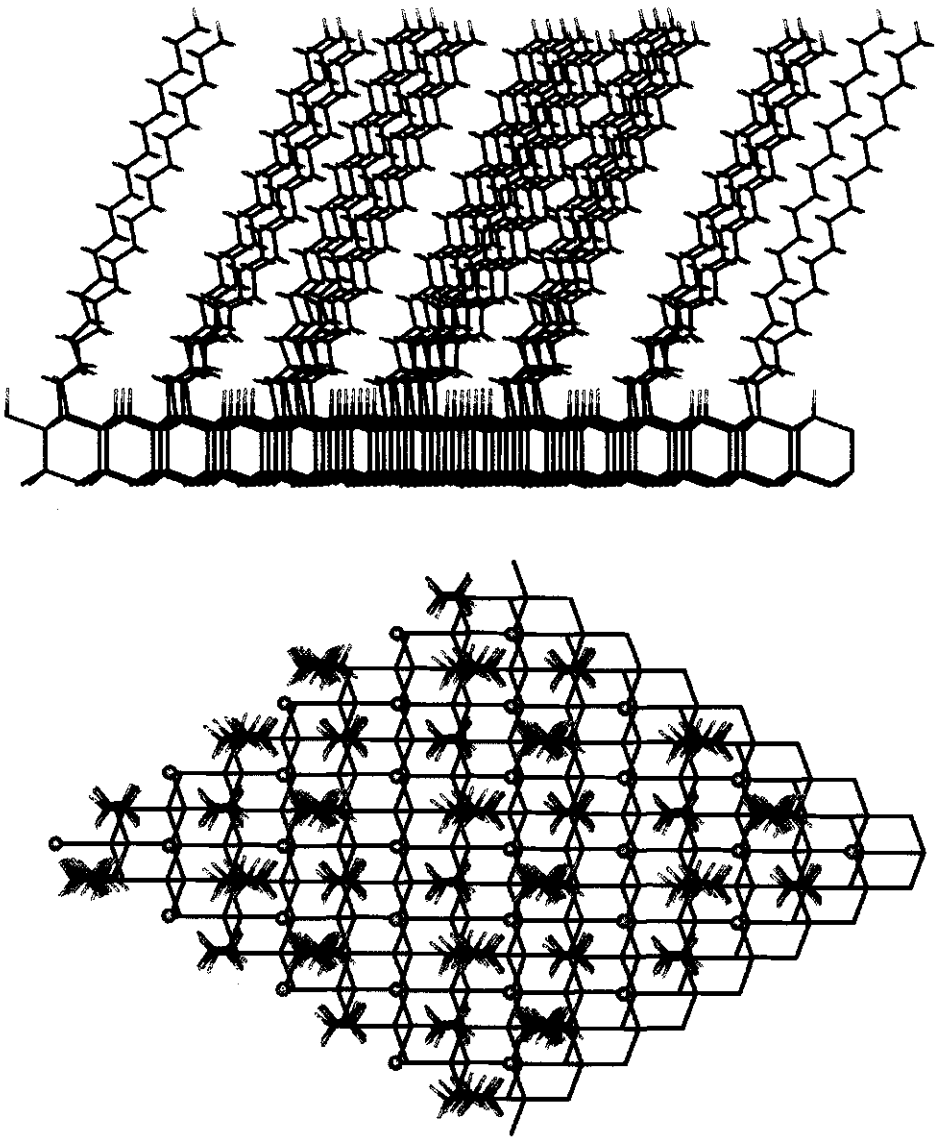

Figure 6. Example of the structure of a monolayer as obtained with the PCFF calculations on the linear patterns **50-A** and **50-B**. Both a side view (top) and a top view (bottom) are shown for a surface with n = 32. In the top view the model is rotated in such a way that the alkyl chains are oriented nearly perpendicular to the plane of paper, to show the all-*trans* conformations of the alkyl chains. For reasons of clarity and to reveal the substitution pattern, the remaining hydrogen atoms at the Si surface are depicted in this top view as blue balls.

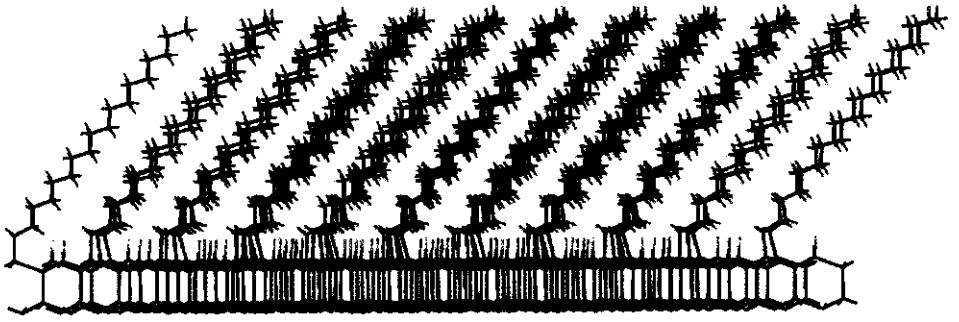

Figure 9. Example of the structure of a monolayer as obtained with the PCFF calculations on the zigzag patterns **50-D** and **50-E**.

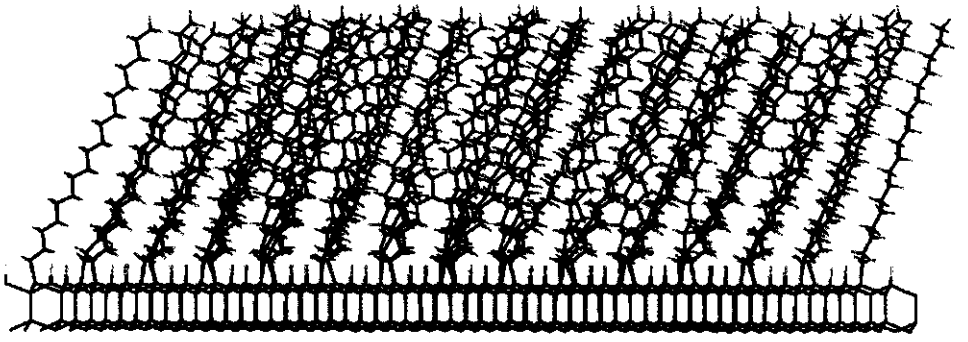

Figure 10. Example of the structure of a monolayer as obtained with the PCFF calculations on the zigzag patterns **50-F** and **50-G**.

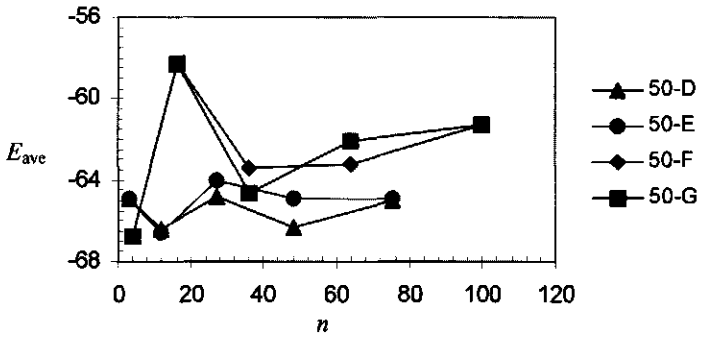

Figure 8. Results (E_{ave} (kcal mol^{-1}) per alkyl chain vs. n) of the PCFF calculations on cells **50-D**, **50-E**, **50-F**, and **50-G**.

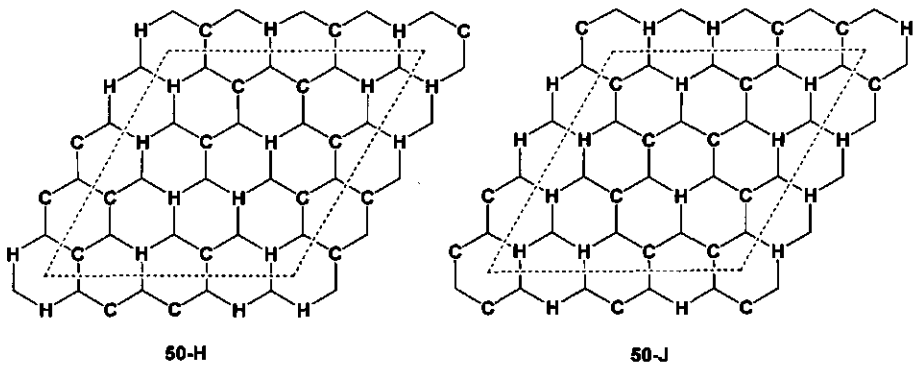

Figure 11. Unit cells **50-H** and **50-J** with disordered patterns and a substitution percentage of 50% of the Si–H for Si–alkyl groups.

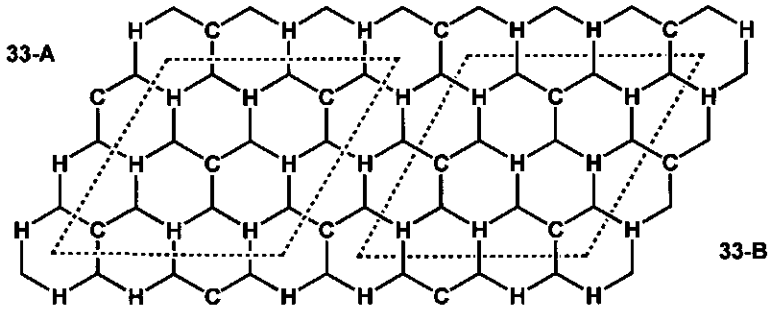

Figure 13. Unit cells **33-A** and **33-B** of the hexagonal patterns with a substitution percentage of 33%.

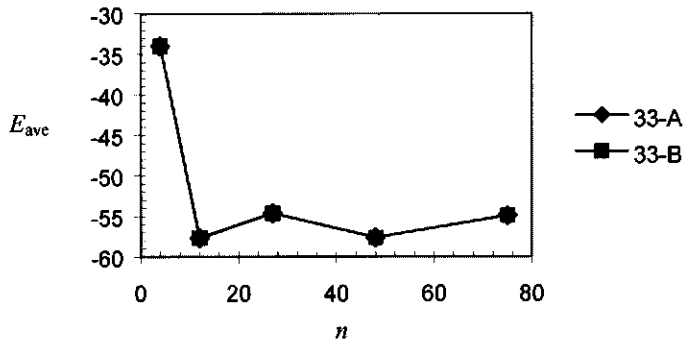

Figure 14. Results (E_{ave} (kcal mol^{-1}) per alkyl chain vs. n) of the PCFF calculations on cells **33-A** and **33-B**.

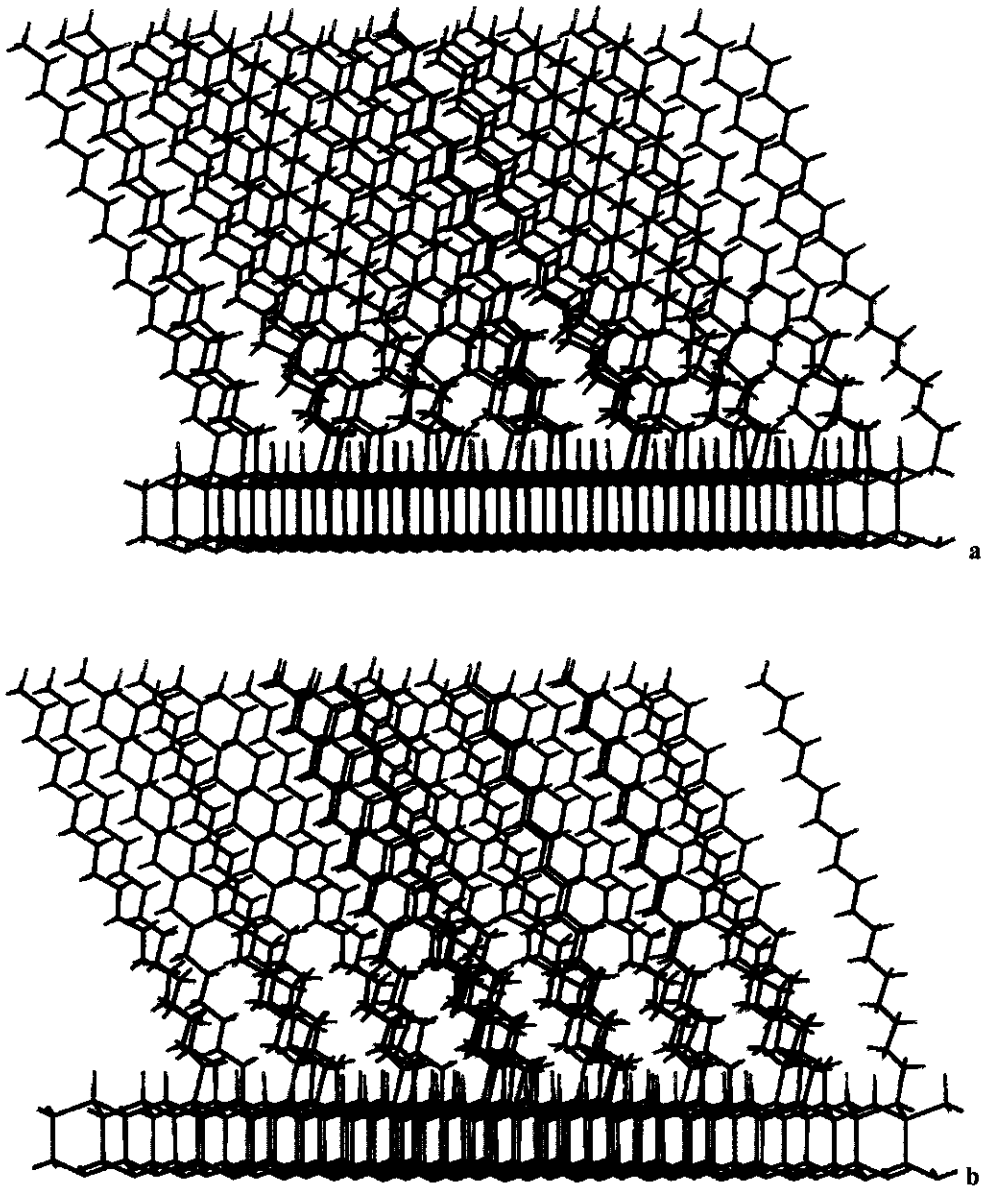

Figure 12. (a) Example of the structure of a monolayer as obtained with the PCFF calculations on pattern **50-H**. (b) Example of the structure of a monolayer as obtained with the PCFF calculations on pattern **50-J**.

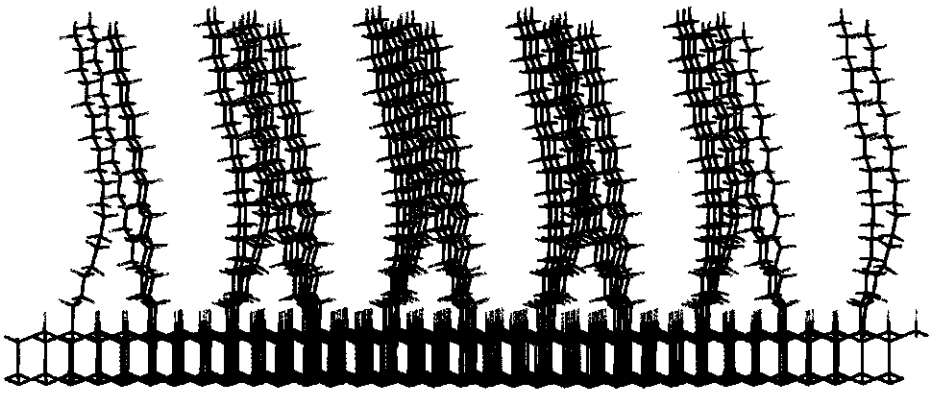

a

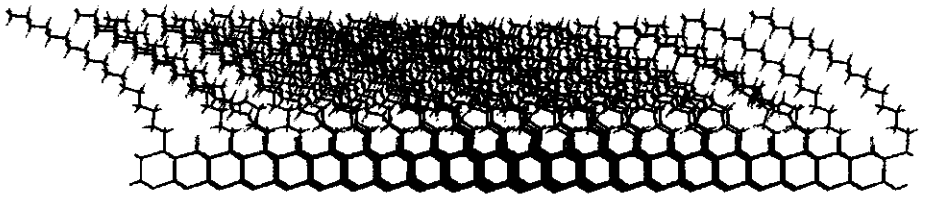

b

Figure 15. (a) Example of the structure of a monolayer as obtained with the PCFF calculations on patterns **33-A** and **33-B**. (b) Example of the structure of a monolayer as obtained with the UFF calculations on patterns **33-A** and **33-B**.

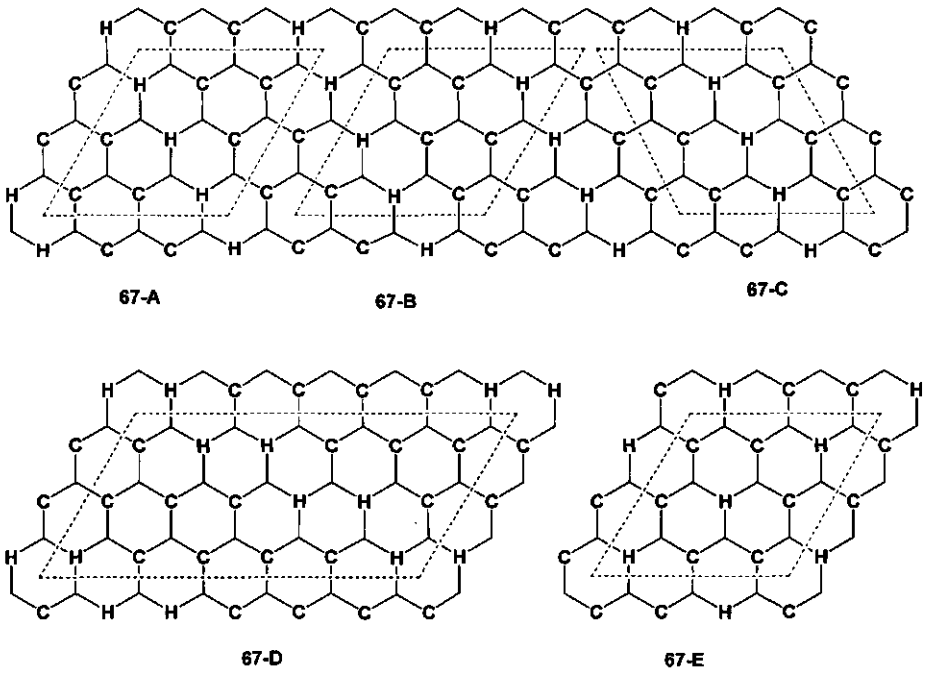

Figure 16. Unit cells **67-A**, **67-B**, **67-C**, **67-D**, and **67-E** of the patterns with a substitution percentage of 67%.

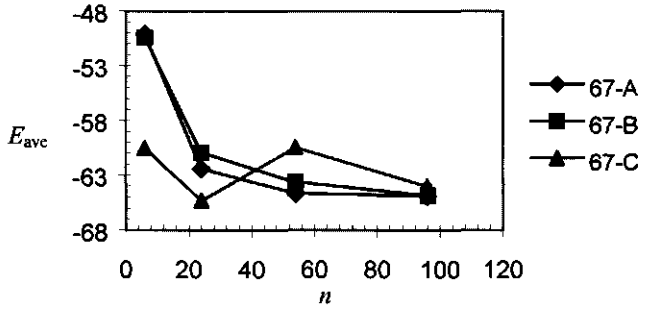

Figure 17. Results (E_{ave} (kcal mol^{-1}) per alkyl chain vs. n) of the PCFF calculations on cells **67-A**, **67-B**, and **67-C**.

6.3.2.3 Ordered, Zigzag-Type Substitution Patterns

Alternatives for the linear substitution patterns are zigzag-type substitution patterns. Four of such structures were investigated, which represent two different types of zigzag patterns (Figure 7). In boxes **50-D** and **50-E** two unit cells are shown in which the alkyl chains form sets of three along the indicated direction (arrows). In the other pattern, described by the boxes **50-F** and **50-G**, the alkyl chains form sets of two molecules. The results obtained on the linear substitution patterns (see Section 6.3.2.2) have shown the usefulness to investigate a substitution pattern with several different unit cells. Therefore, two unit cells were used for each of the two patterns.

The results obtained on these zigzag patterns are shown in Figure 8. The same trends as found for the linear patterns (**50-A** and **50-B**) are observed with these zigzag patterns. For boxes with large n ($n > 20$) the average energy per alkyl chain E_{ave} again becomes nearly independent of the box size, and the resulting monolayer structures are all highly similar. For the patterns **50-D** and **50-E** the average value of E_{ave} (~ -65 kcal mol^{-1} per alkyl chain) is somewhat lower than that of the linear patterns ($E_{ave} \approx$ -64 kcal mol^{-1} per alkyl chain). The average energy of the other zigzag type patterns **50-F** and **50-G** is somewhat higher ($E_{ave} \approx$ -62 kcal mol^{-1} per alkyl chain). This indicates that only small differences exist between the various patterns, either zigzag or linear, which suggests that the various patterns will likely all be present on the modified Si surface.

For all zigzag patterns investigated here the structure of the monolayers, as modeled with large n, is again consistent with the experimental data. The tilt angles of the octadecyl chains are ~25–30° and the molecules are mainly in all-*trans* conformations. Two examples are shown in Figure 9 and 10. This indicates that all these patterns, either linear or zigzag, give similar results for the monolayer structure. Also, the thickness of these monolayers is approximately 19 Å, which agrees within experimental uncertainty with two measured values: 18 Å, as determined with ellipsometry,[1] and 19.7 Å, from X-ray reflectivity measurements.[2] The results do not agree with the results of an earlier X-ray measurement, which yielded a monolayer thickness of only 16 Å.[1] This lower value not only is less likely given the more recent X-ray data,[2] but would also require all alkyl chains to have a considerably large average torsion angle in the Si–C–C–C bond at the surface (estimated to be 37°). In the structures as obtained from the molecular mechanics investigations described in this Chapter no such large twist angles were observed (see, e.g., the top view in Figure 6). Many of the alkyl chains have Si–C–C–C twist angles close to 0°, some are in the range of 5–15°, and only

occasionally values up to 36° are found. However, even the CH_3 groups of these latter alkyl chains are only slightly below the outside of the monolayer surface and a thickness of only 16 Å is not found.

The computations predict that the two zigzag patterns **50-D** and **50-E** yield the lowest energy structures. To the degree that the occurrence of the various patterns formed in the radical-chain reaction is determined by the stability of the product, this would suggest that **50-D** and **50-E** are the most likely substitution patterns. If, on the other hand, the resulting pattern is determined by the kinetics of the reaction, e.g., an irreversible H atom abstraction from the Si surface, then our computations suggest that experimental parameters, such as tilt angles and packing densities as derived from IR dichroism and X-ray reflectivity measurements, can not be used to distinguish between several of the possible substitution patterns. This shows that more information on the mechanism and kinetics of the monolayer formation is necessary.

6.3.2.4 Disordered Patterns

The results of the calculations with a substitution percentage of 50% show a good correlation between experimental data and the computational results. However, so far only monolayers with highly ordered substitution patterns have been investigated. In reality, it may well be the case that several of the highly ordered patterns are simultaneously present as relatively small patches on the surface. The presence of such patches would thus only imply a high short-range two-dimensional organization. Upon increased degrees of coverage, the radical-chain mechanism proposed for the formation of these monolayers[1,7] suggests that the growing domains of alkyl groups will encounter each other on the surface, which will give rise to mismatches in the patterns at the boundaries between the various domains. For example, if one domain is formed with a zigzag pattern and the other with a linear pattern, the structure of the monolayer has to switch abruptly from one pattern to the other at the boundary between these two domains. As a result, disordered patterns will be present on the surface at these boundaries. The consequences of the introduction of such disordered areas on the overall structure of the monolayer are discussed in this section.

The effects of such disorder can be investigated by designing a large box, in which two different patterns are present on the Si surface with a disordered area between these two domains. However, the problem with such an approach is that one would also have to study the effect of the size of the separate domains on the results, as the size of these domains is currently not known from experiments. Besides, if a large surface with only a relatively small

defect area would be investigated, this area will most likely have only a minor effect on the overall monolayer structure. This would result in an average energy per alkyl chain close to the current range of E_{ave} for the various patterns **50-A** to **50-G**. Consequently, such calculations would give little information about the effect of the disorder.

This problem can be solved by using a large surface with many disordered areas, as this increases the effects of disorder on the overall monolayer structure. Two boxes with such disordered patterns were investigated here (Figure 11). Pattern **50-H** is a combination of the two zigzag patterns **50-F** and **50-G**, pattern **50-J** is a more-or-less randomly constructed pattern with an overall substitution percentage of 50%. In these patterns, small areas exist in which several unreacted Si–H groups are still grouped together, whereas clusters of several alkyl chains are present in other areas. Such situations will most likely indeed occur at least at the domain boundaries.

The results of the calculations on these two disordered patterns showed that the energy of these patterns **50-H** and **50-J** is considerably higher compared to that of the ordered patterns (**50-A** to **50-G**). For **50-H** the difference is approximately 1–3 kcal mol^{-1} ($E_{ave} \approx$ -62 kcal mol^{-1} per alkyl chain), i.e., close to the energy of the composing zigzag patterns **50-F** and **50-G**. This difference in the average energy per alkyl chain indicates that this disordered pattern is less favorable than the ordered patterns, which suggests that it will not be present on the surface in significant amounts. For pattern **50-J** the difference in energy with the ordered patterns is approximately 3–5 kcal mol^{-1} ($E_{ave} \approx$ -60 kcal mol^{-1} per alkyl chain), which is even larger. Consequently, this pattern will also only be present on the surface in small amounts.

Interestingly, the structure of the monolayers is still properly described by these two patterns, despite the difference in the energy of the system. Figure 12 shows the results of the PCFF calculations on both patterns (for the boxes with $n = 32$). The tilt angles are near 25° and the alkyl chains are mainly in all-*trans* conformations. This suggests that, if such disordered patterns are indeed present at the boundaries between the ordered domains, the packing of the alkyl chains in the monolayer is not or only slightly disturbed.

The major difference in the energy of these disordered patterns is found in the contribution from favorable Van der Waals interactions, which are usually diminished compared to that in the well-ordered patterns. This is due to the fact that in these disordered patterns there are areas in which the density of alkyl chains is below 50%. Of course this is compensated for by areas that have a higher density of alkyl chains than 50%, however, this does not give a decrease in the total energy of the system, as the steric hindrance between the

alkyl chains in such areas increases strongly (see also Section 6.3.3.2). This steric hindrance is visible in Figure 8, where some of the Si–C bonds show rather large tilt angles.

6.3.3 Different Degrees of Coverage

6.3.3.1 Low Coverage

As already discussed in the Introduction, it has been estimated from experimental data that ~50% of the Si–H groups on the Si(111) surface is replaced by alkyl chains.[1,2,3] In this situation, all alkyl chains have to penetrate the Van der Waals radii of other alkyl groups, especially near the Si surface, as they have to be on neighboring Si surface atoms. This is energetically unfavorable and it might be that the alkyl chains can not be bound to the surface in such patterns, because of steric repulsion. If it is not possible to place two alkyl chains on neighboring Si surface atoms, the closest packing density is the situation where each alkyl chain on the Si(111) surface is surrounded by six Si–H groups. This gives a hexagonal substitution pattern on the surface and the substitution percentage is only 33%, considerably lower than the experimental value of 50–55%. Two such cells, **33-A** and **33-B**, which have the hexagonal substitution patterns that describe such a surface (Figure 13), were investigated. The results of the calculations are depicted in Figure 14.

There are no significant differences between the results for the two cells **33-A** and **33-B**. They give similar structures and approximately the same value for E_{ave} at all n, except for $n = 3$. Therefore only the results on the larger repeating boxes (with $n \geq 12$) are discussed. The energy E_{ave} of these patterns **33-A** and **33-B** is considerably higher (by ~7–10 kcal mol^{-1} per alkyl chain, depending on n) than that of the 50% substituted surfaces, indicating that this substitution percentage of 33% is energetically less favorable. The main factor responsible for this large difference was found in the Van der Waals energy of the two systems, with the 50%-substituted surfaces being more favorable by ~10 kcal mol^{-1} per alkyl chain. The remaining difference in E_{ave} mainly comes from differences in torsion and bond energies. This means that the addition of extra alkyl chains to the 33%-substituted surfaces is energetically favorable. It is therefore expected that this will occur, which shows that the alkyl chains can be on neighboring silicon surface atoms.

That the situation with 33% substitution is not the correct substitution percentage for these alkyl monolayers on the H-terminated Si(111) surface is also evident from the structure

of the monolayers (Figure 15a). The molecules are tilted towards each other, forming small corn sheaf-like clusters in an attempt to maximize the attractive Van der Waals interactions between the alkyl chains. This effect has also been observed for monolayers of alkyl amines on the Si(100) surface investigated with molecular modeling, which do not form close-packed monolayers.[4] Usually, the alkyl chain in the middle of a cluster is oriented nearly perpendicular to the Si surface, whereas the other alkyl chains show a bend, or adopt twisted or banana-like conformations. This results in a disordered monolayer structure, in contradiction with results from IR spectroscopy and X-ray reflectivity.[1,2] On the basis of these results it is concluded that the substitution percentage of 33% is too low and that the alkyl chains in the monolayers can be bound to neighboring silicon surface atoms. The resulting steric hindrance due to interpenetration of Van der Waals radii is apparently compensated for by larger attractive Van der Waals forces between parts of the chains at increased distances from the Si surface.

It is interesting to note that in this particular case a completely different structure was found for the UFF calculations. An example is shown in Figure 15b. In order to maximize the Van der Waals interactions, the alkyl chains have very large tilt angles (up to about 60°). This value does not correspond to that found experimentally (28–36°),[1,2] which again indicates that the substitution percentage of 33% is not correct. The reason for this difference is not known, however, both situations are minima. Also, if a UFF-optimized structure is subsequently investigated with the PCFF force field (or vice versa), this structure has a much higher energy compared to the optimized structure as found with PCFF calculations.

6.3.3.2 High Coverage

In the previous section it has been shown that patterns with a substitution percentage significantly below 50% do not give a good description of the monolayer structure. However, this does not confirm that 50% is indeed the correct substitution percentage for these monolayers of 1-alkenes on the H-terminated Si(111) surface, as higher percentages (60%[8] and even 97%)[3] have been reported. Up to now no high-coverage monolayers have been examined by theoretical calculations. In this section, two of these higher substitution percentages (67% and 100%) are investigated.

Computations on the surfaces with a substitution percentage of 100% (as an approximation[18] for the 97%-occupied surface)[3] are relatively easy, as all Si surface atoms have to be bound to an alkyl chain. Investigation of these structures showed that surfaces with this substitution percentage are very unlikely. The molecules are oriented perpendicular to the

Si surface (tilt angle ~1°) and penetrate each others Van der Waals volume to a large extent,[19] a situation which is highly unfavorable. Serious deformations of the Si–C bonds at the surface occur as well. As a result, the energy of the alkyl chains in these structures is very high (E_{ave} = -14.7 kcal mol^{-1} per alkyl chain), compared to, e.g., 50% substitution ($E_{ave} \approx$ -64 kcal mol^{-1} per alkyl chain). This situation is not expected to be different for molecules that are linked to the surface via a Si–O–C bond instead of a Si–C bond, as is the case for the reaction of octadecanal molecules with the H-terminated Si(111) surface.[3] Therefore, it is evident that this substitution percentage is not possible on the Si(111) surface.

In fact, the substitution percentage of 100% is considerably above the theoretically maximum substitution percentage that is possible on the H-terminated Si(111) surface. This maximum is most likely close to 69%, as can be calculated from the cross section of 18.5–18.6 Å^2 of an alkyl chain in crystalline *n*-alkanes,[20] and the surface area of 12.77 Å^2 of a Si–H group on the Si(111) surface, as can be calculated from the size of the small unit cell shown in Figure 1. Higher percentages are thus very unlikely, but any value below this 69% may well be possible. Interpenetration of alkyl chains is required for such percentages, but the results from the 33%- and 50%-substituted surfaces have shown that this is not problematic if this results in a decrease of the average energy per alkyl chain on a surface.

Unfortunately, structures with this substitution percentage of 69% are again rather difficult to construct, as was already discussed for the situation with 53% substitution.[18] A surface with (multiples of) 100 Si surface sites would again be necessary, this time with (multiples of) 69 alkyl groups and 31 Si–H groups. Therefore, it was chosen to use surfaces with a substitution percentage of 67% (ratio Si–H : Si–alkyl = 1 : 2).

As is the case for the 50%-substituted surfaces, a large variety of substitution patterns is possible for such surfaces with a substitution percentage of 67%. In analogy with **50-A** and **50-B** three cells with linear patterns on the Si(111) surface were investigated: **67-A**, **67-B**, and **67-C** (Figure 16). For large enough values of *n* these unit cells yield highly similar results. The E_{ave} of these structures (Figure 17) is comparable to that of the 50%-substituted surfaces. This indicates that an increase of the substitution percentage from 50% to 67% yields an increase in favorable Van der Waals interactions that is apparently canceled by an increase in unfavorable conformations of the alkyl chains. This increase in unfavorable conformations mainly comes from the considerable deformations of the Si–C bonds and the first C–C bonds at the surface. The Si–C bonds are no longer nearly perpendicular to the Si surface, but make tilt angles >20°, which is energetically unfavorable. The reason for this deformation is most

likely the increased interpenetration of the Van der Waals radii of CH_2 groups at the surface compared to that on the 50%-substituted surfaces. Unlike the CH_2 groups further away from the Si surface, these methylene groups have limited possibilities to move away from each other and deformation of Si–C bonds forms the only possibility to reduce the Van der Waals repulsions.

The deformation of the Si–C bonds was also found for the zigzag pattern **67-D**. Moreover, in this structure even deformation of the Si surface itself was observed. Some of the Si atoms were lifted out of the Si surface plane, as this reduces the steric hindrance between the CH_2 groups at the Si surface. For these structures E_{ave} was somewhat lower (by ~1 kcal mol^{-1} per alkyl chain) than that of the linear patterns **67-A** to **67-C**. Since deformations of the Si surface are, however, not included in this value, due to the method that is used to calculate E_{ave} (see Experimental Section), this does not imply any favorability of this structure.

Hexagonal patterns, i.e., the inverse situations of **33-A** and **33-B**, are another possibility. Given the radical-based reaction mechanism,[1,7] the formation of such a highly ordered system seems somewhat unlikely, as it would require a high selectivity in the reaction to form such an ordered pattern, like **67-E** (Figure 16). The results showed that the energy per alkyl chain E_{ave} of these boxes is comparable to that of the 50%-substituted surfaces, as a result of the increase in energetically favorable Van der Waals interactions in the boxes. However, in all calculations the alkyl chains remained in an almost perpendicular position (tilt angle < 10°), which does not correspond to the experimental data. Considerable deformations of the Si–C bonds occur as well. Thus, this pattern does not give a good representation of the monolayer structure.

The overall structure of the monolayers with the linear patterns **67-A**, **67-B**, and **67-C**, as well as that of the zigzag pattern **67-D**, does not correspond to that determined experimentally. The tilt angle of the molecules is considerably less than 30° (generally < 20°), and in some cases the alkyl chains are almost perpendicular to the Si surface. This shows that with these patterns the Si surface is too crowded, even though this substitution percentage is energetically possible. Combined with the observed deformation of the Si–C bonds at the surface, the deformation of the Si surface, and the lack of gain in energy of the system, it becomes obvious that the octadecyl molecules can only artificially be forced onto the surface to such a degree of substitution. It must therefore be concluded that a substitution percentage of 67% is too high for monolayers of alkyl chains on the H-terminated Si(111) surface.[21]

6.3.4 Implications of the Results on Future Experimental Work

The results from the molecular modeling calculations show that with a substitution percentage of 50% the best correlation is found between the experimentally determined and the theoretically predicted structure of the alkyl monolayers on Si(111) surfaces. Significantly higher (67% and 100%) or lower (33%) substitution percentages give results that do not correlate with the experimental data and, in the case of the higher substitution percentages, result in deformations of the Si–C bonds at the surface.

There is no gain in energy upon going from 50% to 67% substitution, which suggests that the energetic minimum of E_{ave} as a function of the substitution percentage is somewhere in between these two values. This means that for these well-ordered alkyl monolayers on the Si(111) surface the optimal substitution percentage will be somewhere between 50% and 67%, and likely closer to 50%. The long alkyl chains, like the octadecyl groups investigated here, have to be approximately in all-*trans* conformations to form ordered monolayers. Somewhat higher packing densities may be thermodynamically favorable, because of an increase in attractive Van der Waals interactions between the alkyl chains, but will be kinetically problematic, as it becomes increasingly difficult for a new alkyl chain to reach the Si surface. In addition, an increase of the packing density will eventually also be thermodynamically unfavorable, as it deforms Si–Si–C angles and diminishes the flexibility of the C–C bonds near the surface, which is required in order to reduce the steric hindrance that occurs between the CH_2 groups near the Si surface (see the results on 67% substitution in Section 6.3.3.2). Consequently, there is a limit beyond which it becomes too difficult to insert more alkyl groups. This means that the currently reported well-ordered monolayers with long alkyl chains,[1,2,3] with the substitution percentages of 50–55%, display a packing density that is close to the theoretical maximum value for such monolayers.

Currently, two mechanisms for thermal monolayer formation have been proposed. One is based on a zipper-like radical chain reaction,[1,7] whereas the other suggests a 1 : 1 mechanism,[22] in which each formation of an Si–C bond requires a new initiation, i.e., the formation of a Si radical site by an initiator (a solvent radical). The kinetics of the reaction are not well-known, but the present results seem to be in favor of the zipper-like mechanism. With this mechanism the formation of ordered patterns, like **50-A** to **50-G**, is not only thermodynamically more favorable, but also mechanistically more likely than that of disordered patterns, such as **50-H** and **50-J**. In the zipper mechanism each binding of an alkyl chain directly generates a new Si radical site on the next-nearest Si surface atom, and the next 1-alkene molecule that reacts with the surface has little choice but to react at that site, and

subsequently create a Si surface radical closeby. Combined with a self-avoiding random walk,[7] this leads to relatively large areas with ordered substitution patterns. In contrast, if a 1 : 1 mechanism occurs, the formation of ordered patterns is less likely, as statistics predict that the next initiation will in many cases not be on the next-nearest Si surface atom. Consequently, the 1-alkenes will react randomly with the Si surface and almost no ordered patterns will be formed, in contrast with experiment.

Finally, the results from the calculations provide a possible explanation for the somewhat lower substitution percentages that are found when reaction conditions are used that are based on a 1 : 1 mechanism, such as in the case of the Al-catalyzed reaction to prepare the monolayers.[23] In this reaction the catalyst and the 1-alkene have to approach the surface simultaneously. This becomes increasingly difficult upon higher degrees of monolayer formation, because of steric problems, and a lower substitution percentage (~40%, instead of 50%) of the Si–H groups is the result.

6.4 Conclusions

The structure of octadecyl monolayers on the H-terminated Si(111) surface has been investigated by molecular modeling simulations, using the approach of two-dimensionally repeating boxes to mimic the alkyl-modified surface. Calculations without the repeating box, using large alkylated surfaces, fail because of the occurrence of edge effects.

The effects of different substitution percentages (33%, 50%, 67%, and 100%) of the Si–H for Si–alkyl groups on the monolayers structure were investigated. The results show that only with a substitution percentage of 50% there is a good agreement of the structures obtained from molecular modeling and the available experimental data, with the lowest energy results for the zigzag-type patterns **50-D** and **50-E**. Calculations on surfaces with a lower substitution percentage (33%) give structures in which the molecules start to form small clusters on the surface, which leads to disordered monolayers or to structures in which the alkyl chains are tilted too far (~60°) compared to the experimentally observed situation (~30°). This result shows that the steric hindrance due to the required interpenetration of Van der Waals radii, which occurs on surfaces with higher substitution percentages than 33%, is compensated for by larger attractive Van der Waals forces between the alkyl chains.

Calculations on surfaces with high substitution percentages (67% and 100%) show that these surfaces are too crowded. In the case of 100% substitution, a value that is above the

theoretical maximum of ~69%, the molecules are oriented perpendicular to the Si surface and have very high energies. This confirms that this percentage, though reported in literature,[3] is unrealistic. For the surfaces with 67% substitution, a situation that is theoretically and energetically possible, it is observed that highly unlikely deformations of the Si–C bonds at the Si surface (all tilt angles > 20°) are necessary to construct these structures. In addition, the average enthalpy per alkyl chain on the surfaces is very similar to the values obtained for surfaces with 50% substitution. This indicates that there is no driving force to go from 50% to 67% coverage. From these results it is concluded that the optimal substitution percentage for these well-ordered monolayers on the Si(111) surface is between 50 and 67%, presumably close to 55%.

Finally, the results give a possible explanation for the observation[23] that in reactions based on a 1 : 1 addition mechanism between the Si–H groups and the 1-alkene lower substitution percentages are reached compared to in surface modifications that rely on the proposed radical-based mechanism.[1,7]

References and Notes

[1] Linford, M. R.; Fenter, P.; Eisenberger, P. M.; Chidsey, C. E. D. *J. Am. Chem. Soc.* **1995**, *117*, 3145–3155.

[2] Sieval, A. B.; Demirel, A. L.; Nissink, J. W. M.; Linford, M. R.; van der Maas, J. H.; de Jeu, W. H.; Zuilhof, H.; Sudhölter, E. J. R. *Langmuir* **1998**, *14*, 1759–1768 (Chapter 3).

[3] Effenberger, F.; Götz, G.; Bidlingmaier, B.; Wezstein, M. *Angew. Chem., Int. Ed. Engl.* **1998**, *37*, 2462–2464.

[4] Zhu, X.-Y.; Mulder, J. A.; Bergerson, W. F. *Langmuir*, **1999**, *15*, 8147–8154.

[5] Li, T.-W.; Chao, I.; Tao, Y.-T. *J. Phys. Chem. B* **1998**, *102*, 2935–2946.

[6] Some recent examples are: (a) Jung, H. H; Won, Y. D.; Shin, S.; Kim, K. *Langmuir* **1999**, *15*, 1147–1154. (b) Rovillard, S.; Perez, E.; Ionov, R.; Voué, M.; De Coninck, J. *Langmuir* **1999**, *15*, 2749–2754. (c) Okamura, E.; Fukushima, N.; Hayashi, S. *Langmuir* **1999**, *15*, 3589–3594. (d) Tutein, A. B.; Stuart, S. J.; Harrison, J. A. *Langmuir* **2000**, *16*, 291–296.

[7] Cicero, R. L.; Linford, M. R.; Chidsey, C. E. D. *Langmuir* **2000**, *16*, 5688–5695.

[8] (a) Terry, J.; Linford, M. R.; Wigren, C.; Cao, R.; Pianetta, P.; Chidsey, C. E. D. *Appl. Phys. Lett.* **1997**, *71*, 1056–1058. (b) Terry, J.; Linford, M. R.; Wigren, C.; Cao, R.; Pianetta, P.; Chidsey, C. E. D. *J. Appl. Phys.* **1999**, *85*, 213–221.

[9] (a) Cerius^2, version 3.5, Molecular Simulations Inc., September 1997 or version 3.8, 1998. (b) Terms that are specific to the Cerius^2 program have in the text been put between quotes.

[10] The criteria for the high-convergence minimizations are: Atom root mean square force 1 x 10^{-3} kcal mol^{-1} Å^{-1}; atom maximum force 5 x 10^{-3} kcal mol^{-1} Å^{-1}; energy difference 1 x 10^{-4} kcal mol^{-1}; root mean square displacement 1 x 10^{-5} Å; maximum displacement 5 x 10^{-5} Å.

[11] (a) Rappé, A. K.; Casewit, C. J.; Colwell, K. S.; Goddard, W. A., III; Skiff, W. M. *J. Am. Chem. Soc.* **1992**, *114*, 10024–10035. (b) Castongauy, L. A.; Rappé, A. K. *J. Am. Chem. Soc.* **1992**, *114*, 5832–5842. (c) Rappé, A. K.; Colwell, K. S.; Casewit, C. J. *Inorg. Chem.* **1993**, *32*, 3438–3450.

[12] (a) Sun, H.; Mumby, S. J.; Maple, J. R.; Hagler, A. T. *J. Phys. Chem.* **1995**, *99*, 5873–5882, and references therein. (b) Hill, J.-R.; Sauer, J. *J. Phys. Chem.* **1994**, *98*, 1238–1244. (c) Maple, J. A.; Hwang, M. J.; Stockfisch, T. P.; Dinur, U.; Waldman, M.; Ewig, C. S.; Hagler, A. T. *J. Comp. Chem.* **1994**, *15*, 162–182.

[13] Higashi, G. S.; Becker, R. S.; Chabal, Y. J.; Becker, A. J. *Appl. Phys. Lett.* **1991**, *58*, 1656–1658.

[14] Pietsch, G. J.; Köhler, U.; Henzler, M. *J. Appl. Phys.* **1993**, *73*, 4797–4807.

[15] Wagner, P.; Nock, S.; Spudich, J. A.; Volkmuth, W. D.; Chu, S.; Cicero, R. L.; Wade. C. P.; Linford, M. R.; Chidsey, C. E. D. *J. Struct. Biol.* **1997**, *119*, 189–201.

[16] The terraces are several hundred Ångstroms wide and several thousand Ångstroms long, which is considerably larger than the largest surface (with n = 162) that has so far been investigated. A 50%-substituted surface has one alkyl chain per 24–25 Å^2 (see ref 1 and Chapter 3). If, for example, the dimensions of a terrace are 200 x 1000 Å (= 200 x 10^3 Å^2), it would take n = 8000 to describe such a terrace. This suggests that the present surfaces may indeed be too small.

[17] In the present situation, the calculations on a surface with n = 162 take ~60 h on a Silicon Graphics 175 MHZ O_2.

[18] A surface with a substitution percentage of 53% is too difficult to investigate by molecular mechanics calculations, because of two major practical problems: (a) A box with a multiple of 100 surface sites is required, as both 53 and 47 are prime numbers. The number of both alkyl chains and hydrogen atoms on a surface has to be an integer, since it is not possible to put a fractional alkyl chain on the surface. Molecular mechanics calculations are capable of handling such large structures, although at the cost of increased computational demands. (b) The alkyl chains have to be covalently linked to the Si surface. There is no indication which of the many possible substitution patterns should be used for such a surface with 53% substitution of the Si–H groups. Thus, although such calculations are possible, it is necessary to choose a different substitution percentage as an approximation for this theoretical value, to practically be able to construct the repeating boxes.

[19] This was visualized within the Cerius^2 program, which contains an option to show the molecular volume of structures.

[20] Craievich, A. F.; Denicolo, I.; Doucet, J. *Phys. Rev. B* **1984**, *30*, 4782–4787.

[21] The results in Figure 17 show that the energy of the structures **67-A** to **67-C** only converges for relatively large surfaces (repeating boxes with $n = 96$). This may suggest that in this case one could just as well have investigated the 69%-substituted surfaces in the first place, instead of using the 67%-substituted surfaces as an approximation, as these 69%-substituted surfaces would have approximately the same surface size ($n = 100$). However, this assumption is not correct, as one would also have to investigate a larger 69%-substituted surface than $n = 100$, in order to show convergence for E_{ave} for this surface. This larger surface would have $n = 400$, a situation that will give serious problems in handling, because of its size. Thus, the use of the 67%-substituted surfaces is still preferable.

[22] Bateman, J. E.; Eagling, R. D.; Horrocks, B. R.; Houlton, A. *J. Phys. Chem. B* **2000**, *104*, 5557–5565.

[23] Boukherroub, B.; Morin, S.; Bensebaa, F.; Wayner, D. D. M. *Langmuir* **1999**, *15*, 3831–3835.

Chapter 7

Silicon Surface Passivation by Monolayers of 1-Alkenes: Minority Charge Carrier Lifetime Measurements and Kelvin Probe Investigations [1]

Abstract

The possibility to use the monolayers of 1-alkenes for silicon surface passivation is investigated. Modulated free carrier absorption (MFCA) measurements show that on 1–2 Ω·cm p-type Si(100) surfaces modified with a monolayer of CH_2=CH–$(CH_2)_8$–C(O)O–CH_3 maximum effective surface recombination velocities S_{eff} as low as 120 cm/s can be obtained. These values are in the same order of magnitude as those obtained using other passivation techniques, which demonstrates that these monolayers provide an interesting alternative for silicon surface passivation.

During the MFCA measurements an unusual time-dependent behavior of the effective lifetime is observed: τ_{eff} rises continuously during illumination of the substrate. Kelvin probe measurements show that there is a slow shift of the Fermi level of the semiconductor under illumination, which is the result of a slow, reversible filling of surface traps.

[1] The results described in this Chapter will be published:
A. B. Sieval, C. L. Huisman, A. Schönecker, A. S. H. van der Heide, A. Goossens, W. C. Sinke, H. Zuilhof, and E. J. R. Sudhölter, to be published.
A preliminary report has already been published:
A. B. Sieval, H. Zuilhof, E. J. R. Sudhölter, F. M. Schuurmans, and W. C. Sinke *Proceedings of the 2nd World Conference on Photovoltaic Solar Energy Conversion* (Vienna, 1998), 322–325.

7.1 Introduction

The passivation of semiconductor surfaces is a critical step in the fabrication of high-quality silicon devices, like solar cells. Over the years, extensive research has been done to develop easy and cheap methods to reduce the surface recombination velocity of the charge carriers. The aim here is the utility to determine the bulk minority charge carrier lifetime of the semiconductor, which is one of the important intrinsic properties. Two methods for surface passivation are now generally used: submerging of the silicon substrates in solutions of hydrofluoric acid (HF)[1,2,3] or in a solution of I_2 in ethanol.[3,4,5] Both methods give rise to excellent surface passivation. For a 150 Ω·cm n-type float zone Si(111) substrate submerged in HF a surface recombination velocity of 0.25 cm/s has been reported,[1,2] but in general much higher values (100–200 cm/s) are found for substrates with higher doping densities and for p-type Si wafers.[3] For I_2/ethanol surface recombination velocities < 10 cm/s can be obtained,[4] but this again depends on the resistivity of the Si substrate, and in general values < 50 cm/s are measured.[5]

However, both methods have their drawbacks. Hydrofluoric acid is a dangerous, corrosive acid, which means that special safety precautions are required during the measurements if the sample has to remain submerged in the HF solution. Alternatively, the H-passivated Si surface can also be removed from the HF solution and measured in air.[3,6] Under these circumstances the Si surface is not stable, but is slowly oxidized, which results in an increase of the surface recombination velocity. Unfortunately, comparison of the results is often complicated, as the rate of oxidation is strongly influenced by external factors. The formation of a monolayer of silicon oxide on crystalline, H-terminated Si surfaces has been reported to take anywhere from one hour[7,8,9] to a week,[10,11] and up to a month.[12] In these investigations the silicon oxide growth rate has been shown to depend on the properties of the semiconductor substrate (e.g., p-type or n-type; Si(100) or Si(111) oriented surface),[8,9] on the environmental conditions (e.g., the humidity),[9] and on the etching conditions.[8,11] A second problem is that in lifetime measurements an immediate and usually rapid decrease of the surface passivation is seen due to oxidative processes.[3,6] An example is shown in Figure 1. These two problems seriously limit the application of this method as a standard for Si surface passivation.

The other frequently used method for surface passivation involves submerging of a HF-etched wafer in I_2/ethanol. This gives a more stable system, however, this surface also degrades after some time (~30–60 min).[3,13] As with the measurements in the HF solutions, the

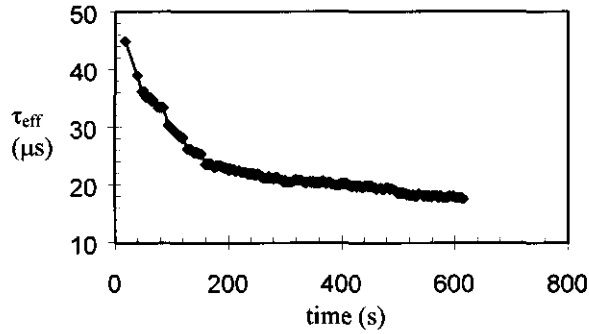

Figure 1. Decreasing effective lifetime τ_{eff} of the minority charge carriers due to surface oxidation as observed for a H-passivated p-type Si(100) surface in air (from ref 6).

wafer again has to be submerged in the liquid during the whole measurement, which is inconvenient from a practical point of view.

The monolayers described in this thesis provide an interesting alternative for silicon surface passivation, as they are easily prepared on the well-known H-terminated Si surfaces, and because the resulting monolayer-modified Si surfaces do not oxidize in air,[14,15,16,17] unlike these H-terminated Si surfaces. An example of this inhibition of surface oxidation is shown in Figure 2. This means that these surfaces are much more stable in time compared to H-terminated Si surfaces, and, thus, that the minority charge carrier lifetime measurements can be done on a system that shows no surface oxidation during the time required for the measurements.[18] Of course other passivation techniques, like the application of a layer of

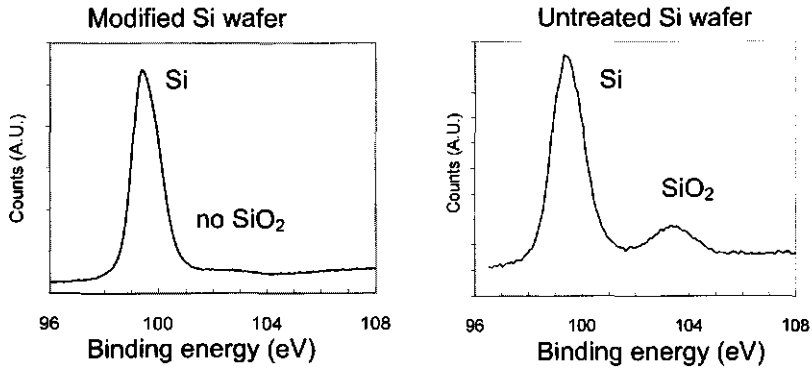

Figure 2. Inhibition of Si surface oxidation by the organic monolayers. XPS spectra (Si 2p region) for a substrate modified with **I** (left) and an untreated Si wafer (right).[15]

silicon oxide and silicon nitride, offer a similar advantage, but the monolayer preparation is done at lower temperatures and does not require special, expensive equipment.

There are two reports on the stabilization of H-passivated Si surfaces with an organic layer. It has been shown that by evaporation of a thin film of a solid aromatic compound (tetracene) on top of a H-terminated Si surface the surface oxidation is inhibited,[19] because the approach of oxygen to the Si surface is blocked by the organic layer. In this modification the Si surface is, however, still passivated by hydrogen, not by the organic compound, as there are no covalent Si–C bonds formed between the organic compound and the Si surface. Very recently, the surface passivation of Cl-terminated Si surfaces that were modified with Grignard compounds was reported.[20] In this reaction Si–C bonds are formed (see Section 2.3.3). Recombination velocities as low as 25 cm/s were reported for very high purity (3800 Ω·cm) n-type float-zone Si(111) surfaces.

In this Chapter the surface passivation of p-type Si(100) wafers (float zone (FZ) quality, 1–2 Ω·cm) by organic monolayers of 1-alkenes is investigated. The Si surfaces were all modified with the functionalized 1-alkene CH_2=CH–$(CH_2)_8$–C(O)O–CH_3 (**I**), as this 1-alkene showed good surface passivating properties in preliminary investigations.[6] The lifetime of the minority charge carriers is determined by Modulated Free Carrier Absorption (MFCA) measurements. The substrates are also investigated by Kelvin probe measurements, as this technique can provide information about possible changes in the electronic properties of the semiconductor substrate upon modification with **I**. Both techniques are non-contact methods, which means that the surface of the modified substrate is not damaged during the measurements.

7.2 Theory

7.2.1 Modulated Free Carrier Absorption (MFCA) Measurements

The Modulated Free Carrier Absorption (MFCA) technique is used to determine the lifetime of the minority charge carriers.[21,22] The measurement is based on the following principle. Charge carriers are generated in the Si substrate by excitation of electrons from the valence band to the conduction band using 848 nm light from a laser diode. These charge carriers are then detected using a 1550 nm laser. The power density (P) of the bias excitation light on the wafer surface can be varied using neutral density filters, thus allowing for

measurements both at high-level and low-level injection conditions. To measure the τ_{eff}, a small intensity modulation with a frequency ω is added to the bias-light power density. The generated excess charge carrier concentration in the sample will vary with this modulated light intensity, however, with a certain shifted phase angle ϕ, which is determined by the recombination properties of the charge carriers in the wafer. At a low modulation frequency the system (= the moving and recombining charge carriers) can keep pace with the changes in light intensity, which means that at a maximum (minimum) in the light intensity the number of charge carriers is also at a maximum (minimum). However, if the modulation frequency is increased the system in the wafer starts to fall behind, because the recombination of the charge carriers is not fast enough. By measuring ω_{45}, the modulation frequency at which the phase shift between the two lasers is 45°, the effective minority charge carrier lifetime τ_{eff} can be determined according to: $\tau_{eff} = 1 / \omega_{45}$. [21,22] This effective lifetime depends on the bulk lifetime τ_b of the Si substrate and on the recombination velocities S_1 and S_2 at the two interfaces of the wafer. As there is a monolayer on both sides of the wafer after the modification, it can be assumed that the recombination velocities on both sides of the wafer are equal, i.e., $S_1 = S_2 = S_{eff}$ (see also Section 7.4.1). Consequently, τ_{eff} is in first approximation:[21,22]

$$\frac{1}{\tau_{eff}} = \frac{1}{\tau_b} + \frac{2S_{eff}}{W}$$

in which S_{eff} is the effective surface recombination velocity, and W is the thickness of the wafer.

7.2.2 Kelvin Probe Measurements

The Kelvin probe is a non-contact, capacitor-based technique to measure the work function difference between two materials.[23] Because the Kelvin probe technique is non-destructive and very sensitive, it is widely used in semiconductor surface science, including in studies of the monolayer coverage by organic molecules.[24] Figure 3 shows a schematic drawing of a typical set-up. It consists of a piezo-driven vibrating gold grid placed in close proximity (< 1 mm) to the sample surface.

In Figure 4 the energy diagram of a p-type semiconductor during a Kelvin probe measurement is shown. The workfunctions (ϕ) of the gold reference electrode (ϕ_M) and of the semiconductor (ϕ_{SC}) are defined as the difference between the Fermi level (E_F) of the material and the vacuum level (E_{vac}). The difference between the two work functions leads to

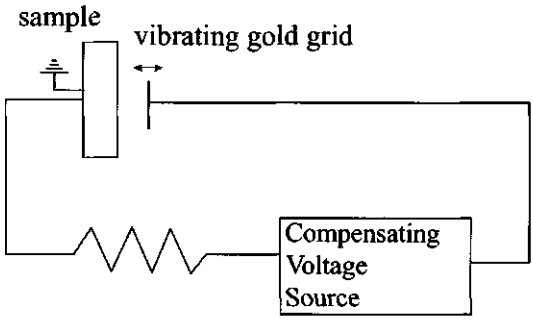

Figure 3. Schematic drawing of the electrical circuit of the Kelvin probe.

a contact potential difference (V_{CPD}), from which the Fermi level of the semiconductor can be derived if that of the reference electrode is known. In the semiconductor, the valence and the conduction band (VB and CB, respectively) are bent due to local surface charging, with the energy being pinned at the surface. The difference between the energy in the bulk and at the surface is called the band bending (V_{bb}). Its value can be deduced from the difference in the Kelvin probe signal in the dark and after saturation with light, as in this latter case the band bending disappears. Finally, the electronegativity (χ) of the semiconductor is the difference between the conduction band edge and the vacuum level.

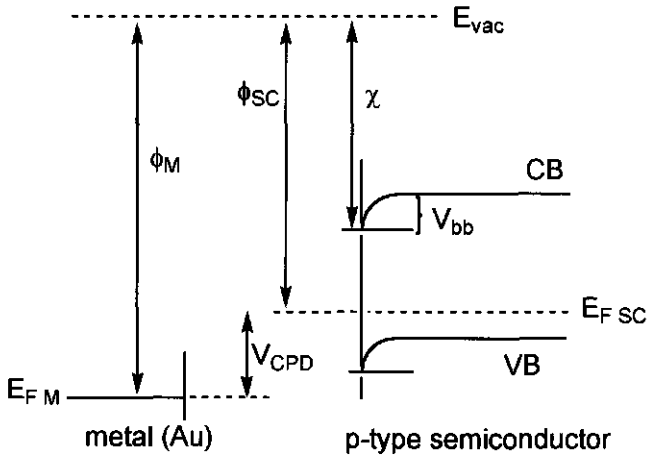

Figure 4. Energy diagram during Kelvin probe measurements on a p-type semiconductor.

In general, the work function of the metal and that of the sample under study are different, i.e., there is a difference between the Fermi levels of the two materials, which leads to a contact-potential difference (V_{CPD}), as discussed above. In the Kelvin probe set-up, this contact potential can be compensated by a bias voltage between the gold reference and the sample. In such a system, the charge on the as-created flat-plate capacitor can be written as:

$$Q = C \times V = C \times (V_{CPD} + V_{comp}) = \frac{\varepsilon\, \varepsilon_o A}{d} \times (V_{CPD} + V_{comp})$$

with Q = charge, C = capacitance, V = potential drop across the air gap, V_{CPD} = contact potential difference, V_{comp} = compensating voltage, ε_o = permittivity of vacuum, ε = dielectric constant, A = capacitor area, and d = interplate distance. When the sum of V_{CPD} + V_{comp} is kept constant and d oscillates, Q will fluctuate in time, which leads to an alternating current (ac current). The amplitude of this modulated current is only zero if $V_{CPD} = -V_{comp}$. In other words, only when the compensating voltage exactly matches the contact potential difference, the ac current, as observed on an oscilloscope or by a phase-locked measuring device, is zero. When charge carriers are generated in the semiconductor by light an additional surface photovoltage (V_{ph}) is created. In this case not only V_{CPD}, but the sum of V_{CPD} + V_{ph} must be compensated by the compensating voltage V_{comp} to reach the state where there is no ac current. The surface photovoltage can either lead to a change of the band bending, if the bands of the semiconductor are not flat, or can result in a (change in the) surface dipole layer, which results in a shift of the band edges. Both processes can be monitored with the Kelvin probe.

7.3 Experimental

7.3.1 General

A total of five batches of methyl 10-undecenoate (**I**) were prepared as described in Chapter 3, each on a 50 g scale. The yields after distillation varied between 84% and 89%. The alkene was distilled twice in vacuo (see Results and Discussion), using a distillation set-up that was cleaned with distilled methanol before use. The distillates were combined and stored in clean bottles. Used alkene could be recycled after one additional redistillation step, without any consequence for the resulting surface passivation. The Si(100) wafers (1–2 Ω·cm, p-type, boron doped, float zone (FZ) quality, 375±15 μm thickness, single polished) were obtained from Wacker Siltronic AG (Bayer Solar, Freiberg, Germany), and had a guaranteed

bulk lifetime τ_b > 1000 µs. In one experiment a shiny-etched wafer of 300 µm thickness (double polished) with the same intrinsic properties was used. The wafers were cut into pieces of ~2.5 x 3 cm^2, which were stored separately in teflon boxes. Solvents for substrate cleaning were distilled. Hydrofluoric acid was semiconductor grade.

7.3.2 Sample Preparation

The Si substrates were modified in a specially designed vessel, which consists of three flattened tubes (inner dimensions of a tube: ~50 x 30 x 5 mm^3; see Section 3.2.3) to allow for the preparation of three samples within a single experiment. This is important for the reproducibility of the measurements, because the monolayer quality is influenced by the concentration of oxygen in the system (see Chapter 4). The vessel was filled with a sufficient amount of **I** to completely fill all three tubes and dry nitrogen gas was bubbled through the solution for at least 1 h. During this time the tubes were partially submerged (~3 cm deep) in an oil bath of 200 °C, to preheat the alkene.[25] Subsequently, the Si substrates were etched in a 2.5% HF solution for 2 min, using a fresh solution for each sample. Each of the etched substrates was immediately transferred into the vessel, temporarily opening the large screw cap under vigorous nitrogen flow. If necessary, residual drops of the HF solution were blown off with N_2. Each Si substrate was placed in a separate section of the vessel (i.e., in one of the flattened tubes), thus avoiding direct contact between the Si substrates. After all three substrates had been inserted the screw cap was closed, the vessel was lowered into the oil bath as deeply as possible, and the system was heated at 200 °C under a slow flow of N_2 for 2 h.

Subsequently, the vessel was removed from the oil bath. The major part of the alkene was poured off and the samples were removed from the vessel using teflon tweezers, again avoiding direct contact between the substrates. The modified substrates were thoroughly rinsed three times in petroleum ether (40–60 °C), three times in methanol, and finally once in dichloromethane (see Chapter 3). For each rinsing step, as well as for each separate substrate, fresh solutions were used. All modified wafers were stored separately in the dark in teflon boxes.

7.3.3 Measurement Procedure for MFCA Measurements

The MFCA set-up used has been described previously in detail.[21,22] After the monolayer preparation all three samples were briefly scanned. Because of the observed time-dependent behavior of τ_{eff} (see Results and Discussion) each sample was first illuminated for 10–15 min at a low power density (P ≈ 200 mW/cm^2) to get a quasi-stable system.

Subsequently, τ_{eff} was rapidly determined at a few (usually four to six) different power densities. After all three samples were measured in this way, more prolonged, detailed studies were performed. To minimize the storage effects the samples that were measured later (samples 2 and 3 from a set of three) were kept in the dark.

7.3.4 Kelvin Probe Measurements

A Kelvin probe unit (Besocke Delta Phi type S) with a vibrating gold-grid with a diameter of 2 mm, operating at a resonance frequency of ~170 Hz, was used. The ac current was monitored on an oscilloscope and was automatically set to zero. This compensating voltage was measured by a Keithley 2001 digital multimeter with intervals of 1 s. Measurements were carried out in ambient atmosphere. Since slow relaxation processes occur, stabilization of the dark signal could take up to 2 h, after which the fluctuations in V_{comp} were less than 10 mV. The workfunction of the gold grid was taken to be 5.0 ± 0.1 V.

Monochromatic irradiation with light with a wavelength of 848 nm was done using a 250 Watt tungsten-halogen lamp (Oriel) in combination with a grating monochromator (ARC Spectrapro 275) and appropriate high-pass filters (Schott). The light was focused on the gold grid with an intensity of approximately 100 $\mu W/cm^2$. A 5-mW diode laser (Coherent) was used for irradiation with 670 nm light.

7.4 Results and Discussion

7.4.1 Lifetime Measurements

Silicon surface passivation is a process that is highly sensitive to contaminations in the reagents that are used.[26] A total of eight batches of three Si substrates each was modified with compound **I** for the lifetime measurements. The samples were indistinguishable according to the results of water contact angle measurements and IR spectroscopy. Nevertheless, significant variations were found for the surface passivation characteristics, which confirms the high sensitivity of these measurements to small amounts of impurities (= defects in the monolayer). In the first experiments the organic compound was distilled only once, as this is in general sufficient for the purification of 1-alkenes that are used for monolayer preparation.[27] For surfaces modified with this singly distilled **I** maximum effective lifetimes τ_{eff} of ~ 50–70 μs were obtained. An untreated (= unpassivated) Si wafer gives a maximum

τ_{eff} of ~5–7 μs, which shows that Si surface passivation has been achieved with these monolayers of **I**. However, effective lifetimes τ_{eff} > 100 μs had already been found in preliminary experiments,[6] which indicates that the Si surfaces were not yet passivated as well as possible.

A likely explanation for this difference is that the Si surfaces were contaminated during the modification, since it is known that contamination of the surface has a negative effect on the charge carrier lifetimes.[26] The most probable cause for contamination is the presence of small amounts of impurities in the organic reagent, which can absorb on the Si surface. As a result the monolayer of **I**, although overall still well-ordered, will have some defects. These defects in the monolayer lead to defects at the Si surface, which will act as sites for charge carrier recombination. Consequently, the maximum effective lifetime of the minority charge carriers will decrease.

The surface passivation was considerably improved when doubly distilled **I** was used for the modifications.[28] The results of an MFCA measurement on such a substrate (Figure 5) show that this sample has a maximum effective lifetime τ_{eff} of 105 μs, which corresponds to a maximum effective surface recombination velocity S_{eff} of 160 cm/s. Different spots on the wafer and a different maximum power density P_{max} for the excitation light[29] yield very similar results (Figure 5).

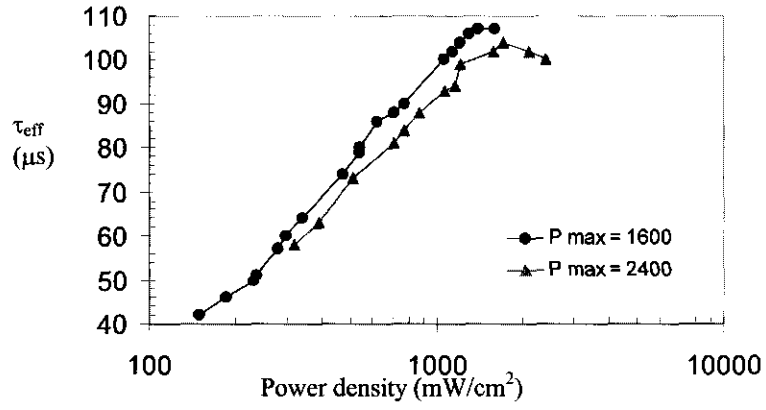

Figure 5. MFCA measurement (P-τ curve; Power density P of the incident light vs. the effective lifetime τ_{eff} of the minority charge carrierrs) on a Si substrate modified with doubly distilled **I**. Two separate measurements with two different maximum power densities (P_{max}, in mW/cm^2) are shown.

It is difficult to compare the S_{eff} of 160 cm/s to literature values, as factors like the doping density and the surface orientation all influence the recombination velocity.[21,30,31] The value of S_{eff} is comparable to the value of S_{eff} of 130 cm/s that was measured on a HF-passivated 7 Ω·cm p-type Si(100) wafer,[3] and approaches the S_{eff} of ~40 cm/s as found for a 1.5 Ω·cm p-type Si(100) wafer passivated with I_2/ethanol.[13] This clearly demonstrates that these monolayers of 1-alkenes are well suited for Si surface passivation.

In all measurements it is found that the τ_{eff} of the minority charge carriers depends on the power density P of the incident light. An increase of P leads to an increase in τ_{eff}, up to a certain maximum value. A similar behavior is known for thermally oxidized[31,32] and for silicon nitride-coated[33,34] p-type Si wafers, where it has been attributed to an injection level-dependent surface recombination velocity. Beyond the maximum value the effective lifetime decreases again. This effect is believed not to originate from an increase in the surface recombination, but from an increased bulk recombination. If the surfaces of the semiconductor are well passivated, so-called Auger recombination in the crystalline bulk of the silicon becomes significant at high injection levels, and can even dominate the measured τ_{eff}.[35]

The two curves in Figure 5 are nearly identical, which shows that there is a good reproducibility of τ_{eff}. As the two measurements were done on different spots on the surface, it also indicates that the whole surface is equally well passivated. This is not unexpected, as the quality of the monolayer should be the same over the sample surface. This observation also confirms that these modified substrates have a good stability, unlike for surfaces passivated by HF[3,6] and I_2/ethanol,[3,13] as there is no degradation of the substrate during the time required for these two measurements.[36]

It is inherent to the modification procedure that near-identical monolayers of **I** are formed on both sides of the Si substrate. This strongly suggests that the resulting surface passivation is also equal on both sides. In Figure 6 the results are shown that were obtained from the front- and backside of a singly polished Si wafer (power density P vs. τ_{eff}). Both sides were investigated under equal measurement conditions, i.e., with the same maximum power density of the excitation light. On the unpolished side the effective lifetimes are only slightly lower (~5–10 μs) than those of the polished side, a difference that is within the variation of values of τ_{eff} as found for the substrates modified with **I**. This shows that both sides of the modified Si substrate are equally well passivated, which means that the surface structure has little influence on the surface passivating properties of the monolayer. This

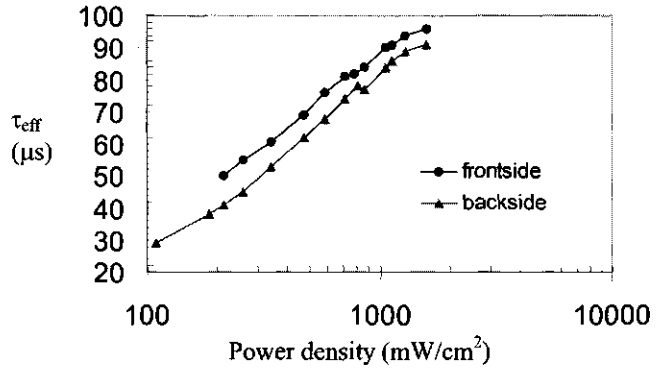

Figure 6. P-τ curves as obtained from MFCA measurements on the front- and backside of a Si substrate passivated with **I**. The maximum power density in both measurements was 1600 mW/cm^2.

result also demonstrates that the assumption that the surface recombination velocity is equal on both sides of the modified wafer, i.e., that $S_1 \approx S_2$, is correct (see Section 7.2.1).

In general, maximum effective lifetimes τ_{eff} of 90–110 μs were obtained for the 375 μm-wafers modified with **I**, with small differences (~5–10 μs) between the three samples from a batch. These values correspond to maximum effective surface recombination velocities S_{eff} of 150–190 cm/s, which are comparable to the S_{eff} of 130 cm/s as obtained with HF passivation (*vide supra*). There are also only small differences between the samples from different batches, as can, e.g., be seen from the results in Figures 5 and 6, which display maximum effective lifetimes of 105 and 95 μs, respectively. This shows that the modification procedure and the resulting surface passivation have a good reproducibility.

The highest maximum lifetime obtained in these investigations with the monolayers of **I** on the singly polished Si(100) substrates was τ_{eff} = 132 μs. This value corresponds to a maximum surface recombination velocity S_{eff} of 125 cm/s. A comparable value was obtained on a different type of Si substrate modified with **I**. This Si wafer had a thickness of only 300 μm and had received a shiny etch, which means that after sawing and polishing of the wafer a thin layer of Si is removed by a chemical etch, to reduce the number of surface defects resulting from the mechanical steps. This substrate shows a maximum τ_{eff} of 110 μs (Figure 7), which in this case corresponds to a maximum surface recombination velocity S_{eff} of 120 cm/s. The values for S_{eff} of these two substrates are approximately equal, which shows that

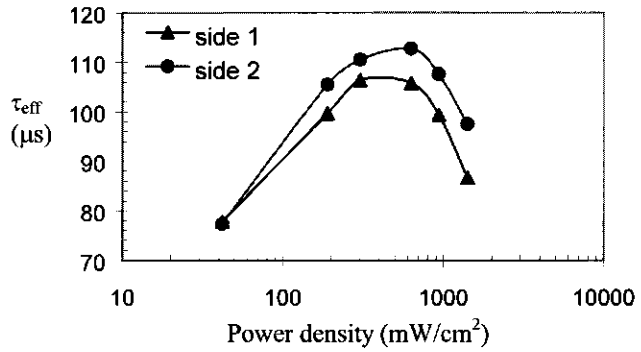

Figure 7. P-τ curves of both sides of the shiny-etched, double-polished p-type Si(100) wafer of 300 μm thickness passivated with **I** (from ref 6).

the surface passivation works equally well for wafers of various thickness. It also suggests that the application of a shiny etch has only a small influence on the surface-passivating effect of a monolayer of **I**. Interestingly, these values of S_{eff} are also somewhat lower than the S_{eff} of 130 cm/s as reported for the HF-passivated Si wafer mentioned above. Combined with the much better stability of the monolayer-modified substrates compared to that of the surfaces passivated with HF and I_2/ethanol (see Introduction), this clearly demonstrates that the monolayers of organic molecules form an interesting and promising alternative for Si surface passivation.

7.4.2 Time-Dependent Behavior of τ_{eff}: MFCA Studies

During the lifetime measurements on these monolayer-passivated Si surfaces a remarkable phenomenon was observed: τ_{eff} continuously increases under illumination at a constant power density P of the excitation light. Such effects are known for SiO_2-passivated silicon surfaces that are illuminated with very high intensity lasers,[37,38] in which case multiphoton absorption takes place, but such processes can be excluded here. Two examples of this time-dependent behavior of τ_{eff} are shown in Figure 8. A rapid increase in τ_{eff} occurs in the beginning, after which τ_{eff} keeps on increasing gradually, as was found for a sample that was illuminated constantly at a constant, low value of P for three days. The effective lifetime τ_{eff} had reached a value of 117 μs, from an initial value of τ_{eff} = 25 μs.

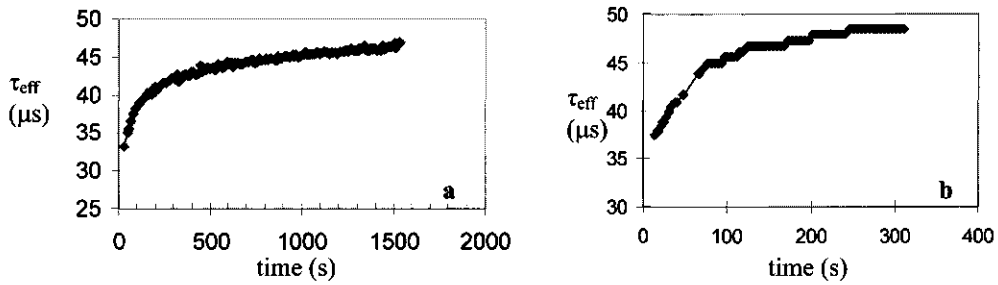

Figure 8. Time-dependent behavior of τ_{eff} as observed for: (a) a wafer passivated with **I**, and (b) a wafer passivated with 1-hexadecene (from ref 6).

This time-dependent behavior of τ_{eff} was found on all monolayer-modified samples, regardless of the power density of the excitation light or of the maximum effective lifetime of the sample. The initial part of the curves usually showed some variation, i.e., some samples showed a faster increase over time in the first few hundreds of seconds compared to other samples, but the slope of the subsequent continuous, approximately linear growth of τ_{eff} is always similar. The effect is observed both for monolayers of functionalized molecules, like **I** (Figure 8a), as well as for monolayers of underivatized 1-alkenes, like 1-hexadecene (Figure 8b). It is not observed for other surface passivation methods, like silicon nitride, which means that it must be a direct result of the surface modification with 1-alkenes.

The time-dependent behavior of τ_{eff} is well reproducible in a series of measurements on a sample. After storage of the wafer in the dark for at least several hours (= longer than the time it had been illuminated during a measurement), approximately the same curve for τ_{eff} is found in a second measurement if the same power density of the excitation light is used. This indicates that in the dark the wafer returns to what can be called its "original state", which means that under illumination neither the composition of the monolayer nor the structure of the Si surface are permanently changed. If such changes did occur, τ_{eff} would have been affected permanently, which would have become clear in subsequent second or third measurements. The reproducibility of the effect also shows that there is no degradation of the Si surface under illumination. This would result in a decrease of τ_{eff}, as degradation would increase the number of defects at the Si surface, and consequently the number of recombination sites.

In experiments with only short intervals between the periods of illumination, i.e., with dark periods that are approximately equal to or even shorter than the period of illumination, the time-τ_{eff} curves are not reproducible. This means that, apparently, the sample does not instantaneously return to its "original state" when the excitation light is switched off. An example of such an experiment is shown in Figure 9, where both the illumination period and the dark period are approximately 15 min. The τ_{eff} of each successive period of illumination starts at a higher value and also gives a higher end value for τ_{eff}, which clearly demonstrates that the substrate did not fully return to its "original state". Moreover, the starting value of τ_{eff} in each successive illumination period is actually close to the last value of the previous illumination period. This indicates that the decay to the "original state" is a rather slow process.

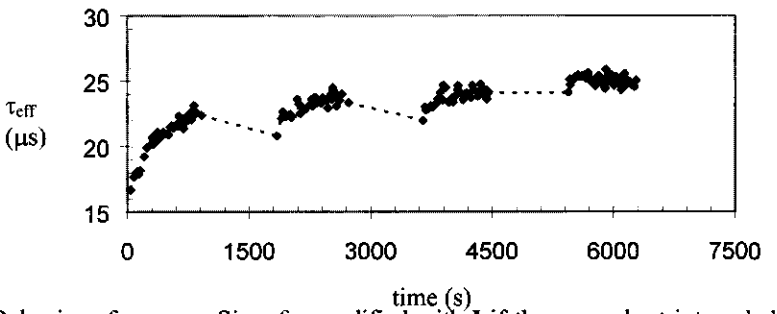

Figure 9. Behavior of τ_{eff} on a Si wafer modified with **I** if there are short intervals between the periods of illumination.

Absorption of light by the monolayer may be responsible for the observed time-dependent behavior of τ_{eff}. The antisymmetric CH_2 stretching vibrations in the organic molecules show infrared absorptions at 2920–2925 cm^{-1}. These values correspond to wavelengths of ~3420–3425 nm, which means that the fourth harmonic of this vibration is around 855 nm, i.e., close to the excitation wavelength of 848 nm. Although the absorption of such overtones is low and will most likely be negligible in a monolayer of an organic compound, the continuous absorption of the 848 nm light by the organic molecules could in theory cause changes in the monolayer structure. The other wavelength used in the MFCA measurements, the detection wavelength of 1550 nm, is not absorbed by the monolayer.

To investigate this absorption of the excitation light by the monolayer two control experiments were performed, in which different wavelengths (950 and 1025 nm) were used to

generate the charge carriers in the semiconductor. For the excitation with light of 950 nm, the 848 nm laser was replaced by a low-intensity Light Emitting Diode (LED), which was placed close to the substrate. For the experiment using 1025 nm light a 500 mW near-infrared laser was used. The results from these experiments showed that also with these two wavelengths the effective lifetime of the sample continuously increases during illumination. Thus, it must be concluded that the observed time-dependent behavior of τ_{eff} is independent of the excitation wavelength, which strongly suggests that it is not related to light absorption by the monolayer.

7.4.3 Time-Dependent Behavior of τ_{eff}: Kelvin Probe Measurements

A possible explanation for the increase of τ_{eff} over time is a change in the properties of the silicon surface itself. If there is a slow filling of surface traps under illumination, the positions of the bands of the semiconductor will shift and the number of recombination centers at the surface is reduced. This results in a decrease of the recombination velocities, which means that τ_{eff} will increase over time. This filling of traps is a reversible and slow process, two features that are observed in our experiments. Unfortunately, MFCA measurements can not provide information about this process, since they only show the net result of these changes on τ_{eff}. Also, the MFCA can not be used to investigate processes that occur in the dark, which are important, because of the reproducibility of the effect and the rather slow decay process that occurs.

The trapping and detrapping of electrons can be investigated by Kelvin probe measurements. In the case of semiconductors the position of the Fermi level of the semiconductor relative to that of a reference electrode is determined. Trapping of charges at the illuminated semiconductor surface will shift the Fermi level of the semiconductor. As discussed above, in the case of the monolayer-modified Si substrates such charging of the semiconductor surface can cause the observed time-dependent behavior of τ_{eff}. With the Kelvin probe this surface charging can be measured by continuously monitoring the position of the Fermi level of the illuminated semiconductor. Also, the Kelvin probe can measure in the dark, which means that these measurements can provide information about the subsequent decay process that occurs. Therefore, it is interesting to investigate the modified Si substrates with this technique.

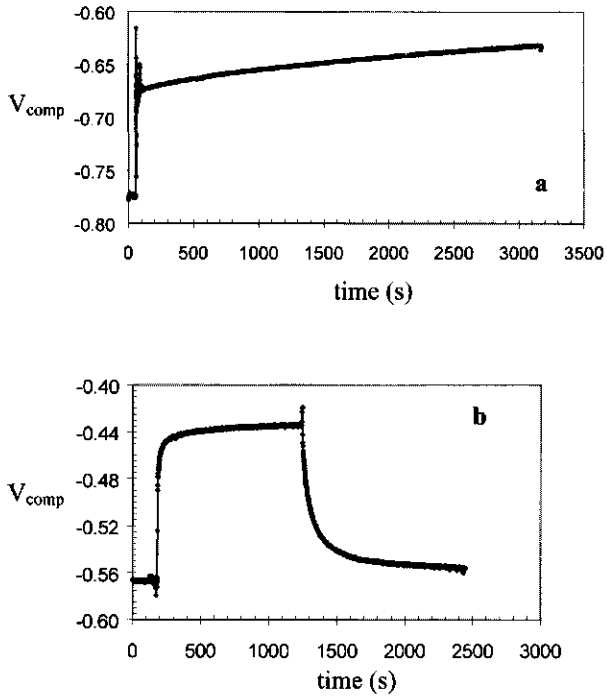

Figure 10. Surface photovoltage measurements on Si wafers passivated with **I**. (a) With light of 848 nm. (b) With light of 670 nm.

Figure 10 shows the results of two measurements on monolayer-modified Si substrates. In Figure 10a the sample was irradiated with low-intensity 848 nm light, in Figure 10b with high-intensity 670 nm light. A fast jump of V_{comp} of +0.10 V is observed when the light is switched on, followed by a slow, continuous increase. The fast jump is due to the light-induced flattening of the bands of the semiconductor, which is a fast process. The subsequent slow increase is due to slow additional charging of the surface. It is interesting to note that there are no differences between the two samples, which means that there is not much effect of either the intensity or the wavelength of the applied irradiation on the rate of the slowly growing surface photovoltage signal. This was also found for the time-dependent behavior of τ_{eff} in the MFCA measurements. Figure 10b shows that when the light is turned off, the same process occurs, though in the other direction: the signal first decreases rapidly due to reoccurrence of the band bending, and then continues to relax slowly towards its initial value.

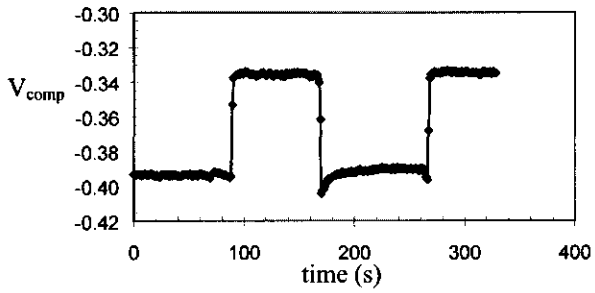

Figure 11. Surface photovoltage measurement on a H-passivated p-type Si wafer. At t = 90 s the light is turned on and at t = 160 s the light is turned off. At t = 270 s the second cycle was started (not fully shown) to test for the stability of the substrate.

Figure 11 shows the result of a measurement on a hydrogen-terminated Si substrate, which was performed as a control experiment. This surface shows a stable contact potential difference versus gold both in the dark and under illumination. The jumps in V_{comp} as a result of switching the light on or off are again instantaneous (within 10 seconds), as already observed for the monolayer-modified Si substrates. This confirms that the lifting of the band bending, which occurs when the light is switched on is a fast process.

The observed jump in V_{comp} upon illumination of the passivated Si substrates indicates that there is little band bending for these surfaces. For the 848-nm irradiated sample this can be calculated to be 0.09±0.02 eV, for the H-terminated Si surface it is 0.06±0.02 eV. This shows that on these Si surfaces the number of electronic defects is negligible, which explains the excellent passivating properties of the organic monolayers.

The observed slow, continuous increase of V_{comp} and of τ_{eff} during illumination is the likely result of changes in the properties of the modified semiconductor substrate. Since under illumination the bands are flat, this response of V_{comp} can not be related to a change in the band bending, which means that it must be due to a change in the position of the band edges (see Section 7.2.2). Such shifts of the band edges can be caused by (additional) polarization of the surface dipole layer. The sign of the slow increase of the signal indicates that a negative charge is formed at the monolayer side of the Si–monolayer interface, and, thus, that positive charges are present on the Si surface itself. This means that electrons are trapped onto the organic molecules or onto adsorbed molecules on the outside of the monolayer.

Once the light is switched off the band flattening will disappear, i.e., the band bending will reoccur. In this situation the monolayer and the Si surface can no longer be permanently charged, and some process starts to reach a thermodynamically stable state again. In general, the electron trapping process is completely reversible, unless a chemical reaction or degradation occurs. This complete reversibility is indeed observed for these monolayer-modified Si substrates, both in the Kelvin probe and the MFCA measurements, which means that chemical and/or degradation reactions can be ruled out. The detrapping of the electrons, like the trapping itself, will be a slow process, because the electrons have to cross the barrier of the organic material again. Therefore, it will take place on a similar timescale as the trapping process, which is confirmed by the result shown in Figure 10b. Thus, it must be concluded that the observed time-dependent behavior of V_{comp} and of τ_{eff} is caused by trapping of electrons at the surface of the monolayer.

A simple calculation can give an estimate of the degree of trapping of electrons, if it is assumed that the electrons are trapped on the organic molecules in the monolayer and that the trapping rate is constant in time. This will give an indication about the number of electrons that is trapped per second and can also indicate how long this process can go on. This is relevant, as in Section 7.4.2 it was already mentioned that τ_{eff} was still not stable after 3 days of continuous illumination. The CPD changes with a rate of ~0.01 mV/s, which means that the current that flows in the process is $dQ/dt = C\ dV/dt \approx 27$ pA cm^{-2}, using an effective dielectric constant of 3 and a distance of 1 nm between the Si surface and the outside of the monolayer. This corresponds to ~1.7 x 10^8 electrons per cm^2 per second. Since the monolayer contains one molecule per 24 Å^2 (see Chapter 3), it would at this rate take approximately 2.5 x 10^6 s, or 29 days, to store one electron on all organic molecules in the monolayer, but, of course, the process would slow down further upon additional charging.

7.5 Conclusions

The possibility to use the monolayers of 1-alkenes for silicon surface passivation was investigated. Modulated free carrier absorption (MFCA) measurements show that maximum effective lifetimes τ_{eff} of the minority charge carriers of 130 μs can be obtained on 1–2 Ω·cm p-type Si(100) surfaces modified with a monolayer of CH_2=CH–$(CH_2)_8$–C(O)O–CH_3 (compound **I**). This lifetime corresponds to a maximum effective surface recombination

velocity S_{eff} of 125 cm/s. The whole surface of the semiconductor is equally well passivated and the values for τ_{eff} and S_{eff} are well reproducible. These values are in the same order of magnitude as those obtained using other passivation techniques, like HF passivation and I_2/ethanol, and clearly demonstrate that monolayers of 1-alkenes, like **I**, can be used for silicon surface passivation.

During the MFCA measurements an unusual time-dependent behavior of the effective lifetime is observed: τ_{eff} rises continuously during illumination of the substrate. The effect is well reproducible and was observed for all Si substrates passivated with monolayers of 1-alkenes, i.e., both for functionalized and underivatized compounds. It was also observed for all power densities of the bias light that were used. Kelvin probe measurements showed that this behavior of τ_{eff} is the result of a slow, reversible filling of surface traps. This leads to charging of the Si surface, which shifts the bands of the semiconductor. The filling of surface traps reduces the number of recombination sites at the surface, thus leading to a decrease of the surface recombination velocity, which is observed as an increase in τ_{eff} in the MFCA measurements.

References and Notes

[1] Yablonovitch, E.; Allara, D. L.; Chang, C. C.; Gmitter, T.; Bright, T. B. *Phys. Rev. Lett.* **1986**, *57*, 249–252.

[2] Yablonovitch, E; Gmitter, T. *Appl. Phys. Lett.* **1986**, *49*, 587–589.

[3] Poortmans, J.; Vermeulen, T.; Nijs, J.; Mertens, R. *Proceedings of the 25th IEEE Photovoltaic Specialists Conference*, Washington D.C., 1996; IEEE: New York, NJ, USA, 1996, 721–724.

[4] Horányi, T. S.; Pavelka, T.; Tüttö, P. *Appl. Surf. Sci.* **1993**, *63*, 306–311.

[5] Stephens, A. W.; Green, M. A. *J. Appl. Phys.* **1996**, *80*, 3897–3903.

[6] Sieval, A. B.; Zuilhof, H.; Sudhölter, E. J. R.; Schuurmans, F. M.; Sinke, W. C. *Proceedings of the 2nd World Conference on Photovoltaic Solar Energy Conversion*, Vienna, 1998; Joint Research Center of the European Commission: Ispra, Italy, 1998, 322–325.

[7] Morita, M.; Ohmi, T.; Hasegawa, E.; Kawakami, M.; Ohwada, M. *J. Appl. Phys.* **1990**, *68*, 1272–1281.

[8] Niwano, M.; Kageyama, J.-i.; Kurita, K.; Kinashi, K.; Takahashi, I.; Miyamoto, N. *J. Appl. Phys.* **1994**, *76*, 2157–2163.

[9] Miura, T.-a.; Niwano, M.; Shoji, D.; Miyamoto, N. *J. Appl. Phys.* **1996**, *79*, 4373–4380.

[10] Gräf, D.; Grundner, M.; Schulz, R.; Mühlhoff, L. *J. Appl. Phys.* **1990**, *68*, 5155–5161.

[11] Kluth, G. J.; Maboudian, R. *J. Appl. Phys.* **1996**, *80*, 5408–5414.

[12] Olsen, J. E.; Shimura, F. *J. Vac. Sci. Technol. A* **1989**, *7*, 3275–3278.

[13] Schönecker, A.; Heasman, K.; Schmidt, J.; Poortmans, J.; Burton, T.; Koch, W. *Proceedings of the 14th European Photovoltaic Solar Energy Conference*, Barcelona, 1997; Stephens: Bedford, UK, 1997, p 666.

[14] Buriak, J. M. *Chem. Commun.* **1999**, 1051–1060.

[15] Sieval, A. B.; Linke, R.; Zuilhof, H.; Sudhölter, E. J. R. *Adv. Mater.* **2000**, *12*, 1457–1460.

[16] Bansal, A.; Li, X.; Lauermann, I.; Lewis, N. S.; Yi, S. I.; Weinberg, W. H. *J. Am. Chem. Soc.* **1996**, *118*, 7225–7226.

[17] Bansal, A.; Lewis, N. S. *J. Phys. Chem. B* **1998**, *102*, 4058–4060.

[18] Care should be taken that the inhibition of the Si surface oxidation is not interpreted as an absolute stability of the modified Si surface. First, the amount of silicon oxide that is formed after a certain period of time can be below the detection limits in the XPS measurements. Second, at defect sites in the monolayer oxidation of the Si surface can certainly occur, although this reaction will probably be on a much slower time-scale compared to the oxidation of the H-terminated surfaces. Water is required for the oxidation (see ref 9), and the (hydrophobic parts of the) organic layer will make it difficult for the water molecules to reach the Si surface. Another point that has to be taken into account is that the oxidation of the H-terminated Si surface takes much longer than the observed decay of the charge carrier lifetimes, as was already discussed in this Introduction. The monolayers inhibit the oxidation of the Si surface for a (very) long time, but this does not automatically imply that the decay of the charge carrier lifetimes, as observed for the H-terminated surfaces, is also decelerated.

[19] Deckman, H. W.; Weinberger, B. R.; Yablonovitch, E. *European Patent EP 0171278* (February 12, 1986).

[20] Royea, W. J.; Juang, A.; Lewis, N. S. *Appl. Phys. Lett.* **2000**, *77*, 1988–1990.

[21] Glunz, S. W.; Sproul, A. B.; Warta, W.; Wettling, W. *J. Appl. Phys.* **1994**, *75*, 1611–1615.

[22] Schönecker, A.; Eikelboom, J. A.; Burgers, A. R.; Lölgen, P.; Leguijt, C.; Sinke, W. C. *J. Appl. Phys.* **1996**, *78*, 1497–1504.

[23] Kelvin, L. *Philos. Mag.* **1898**, *46*, 82.

[24] Lü, J.; Delamarche, E.; Eng, L.; Bennewitz, R.; Meyer, E.; Güntherodt, H.-J. *Langmuir* **1999**, *15*, 8184–8188.

[25] Preheating of the 1-alkene is necessary in this case, because of the large amount of material (~35 ml) that is in the vessel. This takes too long to heat up to ~190 °C, which is the temperature of the 1-alkene if the tube is heated in the oil bath of 200 °C. It is known that at lower reaction temperatures, or when the alkene is still relatively cold when the wafers are inserted, less well-ordered monolayers are formed (see Chapters 3, 4, and 5). Such samples are usually poorly passivated and give rise to

considerably lower maximum effective lifetimes of the minority charge carriers (maximum $\tau_{eff} < 40$ μs).

[26] Itsumi, M.; Sato, Y.; Imai, K.; Yabumoto, N. *J. Appl. Phys.* **1997**, *82*, 3250–3255.

[27] No significant differences were found in the quality of the monolayers prepared with single or double-distilled alkene when they were analyzed with the usual analytical techniques, like contact angle measurements or IR spectroscopy.

[28] Triple distillation of the alkene was also tested, but this gave no further improvement of the surface passivation.

[29] The maximum light intensity has to be set in advance, and can not be changed during the measurement, as this is done by (de)focussing of the excitation laser. To determine the maximum power density, the light intensity is measured (in mW) through a hole with a known diameter (400 μm) before a measurement is started. This means that changing the maximum power density requires removal of the wafer from the set-up, which is undesirable once a measurement has been started, in particular because of the observed time-dependent behavior of τ_{eff}.

[30] Stephens, A. W.; Green, M. A. *Sol. Energy Mater. Sol. Cells* **1997**, *45*, 255.

[31] Stephens, A. W.; Aberle, A. G.; Green, M. A. *J. Appl. Phys.* **1994**, *76*, 363–370.

[32] Aberle, A. G.; Glunz, S. W.; Warta, W. *J. Appl. Phys.* **1992**, *71*, 4422–4431.

[33] Aberle, A. G.; Lauinger, T.; Schmidt, J.; Hezel, R. *Appl. Phys. Lett.* **1995**, *66*, 2828–2830.

[34] Schuurmans, F. M. Ph.D. Thesis, Utrecht University, 1996.

[35] Schmidt, J.; Aberle, A. G. *J. Appl. Phys.* **1997**, *81*, 6189–6199.

[36] The measurement of a curve as shown in Figure 5 can easily take up to 1 h, depending on the number of power densities that is used. As the wafer has to be stored in the dark for at least the same time as the time period that has been used for this measurement before the second measurement can be performed (see the sections on the Time-Dependent Behavior of τ_{eff}), it is clear from the observed reproducibility of τ_{eff} that the samples are stable for at least several hours.

[37] Shamir, N.; Mihaychuk, J. G.; van Driel, H. M. *J. Appl. Phys.* **2000**, *88*, 896–908.

[38] Shamir, N.; van Driel, H. M. *J. Appl. Phys.* **2000**, *88*, 909–917.

Chapter 8

Amino-Terminated Monolayers on Silicon Surfaces [1]

Abstract

A new approach has been developed to prepare well-defined amino-terminated monolayers on H-terminated Si surfaces. This two-step procedure is the first method that provides direct control over the surface density of the amino groups. First, a mixed monolayer of a protected ω-amino-1-alkene and an underivatized 1-alkene is prepared on a H-terminated Si(100) surface, using either phthalimide or acetamide as the NH_2-protecting group. Subsequent removal of the protective groups generates the desired covalently attached NH_2-terminated monolayer.

[1] The results described in this Chapter will be published:
A. B. Sieval, R. Linke, G. Heij, G. Meijer, H. Zuilhof, and E. J. R. Sudhölter, submitted.

8.1 Introduction

Functionalized organic monolayers on solid substrates provide new well-defined means to obtain direct information on biochemical phenomena such as cell adhesion,[1] or to develop new types of (bio)sensors.[2] One particularly interesting class is constituted by monolayers terminated with amino groups,[3] as this functionality can be used for the complexation of biologically active molecules, like DNA[3,4,5] and proteins.[6,7]

Several different methods currently exist for the preparation of these amino-functionalized monolayers. On gold surfaces they can be easily prepared by adsorption of ω-amino thiols onto the surface.[6,8] In this adsorption process the amino groups do not interfere with the monolayer formation by side reactions,[9] which makes this a relatively easy route for the preparation of these monolayers. Also, this method has the advantage that soft lithographical methods such as microcontact printing can be used to obtain precisely defined surfaces.[10] However, subsequent further functionalization of the amino groups is problematic, because thiol monolayers can be relatively easily removed from the surface, e.g., when heated in organic solvents.[11,12]

An alternative route is presented by the monolayers of alkyltrichloro- and alkyltrialkoxysilanes on oxidized silicon. Although there are several problems associated with the use of these compounds (see Section 1.2.2), the resulting monolayers are more stable towards organic solvents,[13] as they are bound to the surface by covalent Si–O–Si bonds. Unfortunately, amino-functionalized compounds can not be used directly in the surface modification. The Si–Cl and Si–OR groups in the organic molecule react with NH_2 groups, which gives rise to the formation of disordered layers (for long alkyl chains)[14,15] or multilayers (for short alkyl chains).[16] This problem can be circumvented by conversion of suitable functional groups in the monolayer into NH_2 groups, as has been shown for the reduction of CN groups[17] and in the two-step sequence –Br → $-N_3$ → $-NH_2$, which involves a nucleophilic substitution and subsequently a reduction step.[17,18]

The monolayers of 1-alkenes on H-terminated Si surfaces described in this thesis constitute a new class that has several advantages over the above-mentioned systems. It has been shown in Chapter 3 that the covalent Si–C bond is stable in organic solvents and towards hydrolysis, and that functional groups in the monolayer can be modified using standard reactions from organic chemistry, like reductions and esterifications.[19] Also, the required ω-functionalized 1-alkenes are often intermediates in the synthesis of thiols[20] and silanes[21]

that are used in the above-mentioned procedures, which implies the relative ease of obtaining these materials.

The preparation of amino-terminated monolayers using this Si surface modification reaction with 1-alkenes has been reported.[3] This route involves a chlorosulfonylation reaction of the terminal methyl groups of an alkyl monolayer, followed by a coupling reaction with ethylenediamine. Although the resulting layer contains NH_2 groups that are capable of binding DNA, there are several drawbacks to this method. First, the chlorosulfonylation procedure requires relatively harsh reaction conditions (two toxic, corrosive gasses, i.e., chlorine and sulfur dioxide, plus UV light). Second, there are difficulties regarding the control over the precise composition of the monolayer, i.e., the percentage of NH_2 groups on the surface.

In this Chapter a new approach is presented to prepare amino-terminated monolayers on Si surfaces (Figure 1). In the Si surface modification reaction protected amines are used; the direct use of ω-amino-1-alkenes is not possible, because in that case the amino groups will also react with the Si surface,[22,23] which results in the formation of disordered monolayers.[19] Subsequently, the protective groups are removed by well-known deprotection reactions. In this approach there is a direct control of the density of the amino groups on the surface, as will be demonstrated by preparing mixed monolayers of the amino-functionalized compound with 1-decene. One route makes use of the Ing-Manske modification of the Gabriel synthesis of amines, i.e., a reaction of phthalimide groups with hydrazine.[24] Such route has been attempted for monolayers of alkylsilanes, however, only disordered monolayers were obtained in that case.[14] The other route involves acidic hydrolysis of acetamide groups.

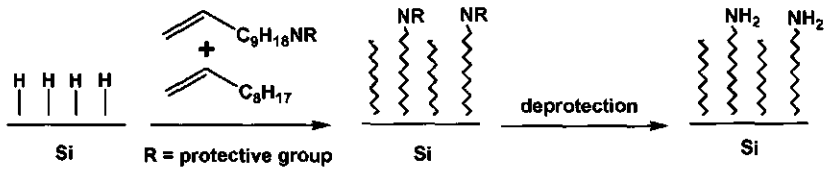

Figure 1. Schematic representation of the procedure developed for the preparation of the amino-terminated monolayers.

8.2 Experimental

8.2.1 General Information

1-Decene (**C10**, > 97%, Fluka) was distilled in vacuo and stored at -20 °C. *N*-(ω-Undecylenyl)-phthalimide (**I**) was recrystallized from distilled methanol, *N*-(ω-undecylenyl)-acetamide (**II**) was used without further purification. The purified compounds **I** and **II** were stored at room temperature under vacuum. Mesitylene (Fluka, 99%) was distilled at atmospheric pressure and stored on $CaCl_2$. Hydrazine monohydrate[25] (99%) was obtained from Acros. All glassware for distillations, recrystallizations, and monolayer preparations was cleaned with distilled solvents only. All other details have been described previously in Chapters 3, 4, and 5.

8.2.2 Synthesis of the Functionalized Alkenes

The protected 1-amino-10-undecene derivatives **I** and **II** were synthesized by the route depicted in Figure 2.

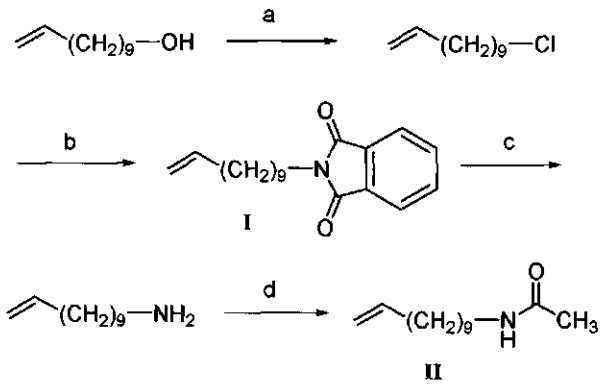

Figure 2. Synthesis of the protected amine derivatives **I** and **II**. (a) $(C_6H_5)_3P$, CCl_4, CH_3CN, reflux, 24 h. (b) Potassium phthalimide, DMF, 90 °C, 24h. (c) $NH_2NH_2.H_2O$, ethanol, reflux, 3 h. (d) Acetic anhydride, reflux, 10 min, followed by chromatography.

1-Chloro-10-Undecene.[26] A mixture of 25.0 g (0.147 mol) of 10-undecylenyl alcohol, 50.0 g (0.190 mol) of triphenylphosphine, 75 ml of carbon tetrachloride, and 75 ml of acetonitril was heated to reflux for 24 h. The resulting brown solution was cooled to room temperature and the solvents were evaporated under reduced pressure. The solid residue was

transferred onto a glass filter and extracted four times with 100 ml of petroleum ether (40–60 °C). The combined extracts were dried over $MgSO_4$ and concentrated in vacuo, which yielded 29.0 g of crude 1-chloro-10-undecene as a yellow oil.[27] Distillation gave 24.8 g (0.131 mol, 89%) of pure 1-chloro-10-undecene (bp 115–116 °C, 13 mmHg; lit 104–105 °C, 6 mmHg).[28]

^{1}H NMR: δ 5.90–5.70 (m, 1H), 5.04–4.88 (m, 2H), 3.52 (t, 2H, J = 6.9 Hz), 2.08–1.98 (m, 2H), 1.82–1.69 (m, 2H), 1.50–1.22 (m, 12H). **^{13}C NMR**: δ 139.15, 114.14, 45.14, 33.81, 32.67, 29.42, 29.39, 29.10, 28.92, 28.89, 26.89. **IR** (cm^{-1}): 3076 (m); 2926 (m); 2854 (m); 1824 (w); 1640 (m); 1463 (m); 1445 (w). **MS**: m/z (relative intensity) 41 (72.4); 55 (100.0); 69 (68.4); 83 (38.5); 97 (26.3); 104 (50.8); 188 (10.4); 190 (2.8). Exact mass: calculated 188.1331 for $C_{11}H_{21}Cl$; found 188.1331.

***N*-(ω-Undecylenyl)-Phthalimide (I).**[29] To a solution of 10.0 g (0.053 mol) of 1-chloro-10-undecene in 25 ml of dry DMF was added 12.8 g (0.069 mol) of potassium phthalimide. The resulting suspension was stirred on an oil bath of 90 °C for 24 h. The obtained reaction mixture was cooled to room temperature and 75 ml of water was added. The aqueous layer was extracted once with 75 ml and subsequently twice with 30 ml of ether. The combined organic layers were washed with 25 ml of a 0.2 M NaOH solution and with 25 ml of brine, and dried over $MgSO_4$. Evaporation of the solvent yielded 15.5 g (0.052 mol, 98%) of the crude product as a yellow solid. Recrystallization from 50 ml of distilled methanol gave, after standing of the solution at 18–20 °C in a closed flask for 18 h, 10.3 g (0.034 mol, 64%) of *N*-(ω-undecylenyl)-phthalimide (**I**) as white needles (mp 42–42.5 °C). The filtrate was subsequently placed at 4 °C in a closed flask for 24 h, which yielded an additional 2.6 g of **I**, which was still pure enough to use. This gave a total yield of 12.9 g (0.043 mol, 83%).

^{1}H NMR: δ 7.86–7.80 (m, 2H), 7.75–7.67 (m, 2H), 5.90–5.71 (m, 1H), 5.04–4.89 (m, 2H), 3.67 (t, 2H, J = 7.3 Hz), 2.06–1.97 (m, 2H), 1.72–1.58 (m, 2H), 1.41–1.19 (m, 12H). **^{13}C NMR**: δ 168.37 (2C), 139.12, 133.75 (2C), 132.10 (2C), 123.06 (2C), 114.04, 37.99, 33.72, 29.34, 29.31, 29.09, 29.00, 28.82, 28.53, 26.78. **IR** (CCl_4, cm^{-1}): 3079 (w); 2929 (m); 2856 (m); 1774 (m); 1718 (s).

1-Amino-10-Undecene.[30] To a solution of 10.0 g (0.033 mol) of *N*-(ω-undecylenyl)-phthalimide (**I**) in 100 ml of ethanol was added 2.5 g (0.050 mol) of hydrazine. The resulting mixture was heated to reflux for 3 h. The solution was cooled to room temperature and acidified to pH = 1–2 by the addition of 100 ml of 1 M HCl. The white suspension was filtered on a glass filter and the residue was washed twice with 20 ml of 1 M HCl. The combined filtrates were made alkaline (pH = 10–11) by the addition of NaOH (tablets) and

concentrated to a volume of ca. 100 ml by evaporation under reduced pressure. The resulting turbid aqueous layer was extracted four times with 50 ml of ether. The combined organic layers were washed once with 20 ml of a 0.2 M NaOH solution and once with 20 ml of brine, to which a few ml of the 0.2 M NaOH solution has been added. The organic layer was dried over NaOH (solid) for 1–2 h. Evaporation of the solvent yielded 4.9 g (0.029 mol, 88%) of crude 1-amino-10-undecene as a yellow oil.

^{1}H NMR: δ 5.92–5.72 (m, 1H), 5.04–4.90 (m, 2H), 2.68 (t, 2H, J = 6.8 Hz), 2.09–1.99 (m, 2H), 1.74 (br. s, 2H), 1.45–1.27 (m, 14H). **^{13}C NMR**: δ 139.19, 114.06, 42.09, 33.76, 33.55, 29.51, 29.42, 29.39, 29.08, 28.88, 26.83. **IR** (cm^{-1}): 3366 (m); 3295 (m); 3076 (w); 2925 (m); 2853 (m); 1640 (m).

***N*-(ω-Undecylenyl)-Acetamide (II).**[31] A mixture of 4.2 g (0.025 mol) of 1-amino-10-undecene and 5 ml (0.053 mol) of acetic anhydride was heated to reflux for 10 min, using a preheated oil bath of 170 °C. The resulting hot solution was immediately poured onto 50 ml of ice water and this mixture was heated to reflux for 20 min. The resulting solution was cooled to room temperature and extracted three times with 50 ml of ether. The combined organic layers were subsequently washed twice with water and once with brine and dried on $MgSO_4$. Evaporation of the solvent gave 5.0 g of a yellow oil, which contained a mixture (ratio ~2 : 1) of the monoacetylated amine (i.e., compound **II**) and the diacetylated amine.

The compounds were separated by chromatography (silica gel) using a 2 : 1 mixture of distilled ethyl acetate and distilled petroleum ether (40–60 °C). The fractions containing **II** were combined and stirred with a small amount of activated carbon (Norit) for 18 h.[32] The resulting solution was dried over $MgSO_4$ and filtered. Subsequent evaporation of the solvents under reduced pressure gave 2.7 g (0.013 mol, 52%) of *N*-(ω-undecylenyl)-acetamide (**II**) as a white solid (mp 29–30 °C). Subsequent recrystallization from 25 ml of distilled ethyl acetate at -20 °C gave 0.90 g (0.0042 mol, 16%) of pure *N*-(ω-undecylenyl)-acetamide (**II**) as white crystals (mp 30–31 °C).

^{1}H NMR: δ 5.90–5.70 (m, 1H), 5.50 (br. s, 1H), 5.02–4.88 (m, 2H), 3.26–3.16 (m, 2H), 2.05–1.96 (m, 2H), 1.96 (s, 3H), 1.50–1.22 (m, 14H). **^{13}C NMR**: δ 170.14, 139.15, 114.08, 39.71, 33.75, 29.51, 29.42, 29.35, 29.22, 29.04, 28.85, 26.87, 23.22. **IR** (KBr, cm^{-1}): 3292 (m, br. peak); 3079 (w); 2928 (m); 2855 (m); 1650 (s); 1553 (m). **MS**: m/z (relative intensity) 30 (100); 41 (24.6); 43 (33.8); 55 (19.49); 60 (30.4); 72 (50.5); 73 (51.6); 86 (22.3); 100 (20.8); 211 (16.6). Exact mass: calculated 211.1936 for $C_{13}H_{25}NO$; found 211.1939.

8.2.3 Monolayer Preparation

For the water contact angle measurements, the monolayers were prepared as described previously in Chapter 3 and 4. The ATR crystals for the IR measurements were modified by the procedure as described in Chapter 5.

8.2.4 Modification of the Monolayers

Monolayer modifications with hydrazine were performed in closed flasks. The samples were placed in a 5% solution (v/v) of hydrazine in distilled ethanol and the solution was stirred at room temperature for 40–48 h. Subsequently, the samples were removed from the solution and cleaned as usual.

Monolayer modifications with 4 M HCl were carried out as described previously in Chapter 3 for the hydrolysis of the ester-terminated monolayers. A reaction time of 20–24 h was used. After the reaction the substrates were rinsed repeatedly in water.

8.2.5 Monolayer Analysis

Water contact angles were determined by the Wilhelmy plate method as described previously (Chapters 3, 4, and 5). The details for the ATR-IR measurements have been described in Chapter 5.

8.3 Results and Discussion

8.3.1 Mixed Monolayers of *N*-(ω-Undecylenyl)-Phthalimide and 1-Decene

Monolayers with different surface densities of the amino groups can be prepared by using mixtures of the protected amine derivative and an underivatized 1-alkene in the surface modification. As there will be no significant difference in the reactivity of the alkene moieties of the two compounds, both 1-alkenes will react with the H-terminated Si surface. Consequently, it is expected that a monolayer will be formed in which both alkenes are incorporated, with their ratio of incorporation approximately equal to the molar ratio as used in the solution for the surface modification.

The results of the water contact angle measurements on mixed monolayers of *N*-(ω-undecylenyl)-phthalimide (**I**) and 1-decene (**C10**) are shown in Figure 3. The molar ratio of the two alkenes was varied from **C10** : **I** = 1 : 2 to 49 : 1. The water contact angles of the resulting monolayers are found to depend on this molar ratio. An increase of the relative

amount of **C10** leads to an increase in the water contact angles. At low concentrations of **I** the water contact angles approach the values of a monolayer of **C10** (Θ_a = 108°, Θ_r = 98°). This shows that both 1-alkenes react with the Si surface and that their ratio in the monolayer depends on the molar ratio in solution, as expected. The water contact angle hysteresis for these monolayers is small (≤ 10°), which indicates that they are well-ordered.

The incorporation of more molecules of **I** in the monolayer decreases the contact angles, as the phthalimide group is a polar, hydrophylic group. An increase in the contact angle hysteresis is observed as well, especially for the monolayers with relatively large percentages of **I** (i.e., for the **C10** : **I** ratios of 1 : 2 and 1 : 1). This effect has previously been reported for similar mixed monolayers on oxidized silicon,[15] where it was attributed to the formation of less ordered monolayers upon increase of the relative amount of phthalimide groups. In the present investigations it was found that for the monolayers with **C10** : **I** ratios of 1 : 1 and 1 : 2 the contact angles also decrease by several degrees (≥ 4°) during the measurement, which indicates the adsorption of water on these monolayers with many polar phthalimide groups. The contact angles of monolayers with relatively high **C10** : **I** ratios (from 3 : 1 up to 49 : 1) were stable (decrease in Θ_a < 2° over 8 successive measurements). Water adsorption will lead to an increase in the polarity of the surface and, thus, to a decrease in the contact angles during the measurement. This means that it is not possible to draw any conclusion about the packing density of these monolayers with high percentages of **I** from the contact angle measurements.

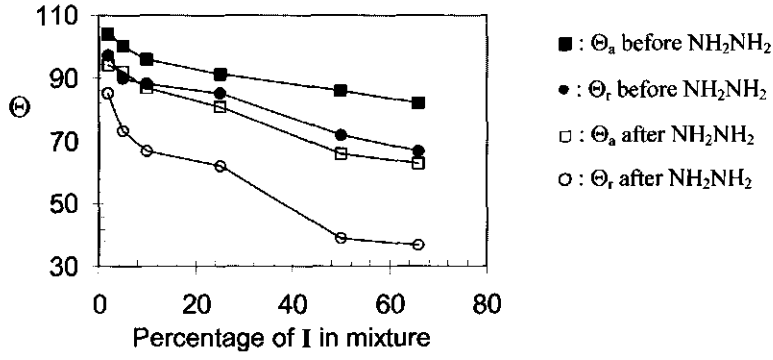

Figure 3. Advancing and receding water contact angles (Θ_a and Θ_r, respectively) of the mixed monolayers of **C10** and **I** before (closed symbols) and after (open symbols) reaction with hydrazine.

More information about the packing density of the alkyl chains in the monolayers can be obtained from IR spectroscopy. The methylene stretching vibrations can be used for this purpose, as the peak positions of these vibrations shift to lower wavenumbers if the ordering of the alkyl chains in the monolayer increases.[33] Unfortunately, the extent of this shift, especially that of the antisymmetric vibration at ~2920 cm^{-1}, also depends on the length of the alkyl chain, which means that for thin monolayers (like decyl chains) the shift is much smaller than the shift observed for thicker layers (like octadecyl chains).[34] This can complicate the analysis of thin monolayer films, like those investigated here, as these monolayers can thus appear disordered according to their IR absorptions, whereas in fact they are ordered.

The IR spectra (C=O and C–H regions) of a 1 : 1 monolayer of **C10** and **I** are shown in Figure 4a. The C=O vibration of the phthalimide groups is clearly visible at 1717 cm^{-1}, which shows that the phthalimide groups have been incorporated in the monolayer. The maxima of the methylene stretching vibrations are observed at 2925 and 2853 cm^{-1}. These values suggest that the alkyl chains in this monolayer are not as densely packed as in a well-ordered monolayer of 1-dodecene, which gives absorptions at 2922 and 2853 cm^{-1} (see Chapter 5). They are closer to the values of a monolayer of 1-decene (**C10**), which gave absorptions at 2923 and 2853 cm^{-1}, however, there is still a difference. Thus, it appears that in a mixed monolayer with a high percentage of **I**, i.e., for the **C10** : **I** ratios of 2 : 1 and 1 : 1, the packing of the alkyl chains is disturbed by the presence of the molecules of **I**, most likely because of steric hindrance between the phthalimide groups. This steric hindrance will also occur during the monolayer formation, and, as a result, less ordered monolayers are formed.

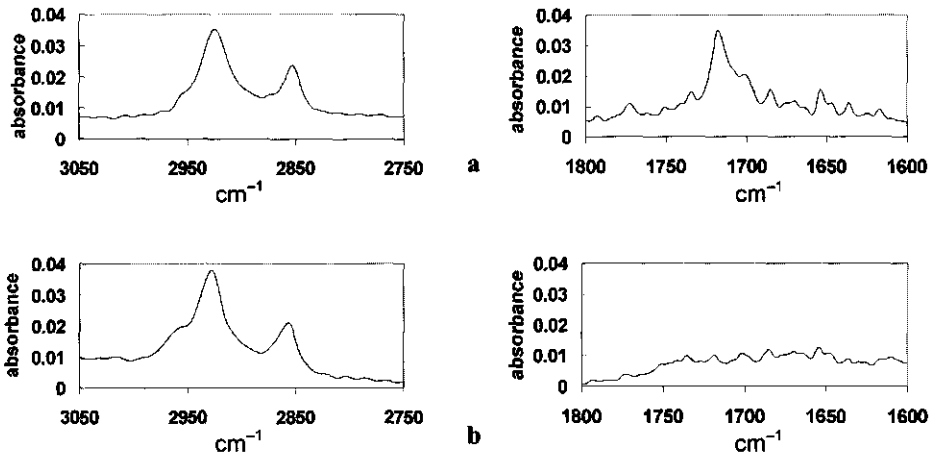

Figure 4. (a) IR spectra (C–H and C=O regions) of a 1 : 1 monolayer of **C10** and **I**. (b) Same as (a), after reaction with hydrazine.

At lower percentages of **I** the packing of the molecules is much better, as evidenced from the small contact angle hysteresis for these monolayers, which means that for these mixtures ordered monolayers will be formed. This was confirmed by an IR measurement on a 3 : 1 monolayer, which gave absorptions at 2922 and 2852 cm^{-1}. However, in this layer the C=O vibration was poorly visible.

Reaction of these monolayers with a 5% solution (v/v) of hydrazine in ethanol (at room temperature, 40–48 h) resulted in a decrease in the water contact angles of the monolayers (Figure 3). For the monolayers with a high **C10** : **I** ratio, i.e., for monolayers with only relatively few phthalimide groups, the decrease in the contact angles is small, whereas for monolayers with many phthalimide groups this decrease is much larger. A reference layer of **C10** did not show such decrease, not even after one week, which indicates that the covalent Si–C linking of the monolayers to the Si surface is not damaged under the reaction conditions. The mixed monolayers showed no decrease in the contact angles in neat ethanol. Thus, the decrease in the contact angles is most likely due to a reaction of hydrazine with the phthalimide groups, which generates hydrophylic amino groups at the outside of the monolayer. These groups are more polar than phthalimide groups, which means that the water contact angles of the modified monolayers will be lower. For the monolayers with high amounts of **I** the contact angles come close to those of a monolayer completely terminated with NH_2 groups, which gives Θ_a = 63–68° and Θ_r = 42°.[17,18] Longer reaction times (up to a week) did not result in a further decrease of the contact angles, which indicates that the reaction is apparently complete after two days. It also confirms that the mixed monolayers are stable under the reaction conditions.

Further evidence for this reaction was obtained from IR spectroscopy. In Figure 4b the IR spectra of the monolayer of **C10** and **I** (ratio 1 : 1) are shown *after* a reaction with the hydrazine solution. The C=O peak has completely disappeared, which confirms the removal of the phthalimide groups. In the C–H region no changes are observed, which shows that the monolayer itself is not damaged by the reaction, as already found with the contact angle measurements. The maxima of the methylene vibrations remained at 2925 and 2853 cm^{-1}. Monolayers with a **C10** : **I** ratio of 1 : 2 were also investigated and gave similar results. No changes in the IR spectra were observed if a mixed monolayer was placed in ethanol without hydrazine for several days. The reference monolayer of **C10** showed no changes when treated with the hydrazine solution, which again confirms that the monolayer is not damaged by the reaction conditions. Thus, on the basis of the results from the water contact angle measurements and IR spectroscopy on these mixed monolayers of **C10** and **I** it must be

concluded that amino-terminated monolayers can be prepared by reaction of a mixed monolayer of **C10** and **I** with a hydrazine solution in ethanol. All phthalimide groups in the monolayer are converted to amino groups, which means that by variation of the **C10** : **I** ratio the density of the amino groups per surface area can be controlled.

8.3.2 Mixed Monolayers of *N*-(ω-Undecylenyl)-Acetamide and 1-Decene

A second route for amino-terminated monolayers can be the preparation of acetamide-terminated monolayers and subsequent acidic hydrolysis of the amide groups to amino groups. To investigate the possibilities and limitations of this route, mixed monolayers of *N*-(ω-undecylenyl)-acetamide (**II**) and 1-decene (**C10**) were prepared. Because the purification of compound **II** is quite elaborate and gives low yields (see Section 8.2.2), only a few experiments were performed.

Three different ratios of **C10** and **II** (i.e., 9 : 1, 3 : 1, and 1 : 1) were used to prepare monolayers. In the water contact angle measurements on the resulting monolayers the same correlation with the relative amount of **II** was observed as was already found with the mixed monolayers of **C10** and **I** (see Section 8.3.1). However, the contact angle hysteresis was larger, most likely because an acetamide group is much more polar that a phthalimide group.

The results from IR spectroscopy on a 1 : 1 monolayer of **C10** and **II** are shown in Figure 5a. It was found that with this ratio an ordered monolayer is still formed, in contrast to the monolayer of **C10** and **I** with the same ratio. The methylene stretching vibrations were found at 2923 and 2853 cm^{-1}, i.e., at the same values as the well-ordered monolayer of **C10** (see Section 8.3.1). Acetamide groups are smaller that phthalimide groups, thus the formation of ordered ω-amino-protected monolayers is easier at high concentrations of the functionalized 1-alkene. Besides, well-ordered monolayers terminated with acetate groups, a functional group that has similar dimensions as an acetamide group, have already been reported in Chapter 3. The C=O vibration of the amide group was clearly visible as a broad peak, with a maximum at ~1730 cm^{-1}, which is a remarkably high value for such a vibration.[35] This shift is most likely the result of a nonplanar conformation of the amide group, which decreases the conjugation between the C=O and N–H bonds and thus shifts the C=O vibration to a higher value.

Reaction of the **C10/II** monolayers (9 : 1 and 3 : 1 ratios only) with a 4 M HCl solution under reflux conditions (20–24 h) resulted in a considerable decrease in the water contact angles of the monolayers. The 9 : 1 monolayer showed a change from Θ_a/Θ_r = 93°/70°

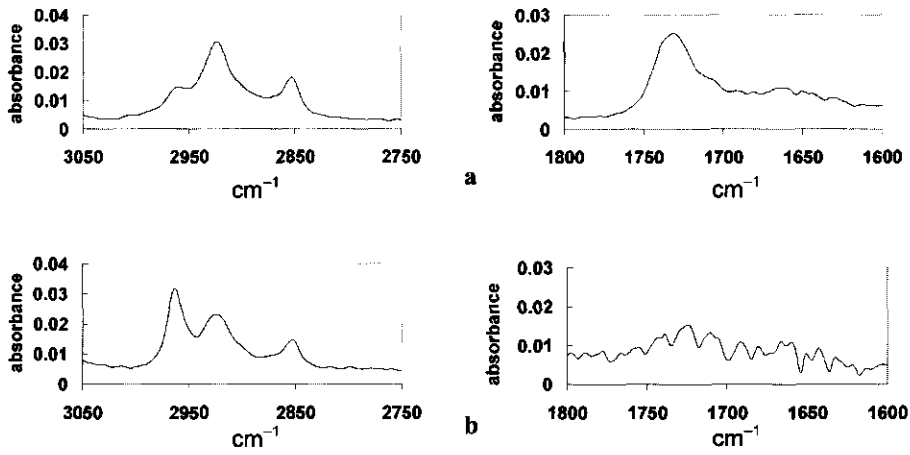

Figure 5. (a) IR spectra (C–H and C=O regions) of a 1 : 1 monolayer of **C10** and **II**. (b) Same as (a), after hydrolysis.

to Θ_a/Θ_r = 85°/55°; for the 3 : 1 monolayer a larger decrease was observed, from Θ_a/Θ_r = 87°/62° to Θ_a/Θ_r = 58°/27°. Amide groups can be hydrolyzed under strong acidic conditions, which will generate a monolayer with NH_3^+ groups on the surface. These groups are more polar than NH_2 groups,[17] and thus these NH_3^+-terminated monolayers give lower contact angles than the corresponding mixed monolayers terminated with NH_2 groups that were prepared using compound **I**. Longer reaction times had no significant effect on the contact angles. Control experiments showed that monolayers of **C10** are perfectly stable under these conditions.

The hydrolysis of the acetamide groups was confirmed by IR spectroscopy. Figure 5b shows the spectra of the 1 : 1 monolayer after this reaction. The C=O vibration has disappeared completely, which shows that the acetamide groups have been removed. The positions of the CH_2 vibrations have not changed, however, their intensities have slightly decreased and the peaks have somewhat broadened, which suggests that some disordering (i.e., increase in gauche conformations) of the alkyl chains has occurred. This effect has been observed previously in the hydrolysis of ester-terminated monolayers (see Section 3.3.3). The intensity of the antisymmetric CH_3 vibration at ~2960 cm^{-1} has increased drastically after the hydrolysis. It is known from IR measurements on monolayers of thiols[36] and of dicarboxylic acids[37] on gold, of alkanoic acids on various metal surfaces,[38] and of alkylsilanes on oxidized silicon[39] that the intensity of this vibration strongly depends on the orientation of the CH_3 group with respect to the surface normal. Apparently, a change in the orientation has also

occurred for the CH_3 groups from the 1-decene molecules in this monolayer after the hydrolysis. The results from IR spectroscopy indicate that the monolayers are not damaged by the reaction conditions. Thus, ordered mixed monolayers of **C10** and **II** can be prepared on the H-terminated Si surface and the acetamide groups in these monolayers can be converted into amino groups by hydrolysis of the amide groups with boiling HCl.

8.4 Conclusions

Two new routes have been developed for the preparation of amino-functionalized monolayers on H-terminated Si surfaces. Both routes are based on a two-step procedure, in which a mixed monolayer is prepared of a protected ω-amino-1-alkene and an underivatized 1-alkene. Subsequent removal of the protective groups generates the desired NH_2-terminated monolayers. As protective groups phthalimide and acetamide moieties have successfully been used. The phthalimide groups are removed by a reaction with hydrazine; the acetamide groups are hydrolyzed under strongly acidic conditions. It was found that both routes are equally suitable for the preparation of the NH_2-terminated monolayers, except when high surface densities (≥ 50%) are desired, in which case only the acetamide route gives well-ordered monolayers. At lower surface densities of the NH_2 groups the phthalimide route is preferable, as this compound is more easily synthesized.

References and Notes

[1] Mrksich, M. *Chem. Soc. Rev.* **2000**, *29*, 267–273.

[2] Sieval, A. B.; Linke, R.; Zuilhof, H.; Sudhölter, E. J. R. *Adv. Mater.* **2000**, *12*, 1457–1460.

[3] Wagner, P.; Nock, S.; Spudich, J. A.; Volkmuth, W. D.; Chu, S.; Cicero, R. L.; Wade, C. P.; Linford, M. R.; Chidsey, C. E. D. *J. Struct. Biol.* **1997**, *119*, 189–201.

[4] Zhao, Y. D.; Pang, D. W.; Hu, S.; Wang, Z. L.; Cheng, J. K.; Dai, H. P. *Talanta* **1999**, *49*, 751–756.

[5] Frutos, A. G.; Brockman, J. M.; Corn, R. M. *Langmuir* **2000**, *16*, 2192–2197.

[6] Silin, V.; Weetall, H.; Vanderah, D. J. *J. Colloid Interface Sci.* **1997**, *185*, 94–103.

[7] Yang, Z.; Frey, W.; Oliver, T.; Chilkoti, A. *Langmuir* **2000**, *16*, 1751–1758.

[8] Nuzzo, R. G.; Fusco, F. L.; Allara, D. L. *J. Am. Chem. Soc.* **1987**, *109*, 2358–2368.

[9] (a) In a broad survey[9b] of potential functional groups that could be used for the preparation of monolayers on gold surfaces, stearamine ($C_{18}H_{37}NH_2$) was also tested. It was found that this

compound does not give (stable) ordered monolayers, which means that this compound only physisorbes on the gold surface. (b) Bain, C. D.; Evall, J.; Whitesides, G. M. *J. Am. Chem. Soc.* **1989**, *111*, 7155–7164.

[10] Xia, Y.; Whitesides, G. M. *Angew. Chem., Int. Ed. Engl.* **1998**, *37*, 550–575.

[11] Jennings, G. K.; Laibinis, P. E. *Langmuir* **1996**, *12*, 6173–6175.

[12] Bain, C. D.; Troughton, E. B.; Tao, Y.-T.; Evall, J.; Whitesides, G. M.; Nuzzo, R. G. *J. Am. Chem. Soc.* **1989**, *111*, 321–335.

[13] Tillman, N.; Ulman, A.; Penner, T. L. *Langmuir* **1989**, *5*, 101–111.

[14] Bierbaum, K.; Kinzler, M.; Wöll, Ch.; Grunze, M.; Hähner, G.; Heid, S.; Effenberger, F. *Langmuir* **1995**, *11*, 512–518.

[15] Heid, S.; Effenberger, F. Bierbaum, K.; Grunze, M. *Langmuir* **1996**, *12*, 2118–2120.

[16] See, e.g., (a) Moon, J. H.; Shin, J. W.; Kim, S. Y.; Park, J. W. *Langmuir* **1996**, *12*, 4621–4624. (b) Moon, J. H.; Kim, J. H.; Kim, K.-i.; Kang, T.-H.; Kim, B.; Kim, C.-H.; Hahn, J. H.; Park, J. W. *Langmuir* **1997**, *13*, 4305–4310.

[17] Balachander, N.; Sukenik, C. N. *Langmuir* **1990**, *6*, 1621–1627.

[18] Heise, A.; Menzel, H.; Yim, H.; Foster, M. D.; Wieringa, R. H.; Schouten, A. J.; Erb, V.; Stamm, M. *Langmuir* **1997**, *13*, 723–728.

[19] Sieval, A. B.; Demirel, A. L.; Nissink, J. W. M.; Linford, M. R.; van der Maas, J. H.; de Jeu, W. H.; Zuilhof, H.; Sudhölter, E. J. R. *Langmuir* **1998**, *14*, 1759–1768 (Chapter 3).

[20] 1-Thioalkanes can be prepared from 1-alkenes by (anti-Markovnikov) addition of thioacetic acid to the C=C bond and subsequent alkaline hydrolysis of the resulting thioester. This reaction is frequently used in literature to prepare ω-functionalized thiols. See: Wardell, J. L., *Synthesis of Thiols* in Patai, S. *The Chemistry of the Thiol Group*; J. Wiley & Sons: London, England, UK, 1974, p 175–178.

[21] See, e.g., Vallant, T.; Kattner, J.; Brunner, H.; Mayer, U.; Hoffmann, H. *Langmuir* **1999**, *15*, 5339–5346.

[22] Bitzer, T.; Alkunshalie, T.; Richardson, N. V. *Surf. Sci.* **1996**, *368*, 202–207.

[23] Zhu, X.-Y.; Mulder, J. A.; Bergerson, W. F. *Langmuir* **1999**, *15*, 8147–8154.

[24] (a) Ing, H. R.; Manske, R. H. F. *J. Chem. Soc.* **1926**, 2348–2351. (b) March, J. *Advanced Organic Chemistry*, 4th ed.; J. Wiley and Sons: New York, NJ., USA, 1992, p 425–426.

[25] The abbreviation hydrazine will be used for this compound throughout this Chapter.

[26] Based on: Cristol, S. J.; Strom, R. M.; Stull, D. P. *J. Org. Chem.* **1978**, *43*, 1150–1154.

[27] The crude material usually contains a small amount of triphenylphosphine and/or triphenylphosphine oxide, thus the apparent yield is always > 100%.

[28] Mirviss, S. B. *J. Org. Chem.* **1989**, *54*, 1948–1951.

[29] Based on: Sheenan, J. C.; Bolhofer, W. A. *J. Am. Chem. Soc.* **1950**, *72*, 2786–2788.

[30] Based on: Vogel's Textbook of Practical Organic Chemistry, 5th ed.; Longman Scientific & Technical: Essex, England, UK, 1989, p 780.

[31] Vogel's Textbook of Practical Organic Chemistry, 5th ed.; Longman Scientific & Technical: Essex, England, UK, 1989, p 1274.

[32] If this step with activated carbon (Norit) is omitted, the obtained product (**II**) is pale yellow instead of white. It should also be noted that the product is not the first to come of the column, which somewhat complicates this purification by chromatography.

[33] This effect is used throughout this whole thesis. See Chapters 3 and 5 for more details.

[34] Porter, M. D.; Bright, T. B.; Allara, D. L.; Chidsey, C. E. D. *J. Am. Chem. Soc.* **1987**, *109*, 3559–3568.

[35] The C=O vibration of amide groups is usually observed at 1700–1670 cm^{-1} (in dilute solutions). In CCl_4 compound **II** gave an absorption at 1686 cm^{-1}.

[36] Nuzzo, R. G.; Dubois, L. H.; Allara, D. L. *J. Am. Chem. Soc.* **1990**, *112*, 558–569.

[37] Colorado, R.; Villanza, R. J.; Lee, T. R. *Langmuir* **1998**, *14*, 6337–6340.

[38] Tao, Y.-T. *J. Am. Chem. Soc.* **1993**, *115*, 4350–4358.

[39] Brunner, H.; Vallant, T.; Mayer, U.; Hoffmann, H. *Surf. Sci.* **1996**, *368*, 279–291.

Appendix

Infrared Spectroscopy of Organic Monolayers on Solid Substrates

Attenuated Total Reflection (ATR) Spectroscopy

Infrared spectroscopy is a valuable tool for the analysis of organic monolayers on solid surfaces. In general, the spectrum is measured by the reflection of infrared light from the substrate. However, such measurements are often hampered by the low signal-to-noise ratio for the absorption of a monolayer.

The problem of the low absorption can be solved by the application of Multiple Internal Reflection (MIR) spectroscopy.[1,2] With this method, which is also often referred to as Attenuated Total Reflection (ATR) spectroscopy, the infrared light is reflected many times at the monolayer–substrate interface. The method is based on the following principle: the monolayer, with refractive index n_2, is prepared on a crystal with a high refractive index n_1. Snell's law of refraction states that

$$n_1 \sin\Theta_1 = n_2 \sin\Theta_2$$

with Θ_1 and Θ_2 the angles of incidence and refraction of the light from the interface between layer 1 and layer 2. If light goes from the crystal (layer 1) to the monolayer (layer 2), this equation has no solution for Θ_2 if

$$\frac{n_1}{n_2}\sin\Theta_1 > 1$$

and total reflection of the light occurs within layer 1 (= in the crystal; see Figure 1a).

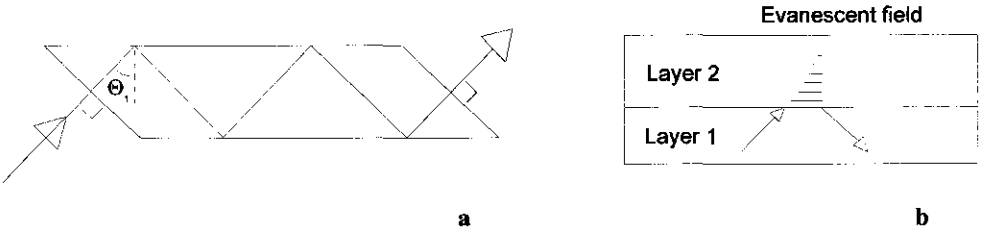

Figure 1. (a) Schematic representation of multiple internal reflection of light through a crystal. (b) Generation of an evanescent field at the crystal–monolayer interface.

The reflecting light at the surface generates an evanescent field outside this surface (Figure 1b). This field will interact with the material in layer 2 (= the monolayer) and thus depends on the infrared characteristics of the monolayer. The strength of the evanescent field

decays with the distance from the surface. The so-called depth of penetration d_p, which is defined as the distance from the surface where the electric field has fallen to 1/e of its original value, is[1,3]

$$d_p = \frac{\lambda}{n_1 2\pi\sqrt{\sin^2(\Theta_1) - n_{21}^2}} \qquad \text{with } n_{21} = \frac{n_2}{n_1}$$

and λ the wavelength of the light. Due to the exponential decay of the field, the spectral characteristics close to the surface mainly determine the obtained spectrum.

The ATR crystals used in this research had an angle of incidence of $\Theta_1 = 45°$, were 50 mm long and had a thickness of 1 mm. The refractive index of Si is $n_1 = 3.5$. The refractive index of organic compounds, like the alkyl monolayers in these investigations, is usually $n_2 \approx 1.5$. In this situation total reflection of the infrared light will occur at the Si–monolayer interface, which results in 50 reflections, and, consequently, in a strongly improved signal-to-noise ratio. In this set-up the depth of penetration for the IR light that probes the C–H stretching vibrations, which are at $\lambda \approx 3.33$ μm (i.e., near 3000 cm^{-1}), is $d_p \approx 270$ nm. This is > 100 times larger than the thickness of the monolayers, thus all vibrations, also those further away from the surface, are measured without any significant effect on their intensity.

Orientation Analysis of Alkyl Monolayers by Infrared Dichroism Measurements

Infrared absorption spectroscopy in combination with polarized light can be used to obtain information about the orientation of (certain parts of) the molecules in a (mono)layer.[4] This requires the determination of the dichroic ratio D of a specific absorption, which is[5]

$$D = \frac{A^S}{A^P}$$

where A^S and A^P are the absorptions of s- and p-polarized light, respectively. In order to find the orientation of the molecules, it is necessary to define a coordinate system. The spherical polar coordinates are generally used, which means that the x- and y-direction are in the surface plane and the z-direction is the surface normal.[6,7] Thus, the s-polarized light is oriented perpendicular to the incident plane (the *s* comes from the German word *senkrecht*, which means perpendicular) and has a component in the y-direction (Figure 2). The p-polarized light is oriented parallel to the incident plane and has components in the x- and z-direction. This transforms the dichroic ratio into[5]

$$D = \frac{A_y}{A_x + A_z}$$

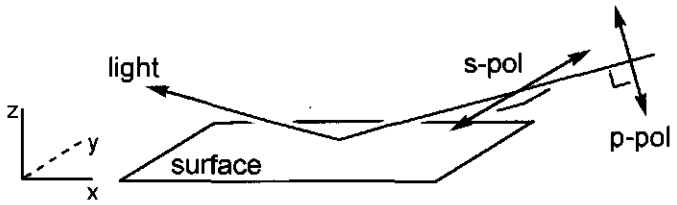

Figure 2. Directions for s- and p-polarized light.

The absorptions A_x, A_y, and A_z are[5]

$$A_x = \tfrac{1}{2} M^2 E_x^2 \sin^2 \alpha$$

$$A_y = \tfrac{1}{2} M^2 E_y^2 \sin^2 \alpha$$

$$A_z = M^2 E_z^2 \sin^2 \alpha$$

where M is the transition dipole moment of the vibration, α is the angle between M and the surface normal, and E_x, E_y, and E_z are the different components of the electric field at the surface. These are given by[8]

$$E_x = \frac{2\cos\Theta\left(\sin^2\Theta - n_{31}^2\right)^{1/2}}{\left(1 - n_{31}^2\right)^{1/2}\left[\left(1 + n_{31}^2\right)\sin^2\Theta - n_{31}^2\right]^{1/2}}$$

$$E_y = \frac{2\cos\Theta}{\left(1 - n_{31}^2\right)^{1/2}}$$

$$E_z = \frac{2n_{32}^2\cos\Theta\sin\Theta}{\left(1 - n_{31}^2\right)^{1/2}\left[\left(1 + n_{31}^2\right)\sin^2\Theta - n_{31}^2\right]^{1/2}}$$

where Θ is the angle of incidence of the infrared light, and n_{31} and n_{32} are defined as

$$n_{31} = \frac{n_3}{n_1} \text{ and } n_{32} = \frac{n_3}{n_2}$$

with n_1 the refractive index of the ATR crystal, n_2 the refractive index of the organic layer, and n_3 the refractive index of air. Using values of $n_1 = 3.5$, $n_2 = 1.5$, and $n_3 = 1.00$, combined with $\Theta = 45°$ as the angle of incidence, this results in

$$E_x = 1.4086,\ E_y = 1.4757, \text{ and } E_z = 0.6844.$$

Substitution of the formulas for A_x, A_y, and A_z gives

$$D = \frac{\tfrac{1}{2} E_y^2 \sin^2 \alpha}{E_z^2 \cos^2 \alpha + \tfrac{1}{2} E_x^2 \sin^2 \alpha}$$

which, after some mathematics, transforms in

$$\alpha = \tan^{-1}\left[\frac{2DE_z^2}{E_y^2 - DE_x^2}\right]^{1/2}$$

The absolute absorptions A, which determine D, can be directly measured in the IR spectra. The values for E are known (*vide supra*). Thus, one can calculate the α of a certain vibration by measuring the polarized IR spectra. In order to determine the tilt angle of an alkyl chain, the measurement of two independent α's is sufficient. Generally, in the analysis of alkyl monolayers the antisymmetric (α_a) and symmetric (α_s) methylene stretching vibrations are used.[6] These absorptions are at approximately 2920 and 2850 cm^{-1}, respectively.

The tilt angle Θ_{tilt} of the alkyl chain, which is defined as the angle between the molecular axis of the alkyl chain and the surface normal, is perpendicular to the two methylene stretching vibrations and can be determined from[6]

$$\cos^2 \alpha_s + \cos^2 \alpha_a + \cos^2 \Theta_{tilt} = 1 \qquad \text{(normalization of vectors)}$$

with $\alpha_s = \alpha$ of symmetric stretching vibration, $\alpha_a = \alpha$ of antisymmetric stretching vibration, and Θ_{tilt} = tilt angle of the alkyl chain.

This gives

$$\Theta_{tilt} = \cos^{-1}\sqrt{1 - \cos^2 \alpha_s - \cos^2 \alpha_a}$$

which thus allows for directly determining the tilt angle of an alkyl chain in a monolayer on a silicon substrate from the measurement of the s- and p-polarized infrared spectra.

References

[1] Harrick, N. J. *J. Phys. Chem.* **1960**, *64*, 1110–1114.

[2] Fahrenfort, J. *Spectrochimica Acta* **1961**, *17*, 698–709.

[3] Yalamanchili, M. R.; Atia, A. A.; Miller, J. D. *Langmuir* **1996**, *12*, 4176–4184.

[4] Simpson, G. J.; Rowlen, K. L. *J. Phys. Chem. B* **1999**, *103*, 3800–3811.

[5] Tillman, N.; Ulman, A.; Schildkraut, J. S.; Penner, T. L. *J. Am. Chem. Soc.* **1988**, *110*, 6136–6144.

[6] Higashiyama, T.; Takenaka, T. *J. Phys. Chem.* **1974**, *78*, 941–947.

[7] For a short explanation of spherical polar coordinates see, e.g., Atkins, P. W. *Molecular Quantum Mechanics*, 2nd ed.; Oxford University Press: Oxford, Great Britain, 1983, p 64.

[8] Haller, G. L.; Rice, R. *J. Phys. Chem.* **1970**, *74*, 4386–4393.

Summary

Silicon is the basis material for a large variety of electronic devices, such as microprocessor chips and sensors. Upon continuous downsizing of these devices the properties of the silicon surface become more and more important for determining the performance of the device. This means that careful control is required over the structure and chemical composition of the surface. Preferably, this control should be possible all the way down to the molecular level.

Monolayers of organic compounds on solid substrates form an important candidate for such control over the surface properties of inorganic materials. These monolayers consist of (mixtures of) separate, single organic molecules and the properties of individual molecules can be easily controlled, e.g., by the incorporation of functional groups. Also, the exact position of these functional groups in the molecule can be varied, which allows for a further finetuning of the properties of the inorganic substrate, as the effect of the functional group in general depends on the distance to the surface of the substrate. This means that it is in principle possible to have control down to the molecular level, as desired.

In Chapter 1 a brief review is given of three important types of monolayers that have been investigated during the past decades, i.e., Langmuir-Blodgett monolayers, monolayers of thiols on gold, and monolayers of silanes on oxidized silicon.

Chapter 2 describes the preparation of a new, different class of covalently bound organic monolayers on oxide-free silicon surfaces by (wet-)chemical reactions between organic molecules and Si surfaces, for which several different methods are currently available. The resulting organic monolayers can be linked to the Si surface via several different covalent bonds: Si–C, Si–O–C, and Si–N–C, depending on the type of functionalized (reactive) Si surface and the organic reagents that are used. Both wet-chemical reactions as well as high-vacuum processes are discussed. This Chapter also gives a short introduction into the field of clean and hydrogen-terminated silicon surfaces, as an understanding of the structure of these surfaces is essential in studying the reactivity and modification of the Si surfaces.

Chapter 3 describes the preparation of monolayers of 1-alkenes on H-terminated Si(100) surfaces by a thermal reaction at 200 °C. In this reaction the 1-alkenes react with Si–H groups on the surface, which results in highly stable, covalently bound, Si–C linked monolayers. Both underivatized and functionalized 1-alkenes have been used, and the resulting monolayers have been characterized by three techniques: water contact angle measurements, infrared spectroscopy, and X-ray reflectivity. The results show that underivatized 1-alkenes give densely packed monolayers. They are hydrophobic, with advancing and receding water contact angles of Θ_a = 109–110° and Θ_r = 94–96°, respectively. The IR spectra show C–H absorptions at 2920–2921 cm^{-1} and 2851–2852 cm^{-1} for the antisymmetric and symmetric methylene stretching vibrations. These values all correspond well to those of other systems that give densely packed, well-ordered monolayers, like the thiols on gold and the alkyltrichlorosilanes on oxidized silicon. From the results from X-ray reflectivity, which confirmed the dense packing of the molecules in the monolayers, a tilt angle of 28±1° with respect to the surface normal was calculated for the alkyl chains. Experiments using ω-functionalized 1-alkenes showed that these compounds also give densely packed monolayers, provided that the functional groups are properly protected. Disordered monolayers are obtained if the functional groups are too close to the alkene moiety. The interconversion of the functional groups in the ω-functionalized monolayers is also investigated. It is shown that ester groups can be hydrolyzed to generate carboxylic acid groups, which can be reacted with an alcohol to generate a new ester group. Acetate groups have also been converted into alcohol groups by a reduction.

The surface modification in Chapter 3 requires the use of neat 1-alkenes. This can in some cases be problematic, as relatively large quantities of the 1-alkene are required, which are not always available. Also the high reaction temperature of 200 °C limits the range of organic compounds that can be used, as the boiling point of the 1-alkene has to be above this temperature. In Chapter 4 an improved method for the preparation of these monolayers of 1-alkenes is presented. It is shown that the monolayers can also be prepared in boiling aromatic solvents, and that the quality of the resulting monolayers is (as least) as good as those prepared using neat 1-alkenes. At a relatively high concentration of the 1-alkenes (10% v/v) several substituted aromatic solvents, like xylenes and *t*-butyl benzene, are suitable for the modification. The "best" solvent, i.e., the solvent of choice, is mesitylene (1,3,5-trimethylbenzene), as only with this solvent well-ordered monolayers are obtained at low concentrations of the 1-alkene (2.5% v/v, ~0.1 M). The new method, which is called the

solution procedure, reduces the amount of 1-alkene required for a surface modification by a factor of 20–40. Also, the range of 1-alkenes that can be used is extended, as the aromatic solvents have boiling points that are considerably lower than the above-mentioned reaction temperature of 200 °C that is required with neat 1-alkenes.

On the H-terminated Si(100) surface the Si surface atoms are terminated with two hydrogen atoms. Three-dimensional models of this surface suggest that with 1-alkynes it would be possible to make two covalent Si–C bonds to the Si surface per reacting organic molecule. In other words, the alkenyl-type structure that is formed after a 1-alkyne has formed a Si–C bond to the Si surface could, in principle, react with a second Si–H group on the surface. This is investigated in Chapter 5, where the preparation of monolayers of 1-alkynes on the H-terminated Si(100) surface is described. For the surface modification the solution procedure is used and the properties of the resulting monolayers are compared to those of monolayers of the corresponding 1-alkenes. The results from water contact angle measurements (Θ_a = 109–110°, Θ_r = 98–101°), IR spectrocopy (ν_a = 2921–2922 cm^{-1}, ν_s = 2852 cm^{-1}), and X-ray reflectivity show that the 1-alkynes form monolayers that are at least as ordered as those of the corresponding 1-alkenes. The results from IR spectroscopy and X-ray reflectivity measurements indicate that the 1-alkynes form two covalent Si–C bonds to the Si(100) surface per reacting molecule. Quantum chemical calculations on small Si clusters, in which the organic molecule is bound to the surface in this way, confirm and clarify this situation, which is also shown to be energetically more favorable than the formation of only one Si–C bond. Thus, it is concluded that the 1-alkynes make two Si–C bonds per reacting molecule.

Chapter 6 describes the investigation of the monolayers by molecular modeling simulations. These calculations can provide more detailed information about the structure of (the molecules in) the monolayers on a molecular scale. This is important, as such information in general can not be derived from experimental data, because the techniques used to investigate the monolayers only measure over a large area. In the calculations the monolayers are described using the approach of two-dimensionally repeating boxes. Calculations without this approach are unsuccessful. All calculations were done on octadecyl monolayers on the H-terminated Si(111) surface, as for this monolayer a large amount of experimental data is available. The results show that the simulations are successful with boxes that contain a minimum of ~30 alkyl chains. For boxes with a substitution percentage of 50% of the Si–H for Si–alkyl groups a good correlation is found between the obtained structures and the available experimental data. The alkyl chains are in all-*trans* conformations and make tilt

angles of 25–30°, which correspond well with the experimental value of 28°. Calculations with different substitution percentages (33%, 67%, and 100%) of the Si–H for Si–alkyl groups showed that much higher packing densities than 50% are unlikely, because of an increase in the steric hindrance between the alkyl chains near the Si surface, which is unfavorable. Much lower packing densities were also found to be unfavorable, because of a serious decrease in the favorable Van der Waals interactions between the alkyl chains when compared to the 50%-substituted surfaces. Therefore it was concluded that the substitution percentage of 50–55% that is obtained experimentally is close to the maximum that can be achieved on this Si surface.

Silicon surface passivation is an important process in the semiconductor industry. In Chapter 7 the possible application of the covalently attached monolayers for this purpose is investigated. Monolayers of 1-alkenes are prepared on high-quality, p-type, float zone Si wafers (1–2 Ω·cm) and the effective lifetime of the minority charge carriers, which is a measure for the resulting surface passivation, is determined by modulated free carrier absorption (MFCA) measurements. On non-passivated surfaces the effective lifetime is ~5–7 μs. The results showed that by modification of the Si substrates with a monolayer of undecylenic acid methyl ester (CH_2=CH–$(CH_2)_8$–C(O)O–CH_3) effective lifetimes up to 130 μs can be obtained. This lifetime corresponds with a maximum surface recombination velocity of 125 cm/s, a value that is in the same order of magnitude as that obtained using other chemical passivating techniques, like hydrogen passivation. However, the stability of the monolayer-modified surfaces is much better than that of hydrogen-passivated surfaces, as the monolayers inhibit the oxidation of the Si surface for at least several weeks (XPS measurements). This indicates that silicon surface passivation with these monolayers is indeed an interesting alternative method. The modified substrates were also investigated by Kelvin probe measurements, to study a reversible time-dependent behavior of the charge carrier lifetimes that was observed in the MFCA measurements. It was found that this effect is due to trapping of charges in surface states that are in the bandgap.

Amino-functionalized monolayers on silicon substrates are interesting for the development of new types of (bio)sensors. Chapter 8 describes a new, facile approach for the preparation of such monolayers. Unlike other methods, this new approach allows for complete control over the surface density of the amino groups. Mixed monolayers of a protected ω-amino-1-alkene and an underivatized 1-alkene of comparable length are prepared by the solution procedure. Subsequently, the protective groups are removed by deprotection

reactions that do not damage the underlying monolayer or the Si substrate. Evidence for the successful deprotection of the amino groups as well as for the stability of the monolayers is derived from a combination of water contact angle measurements and IR spectroscopy. If high surface densities (≥ 50%) of the amino groups are desired the use of an acetamide-protected amino derivative is required. For lower surface densities a phthalimide-protected derivative can be used, which is easier to synthesize.

Samenvatting

Silicium vormt de basis van een breed scala aan elektronische componenten en systemen, zoals microprocessor chips en sensoren. Door het almaar kleiner worden van de dimensies van dergelijke systemen krijgen de eigenschappen van het siliciumoppervlak een steeds grotere invloed op het functioneren ervan. Een nauwgezette controle over de structuur en samenstelling van dit oppervlak wordt dan ook noodzakelijk. Deze controle moet bij voorkeur mogelijk zijn tot op moleculair niveau.

Monolagen van organische verbindingen op vaste substraten zijn een belangrijke kandidaat om de eigenschappen van de oppervlakken van anorganische materialen te kunnen beïnvloeden. Dergelijke monolagen bestaan uit (mengsels van) onafhankelijke, afzonderlijke organische moleculen. De eigenschappen van de individuele moleculen kunnen eenvoudig beïnvloed worden, bijvoorbeeld door het invoeren van functionele groepen in de moleculen. Tevens kan men de positie van een functionele groep binnen het molecuul variëren, wat een verdere verfijning van de eigenschappen van het anorganische substraat mogelijk maakt, omdat de grootte van het effect van de functionele groep op die eigenschappen gewoonlijk afhangt van de afstand van die groep tot het oppervlak van het substraat. Dit betekent dat men met deze monolagen in principe de gewenste controle tot op moleculair niveau kan bereiken.

In Hoofdstuk 1 wordt een kort overzicht gegeven van drie belangrijke klassen van monolagen die in de afgelopen decennia uitgebreid zijn onderzocht. Deze monolagen zijn de *Langmuir-Blodgett monolagen*, de *monolagen van thiolen op goud* en de *monolagen van silanen op geoxideerd silicium*.

In Hoofdstuk 2 wordt een nieuwe klasse van monolagen besproken, die worden gemaakt middels chemische reacties tussen organische moleculen en siliciumoppervlakken: de covalent gebonden, organische monolagen op oxidevrije siliciumoppervlakken. Er zijn momenteel diverse methoden beschikbaar om dergelijke monolagen te maken. De organische moleculen kunnen tevens op verschillende manieren aan het siliciumoppervlak gebonden zijn: middels covalente Si–C, Si–O–C, of Si–N–C bindingen, afhankelijk van het gebruikte gefunctionaliseerde, reactieve siliciumoppervlak en het organische reagens. Zowel de natchemische als de hoogvacuüm reacties worden in dit hoofdstuk besproken. Tevens wordt

een kort overzicht gegeven over de oxidevrije ("schone") en de waterstof-getermineerde siliciumoppervlakken, omdat kennis van de structuur van deze oppervlakken essentieel is bij het bestuderen van de reactiviteit en de modificatie van de siliciumoppervlakken.

In Hoofdstuk 3 worden de monolagen van 1-alkenen op waterstof-getermineerde Si(100) oppervlakken beschreven, die gemaakt worden via een thermische reactie bij 200 °C. Onder deze condities reageren de 1-alkenen met de Si–H groepen op het siliciumoppervlak. Dit resulteert in de vorming van zeer stabiele monolagen, die met een covalente Si–C binding aan het siliciumoppervlak gebonden zijn. Zowel 1-alkenen met en zonder een tweede functionele groep zijn gebruikt in de reactie. De gevormde monolagen zijn geanalyseerd met drie verschillende analysetechnieken: watercontacthoekmetingen, infraroodspectroscopie en Röntgenreflectie. De resultaten van deze metingen laten zien dat dicht gepakte monolagen worden gevormd als er geen verdere functionele groepen aanwezig zijn in de 1-alkenen. Deze monolagen zijn hydrofoob, met zogenaamde voortgaande ("advancing") en teruggaande ("receding") watercontacthoeken van respectievelijk Θ_a = 109–110° en Θ_r = 94–96°. In de IR spectra zijn de anti-symmetrische en symmetrische CH_2 vibraties te zien bij ν_a = 2920–2921 cm^{-1} en ν_s = 2851–2852 cm^{-1}. Al deze waarden corresponderen goed met die van andere, vergelijkbare systemen waarin goed geordende, dicht gepakte monolagen worden gevormd, zoals de monolagen van thiolen op goud en van alkylsilanen op geoxideerd silicium. Uit de resultaten van de Röntgenreflectiemetingen, die de dichte pakking van de moleculen in de monolagen nogmaals bevestigden, werd een tilthoek ten opzichte van de normaal van 28±1° bepaald voor de alkylketens in deze monolagen. Experimenten met ω-gefunctionaliseerde 1-alkenen tonen aan dat ook met dergelijke verbindingen dichtgepakte, geordende monolagen worden gevormd, mits de tweede functionele groep beschermd is. Als de functionele groep te dicht bij de eindstandige alkeengroep zit, worden echter monolagen verkregen die slecht geordend zijn. De interconversie van de functionele groepen in de ω-gefunctionaliseerde monolagen is ook onderzocht. Het blijkt mogelijk om estergroepen te hydrolyseren tot carboxylgroepen, die daarna in een nieuwe estergroep omgezet kunnen worden door ze met een alcohol te laten reageren. Daarnaast zijn acetaatgroepen omgezet in hydroxylgroepen door middel van een reductie.

De oppervlaktemodificatie zoals beschreven in Hoofdstuk 3 vereist het gebruik van puur 1-alkeen. Dit kan soms aanleiding geven tot problemen, omdat dit betekent dat er relatief grote hoeveelheden van het 1-alkeen nodig zijn, die niet altijd beschikbaar zullen zijn. Daarnaast kan men door de relatief hoge reactietemperatuur van 200 °C veel alkenen niet

gebruiken, omdat het kookpunt van het alkeen boven deze temperatuur moet liggen. In Hoofdstuk 4 wordt een verbeterde methode gepresenteerd voor het maken van de monolagen van 1-alkenen. Het blijkt mogelijk de reactie uit te voeren in kokende aromatische oplosmiddelen. De eigenschappen van de gevormde monolagen blijken tenminste net zo goed te zijn als die van monolagen gemaakt met het pure 1-alkeen. Bij een relatief hoge concentratie van het 1-alkeen (10% v/v) zijn verschillende gesubstitueerde aromatische oplosmiddelen, zoals xylenen en *t*-butylbenzeen, geschikt. Het "beste" oplosmiddel, ofwel het oplosmiddel dat men bij voorkeur moet gebruiken, is mesityleen (1,3,5-trimethylbenzeen), omdat alleen in dit oplosmiddel ook bij lagere concentraties van het alkeen (2,5 % v/v; ~0,1 M) goed geordende, dicht gepakte monolagen worden gevormd. Deze nieuwe methode, die de oplosmiddelmethode wordt genoemd, reduceert de hoeveelheid 1-alkeen die nodig is voor een modificatie met een factor 20–40. Tevens kunnen er nu meer 1-alkenen gebruikt worden voor de oppervlaktemodificatie, omdat de kookpunten van de aromatische oplosmiddelen aanzienlijk lager liggen dan de bovengenoemde reactietemperatuur van 200 °C, die nodig was als pure 1-alkenen werden gebruikt.

Op het waterstof-getermineerde Si(100) oppervlak zijn er twee waterstofatomen gebonden aan de Si atomen aan het oppervlak. Driedimensionale modellen van dit oppervlak suggereren dat het mogelijk moet zijn om met 1-alkynen per reagerend molecuul twee covalente Si–C bindingen naar het siliciumoppervlak te vormen. Anders gezegd, de alkenylachtige structuur, die ontstaat nadat het 1-alkyn een Si–C binding heeft gevormd naar het oppervlak, zou in principe nog met een tweede Si–H groep op het oppervlak kunnen reageren. Dit wordt onderzocht in Hoofdstuk 5, waarin de vorming van monolagen van 1-alkynen op het waterstof-getermineerde Si(100) oppervlak wordt beschreven. De oplosmiddelmethode wordt gebruikt voor de oppervlaktemodificatie en de eigenschappen van de gevormde monolagen worden vergeleken met die van de monolagen van de overeenkomstige 1-alkenen. De resultaten van de watercontacthoekmetingen (Θ_a = 109–110°, Θ_r = 98–101°), infraroodspectroscopie (ν_a = 2921–2922 cm^{-1}, ν_s = 2852 cm^{-1}) en Röntgenreflectie tonen aan dat met 1-alkynen monolagen gevormd worden die tenminste net zo goed geordend zijn als die van de overeenkomstige 1-alkenen. De resultaten van de infraroodspectroscopie en de Röntgenreflectie geven sterke aanwijzingen dat er twee covalente Si–C bindingen gevormd worden per reagerend organisch molecuul. Quantumchemische berekeningen aan kleine clusters van silicium, waarbij een organisch molecuul op deze wijze aan het oppervlak van deze clusters is gebonden, bevestigen deze waarneming. Tevens geven ze extra inzicht in deze situatie, omdat ze ook aangeven dat de

vorming van twee Si–C bindingen energetisch gunstiger is dan de vorming van slechts één Si–C binding. Dit betekent dat 1-alkynen per reagerend molecuul twee Si–C bindingen naar het Si(100) oppervlak maken.

In Hoofdstuk 6 worden de resultaten beschreven van het onderzoek aan de monolagen met molecular modeling simulaties. Dergelijke berekeningen kunnen meer inzicht geven in de structuur, op moleculair niveau, van (de moleculen in) de monolagen. Dit is belangrijk, omdat dit soort informatie meestal niet afgeleid kan worden uit experimentele gegevens, omdat de technieken die gebruikt worden voor de analyse van de monolagen alleen over relatief grote oppervlakken meten. In de berekeningen worden de monolagen beschreven met tweedimensionale, repeterende eenheden. Berekeningen zonder deze aanpak blijken geen goede resultaten op te leveren. Alle berekeningen zijn gedaan aan monolagen van octadecyl ketens op het waterstofgetermineerde Si(111) oppervlak, omdat voor deze monolaag een grote hoeveelheid experimentele gegevens beschikbaar is. De resultaten van de berekeningen geven aan dat alleen goede resultaten verkregen worden met repeterende eenheden die minimaal ~30 alkylketens bevatten. Voor de situatie waarin 50% van de Si–H groepen op het oppervlak is vervangen door Si–alkyl groepen wordt een goede correlatie gevonden tussen de berekende structuren en de beschikbare experimentele gegevens. De alkylketens hebben all-*trans* conformaties en maken een tilthoek van 25–30° ten opzichte van de normaal, welke goed correspondeert met de experimentele waarde van 28°. Berekeningen met andere substitutiepercentages (33%, 67% en 100%) van de Si–H voor Si–alkyl groepen tonen aan dat veel hogere substitutiepercentages dan 50% onwaarschijnlijk zijn, omdat de sterische hindering tussen de alkylketens nabij het oppervlak behoorlijk toeneemt, wat energetisch ongunstig is. Veel lagere substitutiepercentages dan 50% blijken eveneens ongunstig, omdat dan de attractieve, energetisch gunstige Van der Waals interacties tussen de alkylketens in de monolaag behoorlijk afnemen. Dit alles geeft aan dat het substitutiepercentage van 50–55%, dat momenteel experimenteel wordt verkregen, dicht bij met maximaal haalbare substitutiepercentage voor dit siliciumoppervlak moet liggen.

Oppervlaktepassivering van silicium is een belangrijk proces in de halfgeleiderindustrie. In Hoofdstuk 7 wordt de resultaten beschreven van het onderzoek naar het gebruik van de covalent gebonden monolagen voor dit doel. Monolagen van 1-alkenen worden gemaakt op hoge kwaliteit, p-type, float zone siliciumwafers (1–2 Ω·cm) en de effectieve levensduur van de minderheidsladingsdragers, die een maat is voor de bereikte oppervlaktepassivering, wordt gemeten met modulated free carrier absorption (MFCA) metingen. Voor oppervlakken die niet gepassiveerd zijn is deze effectieve levensduur ~5–7

μs. De resultaten laten zien dat effectieve levensduren tot 130 μs kunnen worden bereikt door een monolaag van undecyleenzuur methyl ester (CH_2=CH–$(CH_2)_8$–C(O)O–CH_3) aan te brengen op de siliciumsubstraten. Deze levensduur correspondeert met een maximale oppervlakterecombinatiesnelheid van 125 cm/s, een waarde die in dezelfde orde van grootte ligt als de recombinatiesnelheid die gehaald wordt met andere chemische passiveringsmethoden, zoals waterstofpassivering. De stabiliteit van de met een alkylmonolaag gemodificeerde oppervlakken is echter veel beter dan die van de met waterstof gepassiveerde oppervlakken, omdat de organische monolagen de oxidatie van het silicium voor tenminste enkele weken volledig tegengaan (XPS metingen). Dit toont aan dat oppervlaktepassivering van silicium met deze monolagen van 1-alkenen inderdaad een interessante alternatieve methode is. De gemodificeerde substraten zijn ook onderzocht met Kelvin probe metingen, om een reversibel tijdsafhankelijk gedrag van de levensduur van de ladingsdragers te onderzoeken, dat bij de MFCA metingen gevonden werd. Uit de resultaten van deze Kelvin probe metingen bleek dat dit gedrag het gevolg is van het fixeren van ladingen in oppervlaktetoestanden die zich in de bandgap bevinden.

Monolagen op silicium, die zijn gefunctionaliseerd met aminogroepen, zijn interessant voor het ontwikkelen van nieuwe typen (bio)sensoren. In Hoofdstuk 8 wordt een nieuwe, eenvoudige aanpak beschreven om dergelijke monolagen te maken. In tegenstelling tot bij andere methoden is er met deze aanpak volledige controle mogelijk over de dichtheid van de aminogroepen aan het oppervlak. Met de oplosmiddelmethode worden gemengde monolagen gemaakt van een beschermd ω-amino-1-alkeen en een niet gefunctionaliseerd 1-alkeen van vergelijkbare lengte. Vervolgens worden de beschermgroepen verwijderd door ontschermingsreacties, die noch de onderliggende monolaag noch het siliciumsubstraat zelf aantasten. Het succes van de ontscherming van de aminogroepen is aangetoond met een combinatie van watercontacthoekmetingen en infraroodspectroscopie. Als een hoge dichtheid (≥50%) van aminogroepen aan het oppervlak gewenst is, is het nodig een aminoderivaat te gebruiken dat beschermd is met aceetamide groepen. Voor lagere dichtheden kan een ftaalimidederivaat gebruikt worden, dat eenvoudiger te synthetiseren is.

Curriculum vitae

Alexander Bernardus Sieval werd op 6 september 1971 geboren te Leiden. Na het behalen van het gymnasiumdiploma aan het Bonaventuracollege in diezelfde plaats werd in september 1989 begonnen met de studie Scheikunde aan de Rijksuniversiteit Leiden. Het doctoraal examen werd afgelegd op 31 augustus 1994. Tijdens deze studie werd, onder leiding van dr. H. M. Barentsen en prof. dr. J. Cornelisse, een afstudeeronderzoek verricht op het gebied van de intramoleculaire metafotocycloadditie bij de vakgroep Fysisch-Organische Fotochemie. Van augustus 1995 tot februari 1996 was hij, in het kader van een KNCV werkervaringsplaats, werkzaam bij de vakgroep Farmaceutische Technologie van prof. dr. H. E. Junginger, een onderdeel van het Leiden/Amsterdam Center for Drug Research. Hier werd, in samenwerking met dr. A. F. Kotzé en dr. M. Thanou, onderzoek verricht naar de modificatie van het polymeer chitosan, met als doel het wateroplosbaar maken van dit polymeer, zodat dit geschikt werd voor farmaceutische toepassingen. Van maart 1996 tot maart 2000 was hij werkzaam als onderzoeker in opleiding (OIO) in het laboratorium voor organische chemie van Wageningen Universiteit. Hier werd het in dit proefschrift beschreven onderzoek uitgevoerd onder leiding van dr. H. Zuilhof en prof. dr. E. J. R. Sudhölter. Dit onderzoek maakte deel uit van het prioriteitsprogramma 'Zonnecellen voor de 21e eeuw' van NWO. Sinds januari 2001 is hij werkzaam als post-doc onderzoeker aan de Rijksuniversiteit Groningen.

List of Publications

This Thesis

A. B. Sieval, A. L. Demirel, J. W. M. Nissink, M. R. Linford, J. H. van der Maas, W. H. de Jeu, H. Zuilhof, and E. J. R. Sudhölter
Highly Stable Si-C Linked Functionalized Monolayers on the Silicon(100) Surface.
Langmuir **1998**, *14*, 1759–1768.

A. B. Sieval, H. Zuilhof, E. J. R. Sudhölter, F. M. Schuurmans, and W. C. Sinke
Surface Passivation of Silicon by Organic Monolayers.
Proceedings of the 2nd World Conference on Photovoltaic Solar Energy Conversion (Vienna, 1998); Joint Research Center of the European Commission: Ispra, Italy, 1998, 322–325.

A. B. Sieval, V. Vleeming, H. Zuilhof, and E. J. R. Sudhölter
An Improved Method for the Preparation of Organic Monolayers of 1-Alkenes on Hydrogen-Terminated Silicon Surfaces.
Langmuir **1999**, *15*, 8288–8291.

A. B. Sieval, B. van den Hout, H. Zuilhof, and E. J. R Sudhölter
Molecular Modeling of Alkyl Monolayers on the Si(111) Surface.
Langmuir **2000**, *16*, 2987–2990.

A. B. Sieval, R. Opitz, H. P. A. Maas, M. G. Schoeman, G. Meijer, F. J. Vergeldt, H. Zuilhof, and E. J. R. Sudhölter
Monolayers of 1-Alkynes on the H-Terminated Si(100) Surface.
Langmuir **2000**, *16*, 10359–10368.

A. B. Sieval, B. van den Hout, H. Zuilhof, and E. J. R. Sudhölter
Molecular Modeling of Covalently Attached Alkyl Monolayers on the Hydrogen-Terminated Si(111) Surface.
Langmuir, in press.

A. B. Sieval, R. Linke, G. Heij, G. Meijer, H. Zuilhof, and E. J. R. Sudhölter
Amino-Terminated Organic Monolayers on Hydrogen-Terminated Silicon Surfaces.
Submitted.

A. B. Sieval, C. L. Huisman, A. Schonecker, A. S. H. van der Heide, W. C. Sinke, A. Goossens, H. Zuilhof, and E. J. R. Sudhölter
Silicon Surface Passivation by Organic Monolayers: Minority Charge Carrier Lifetime Measurements and Kelvin Probe Investigations.
Manuscript in preparation.

Other Publications

H. M. Barentsen, A. B. Sieval, and J. Cornelisse
Intramolecular Meta Photocycloaddttion of Conformationally Restrained 5-Phenylpent-1-enes. Part II: Steric and Electronic Effects Caused by 4-Mono- and 4-Disubstitution.
Tetrahedron **1995**, *51*, 7495–7520.

A. B. Sieval, M. Thanou, A. F. Kotzé, J. C. Verhoef, J. Brussee, and H. E. Junginger
Preparation and NMR Characterization of Highly Substituted *N*-Trimethyl Chitosan Chloride.
Carbohydrate Polymers **1998**, *36*, 157–165.

M. Thanou, A. B. Sieval, A. F. Kotzé, A. G. de Boer, J. C. Verhoef, and H. E. Junginger
N,N,N-Trimethyl Chitosan Chloride (TMC) of High Degree of Substitution as a Potential Absorption Enhancer for Hydrophilic Drugs.
Advances in Chitin Sciences **1997**, *2*, 384–389.

E. P. K. Currie, A. B. Sieval, M. Avena, H. Zuilhof, E. J. R. Sudhölter, and M. A. Cohen Stuart
Weak Polyacid Brushes: Preparation by LB-Deposition and Optically Detected Titrations.
Langmuir **1999**, *15*, 7116–7118.

E. P. K. Currie, A. B. Sieval, G. J. Fleer, and M. A. Cohen Stuart
Polyacrylic-Acid Brushes: Surface Pressure and Salt-Induced Wetting.
Langmuir **2000**, *16*, 8324–8333.

C. W. Struijk, A. B. Sieval, J. E. D. Dakhorst, M. van Dijk, P. Kimkes, R. B. M. Koehorst, H. Donker, T. J. Schaafsma, S. J. Picken, A. M. van der Craats, J. M. Warman, H. Zuilhof, and E. J. R Sudhölter
Liquid Crystalline Perylene Diimides: Architecture and Charge Carrier Mobilities.
J. Am. Chem. Soc. **2000**, *122*, 11057–11066.

C. van den Boom, M. de Roode, and A. Sieval
On the Anatomy of Hans Brinker.
Annals of Improbable Research, in press.

J. H. Maas, M. A. Cohen Stuart, A. B. Sieval, H. Zuilhof, and E. J. R. Sudhölter
Preparation of Polystyrene Brushes by Reaction of Terminal Vinyl Groups on Silicon and Silica Surfaces.
Submitted.

This research was sponsored by The Netherlands Organization for Scientific Research (NWO-Priority), as part of the national project "Solar Cells for the 21st Century", and by The Netherlands Agency for Energy and the Environment (NOVEM).

ISBN 90-5808-384-5